Université de Montréal

Rôle de l'isoforme p35 de la chaîne invariante humaine dans la formation et le transport de complexes de CMH II

par Catherine Gauthier

Département de microbiologie, infectiologie et immunologie
Faculté de médecine

Mémoire présenté en vue de l'obtention du grade de
Maître *ès* sciences (M. Sc.) en Microbiologie et Immunologie

Août 2015

Université de Montréal
Faculté des études supérieures

Ce mémoire intitulé :

Rôle de l'isoforme p35 de la chaîne invariante humaine dans la formation et le transport de complexes de CMH II

présenté par :

Catherine Gauthier

a été évalué par un jury composé des personnes suivantes :

Dre France Daigle, présidente-rapporteuse
Dr Jacques Thibodeau, directeur de recherche
Dr Claude Daniel, membre du jury

Résumé

La présentation antigénique par les molécules de classe II du complexe majeur d'histocompatibilité (CMH II) est un mécanisme essentiel au contrôle des pathogènes par le système immunitaire. Le CMH II humain existe en trois isotypes, HLA-DP, DQ et DR, tous des hétérodimères composés d'une chaîne α et d'une chaîne β. Le CMH II est entre autres exprimé à la surface des cellules présentatrices d'antigènes (APCs) et des cellules épithéliales activées et a pour fonction de présenter des peptides d'origine exogène aux lymphocytes T CD4+. L'oligomérisation et le trafic intracellulaire du CMH II sont largement facilités par une chaperone, la chaîne invariante (Ii). Il s'agit d'une protéine non-polymorphique de type II. Après sa biosynthèse dans le réticulum endoplasmique (ER), Ii hétéro- ou homotrimérise, puis interagit via sa région CLIP avec le CMH II pour former un complexe αβIi. Le complexe sort du ER pour entamer son chemin vers différents compartiments et la surface cellulaire.

Chez l'homme, quatre isoformes d'Ii sont répertoriées : p33, p35, p41 et p43. Les deux isoformes exprimées de manière prédominante, Iip33 et p35, diffèrent par une extension N-terminale de 16 acides aminés portée par Iip35. Cette extension présente un motif de rétention au réticulum endoplasmique (ERM) composé des résidus RXR. Ce motif doit être masqué par la chaîne β du CMH II pour permettre au complexe de quitter le ER.

Notre groupe s'est intéressé au mécanisme du masquage et au mode de sortie du ER des complexes αβIi. Nous montrons ici que l'interaction directe, ou en *cis*, entre la chaîne β du CMH II et Iip35 dans une structure αβIi est essentielle pour sa sortie du ER, promouvant la formation de structures de haut niveau de complexité. Par ailleurs, nous démontrons que NleA, un facteur de virulence bactérien, permet d'altérer le trafic de complexes αβIi comportant Iip35. Ce phénotype est médié par l'interaction entre p35 et les sous-unités de COPII. Bref, Iip35 joue un rôle central dans la formation des complexes αβIi et leur transport hors du ER. Ceci fait d'Iip35 un régulateur clef de la présentation antigénique par le CMH II.

Mots clés : Présentation antigénique, CMH de classe II, chaîne invariante, COPII, NleA, motif de rétention au ER, motif RXR

Summary

Antigen presentation by the major histocompatibility complex class II molecules (MHCII) is a pathway essential to the immune system control over pathogens. There are three MHCII isotypes in humans, which are HLA-DP, DQ and DR. These are all heterodimers made of an α and a β chain. MHCII is expressed at the cell surface of antigen presenting cells (APCs) and activated epithelial cells and its role is mainly to present peptides of exogenous origin to CD4+ T lymphocytes. MHCII oligomerization and trafficking are largely favored by its chaperone, the invariant chain (Ii). Ii is a non-polymorphic type II protein. It hetero- or homotrimerizes right after biosynthesis in the endoplasmic reticulum (ER), and then its CLIP region interacts with MCHII to form a αβIi structure. This multimer exits the ER and starts its journey towards numerous compartments and the cell surface.

Humans have four Ii isoforms: p33, p35, p41 et p43. The two most predominantly expressed are Ii p33 and p35. They differ in a N-terminal extension long of 16 amino acids that is displayed by Iip35. This extension bears an ER retention motif (ERM) made of the RXR residues. The RXR motif must be masked by the MHCII β chain in order for the αβIi multimer to exit the ER.

Our group investigated the masking and ER exit mechanisms of the αβIi structures. Here we show that a direct (*cis*) interaction between the MHCII β chain and Iip35 is essential for ER exit, thus promoting the formation of high order αβIi structures. Moreover, we demonstrate that the bacterial virulence factor NleA impairs the trafficking of Iip35-containing αβIi multimers. This observation is mediated by an interaction between COPII subunits and Iip35. Altogether, Iip35 plays a crucial role in the αβIi multimer formation and ER exit. Iip35 is therefore a key regulator for MHCII antigen presentation.

Keywords : Antigen presentation, MHC class II, Invariant chain, COPII, NleA, ER retention motif, RXR motif

Table des matières

Liste des figures

Liste des abréviations

aa : Acide aminé
αβ : Dimère de CMH II
αβIi : Complexe comprenant les chaînes α et β du CMH II et la chaîne invariante
ADP : Adénosine diphosphate
AE : Attachement-effacement
APC : Cellule présentatrice d'antigène
ARF : ADP-*ribosylation factor*

β_2m : β_2-microglobuline

Canaux K_{ATP} : Canaux à potassium dépendants de l'ATP
CD : *Cluster of differenciation*
CD74 : Chaîne invariante
CIITA : *MHC class II transactivator*
CLIP : C*lass II-associated invariant chain derived peptide*
CMH : Complexe majeur d'histocompatibilité
CMH I, CMH II : CMH de classes I et II
COP : Protéine de manteau, *coat protein*
COPI, COPII : Vésicules COP de type I et II
C. rodentium : *Citrobacter rodentium*

DCLS : Dysplasie craniolenticulosuturale, ou syndrome de Boyadjiev-Jabs
DTT : Dithiothreitol

EBV: virus Epstein-Barr
E. coli : *Escherichia coli*
EHEC : *E. coli* entérohémorrhagique
Endo H : Endo-β-N-acétylglucosaminidase H
EPEC : *E. coli* entéropathogène
ER : Réticulum endoplasmique
ERAAP : Aminopeptidase résidente du ER (*ER-associated aminopeptidase*)
ERES : ER *exit site*
ERGIC : ER-Golgi *intermediate compartment*
ERM : Motif de rétention au réticulum endoplasmique

GAG : Glycosaminoglycane
GDP : Guanoine diphosphate
GEF : G*uanine nucleotide exchange factor*
GTP : Guanosine triphosphate
H-2 : Complexe majeur d'histocompatibilité murin
HA : Hémagglutinine du virus influenza
HLA : Système d'antigènes leucocytaires humains, CMH humain

IFN : Interféron
Ii : Chaîne invariante
IL : *Interleukin*

K_{ATP} : Canaux de potassium dépendants de l'ATP
LEE : Locus d'effacement des entérocytes
Ler : *LEE-encoded regulator*
Lésions A/E : Lésions d'attachement-effacement
LIP : L*eupeptin-induced protein*, p22
Lymphocyte T_H : Lymphocyte T auxiliaire

MIIC : Compartiment riche en CMH II, *MHC class II containing compartment*
MMTV : *Mouse mammary tumor virus*

NFκB : *Nuclear factor kappa B*
Nle : Effecteur encodé à l'extérieur du LEE, *non-LEE effector*
NleA : *non-LEE-encoded effector* A, ou EspI

Per : *Plasmid-encoded regulator*

PKC : Protéine kinase C

SAG : Superantigène
SE : *Staphylococcal enterotoxin*
SNARE : *Soluble* N-*ethylmaleimide-sensitive factor attachment-protein receptor*
SST3 : Système de sécrétion de type III

TCR : récepteur des cellules T
tER : Région transitionnelle du réticulum endoplasmique
TGN : Réseau *trans*-Golgi
TNF : *Tumor necrosis factor*
t-SNARE : SNARE du compartiment ciblé (*target*)
TSST : *Toxic shock syndrome toxin*

v-SNARE : SNARE de la vésicule
VSV-G: Protéine G du *Vesicular stomatitis virus*

Remerciements

Merci...

À Maxime, Tristan, Auriane, Antoine, Alex et Renaud pour les conseils et les discussions, mais également pour les moments de folie qui nous ont permis de garder le moral;

À Jacques, France, Joëlle, Martin, Jean et Serge pour votre expertise, que vous n'hésitiez jamais à partager;

À Louise, Line, Arnaud, Lucie C. et Anne pour le soutien technique et vos beaux sourires chaque matin;

À Joëlle (encore!), Lamia, Fée-Ann, Nathalie, Geneviève, Danielle, Lucie L., Marie-Hélène et Marie-Élaine pour les pauses quotidiennes que vous m'avez permis de partager avec vous;

À Catherine, Martine, Ariane et Marie pour votre support et votre amitié inépuisable, malgré le manque de temps à partager ensemble;

À Hélène, Guy-Alain et Simon pour votre soutien inconditionnel;

À Eric pour chaque fois où je t'ai appelé en panique et où tu m'as écoutée, chaque fois où tu m'as fait à manger parce que j'étais trop absorbée par le travail, chaque fois où tu as subi un crochet par le laboratoire la fin de semaine, chaque fois où tu m'as encouragée. Merci pour chaque fois où tu m'as fait sentir que tu m'aiderais jusqu'au bout, peu importe ce que ça impliquait.

Chapitre 1. Revue de littérature

1.1 Complexe majeur d'histocompatibilité

Le complexe majeur d'histocompatibilité (CMH), dont l'appellation réfère à son rôle dans la compatibilité de tissus à des fins de transplantation, est un système présent dans l'évolution depuis les vertébrés à mâchoire (1, 2). Le CMH humain, ou système d'antigènes leucocytaires humains (HLA), est situé sur le chromosome 6 et a été identifié par Jean Dausset; le CMH murin encode les protéines du système H-2 au niveau du chromosome 17 et a été découvert par Gorer et Snell (2-5). Les glycoprotéines du CMH peuvent être séparées en deux grandes catégories : les classes I et II (3).

1.1.1. CMH de classe I

Le CMH de classe I (CMH I) est composé de deux glycoprotéines : la chaîne alpha et la β_2-microglobuline (β_2m) (Figure 1-1, p.2). La première est composée de trois domaines dans sa région luminale (α1, α2, α3), d'un passage transmembranaire et d'une courte queue cytoplasmique. La β_2m est une protéine soluble du cytoplasme (6). Les domaines α1 et α2 forment une cavité appelée niche peptidique, qui est exposée vers le milieu extracellulaire. La niche est bordée de chaque côté par une hélice α et son plancher est formé d'une structure en feuillets β. Elle peut accueillir de courts peptides de 8-10 acides aminés (aa) (7). Le plancher irrégulier de la niche présente six poches jouant un rôle important dans l'affinité du CMH I pour un peptide. Les acides aminés N et C-terminaux du peptide se logent dans la première et la dernière poche (1, 7). Dans certains cas, de plus longs peptides peuvent interagir avec la niche peptidique du CMH I : le peptide forme un renflement (du terme anglais *bulge*) en son centre alors que ses extrémités peuvent toujours s'ancrer dans les poches aux extrémités de la niche (7).

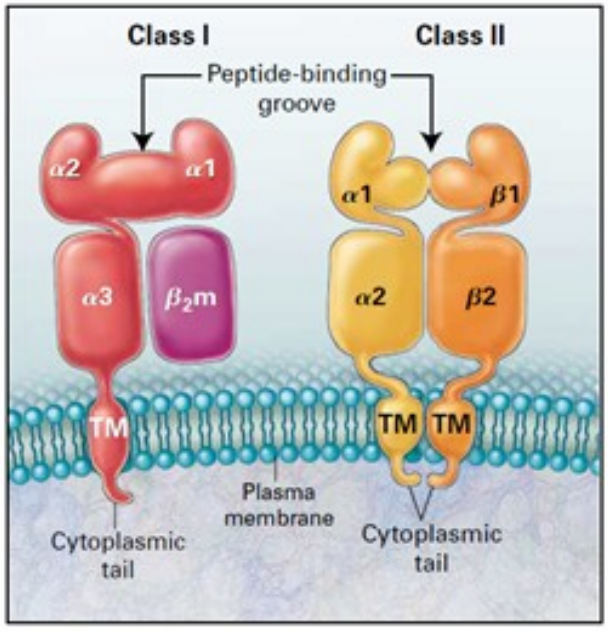

Figure 1-1. Complexe majeur d'histocompatibilité de classes I et II. Représentation des molécules du CMH de classe I et II montrant leur structure en dimère et les cavités correspondant à leur niche peptidique respective. Reproduced with permission from [Klein J, Sato A. *The HLA system. First of two parts*. The New England journal of medicine. 2000;343(10):702-9], Copyright Massachusetts Medical Society. Reproduit avec permission de (1).

Il existe plusieurs loci codant pour le CMH I tant chez l'humain (HLA-A, -B et -C) que chez la souris (H2-D, -K et –L), donnant lieu à divers isotypes hautement polymorphiques (2, 8). L'IFN-β et l'IFN-γ régulent l'expression de NLRC5, aussi appelé transactivateur du CMH de classe I, qui à son tour induit l'expression du CMH I (9, 10). L'expression du CMH I est aussi inductible via l'IFN-α et le TNF-α, et est détectée à des niveaux variables chez tous les types cellulaires nucléés (9, 11).

1.1.2. CMH de classe II

Le CMH de classe II (CMH II) est également composé de deux glycoprotéines (Figure 1-1, p.2) (12). La chaîne alpha (34kDa) ainsi que la chaîne bêta (28kDa) ont chacun deux domaines extracellulaires (α1 et α2; β1 et β2), une région transmembranaire et une courte

queue cytoplasmique (1, 3). Les domaines α1 et β1, au sommet de l'hétérodimère αβ, forment la niche peptidique du CMH II (13). Celle-ci est bordée par deux hélices α antiparallèles, dont l'une appartient à chacune des chaînes (7). Des huit feuillets du plancher de la niche, quatre appartiennent à chacune des chaînes (7). Contrairement au CMH I, la niche du CMH II est ouverte à ses extrémités; ceci permet d'accommoder de plus longs peptides (13-25aa) pouvant dépasser de la niche (1, 7, 14). L'interaction du CMH II avec le peptide est stabilisée par des interactions hydrophobes au niveau des poches de la niche et par des ponts hydrogènes entre les chaînes latérales des acides aminés, comme dans le cas du CMH I (14).

Différents isotypes dits classiques du CMH II sont répertoriés, en l'occurrence HLA-DP, -DQ et -DR chez l'homme et I-A et -E chez la souris. Les dimères humains HLA-DM et -DO, de même que les H2-M et H2-O murins, sont plutôt dits non-classiques. Cette catégorisation des isotypes de CMH II est relative à leur fonction de présentation (classique) ou d'édition du répertoire (non-classique) (2, 15-17).

À la différence du CMH I, l'expression physiologique du CMH II est restreinte aux cellules présentatrices d'antigènes (APCs), dont les cellules B, monocytes, macrophages, cellules dendritiques, ainsi qu'aux cellules épithéliales activées et thymiques (1, 18). L'IFN-γ régule la transcription du gène *MHC class II transactivator* (CIITA), induisant l'expression du CMH II (Figure 1-2, p.4) (19). L'expression peut aussi être induite par le TNF-α (11).

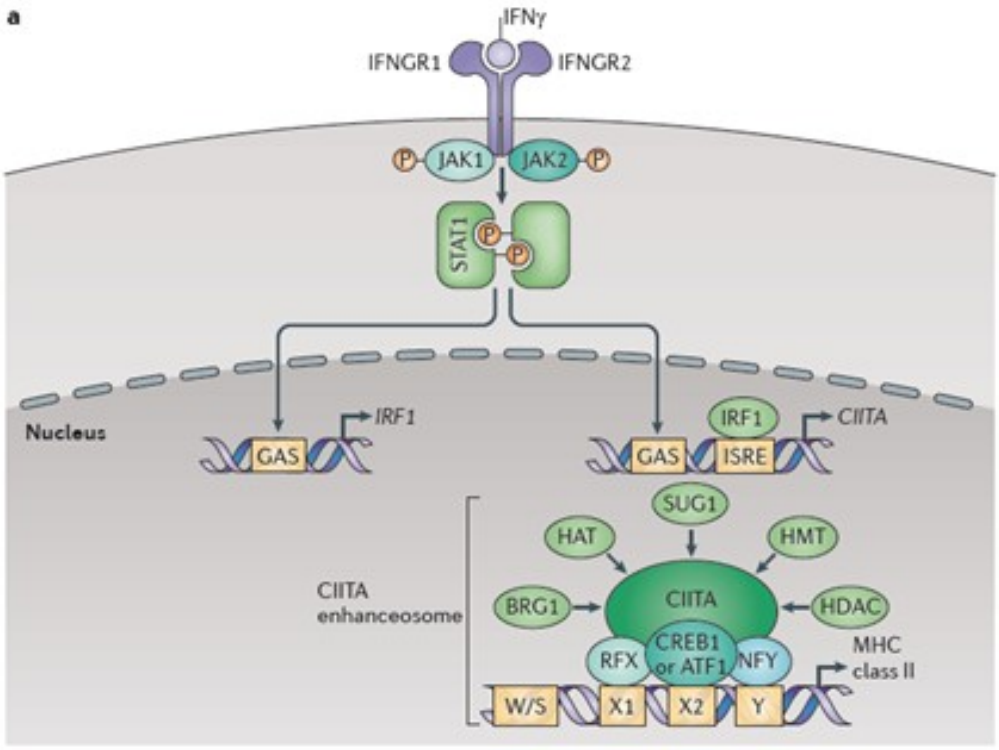

Figure 1-2. Voie de signalisation menant à la transcription du CMH II. La stimulation des APCs et des cellules épithéliales par l'IFN-γ induit une cascade de signalisation qui mène à la transcription de CIITA, qui induit l'expression des molécules du CMH de classe II à l'aide de facteurs de liaison à l'ADN. Reproduit avec permission de (10).

1.2. Présentation antigénique

Les cellules exprimant le CMH I/II à leur surface en sont recouvertes; chaque isotype est présent entre 100 000 et 300 000 fois, et chacun porte un peptide (1). La fonction du complexe majeur d'histocompatibilité est, d'abord et avant tout, de présenter des peptides antigéniques aux lymphocytes T (2, 8). Effectivement, le CMH d'un individu permet d'afficher aux lymphocytes T des éléments extrinsèques possiblement d'origine pathogène, ou encore des éléments intrinsèques altérés, de sorte que ces lymphocytes T puissent déclencher une réponse immunitaire (Figure 1-3, p.5). Ainsi, le CMH peut être vu comme un élément de restriction pour la reconnaissance antigénique, d'où le concept de « restriction par le CMH », introduit par Zinkernagel et Doherty (2, 20-22).

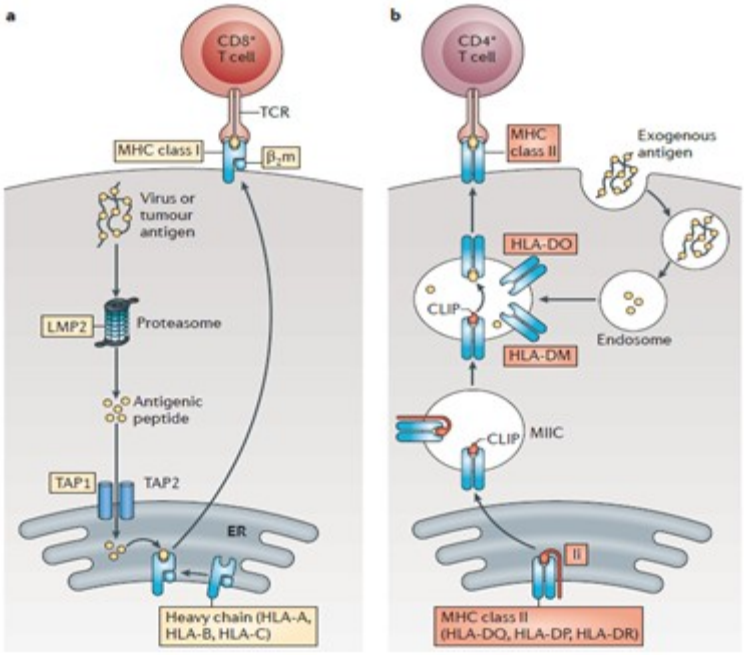

Figure 1-3. Présentation antigénique par le CMH I et le CMH II. Représentation des principales étapes menant à la présentation antigénique (A) par le CMH I et (B) par le CMH II, de la protéolyse des antigènes à la présentation du peptide aux lymphocytes T. Reproduit avec permission de (10).

1.2.1. Présentation par le CMH de classe I

Des approches expérimentales diversifiées, dont beaucoup faisant appel à la virologie, ont permis d'élucider les mécanismes menant à la présentation antigénique par le CMH de classe I (6, 23, 24). Après sa biosynthèse dans le réticulum endoplasmique (ER), la chaîne lourde (α) s'associe à sa chaperonne, la calnexine, puis entame son repliement et la formation des ponts disulfure internes, lui conférant sa conformation (6, 25). Sa dissociation de la calnexine permet à la chaîne lourde de lier la β_2-microglobuline, de manière à charger des peptides (6). Pour ce faire, le CMH I doit se trouver au centre du complexe de liaison du peptide (*peptide-loading complex*), composé des transporteurs protéiques TAP1 et TAP2, des chaperonnes calréticuline et tapasine, et de l'enzyme ERp57 (6, 26). Généralement, le CMH I présente des peptides endogènes, c'est-à-dire qu'ils proviennent d'éléments présents à l'intérieur de la cellule qui sont détruits par le protéasome (Figure 1-3, p.5) (1, 7). Incidemment, les transporteurs TAP sont impliqués dans l'importation de ces fragments protéiques depuis le cytosol vers le ER (1, 6, 7). Ils peuvent ensuite être apprêtés une nouvelle

fois par une aminopeptidase résidente du ER (*ER-associated aminopeptidase*, ERAAP) (27-29). L'association entre un dimère de CMH I et un peptide de haute affinité permet la dissociation du complexe, la sortie du ER, le passage à travers l'appareil de Golgi et vers la membrane plasmique (6). Ainsi, une fois qu'il atteint la surface cellulaire, le CMH I affiche le plus souvent des peptides dérivés de protéines intracellulaires, telles des protéines virales (1, 7, 30), qu'il présente aux lymphocytes T CD8+ (2). Comme le CMH I est présent à la surface de toute cellule nucléée, ceci permet aux lymphocytes T CD8+ de cibler et d'attaquer directement toute cellule infectée par un pathogène intracellulaire (1).

1.2.2. Présentation par le CMH de classe II

Le CMH II présente plutôt des peptides d'origine exogène aux lymphocytes T CD4+ (1, 2, 7). Les peptides proviennent de la dégradation d'éléments endocytés par les cellules présentatrices d'antigènes, donc généralement des pathogènes extracellulaires (1, 8, 30). Après la biosynthèse et la dimérisation des chaînes α et β dans le ER, le dimère αβ du CMH II transite par l'appareil de Golgi pour se rendre jusqu'au compartiment riche en CMH II (*MHC class II containing compartment*, MIIC,), où il rencontrera son peptide (1, 8). Ce compartiment marque l'intersection entre la voie d'importation des antigènes endocytés et la voie d'exportation du CMH II vers la surface cellulaire, et contient tous les éléments nécessaires à la dégradation des antigènes en peptides pour être chargés sur le CMH II (Figure 1-3, p.5) (30-32).

Cette transition du CMH II du ER au MIIC est largement aidée par son association à une protéine non-polymorphique : la chaîne invariante (Ii, CD74) (8, 33). Le CMH II rencontre et charge un peptide de haute affinité, puis se rend en surface pour que le complexe soit reconnu par un lymphocyte T CD4+ qui lui est spécifique (1). L'interaction entre l'APC portant le peptide et un lymphocyte T induit chez cette dernière la production de cytokines comme l'IL-2, l'IL-4, l'IL-5 ou l'IFN-γ, dont l'action vise à amplifier la réponse immunitaire en stimulant la prolifération de lymphocytes T et B, mais également l'activation de macrophages, et la différenciation de cellules B (7).

1.2.3. Présentation croisée

Les premières évidences de la présentation de peptides exogènes par le CMH I proviennent du groupe de Bevan et al. (34). En effet, le CMH I des APCs peut constitutivement porter dans sa niche des peptides exogènes, traditionnellement retrouvés sur le CMH II (35, 36). Plusieurs groupes ont exploré les possibilités mécanistiques de la présentation croisée durant les années 1990 (35, 37-46). Quelques mécanismes sont aujourd'hui suggérés et plus ou moins acceptés : les peptides exogènes peuvent provenir de leur injection directe dans le cytosol par un agent infectieux, par exemple un virus ou une bactérie; de leur transfert direct entre cellules alors que le CMH I est exprimé en surface (*cross-dressing*); de leur échappement à partir des phagosomes vers le cytosol pour dégradation par le protéasome; de leur chargement sur le CMH I dans la voie endosomale; de l'autophagie (Figure 1-4, p.8) (36, 47, 48). La présentation croisée par le CMH I est particulièrement impliquée dans l'activation de cellules T CD8+ par les APCs en présence d'agents infectieux, de cellules tumorales ou de greffon (49-52).

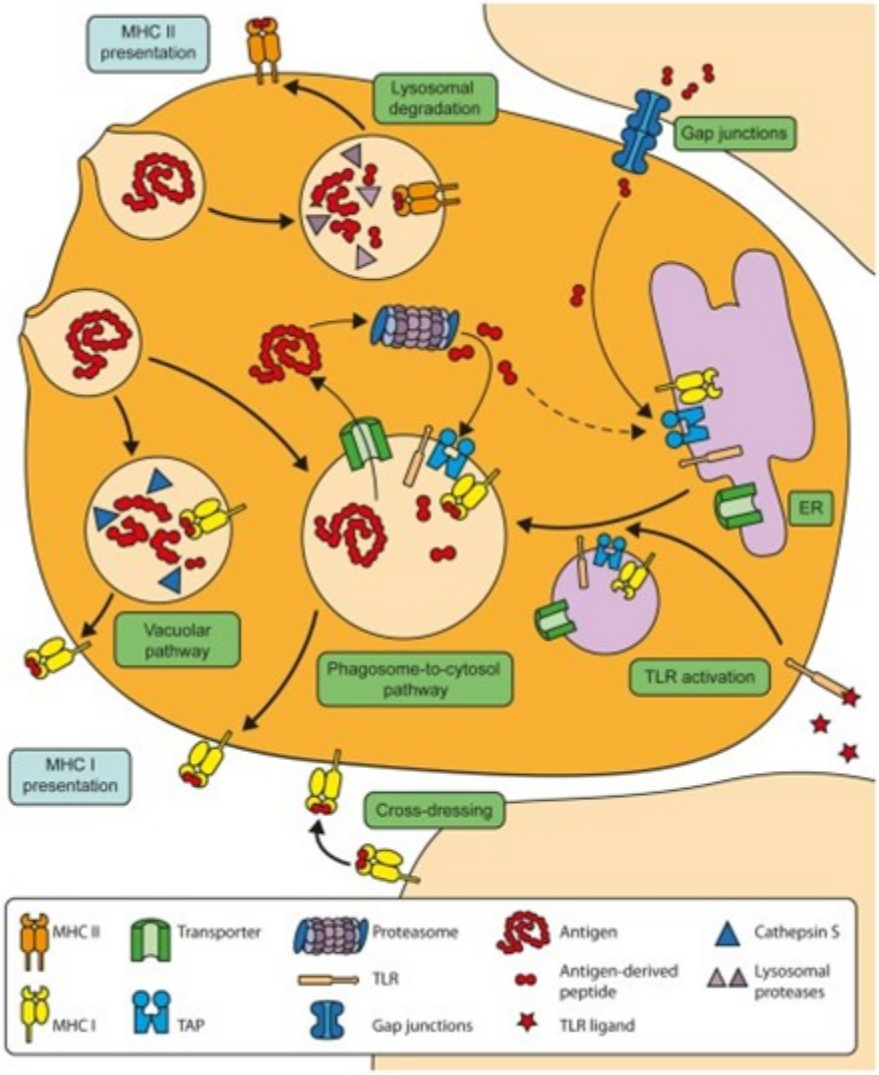

Figure 1-4. Origines postulées pour la présentation croisée. Représentation des mécanismes actuellement suggérés pour être à l'origine de la présentation par le CMH I de peptides traditionnellement portés sur le CMH II. Reproduit avec permission de (36).

1.2.4. Superantigènes

À la différence des antigènes classiques qui lient le CMH par sa niche et interagissent avec plusieurs régions du récepteur des cellules T (TCR), les superantigènes (SAGs) sont des antigènes ayant la particularité de stimuler les lymphocytes T par la région variable de la chaîne β du TCR (53-57). Alors qu'un seul antigène ne stimule normalement que 0,0001% du répertoire de cellules T, un seul superantigène peut en stimuler jusqu'à 20%, justifiant son appellation (55, 58, 59). Parmi cette famille, on retrouve des superantigènes « du soi » et

« étrangers » (57). Les SAGs dits « du soi » sont d'origine virale, dont ceux encodés par le MMTV (*mouse mammary tumor virus*) chez la souris (60-64). Les SAGs « étrangers » sont plutôt d'origine bactérienne, telles des toxines produites par les staphylocoques, notamment les SEs (*staphylococcal enterotoxins*) SEA, B, C1-3, D et E, ou par des streptocoques, comme la TSST (*toxic shock syndrome toxin*) (57, 65-69).

En plus de stimuler un éventail de cellules T, plusieurs études ont porté sur le site d'interaction entre les SAGs et le CMH : comme il se situe à l'extérieur de la niche, un SAG peut lier une plus grande variété de dimères de CMH, et la contrainte d'affinité du CMH pour son peptide se trouve contournée (55, 70-82). Par ailleurs, l'affinité pour le CMH des SAGs varie selon les isotypes et allèles (77, 83). Si le mode et le site d'interaction entre les SAGs bactériens et le CMH sont assez bien caractérisés, la réalité est différente pour les superantigènes viraux (84, 85). Cette problématique a été explorée récemment par notre groupe : il s'avère que le SAG MMTV7 s'attache à l'extérieur de la niche comme les SAGs bactériens, en plus d'avoir la particularité de lier à la fois la chaîne α d'un dimère de CMH II et la chaîne β d'un second, reliant les dimères ensemble (*cross-link*) (Annexe 1) (86). La présentation des SAGs induit la prolifération des lymphocytes et la production de cytokines : incidemment, une partie des lymphocytes meurt, alors que l'autre entre en état d'anergie (55).

1.3. Chaîne invariante

Détectée pour la première fois en 1979 par le groupe de Jones et al. (87), la chaîne invariante est une glycoprotéine non-polymorphique de type II qui, lorsqu'associée au CMH II sous forme αβIi, contribue considérablement au trafic et à la protection du CMH II chez les APCs (1, 7, 8, 88). Elle est encodée sur le chromosome 5 de l'homme, et sur le chromosome 18 de la souris (4, 89). Son expression est régulée par l'IFN-γ et par le TNF-α, comme celle du CMH II (11, 19, 90).

1.3.1. Isoformes de la chaîne invariante

Plusieurs isoformes sont connues pour la chaîne invariante. Chez la souris, on trouve p31 et p41; ces deux formes, nommées d'après leur poids moléculaire respectif sur SDS-PAGE, diffèrent par la présence d'un exon supplémentaire (6b) dans la région luminale de p41 (91). L'homme possède deux isoformes de plus, soit p35 et p43, qui portent une extension de 16 acides aminés dans leur portion cytosolique, les différenciant de p33 (homologue de p31 murin) et p41, respectivement (Figure 1-5, p.10) (88, 91, 92). Parmi les quatre isoformes humaines, p33 et p35 sont exprimées de manière prédominante, c'est-à-dire jusqu'à dix fois plus que p41/p43 (92, 93). Iip35 représente environ 20% du pool d'Ii (94). L'exon 6b (64 acides aminés) présent chez les isoformes p41 et p43 code pour un domaine riche en cystéines présentant une forte homologie avec la thyroglobuline (*thyroglobulin-like domain*) (91, 93, 95). Tous ces variants d'Ii sont encodés par le même gène; ils sont le produit d'épissage alternatif de l'ARN, suivi de l'initiation de la traduction à l'un ou l'autre des codons initiateurs sur le brin d'ARNm (7, 88, 91, 95).

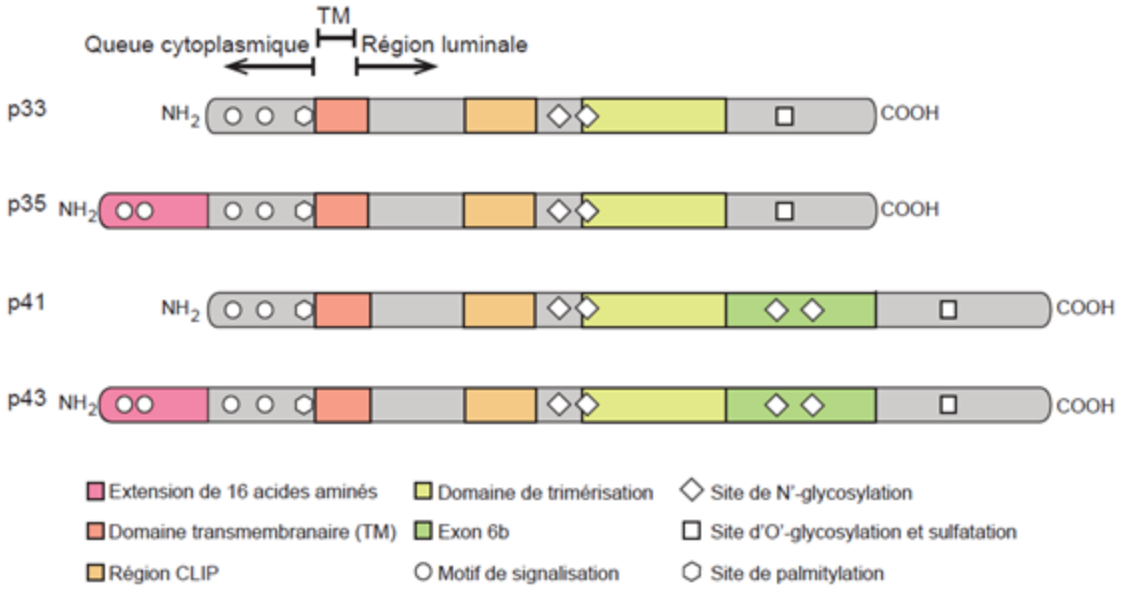

Figure 1-5. Isoformes de la chaîne invariante. Représentation schématisée des domaines d'intérêt, motifs de signalisation et sites de modification post-traductionnelle des quatre isoformes de la chaîne invariante humaine.

1.3.2. Motifs de localisation

La queue cytoplasmique de la chaîne invariante présente différents motifs régulant ses déplacements entre les différentes organelles (Figure 1-6, p.11). En tronquant complètement la région cytoplasmique d'Ii, elle se dirige à la surface cellulaire au lieu des divers compartiments normalement visés, induisant un défaut dans la présentation antigénique (25). En plus du poids moléculaire, ces motifs sont un outil discriminant pour les différentes isoformes d'Ii (92, 96).

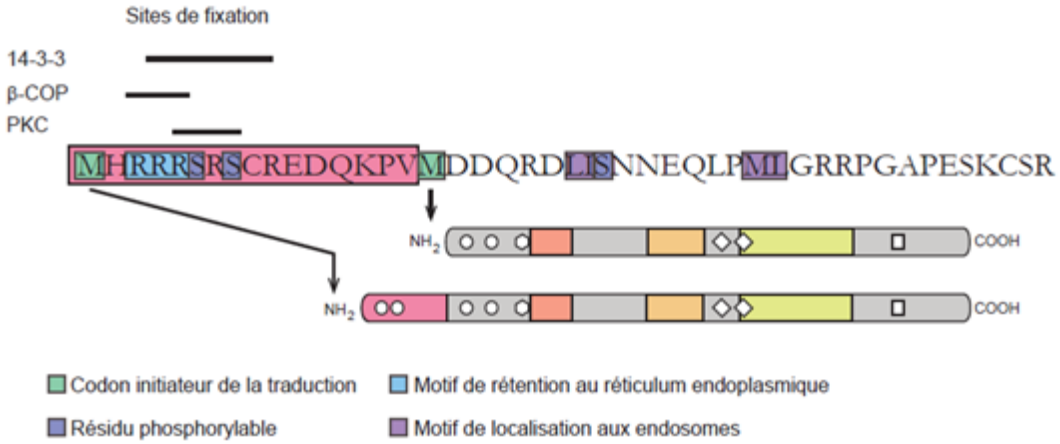

Figure 1-6. Queue cytoplasmique de l'isoforme p35 d'Ii. Représentation des résidus, motifs et sites déterminants de la queue cytoplasmique d'Iip35 dans sa caractérisation fonctionnelle par rapport à Iip33

1.3.2.1. Motif di-arginine

En l'absence de CMH II, les isoformes p35 et p43 de la chaîne invariante demeurent dans le réticulum endoplasmique (88, 93). Des études menées chez Peter Cresswell ont montré que les isoformes p33/p41, exprimées seules, parviennent à quitter le ER pour rejoindre un compartiment endosomal qui colocalise avec des peptides du virus de l'influenza (92, 93). La coexpression de p35/p43 abroge ce phénotype et la chaîne invariante demeure emprisonnée dans le réticulum endoplasmique (92, 93). Ainsi, l'extension de 16 acides aminés de p35 et

p43 comporte un signal fort de rétention au réticulum endoplasmique, absent chez p33 et p41 (Figure 1-6, p.11) (92).

Il s'agit d'un motif de rétention au réticulum endoplasmique (ERM) di-basique de type RXR (97). Si la chaîne invariante a été la première protéine chez laquelle ce motif a été identifié, il est maintenant répertorié dans d'autres complexes, comme les sous-unités Kir6.1/2 et SUR1/2 des canaux de potassium dépendants de l'ATP (K_{ATP}), le récepteur de neurotransmetteur $GABA_B$ et le récepteur du glutamate NMDA (97).

1.3.2.2. Motif di-leucine

Le motif di-leucine est présent au niveau de la queue cytoplasmique de toutes les isoformes de la chaîne invariante (96, 98). Il s'agit en fait de deux motifs distincts – le premier Leu7 Ile8 et le second Pro15 Met16 Leu17 – permettant la localisation aux endosomes (Figure 1-5, p.10) (99, 100). Lorsque les deux motifs sont intacts chez un homotrimère p33/p41, il semblerait que celui-ci contourne l'appareil de Golgi pour se rendre aux endosomes précoces; lorsque seul le deuxième motif est intact, des preuves du passage par le Golgi sont détectables via la glycosylation d'Ii (section 1.3.3.2) (33, 96). En abrogeant les deux motifs, la chaîne invariante est dirigée vers la surface cellulaire (96, 101). La substitution des résidus leucine pour des alanines permet l'inactivation du motif (102). Une étude complémentaire d'Arneson et al. démontre que les motifs de deux chaînes sur trois dans le trimère d'Ii doivent être intacts pour diriger correctement le complexe (103).

De plus, la localisation aux endosomes en vertu du motif di-leucine est indépendante de l'interaction avec le CMH de classe II, tel que la chaîne invariante est détectable dans le ER, le Golgi et les endosomes dans des cellules n'exprimant pas le CMH II (101).

Considérant l'existence possible d'une voie alternative directe entre le ER et les endo-lysosomes, le groupe de Lotteau et al. souligne la pertinence de mieux caractériser les chemins empruntés par les différentes formes d'Ii en sortant du ER (96, 104, 105).

1.3.3. Modifications post-traductionnelles

Un autre outil discriminant dans l'étude des isoformes d'Ii est la gamme de modifications post-traductionnelles dont la chaîne invariante fait l'objet (Figure 1-5, p.10). Ces modifications sont essentielles au repliement, à l'appariement et au trafic approprié des complexes αβIi chez les APCs (106, 107). Elles sont également utiles dans le but de traquer la maturation d'Ii dans des études fondamentales sur la présentation antigénique (93, 106).

1.3.3.1. Phosphorylation

Des résidus phosphorylables ont été identifiés pour la première fois chez la chaîne invariante en 1989 (108). En plus de leur motif de rétention au ER, les isoformes p35 et p43 présentent également un motif phospho-sérine dans leur extension, les distinguant encore de p33 et p41 : Anderson et al. ont identifié les Ser6 et Ser8 de l'extension comme étant les résidus déterminants (Figure 1-6, p.11) (107). Ces deux sérines jouent sur le passage du complexe αβIi à travers le Golgi; par l'utilisation de staurosporine, un inhibiteur de sérine/thréonine kinase, il a été exposé que les complexes n'atteignaient pas les endosomes (107). Il s'avère que la phosphorylation par PKC (protéine kinase C, une sérine/théronine kinase) des résidus sérine, surtout celle de la Ser8, est nécessaire pour la sortie du ER des complexes contenant p35 (94, 109). Cette idée est renforcée par la sialylation faible ou nulle chez des variants portant des mutations ponctuelles aux résidus sérine (94, 109). Le rôle des résidus phosphorylables sera plus longuement discuté à la section 1.5.2.2.1.

L'isoforme p33 peut également être phosphorylée au niveau de sa Ser9, mais seulement chez la forme sialylée, impliquant que la phosphorylation de p33 survient dans le *trans* Golgi ou ultérieurement (107). Ainsi, la Ser9 phosphorylée ne constitue pas un motif de localisation au même titre que les sérines de l'extension de p35/p43 (107).

1.3.3.2. Glycosylation

Ii, comme le CMH II, acquiert des sucres à la suite de sa biosynthèse dans le ER. Des phénomènes de N- et de O-glycosylation ont été répertoriés tant chez la protéine murine qu'humaine (12, 88, 110). Ces sucres subissent une maturation au cours de la progression à travers le Golgi. L'endo-β-N-acétylglucosaminidase H, ou Endo H, est une enzyme clivant les sucres N-glycosylés; la maturation à travers le Golgi permet d'atteindre un état de résistance à l'Endo H (93, 111). Les isoformes p33 et p41, exprimées seules, deviennent résistantes à l'Endo H, alors qu'elles demeurent sensibles lorsque coexprimées avec p35/p43 (93). Les isoformes p33/p35 comportent deux sites de N'-glycosylation (Asn113 et Asn119 de p33); la région supplémentaire de p41/p43 comporte deux sites additionnels, pour un total de quatre chez ces deux isoformes (Figure 1-5, p.10) (7, 112).

1.3.3.3. Acylation

Il a également été montré chez la souris que la chaîne invariante est acylée avant sa progression vers le Golgi, tel que l'administration de cérulénine, un inhibiteur de l'incorporation d'acide gras, prévient la maturation des sucres (106). L'incorporation d'acide palmitique au niveau de la Cys28 préviendrait la formation de ponts disulfure dans la région transmembranaire d'Ii, et participerait ainsi à l'atteinte d'une conformation optimale (Figure 1-5, p.10) (106, 113). La sialylation de la chaîne invariante humaine est également détectée chez p33/p41 après passage par le compartiment *trans* Golgi (93, 106).

1.3.3.4. Sulfatation

Par l'emploi de cellules primaires d'amygdales humaines et de sulfate radioactif, le groupe de Sant et al. a pu démontrer que la chaîne invariante, de même que le CMH II, a la capacité d'incorporer des groupements sulfates (114). Corroborant ces observations, Miller et al. ont pu identifier la Ser201 d'Ii murin (Ser202 chez l'humain) comme étant le site d'incorporation de glycosaminoglycane (GAG) de type chondroïtine sulfate, autant chez

l'homme que la souris (110). Le GAG s'attache à un sucre O-glycosylé sur ce résidu sérine (Figure 1-5, p.10) (110).

1.4. Complexe αβIi

Après leur biosynthèse dans le réticulum endoplasmique, moins de 10 minutes sont requises pour que trois chaînes invariantes s'associent en un trimère grâce à la région entre les acides aminés 163-183 de leur portion luminale (Figure 1-5, p.10) (88, 115). La région transmembranaire est également impliquée dans l'association des trois chaînes (116). Il peut s'agir d'homotrimères (trois chaînes de même isoforme) comme d'hétérotrimères (chaînes d'isoformes diverses) (92, 93). Bertolino et al. ont démontré en 1995 que la trimérisation est essentielle à la fonction d'Ii, tel que la présentation antigénique se trouve altérée lorsque le site de trimérisation est tronqué (117). Les trimères contenant l'isoforme p35 demeurent dans le ER et retiennent p33 jusqu'à l'association au CMH II (92, 111). Le même principe s'applique aux complexes contenant les isoformes p41 et p43 (93). Le groupe de Lamb et al. propose qu'un trimère d'Ii dépourvu de CMH II, qu'il contienne ou non une chaîne p35, n'aurait pas une conformation optimale pour sortir du ER; ceci expliquerait le fait que la sortie d'un homotrimère de p33 soit ralentie par rapport à celle du même trimère portant du CMH II, et ce, malgré l'absence de motif de rétention (92).

Par ailleurs, la région supplémentaire contenant cinq cystéines des isoformes p41/p43 semble affecter le transport de la chaîne invariante. L'utilisation d'agents réducteurs comme le DTT (dithiothréitol) nuit à la formation de ponts disulfure et a pour effet de prévenir la sortie du réticulum endoplasmique de p41, tel que détecté par leur sensibilité à l'Endo H (93). L'isoforme p33, qui ne contient pas de cystéine dans sa portion luminale, ne se trouve pas affectée par la présence de DTT et traverse le Golgi, comme en témoigne sa résistance à l'Endo H (93). Ceci semblerait indiquer un rôle de l'exon 6b dans l'adoption d'une conformation promouvant la sortie du ER des complexes contenant p41/p43 (93).

Plusieurs groupes soulèvent également la question du masquage du motif de rétention au ER médié par l'association avec le CMH II, soit par encombrement stérique ou par induction d'un changement conformationnel (12, 92, 93, 96, 111). Cette question a été partiellement abordée dans notre laboratoire par Khalil et al. (118). À l'aide d'un système utilisant des chaînes α ou β tronquées au niveau de leur portion cytosolique, notre groupe a pu démontrer que la queue cytoplasmique de la chaîne β du CMH II est responsable du masquage (118). De surcroît, une queue longue de seulement trois acides aminés suffit à réaliser ce masquage du ERM de p35 (118). Néanmoins, le mécanisme permettant à la chaîne β d'effectuer le masquage demeure inconnu.

1.4.1. Stœchiométrie du complexe αβIi

Après la biosynthèse des chaînes α et β au niveau du réticulum endoplasmique, elles s'associent à un trimère préformé d'Ii pour former des structures de haute complexité (92). Quelques évidences montrent que la chaîne α serait la première à s'apparier à la chaîne invariante (119). L'association avec la calnexine, une protéine résidente du ER également impliquée dans l'appariement du CMH I, pourrait stabiliser le complexe αβIi durant sa formation (25, 120, 121). Selon le nombre de dimères de CMH II liés séquentiellement, on parle de structures en pentamère $\alpha\beta Ii_3$, en heptamère $(\alpha\beta)_2Ii_3$, ou en nonamère $(\alpha\beta)_3Ii_3$ (complexe saturé) (92, 122). L'association, stabilisée par des ponts hydrogène, s'effectue entre la niche peptidique du CMH II et la région CLIP (*class II-associated invariant chain derived peptide*, acides aminés Leu81-Met104) de la chaîne invariante (115, 123, 124). La cristallisation du complexe HLA-DR3-CLIP par le groupe de Ghosh et al. a permis de remarquer la ressemblance frappante dans l'interaction de la niche avec CLIP versus son interaction avec un peptide antigénique dérivé de l'hémagglutinine (HA) du virus de l'influenza (124).

La stabilité de l'association du CMH II avec Ii peut varier selon les allèles et isotypes, compte tenu des variations dans la séquence (125). Par contre, plusieurs autres régions d'Ii, en C' (acides aminés 81-89) et en N' (acides aminés 101-110) du CLIP, sont suggérées pour stabiliser cette association, en plus de sites sur le CMH de classe II qui contribueraient à

l'interaction (126-131). En l'occurrence, dans un système où un peptide est lié de façon covalente au CMH II, Wilson et al. ont rapporté une interaction résiduelle avec la chaîne invariante, malgré l'occupation de la niche (132).

Il a été proposé en 1982 par de Kretser et al. que des isotypes différents de CMH II puissent se trouver montés sur le même trimère d'Ii (133). Effectivement, ce groupe a observé dans des lignées de cellules B transformées par le virus Epstein-Barr (EBV) que des dimères de HLA-DQ pouvaient être co-immunoprécipités avec HLA-DR (133). Cette observation corrobore les résultats de migration sur gel du groupe de Peter Cresswell, rapportant l'existence de structures correspondant en poids moléculaire à une structure nonamérique (122). Par contre, un groupe allemand a récemment mis de l'avant des résultats défiant ces conventions, démontrant que des dimères de HLA-DP, -DQ et -DR ne pouvaient être isolés sur un même trimère de chaînes invariantes (134). Pour justifier l'inexistence d'heptamères et de nonamères, ce groupe suggère qu'il y a induction d'un changement conformationnel de la région CLIP à cause de l'association avec le CMH II (134). Devant cette contradiction, notre groupe a dernièrement démontré à l'aide d'un système de transfection en lignée HEK293T que plusieurs formes distinctes de HLA-DR peuvent se trouver montées sur un même trimère d'Ii; nos résultats vont donc à l'encontre de cette théorie suggérée par le groupe de Norbert Koch, mais corroborent les résultats originaux obtenus par les groupes de de Kretser et de Roche (Annexe 2) (122, 133-135).

1.4.2. Transport et maturation des complexes αβIi

À la suite de son assemblage, le complexe αβIi néoformé doit entamer sa progression à travers les différentes organelles pour maturer et, ultimement, remplir sa fonction dans la présentation antigénique (Figure 1-7, p.18).

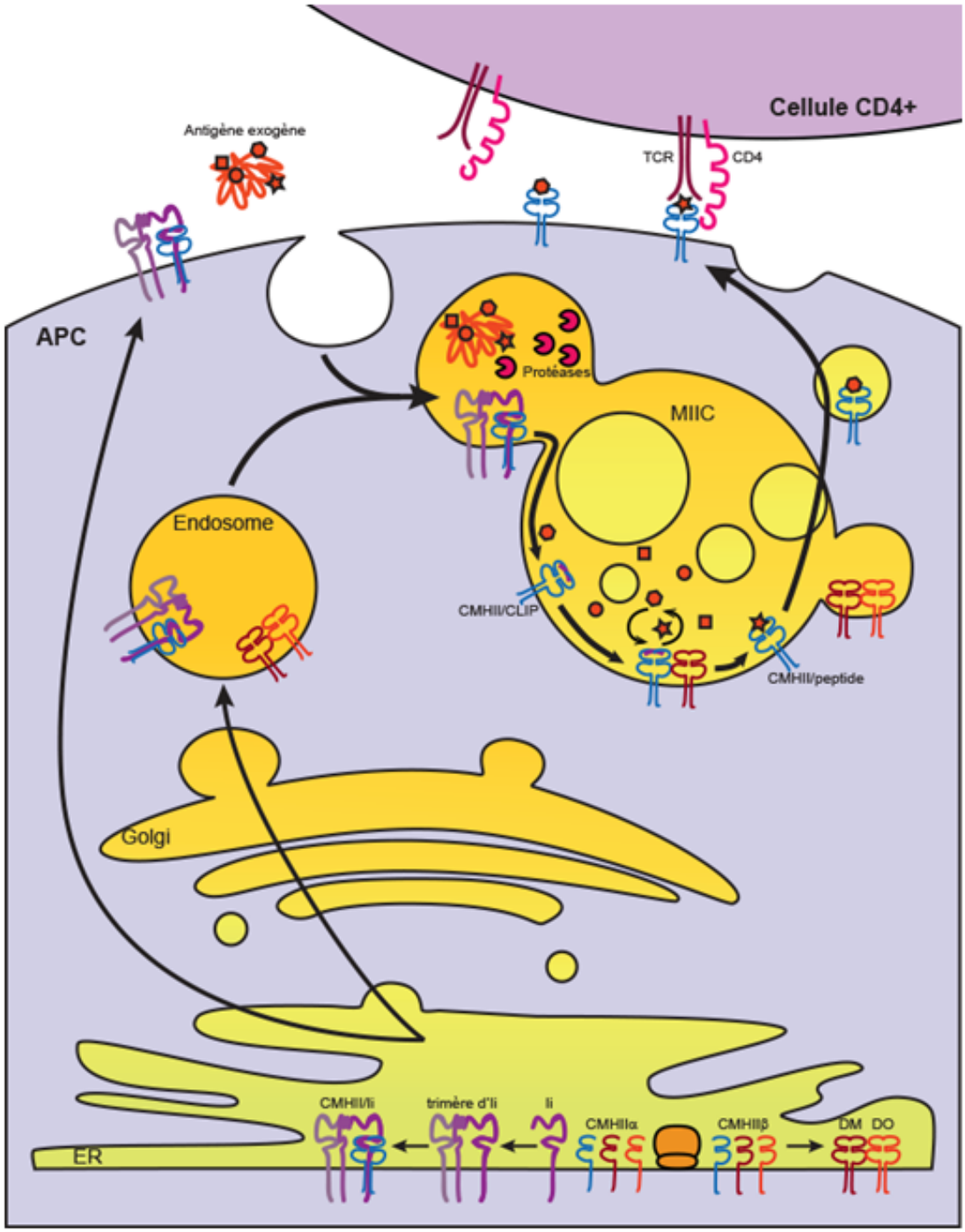

Figure 1-7. Trafic intracellulaire du CMH II et d'Ii menant à la présentation antigénique. Représentation des étapes franchies par le complexe αβIi pentamérique, HLA-DM et HLA-DO depuis leur biosynthèse et leur oligomérisation jusqu'à la présentation du peptide par le CMH II au lymphocyte T CD4+.

1.4.2.1. Sortie du ER par le complexe αβIi

La sortie du réticulum endoplasmique des complexes αβIi dépend largement des motifs de localisation des isoformes dont est composé ce complexe. Effectivement, les complexes contenant uniquement de p33/p41 sortent plus rapidement du ER en raison de l'absence d'ERM; inversement, ceux contenant p35/p43 requièrent le masquage du motif pour progresser dans la cellule (92, 93). Tel que mentionné plus haut, la chaîne β du CMH II permet le masquage de ce motif (118). Un complexe αβIi dont tous les ERM sont masqués correctement et ne permettant pas l'association aux composantes du système COP I progresse à travers le Golgi, tel que démontré par la maturation des sucres. Alternativement, le complexe peut passer du ER vers la surface cellulaire, puis être rapidement endocyté (33, 136). Les phénomènes de rétention et de sortie seront expliqués de façon exhaustive à la section 1.5. Dans tous les cas, qu'il vienne du Golgi ou de la surface, le complexe αβIi passe ensuite aux endosomes (Figure 1-7, p.18) (33).

1.4.2.2. Dégradation du complexe αβIi

D'abord dirigés vers les endosomes précoces, les complexes αβIi s'accumulent, puis Ii altère la physiologie du compartiment : l'endosome riche en Ii augmente en taille et s'acidifie (33, 93). Ce compartiment, le MIIC, a été scrupuleusement caractérisé chez les lymphocytes B, les cellules dendritiques et les macrophages durant les années 1990 par plusieurs groupes néerlandais (31, 32, 137-140). Il a été démontré que le MIIC marque l'intersection entre la voie de biosynthèse des protéines et la voie endocytaire (31). Par microscopie électronique, la morphologie et la nature du MIIC ont également été étudiées, permettant de comprendre qu'il s'agit d'un compartiment présentant un grand réseau membranaire, dérivé d'un endosome précoce, et se rapprochant du lysosome (32). Le MIIC est aussi connu sous les noms de MLB (*multilamellar body*) ou MVB (*multivesicular body*), en référence à sa morphologie et selon son stade de maturation (139). Son diamètre est situé entre 200 et 300nm, et il est présent en environ sept exemplaires par cellule (32). Peters et al. ont également confirmé que le CMH II parvient au MIIC par la voie de biosynthèse, plutôt que par l'endocytose de complexes exprimés en surface (32).

Le MIIC regroupe plusieurs conditions essentielles à la dégradation du complexe αβIi (32). Dans des expériences utilisant le virus de l'influenza, l'atteinte d'une conformation pH-dépendante par l'hémagglutinine virale a démontré qu'il s'agissait d'un compartiment de pH acide (111). Par contre, l'usage de chloroquine sur des cellules de lignée de lymphocytes B cancéreux (B-LCL) a montré que l'acidification du MIIC est nécessaire, mais non suffisante à la dissociation d'Ii du dimère de CMH II; le fait d'abaisser le pH en-deçà 5,0 *in vitro* ne permet pas cette dissociation (141). Les enzymes protéolytiques contenues dans le MIIC jouent un rôle prépondérant dans la dégradation séquentielle de la chaîne invariante (Figure 1-8, p.21) (30). D'abord, la cathepsine D permet la dégradation d'Ii en LIP (*leupeptin-induced protein*, p22) (33, 141, 142). À ce stade de protéolyse, LIP est encore sous forme de trimère (143). Puis, la digestion des complexes par la cathepsine B, et potentiellement d'autres protéases, permet la perte de la portion en C' du CLIP, comprenant le domaine de trimérisation, pour obtenir une forme d'Ii appelée p10 (7, 142). La cathepsine S clive en N' de CLIP, isolant cette fraction dans la niche peptidique (142). Le fragment représentant les acides aminés 1-42 de p33, de son côté, a le potentiel d'activer la voie de signalisation NFκB, notamment pour activer les cellules B (142, 144, 145).

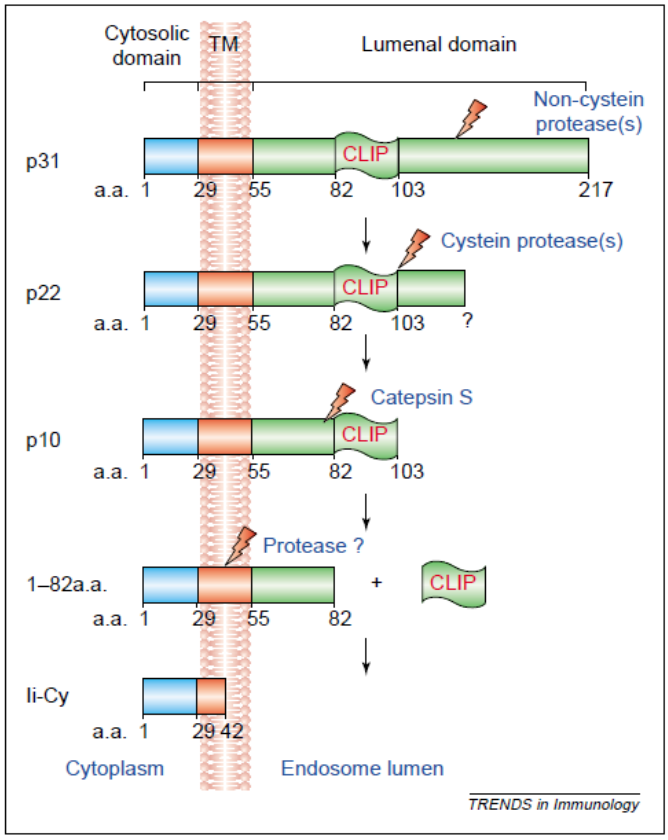

Figure 1-8. Séquence de protéolyse d'Ii. Représentation séquentielle des produits catalytiques issus de la dégradation d'Ii par des protéases dans le MIIC. Reproduit avec permission de (144).

1.4.2.3. Échange de peptide

C'est également au niveau du MIIC que les protéines non-classiques jouent leur rôle (146). Un dimère de HLA-DM, indépendamment de la chaîne invariante, s'associe à un dimère de HLA-DO dans le ER après sa biosynthèse (Figure 1-7, p.18) (16, 147). Par cette association, HLA-DO inhibe la fonction de DM (16). Grâce à un motif de signalisation présent sur la queue cytoplasmique de DMβ, ils transitent vers le MIIC où ils s'accumulent (147-149). Ultimement, la dissociation des deux dimères et le pH acide du MIIC permettent à HLA-DM de s'associer à un dimère de CMH II classique pour catalyser l'échange de CLIP contre un peptide de haute affinité (15, 16, 148, 150-152). En l'absence de DM, des complexes CMH II-CLIP s'accumulent, marquant l'importance de DM dans l'échange de peptide (146).

1.4.3. Fonctions d'Ii reliées au CMH de classe II classique

Dès sa découverte, plusieurs fonctions ont été postulées pour la chaîne invariante par rapport à la présentation antigénique (12). À la fin des années 1980, ces rôles ont commencé à se préciser (153). Par des études de morphologie dans des lignées cancéreuses de cellules B humaines, le groupe de Guagliardi et al. a pu corroborer quelques unes de ces hypothèses fondamentales, reprises jusqu'à aujourd'hui : les rôles de chaperon, de protecteur de la niche et de guide (30, 154).

1.4.3.1. Rôle de chaperon

Il est connu que le squelette formé par le trimère d'Ii dans le réticulum endoplasmique favorise le repliement approprié des chaînes α et β autour du CLIP (123, 155). Effectivement, des phénomènes de mésappariement, de mauvais repliement et d'immaturité (sensibilité à l'Endo H) des dimères de CMH II sont observables en l'absence d'Ii (155, 156). Cette assistance procurée par Ii est importante, considérant que des protéines mal repliées ou incorrectement appariées dans le ER tendent à être retenues et dégradées (88, 120, 155). Le groupe de Schaiff et al. a d'ailleurs montré l'association du CMH II, en absence de la chaîne invariante, avec des marqueurs de stress résidents du ER, comme GRP94 et ERp72 (156). Les dimères échappant néanmoins à la dégradation dans le ER peuvent atteindre la surface cellulaire et sont connus pour être limités dans leur fonction de présentation (4, 157, 158). L'excès d'Ii dans les cellules exprimant le CMH II permet d'éviter cette dégradation; des trimères disponibles demeurent dans le ER jusqu'à association avec les chaînes α et β du CMH II (88).

1.4.3.2. Rôle de protecteur de la niche peptidique

Les premières évidences expérimentales de la protection de la niche par la chaîne invariante proviennent de Roche et Cresswell en 1990; ils ont montré qu'Ii obstruait la niche, ou du moins empêchait l'association d'un peptide du virus de l'influenza avec la niche peptidique du CMH II (159). Ceci a été corroboré par le groupe de Teyton et al, qui indique

que la chaîne invariante prévient la liaison de peptides endogènes (160). En outre, dans le cas d'une structure de haute complexité comme un nonamère, il a été suggéré que ce soit la conformation générale du multimère qui empêche l'appariement d'un peptide dans la niche peptidique (122). Ultérieurement, la dissociation d'Ii permet au CMH II d'interagir avec le même peptide viral (8). Par l'élution et le séquençage de peptides contenus dans la niche peptidique de HLA-DR chez des cellules de lignée B-LCL, il a également été montré que le seul peptide élué est la séquence des acides aminés 81-105 de la chaîne invariante; Ii prévient donc la liaison de peptides par la niche (161). De surcroît, Bijlmakers et al. ont exposé que le CMH II ne fait pas la différence entre des peptides endogènes ou exogènes en l'absence d'Ii, suggérant que la chaîne invariante prévient la capture de peptides dans le réticulum endoplasmique (162). Effectivement, les travaux de Long et al. confirment que la présence d'Ii empêche la présentation aux lymphocytes T CD4+ d'un peptide cytosolique de l'influenza, mais permet celle d'un peptide exogène du même virus, attestant que la chaîne invariante empêche la liaison de peptides dans le ER, au profit des peptides du MIIC (163).

1.4.3.3. Rôle de guide

Bien que son association à la chaîne invariante ne soit pas nécessaire pour que le CMH II atteigne la surface, sa localisation cellulaire se trouve largement affectée lorsqu'il est complexé à un trimère d'Ii (96, 111). Grâce aux multiples motifs de localisation contenus tout au long de la queue cytoplasmique d'Ii (Figure 1-6, p.11), le trimère peut agir comme guide pour le CMH II à travers les différents compartiments cellulaires et contribuer à le diriger jusqu'au MIIC pour rencontrer son peptide. Pour preuve, les travaux de Lotteau et al. montrent que le patron de glycosylation du CMH II est identique à celui du squelette d'Ii auquel il est associé, et que ce patron dépend directement des motifs de localisation présents au niveau de la queue cytoplasmique d'Ii (96). Par ailleurs, dans des cellules n'exprimant pas Ii, le patron de glycosylation des dimères de CMH II qui évitent la dégradation dans le ER est aberrant (155). D'autres travaux par Roche et al. exposent que des complexes pour lesquels la queue cytoplasmique d'Ii est tronquée s'accumulent en surface et, ultimement, peu de dimères de

CMH II parviennent à présenter des peptides antigéniques (25). Ainsi, c'est bien la chaîne invariante qui régule les déplacements des complexes αβIi d'un compartiment à l'autre (96).

1.5. Trafic intracellulaire

Le chemin classiquement emprunté par une protéine dans la cellule implique la sortie du ER, l'accès à l'appareil de Golgi, puis le tri dans le réseau *trans* Golgi (TGN) pour être envoyée vers le compartiment approprié (Figure 1-9, p.25) (164). Pour passer d'un compartiment à l'autre dans la cellule, une protéine ou un complexe protéique peut emprunter les vésicules formées par les protéines de manteau (*coat proteins*, COP) (164-166). Ces COP sont recrutées depuis le cytosol pour polymériser et former un bourgeon à la surface d'une organelle spécifique (164, 166, 167). Le bourgeon forme une vésicule en se détachant, puis transporte le cargo vers une autre organelle également spécifique, où il y a fusion des membranes et libération du cargo (164, 166, 168). Chaque système COP emprunte un trajet et sélectionne un cargo qui lui est particulier (164, 166, 168, 169). Chacun de ces types vésiculaires distincts est nommé d'après le système COP qui le constitue (166). À titre d'exemple, les vésicules de type COPII sont constituées de protéines du système COPII. L'assemblage des vésicules COP nécessite également l'action de GTPases de la famille ARF (*ADP-ribosylation factor*) (166).

Le principe de directionnalité du transport vésiculaire, mis de l'avant par Söllner et al., dépend de protéines appelées SNAREs (*Soluble* N-*ethylmaleimide-sensitive factor attachment-protein receptors*); la spécificité entre les SNAREs à la surface des vésicules (v-SNAREs) pour ceux du compartiment ciblé (t-SNAREs) permet l'attachement par la formation d'un complexe *trans*-SNARE et la fusion d'une vésicule avec son organelle cible formant un complexe *cis*-SNARE (170-172). Deux types vésiculaires différents interviennent entre le ER et le Golgi : COPI et II (173). Cette région de la cellule est hautement dynamique, plastique, tubulaire et connue sous plusieurs appellations; pour la suite, elle sera appelée ERGIC (ER-Golgi *intermediate compartment*) (164). Le transport entre le ER et le Golgi est facilité par un réseau de microtubules qui supporte le mouvement des différentes vésicules

entre les compartiments (174). D'autres types de vésicules de transport existent dans la cellule, notamment les vésicules recouvertes de clathrine, qui transitent plutôt entre le réseau *trans* Golgi, les endosomes et la surface cellulaire (Figure 1-9, p.25) (164, 175-177).

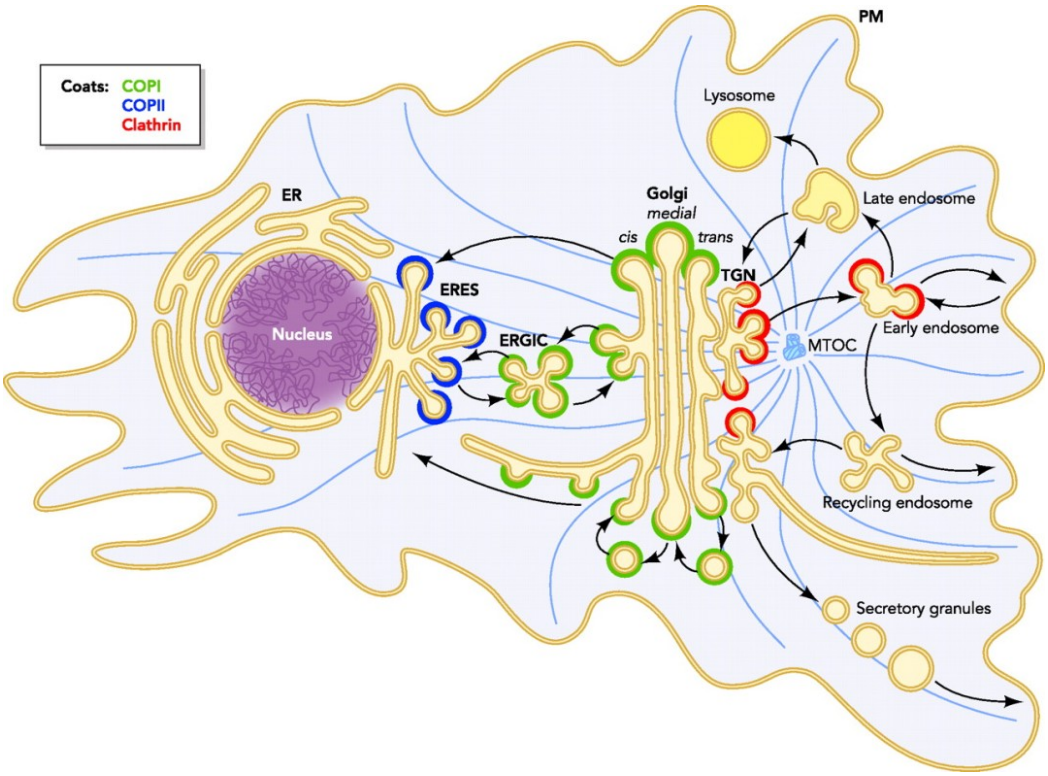

Figure 1-9. Principaux systèmes de transport vésiculaire. Représentation des circuits intracellulaires couverts par les trois principaux types vésiculaires associés à la voie endosomale et à la voie de sécrétion. Reproduit avec permission de (178).

1.5.1. Vésicules COPII

Il est postulé que le tiers des protéines produites au niveau du réticulum endoplasmique chez les mammifères doit être exporté; pour y parvenir, le système de vésicules COP de type II (COPII) est largement impliqué (179). Il a été identifié et caractérisé chez la levure dans les années 1980 en grande partie par l'équipe de Randy Schekman, puis chez l'humain dans les années 1990 (180-187). Ces vésicules prennent naissance à des sites d'export (ER *exit sites*, ERES) au niveau de la région transitionnelle du réticulum endoplasmique (*transitionnal* ER, tER), qui est dépourvue de ribosome et fait face à l'appareil de Golgi, et ont pour destination

le ERGIC ou l'appareil de Golgi (Figure 1-10, p.26) (166, 179, 188-190). Les cargos transportés sont très diversifiés par rapport à leur topologie, leur taille, leur état d'agrégation et leur destination (179).

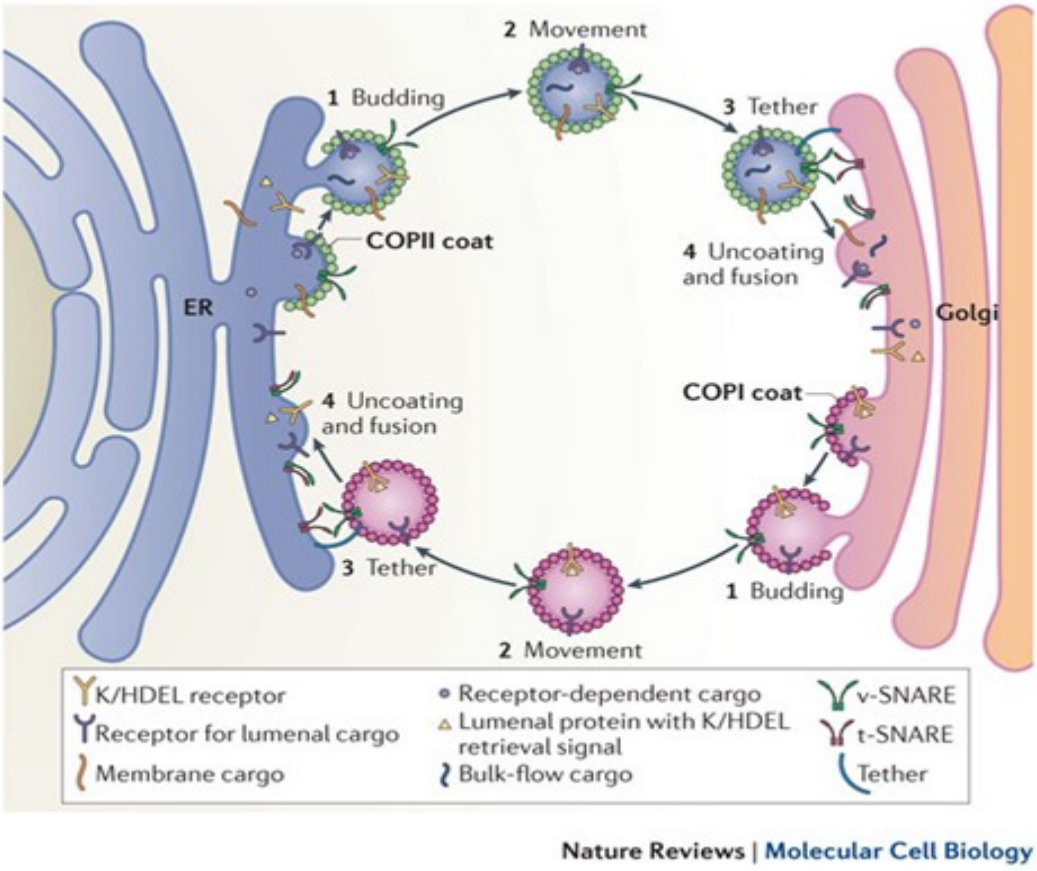

Figure 1-10. Séquence événementielle du transport vésiculaire par COPI et COPII. Représentation des composés impliqués dans chaque phase du transport des vésicules COPI et COPII entre le réticulum endoplasmique et l'appareil de Golgi. Reprinted by permission from Macmillan Publishers Ltd: [Nature Reviews Molecular Cell Biology] (Brandizzi F, Barlowe C. *Organization of the ER-Golgi interface for membrane traffic control*. Nat Rev Mol Cell Biol. 2013;14(6):382-92.), copyright (2013). Reproduit avec permission de (179).

1.5.1.1. Composantes et assemblage des vésicules COPII

Pour donner naissance à une vésicule, séquentiellement, la protéine résidente du ER Sec16 est localisée au ERES du tER afin d'organiser l'assemblage en recrutant différentes sous-unités (187, 191, 192). Le premier acteur, Sec12, induit le passage de la forme GDP à la forme GTP chez la protéine G de la famille ARF nommée Sar1, lui permettant de s'ancrer à la

membrane du tER via la libération de son extrémité N'-terminale (165, 166). L'activation de Sar1 induit une légère courbure dans la membrane du ER et le recrutement subséquent des composantes des vésicules COPII (Figure 1-11, p.28) (166, 192).

D'abord, l'hétérodimère de Sec23 et Sec24 (Sec23/24) s'associe à Sar1 sur la face formant l'intérieur de la vésicule pour former une structure en nœud-papillon (166, 167, 193). L'appellation Sec fait référence à l'indentification initiale de ces protéines dans des groupes de complémentation de mutants de sécrétion chez *Saccharomyces cerevisiae* (180). La nature concave de l'hétérodimère pourrait contribuer à déformer la membrane (192). Le complexe Sec23/24-Sar1 peut recruter les molécules formant le cargo, mais également des récepteurs du cargo et des SNAREs individuels – Bet1p, Bos1p, Sec22p, Sed5p – exposant leur motif de sélection; cette structure est un pré-bourgeon (*pre-budding complex*) (166, 172, 192).

L'hétérodimère Sec13/31 permet par la suite de déformer suffisamment la membrane du tER pour détacher le bourgeon de l'organelle et former une vésicule (166). La sous-unité Sec23, grâce à un résidu arginine conservé, et Sec13/31 peuvent catalyser l'activité GTPase de Sar1, de manière à hydrolyser GTP en GDP et induire la dissociation du bourgeon ou de la vésicule (165, 166). Il est estimé que l'action de Sar1 conjointement à celle de Sec23 met 30 secondes à hydrolyser GTP, et que la réaction est dix fois plus rapide en présence de Sec31 (165). La capacité intrinsèque du complexe à induire sa propre dissociation implique une fenêtre de temps restreinte pour l'assemblage de la vésicule, justifiant l'importance du rôle stabilisateur de Sec12 (166). Le bourgeonnement des vésicules COPII peut ainsi être visualisé comme un processus dynamique (166). Il est généralement accepté que le cargo ait un rôle à jouer dans la stabilisation de l'assemblage de la vésicule, en plus d'en moduler la forme, et potentiellement d'attirer les composantes aux ERES (179).

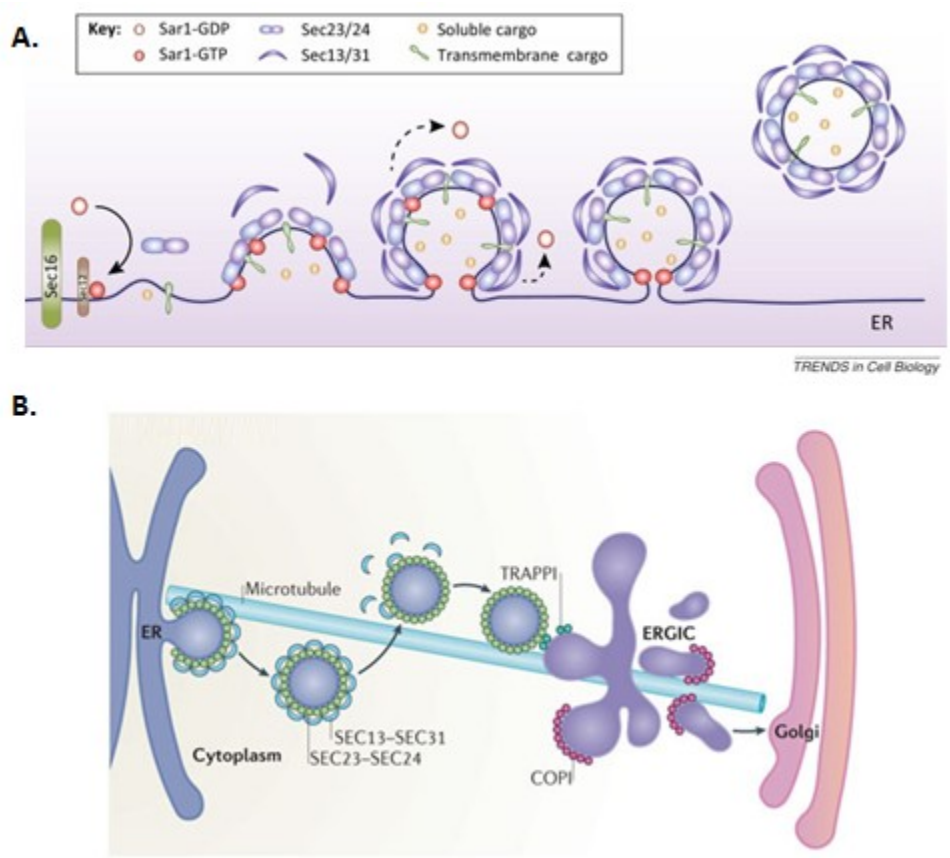

Figure 1-11. Transport de cargo par les vésicules COPII. (A) L'assemblage de la vésicule et la sélection du cargo sont opérés simultanément. Reproduit avec permission de (179). (B) Le bourgeon se détache du Golgi, transite sur le réseau de microtubules et rejoint le ERGIC. Reproduit avec permission de (194).

Un fait important à considérer dans l'étude du système COPII des mammifères est l'existence de diverses isoformes pour la plupart des composantes : deux chacune pour Sar1, Sec23, Sec31 et Sec16 (A, B) et quatre pour Sec24 (A, B, C, D) (179, 195). De son côté, Sec13 n'est exprimé qu'en une isoforme (179). Le niveau d'expression des différents paralogues varie d'un type cellulaire à l'autre, expliquant l'apparition de phénotypes tissu-spécifiques dans le cas de mutations particulières (179, 187, 196). Plusieurs maladies sont associées à des mutations dans le système COPII, comme la dysplasie craniolenticulosuturale (DCLS, ou syndrome de Boyadjiev-Jabs), qui résulte d'une mutation dans Sec23A et du faible taux de Sec23B chez les ostéoblastes crâniens (179, 197). Chez *Saccharomyces cerevisiae*, toutes ces composantes n'ont qu'une isoforme, excepté Sec24 qui en a deux (165, 179).

1.5.1.2. Sélection du cargo par les vésicules COPII

La composante Sec24 est connue pour son rôle majeur dans la sélection du cargo, tel qu'elle présente trois sites d'attachement distincts (A, B et C) (166). Dans les dernières années, il a également été montré que Sar1 pouvait être impliquée dans la sélection de cargo (198). Il est à noter que certaines protéines, notamment des protéines solubles, requièrent un récepteur afin d'être indirectement sélectionnées par les composantes du système COPII (191). Quelques exemples de récepteurs connus sont ERGIC-53 et les protéines de la famille p24 (199-201). À l'opposé, d'autres protéines solubles sont transportées dans les vésicules COPII sans appariement spécifique, un procédé appelé sortie par mouvement de masse, ou *bulk flow exit* (202). Ce processus passif montre une faible efficacité au niveau du ER, mais l'exclusion des vésicules COPI dans le ERGIC permet la concentration des protéines en question pour leur progression à travers l'appareil de Golgi (202). Les modèles de sortie médiée par un récepteur et par mouvement de masse ne sont pas mutuellement exclusifs (201).

1.5.1.2.1. Motifs reconnus par Sec24

Plusieurs sites différents de la sous-unité Sec24 permettent l'appariement à une gamme de motifs (166). En ce sens, le site A reconnaît le motif YNNSNPF, présent chez la syntaxine Sed5; le site B est une cavité étroite accomodant le motif LXX-L/M-E de Bet1 et Sed5, ainsi que le signal D/E-X-D/E présent chez Sys1, Kir2.1 et VSV-G (*vesicular stomatitis virus protein* G); le site C s'associe à Sec22 (166, 188, 201). Différents motifs hydrophobes di-aromatiques C' terminaux sont également reconnus par Sec24 : FF (ERGIC-53), VV (récepteur NMDA), FY (Erv46p) et LL (Emp46p) (166, 201, 203).

1.5.1.2.2. Motifs reconnus par Sar1

Les premières évidences de sélection de protéines au niveau du tER par la protéine Sar1 ont été obtenues lorsque Springer et Schekman ont démontré son association avec deux SNAREs du système COPII : les protéines Bet1 et Bos1 (204). Cette sélection des SNAREs pourrait contribuer à l'assemblage des sous-unités du manteau vésiculaire, puisqu'une autre

région de Bet1 permet de lier Sec24 (166, 204). Ultérieurement, le rôle de sélection de Sar1 a pu être étendu à des protéines de cargo (205). L'utilisation de mutants distincts de Sar1 – l'un restreint à l'état GDP et inactif (Sar1[T39N]), l'autre restreint à l'état GTP et constitutivement actif (Sar1[H79G]) – a permis de constater que Sar1 interagit avec la queue cytoplasmique de VSV-G avant son activation à l'état GTP, donc avant le recrutement des autres sous-unités du complexe de bourgeonnement (205). Sachant que le motif DXE de VSV-G est reconnu par Sec24, Aridor et al. suggèrent que le motif complet permettant aussi la sélection par Sar1 soit plutôt YXDXE (205-207). Chez la levure, Sar1 a également été associé au recrutement de la protéine Emp24 de la famille de protéines p24 (200). Ceci implique que Sar1 a pour fonction de concentrer certains cargos aux ERES. De surcroît, Sar1 est la composante de la vésicule COPII étant responsable du recrutement du moteur de kinésine nécessaire au transport de la vésicule sur le réseau de microtubules, mettant de l'avant le caractère essentiel de Sar1 dans ce système (205).

Le motif di-hydrophobe IL rencontré chez les protéines Erv41 et Erv46 a été identifié comme un motif reconnu par Sar1 (203). Ces protéines ont leurs régions N et C-terminales dans le cytosol (203). Le groupe de Maccioni a plutôt étudié le sort de protéines de type II, en l'occurrence de glycosyltransférases (198, 208). Pour suivre les motifs di-acides et di-hydrophobes déjà connus, ils mettent en lumière la capacité de sélection pour l'export de motifs di-basiques (208). Ils répertorient plus d'une cinquantaine de protéines de la famille des glycosyltransférases, tant chez la levure que chez les animaux, possédant un motif composé de lysines et ou d'arginines, représenté [R/K]X[R/K] (208).

1.5.1.2.3. Sélection du complexe αβIi par COPII

Le motif di-basique identifié chez les glycosyltransférases peut également être observé chez la chaîne invariante; l'isoforme p35 possède un motif RRR dans son extension la différenciant de p33, et les deux isoformes ont un motif RR près de la région transmembranaire (Figure 1-6, p.11) (101, 107, 208). La présence de ces résidus arginine au niveau de la queue cytoplasmique d'Ii suggère une interaction potentielle entre le complexe αβIi et Sar1. Pour ce qui est du CMH I, il est concentré aux ERES pour sélection par les

vésicules COPII après avoir lié son peptide (209). Il a été démontré que l'acide aminé en C' de sa chaîne α est crucial à la sélection dans les vésicules COPII (210). Ceci suggère l'existence potentielle un récepteur médiant cette association pour le transport antérograde du CMH I (209, 210). Ce cas de figure peut aussi être envisageable en ce qui concerne le CMH II, avec ou sans la chaîne invariante.

1.5.2. Vésicules COPI

Ces vésicules sont impliquées dans le transport rétrograde de molécules la plupart du temps depuis le ERGIC, et quelque fois du Golgi, vers le réticulum endoplasmique (164). Elles peuvent également contribuer au transport antérograde du ER et du ERGIC vers le Golgi, ainsi qu'entre les compartiments du Golgi (190, 211). Ceci suggère donc l'existence de deux sous-types de vésicules COPI, selon qu'elles ramènent des protéines résidentes du ER ou qu'elles assurent la progression d'autres cargos (Figure 1-9, p.25) (212). Une fonction primordiale du système COPI est d'une part de distinguer les protéines devant progresser vers et à travers le Golgi, et d'autre part d'assurer le retour des composantes essentielles du réticulum endoplasmique pour en conserver l'intégrité (188, 213, 214). Effectivement, il est évident que de court-circuiter le transport rétrograde par COPI a pour effet d'altérer grandement le transport antérograde, étant donné que le retour des protéines essentielles à l'homéostasie du ER, des lipides et de la machinerie d'exportation est arrêté (189, 194, 215-221).

1.5.2.1. Composantes et assemblage des vésicules COPI

Des analyses quantitatives en microscopie électronique révèlent entre autres que la moitié des composantes de COPI (β-COP) se trouvent autour du ERGIC, du *cis*-Golgi et aux extrémités des compartiments du Golgi; le reste est dispersé dans le cytosol (Figure 1-9, p.25) (222). L'assemblage des vésicules COPI requiert, en plus d'ARF, la présence de sept sous-unités solubles dans le cytosol : α, β, β', ε, γ, δ et ζ-COP (164, 214, 223). L'appariement des sous-unités peut être vu comme spontané, considérant que seulement peu de sous-unités

individuelles sont détectées, exception faite de ζ-COP (164). Les composantes du système COPI sont donc appariées de manière beaucoup stable que celles de COPII (164, 166). Il existe en fait deux sous-complexes distincts : le premier, composé des sous-unités β, γ, δ et ζ-COP forment la couche interne de COPI, c'est-à-dire qu'elle est adjacente à la membrane vésiculaire; le second comprend les composantes α, β' et ε-COP et constituent la couche externe (224). La sous-unité ε-COP est responsable du phénotype de la lignée cellulaire LdlF dérivée des cellules CHO; une mutation thermosensible dans cette protéine court-circuite le système COPI à 37°C (164).

Séquentiellement, comme pour les vésicules COPII, la formation des vésicules COPI requiert l'ancrage d'ARF à la membrane du Golgi ou du ERGIC via son activation par l'échange de GDP pour GTP par GEF (*guanine nucleotide exchange factor*) (Figure 1-12, p.32) (178). ARF procède ensuite au recrutement des sept sous-unités pré-assemblées de COPI depuis le cytosol vers la membrane (178).

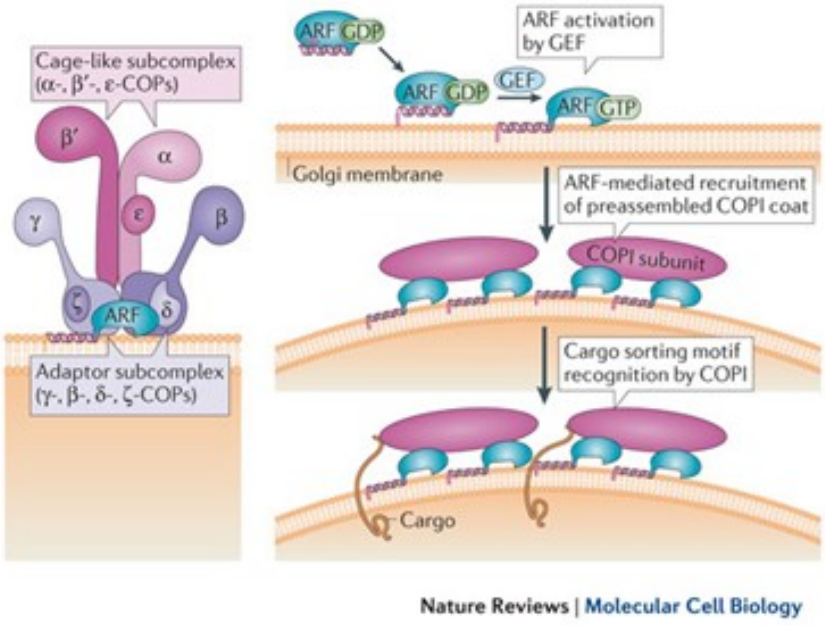

Figure 1-12. Structure et assemblage des vésicules COPI. L'ancrage de la protéine de la famille ARF initie l'assemblage de la vésicule en recrutant les sous-unités pré-assemblées de COPI, qui recrutent le cargo. Reproduit avec permission de (194).

1.5.2.2. Sélection du cargo par les vésicules COPI

Les composantes α, β', γ et δ du système COPI sont chargées de la sélection du cargo (178). Elles parviennent entre autres à reconnaître certains motifs des protéines résidentes du réticulum endoplasmique. En l'occurrence, on parle des motifs cytosoliques C-terminaux K/H-DEL ou KKXX de protéines de type I (164, 190, 194, 200, 216, 225, 226). Pour être sélectionnées, les protéines portant l'ERM KDEL doivent être phosphorylées en position Ser209 par PKA (227). Assurant un certain « contrôle de qualité » des protéines pouvant progresser dans la cellule, les vésicules COPI font également la sélection parmi leur cargo des protéines mal repliées, des complexes mal associés, ou des protéines dirigées vers le Golgi par erreur (164, 190, 213). La sous-unité δ-COP reconnaît spécifiquement un motif présent dans la région cytoplasmique de Sec71p et CD3-ε pour les retourner au ER (211).

La progression dans le Golgi des protéines solubles ayant atteint le ERGIC par *bulk flow* est assurée par l'exclusion du transport rétrograde (214). À l'inverse, pour des protéines devant retourner vers le ER et n'étant pas sélectionnées par COPI, il semble que le transport rétrograde puisse être assuré par un mécanisme indépendant (228). L'inhibition de COPI par microinjection d'anticorps dirigés contre ses composantes court-circuite le retour vers le Golgi de la toxine du choléra et de l'entérotoxine de *Pseudomonas*, qui portent l'ERM KDEL, mais pas celui de la toxine Shiga ni des toxines Shiga-*like* d'*Escherichia coli*, dépourvues de ce motif (228). Cet autre mécanisme serait Rab6-dépendant (228).

1.5.2.2.1. Sélection du complexe αβIi par les vésicules COPI

Le système de vésicules COPI est responsable du retour de complexes devant être retenus au ER; un complexe αβIi atteignant le *cis*-Golgi et dont le motif RXR n'est pas masqué peut s'associer à la sous-unité β-COP du système de vésicules COPI, de manière à retourner vers le réticulum endoplasmique (229). D'autre part, la phosphorylation des sérines 6 et 8 de l'extension de p35/p43 par PKC permet l'interaction avec 14-3-3β, qui rencontre son signal consensus chez ces isoformes ($RSXS^{P}XP$), permettant la progression au-delà du ER (94, 107, 109, 229). Étant donné que les sites reconnus par β-COP et 14-3-3β sont tous deux situés dans la même région de la queue cytoplasmique, l'interaction avec l'une ou l'autre de

ces protéines est de nature compétitive (Figure 1-6, p.11) (229). Incidemment, la progression du complexe dépend du niveau de phosphorylation : un complexe aux sérines phosphorylées s'associe à 14-3-3 et progresse dans la cellule, alors qu'un complexe non-phosphorylé est capté dans les vésicules COPI pour retourner au réticulum endoplasmique (Figure 1-13, 34) (229). Le concept d'assemblage et de masquage appropriés du complexe αβIi pour permettre la progression à travers le Golgi rappelle le phénomène observé chez les canaux K_{ATP}; le motif de rétention RKR de la sous-unité Kir6.2 oblige l'association du complexe avec 14-3-3 afin de prévenir la capture par les vésicules COPI (230).

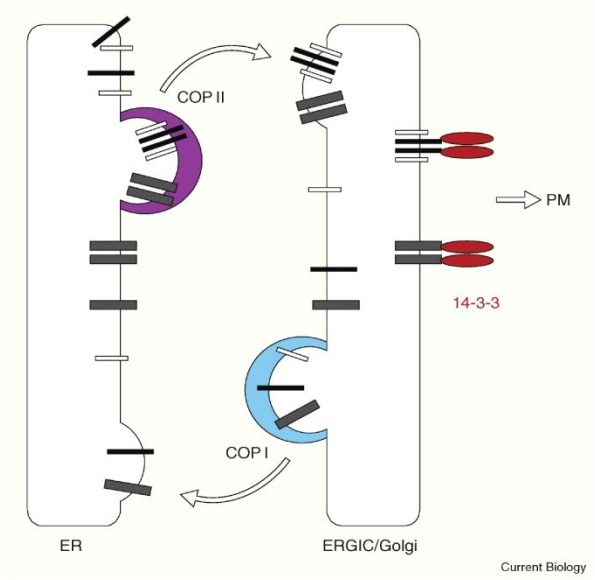

Figure 1-13. Systèmes et molécules associés au trafic de complexes multimériques. Les différentes sous-unités des complexes multimériques sont représentées par les rectangles blancs, gris et noirs. Lorsqu'un multimère est correctement assemblé et que tout ERM est masqué, l'association du multimère à 14-3-3 prévient sa recapture par COPI et permet la progression du complexe. Reproduit avec permission de (231).

1.6. *Escherichia coli* entéropathogène et entérohémorragique

La bactérie *Escherichia coli* est un important pathogène de l'homme comme de plusieurs mammifères (232-239). Si les souches entéropathogènes(EPEC) sont la première cause de diarrhées infantiles, les souches entérohémorrhagiques (EHEC), comprenant le

sérotype O157 :H7, provoquent en plus des symptômes graves comme des colites hémorragiques et un syndrome hémolytique urémique (232, 233, 240). Leur pathogénicité peut être attribuée à plusieurs gènes codant pour des facteurs de virulence ayant un rôle dans l'attachement aux microvilli intestinaux et dans leur effacement (241-244). Les bactéries induisent ensuite le réarrangement du cytosquelette des entérocytes afin de former une structure en piédestal au sommet duquel elles trônent individuellement (243-246).

1.6.1. Îlot de pathogénicité LEE

En 1995, un courant de recherche a été lancé lorsque McDaniel et al. ont observé chez les EPEC la présence d'un locus conférant aux bactéries leur capacité de produire les lésions d'attachement-effacement (AE) (233). Ils ont de surcroît réussi à retracer à l'aide de sondes à ADN l'équivalent de ce locus chez plusieurs bactéries causant des lésions similaires (233). Parmi celles-ci, on compte notamment un pathogène de la souris, *Citrobacter rodentium* (233, 247). Ce locus, baptisé locus d'effacement des entérocytes (LEE), concentre plusieurs facteurs de virulence en un îlot de pathogénicité (233, 248). Cependant, le transfert du LEE chez une souche d'*E. coli* non-pathogène ne suffit pas à conférer le phénotype produisant les lésions d'AE (249).

L'étude chez les EPEC de la composition du LEE et de sa régulation a permis de découvrir le régulateur Ler, ou *LEE-encoded regulator* (244, 248, 250-254). Celui-ci est situé sur le premier de cinq opérons polycistroniques (LEE1 à 5) (254). Le régulon Per (*plasmid-encoded regulator*) du plasmide des EPEC induit l'expression de Ler du LEE1, et Ler induit à son tour l'expression en *trans* des LEE2 et 3, et dans une certaine mesure celle du LEE4 (Figure 1-14, p.36) (254). En plus de réguler la production de facteurs de virulence du LEE et les composantes du système de sécrétion de type III (SST3), il s'avère que Ler régule également l'expression de facteurs de virulence à l'extérieur de l'îlot de pathogénicité LEE (254). Plus récemment, il a été montré chez une souche de EHEC O157:H7 que plusieurs régulateurs, tels que Ler, GrlA, HNS et RpoS, sont impliqués dans l'activation du LEE (255).

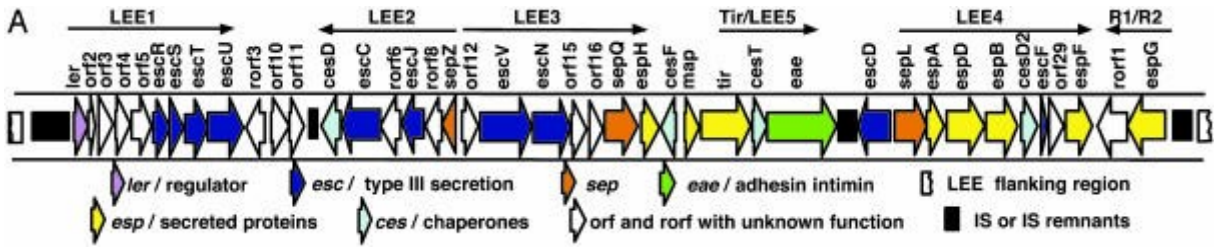

Figure 1-14. Locus d'effacement des entérocytes. Représentation de l'organisation génétique du LEE de *Citrobacter rodentium*. Reproduit de [Deng W, Puente JL, Gruenheid S, Li Y, Vallance BA, Vazquez A, et al. *Dissecting virulence: systematic and functional analyses of a pathogenicity island*. Proceedings of the National Academy of Sciences of the United States of America. 2004;101(10):3597-602]. Copyright (2004) National Academy of Sciences, U.S.A. Reproduit avec permission de (256).

L'expression du LEE permet ainsi le déploiement du SST3, ayant la forme d'une aiguille moléculaire qui peut injecter du matériel effecteur directement dans le cytoplasme d'une cellule-cible : ceci rend possible le contrôle de cette cellule par la bactérie depuis le lumen intestinal (257). Le SST3 est composé entre autres d'un long polymère d'EspA entre les membranes bactérienne et eucaryote, puis le pore est formé dans l'entérocyte par EspB et EspD (245, 258). Parmi les effecteurs transloqués, on compte Tir, EspF, EspG, EspH, EspZ et Map (257, 259). L'effecteur Tir, attaché directement au cytosquelette par sa région cytosolique, interagit avec l'intimine de la membrane bactérienne via sa portion luminale, permettant le contact rapproché entre l'entérocyte et la bactérie (260-263). Tir est également impliqué dans le recrutement d'adapteurs pour la polymérisation de l'actine en un piédestal (264). L'intégrité des jonctions adhérentes entre les entérocytes, qui maintiennent une barrière primordiale entre le lumen intestinal et la sous-muqueuse, pourrait être déstabilisée par l'action d'EspF (265-267).

1.6.2. Effecteurs de type non-LEE

Les quelques effecteurs très potents encodés sur l'îlot de pathogénicité LEE ne suffisent pas à expliquer les changements chez les entérocytes de l'organisme infecté, ce qui a été confirmé par la découverte d'effecteurs encodés à l'extérieur du LEE, appelés *non-LEE effectors* (Nle) (256, 259, 268-270). Le premier effecteur non-LEE transloqué par le SST3 qui

a été identifié est Orf3, un homologue de EspG (271). Il s'avère que, en plus de la coopération rapportée entre les effecteurs du LEE, il existe une collaboration entre les effecteurs LEE et non-LEE (272). En ce sens, un homologue non-LEE d'EspF identifié chez *E. coli* O157 :H7 peut substituer à EspF dans la déstabilisation des jonctions adhérentes, et ce, en plus d'être essentiel à l'action de Tir pour le réarrangement du réseau d'actine (270, 273, 274).

1.6.2.1. Effecteur NleA

En 2004, des études conduites dans le laboratoire de Brett Finlay ont permis de découvrir chez *Citrobacter rodentium*, en plus de 33 facteurs de virulence et 2 régulateurs du LEE, sept effecteurs non-LEE transloqués par le SST3 (256). Cette bactérie présente un LEE hautement similaire à celui des EPEC comme des EHEC, et a l'avantage d'être la seule à pouvoir être étudiée chez un petit animal de laboratoire : la souris (247, 275). Parmi les protéines identifiées, l'effecteur NleA (*non-LEE-encoded effector* A, ou EspI), a été découvert parmi les effecteurs transloqués par le SST3 d'EHEC (269, 276). Par la suite, sa présence chez les EPEC et *C. rodentium*, de même que son absence chez des souches d'*E. coli* non-pathogènes et des bactéries pathogènes non-LEE, a été confirmée (276). Par des infections en modèle murin, il a également été démontré que, malgré que cet effecteur ne provienne pas de l'îlot de pathogénicité LEE, il est essentiel à la virulence de *C. rodentium* (276).

Par la visualisation en microscopie confocale de cellules HeLa infectées par des EHEC ou transfectées avec un plasmide codant pour NleA, il été possible d'établir que cet effecteur se concentre au niveau de l'appareil de Golgi (276). Il s'avère qu'un effet majeur de cet effecteur dans la cellule survient au niveau du système COPII : NleA interagit directement avec chacune des quatre formes (A-D) de la sous-unité Sec24 via sa région C-terminale, déstabilisant l'hétérodimère Sec23/24, et inhibant de ce fait l'export de cargo depuis le ER via les vésicules COPII (277, 278). Cette interaction permet à NleA d'être dirigé dans le système sécrétoire de la cellule (278). Par ailleurs, NleA s'ajoute à EspF et Map sur la liste des effecteurs ayant la capacité de déstabiliser les jonctions adhérentes, mais cet effet est indépendant de son domaine d'attachement à PDZ (279-281). Le groupe mené par Samantha Gruenheid propose que ces fonctions de déstabilisation de la voie de sécrétion et des jonctions

adhérentes soient reliées, en ce sens que l'effet prolongé de NleA sur le transport vésiculaire COPII perturbe l'équilibre dans le recyclage des composantes assurant le maintien des jonctions adhérentes (281). Ultimement, l'architecture de l'épithélium intestinal se trouve affectée, donnant lieu à l'apparition de symptômes diarrhéiques (281).

1.7. Hypothèses et objectifs

Depuis sa découverte en 1979, beaucoup d'efforts ont visé à caractériser de manière exhaustive la chaîne invariante au niveau des différences dans les motifs et modifications post-traductionnelles des diverses isoformes, et au niveau de la fonction globale d'Ii dans la présentation antigénique par le CMH II (section 1.3.). Néanmoins, peu se sont concentrés à combiner ces deux champs de recherche (282, 283) : ces isoformes d'Ii ont-elles des fonctions redondantes, ou ces divergences dans leur séquence respective leurs permettent-elles d'occuper des fonctions distinctes?

Le rôle central de la chaîne invariante dans la présentation antigénique par le CMH II est indéniable. Ii peut être reliée à plusieurs pathologies comme différents cancers, l'arthrite ou le lupus érythémateux (284-294). Il a d'ailleurs été exposé à quelques reprises qu'un déséquilibre dans les taux des isoformes p33 et p35 est observable chez des individus atteints de diabète auto-immun ou de leucémie lymphoïde chronique (295-301). Ceci met de l'avant qu'un état d'homéostasie existe entre les variants d'Ii, et que de troubler cet équilibre induit un effet pathologique, supportant que les isoformes ne soient ni équivalentes, ni redondantes.

Dans cette optique, il est de prime importance d'étudier l'extension cytosolique de 16 acides aminés différenciant les deux isoformes humaines prédominantes d'Ii, p33 et p35, car elle occupe certainement un rôle primordial dans la fonction de p35 par rapport à p33 (92, 93).

D'une part, comme l'extension comprend un motif RXR de rétention au réticulum endoplasmique, le masquage de celui-ci par la chaîne β du CMH II régule nécessairement l'assemblage du complexe αβIi (118, 229). L'étude de ce mécanisme est également une manière d'aborder le dilemme entourant la stœchiométrie d'αβIi, car, en cas de masquage

direct (en *cis*), le niveau de complexité de la structure serait relatif au nombre de ERM présents (122, 134). D'autre part, ce même motif triple-arginine de p35 peut certainement être reconnu comme un signal d'exportation par la sous-unité Sar1 des vésicules COPII (208). Cette dualité entre les deux fonctions d'un même motif doit être investiguée, puisque le recyclage du complexe αβIi entre le ER et l'appareil de Golgi retarde directement son transport vers le MIIC et ultimement la fonction de présentation (208, 229). Ainsi, si l'isoforme humaine p35 présente des contraintes additionnelles par rapport à p33 quant à sa sortie du ER, alors nous suggérons que son extension cytosolique influence directement la stœchiométrie du complexe αβIi, et ce, en plus de gouverner l'exportation de ce complexe via les vésicules COPII. Pour répondre à cette problématique, plusieurs objectifs devront être atteints :

- Caractériser le mode par lequel la chaîne β du CMH II parvient à masquer le motif RXR de p35
- Évaluer l'effet de p35 sur la stœchiométrie globale du complexe αβIi
- Identifier les voies empruntées par les différents complexes αβIi pour sortir du réticulum endoplasmique

Pour y parvenir, il faudra concevoir par biologie moléculaire une banque de plasmides codant pour des protéines humaines sauvages et mutantes du CMH II et de la chaîne invariante. Ceci permettra la mise en place d'un système de transfection en lignées cellulaires humaines, dans le but de constituer des APCs artificielles. Ces cellules pourront être marquées d'anticorps fluorescents pour observation par cytométrie en flux ou en microscopie, ou encore être lysées et soumises à des immunoprécipitations pour analyse par immunobuvardage de type Western.

Considérant l'importance du motif RXR dans la recapture des complexes αβIi par les vésicules COPI, on peut supposer que chacun des ERM présents dans un trimère contenant Iip35 doit être directement masqué pour empêcher la recapture. Ceci impliquerait des contraintes stœchiométriques particulières dans l'oligomérisation des chaînes invariantes avec

les dimères de CMH II, c'est-à-dire la formation de structures comprenant plusieurs CMH II. De plus, l'analogie entre le motif reconnu par Sar1 chez les glycosyltransférases et la séquence de la queue cytoplasmique d'Iip35 permet de suggérer que ses résidus arginine et lysine soient impliqués dans la sélection de complexes αβIi par les vésicules COPII.

Chapitre 2. Résultats de l'article 1

Cet article est reproduit avec la permission de l'éditeur et de tous les auteurs.

2.1. Contribution des auteurs

J'ai procédé aux expériences avec Maryse Cloutier. J'ai préparé les figures supplémentaires et Maryse Cloutier les trois autres figures. J'ai procédé à l'expérience de co-immunoprécipitation présentée en matériel supplémentaire. Kyungho Kim et Jinoh Kim ont procédé à l'expérience de bourgeonnement. Les chimères ont été produites par Maryse Cloutier, Jean-Simon Fortin et Laetitia Genève. Jacques Thibodeau a planifié le projet et les expériences de pair avec Maryse Cloutier, Jean-Simon Fortin et Laetitia Genève. Jinoh Kim et Samantha Gruenheid ont été consultés pour leur expertise. Jacques Thibodeau, Maryse Cloutier, Jean-Simon Fortin et Laetitia Genève ont écrit l'article.

2.2. ER egress of invariant chain isoform p35 requires direct binding to MHCII molecules and is inhibited by the NleA virulence factor of enterohaemorrhagic *Escherichia coli*

Maryse Cloutier [a], Catherine Gauthier [a], Jean-Simon Fortin [a], Laetitia Genève [a], Kyungho Kim [b], Samantha Gruenheid [c], Jinoh Kim [b], Jacques Thibodeau [a, ⇑]

[a] Laboratoire d'Immunologie Moléculaire, Département de Microbiologie et Immunologie, Université de Montréal, Montréal, Qué., Canada

[b] Department of Pediatrics, UC Davis Medical Center, M.I.N.D. Institute, Sacramento, CA, USA

[c] Department of Microbiology and Immunology, McGill Life Sciences Complex, Bellini Pavilion, Montreal, Qué., Canada

Status: published in Human Immunology

Address correspondence and reprint requests to Dr. Jacques Thibodeau, Laboratoire d'Immunologie Moléculaire, Département de Microbiologie, Infectiologie et Immunologie, Université de Montréal, CP 6128, Succursale Centre-Ville, Montreal, QC H3C 3J7, Canada.

2.3. Abstract

Four invariant chain (Ii) isoforms assist the folding and trafficking of human MHC class II (MHCIIs). The main isoforms, Iip33 and Iip35, assemble in the ER into homo- and/or hetero-trimers. The sequential binding of up to three MHCII αβ heterodimers to Ii trimers results in the formation of pentamers, heptamers and nonamers. MHCIIs are required to overcome the p35-encoded di-arginine (RxR) ER retention motif and to allow anterograde trafficking of the complex. Here, we show that inactivation of the RxR motif requires a direct *cis* interaction between p35 and the MHCII, precluding ER egress of some unsaturated Ii trimers. Interestingly, as opposed to MHCII/p33 complexes, those including p35 remained in the ER when co-expressed with the NleA protein of enterohaemorrhagic *Escherichia coli*. Taken together, our results demonstrate that p35 influences distinctively MHCII/Ii assembly and trafficking.

Keywords: Antigen presentation, COPII, NleA, Di-arginine, Invariant chain, MHC class II

2.4. Introduction

The invariant chain (Ii; CD74) is a type II protein that chaperones MHC class II molecules (MHCIIs). Humans express four Ii isoforms from the same mRNA precursor: p33, p35, p41 and p43. The longer p35 and p43 isoforms differ from p33 and p41, respectively, by the presence of a 16 amino acid N-terminal extension resulting from the use of an alternative upstream start codon (1). This cytoplasmic extension encompasses a strong di-arginine (RxR) ER retention motif and two phosphorylation-prone serines (2). Our group has shown that the RxR motif of p35 is masked by the cytoplasmic tail of the MHCII β chain upon assembly in the ER (3). In the ER, the various Ii isoforms form homo- and heterotrimers immediately after biosynthesis. Then, MHCII αβ heterodimers sequentially incorporate Ii trimers, generating pentamers, heptamers and, ultimately, nonamers (4, 5). It was recently suggested that nonamers are experimental artefacts and that structural constraints might only allow the formation of pentamers (6). However, half of the Ii pool is part of trimers containing at least one p35 moiety and there is no evidence for the preferential binding of MHCII to p35 over p33 (7). Thus, in conditions where the MHCII binds the p33 moiety of a p35-containing Ii heterotrimer, this pentamer model implies that the MHCII has to overcome the RxR motif in *trans*. Here, we have addressed the assembly and trafficking of the p35-containing MHCII/Ii complex.

2.5. Material and Methods

Plasmids and mutagenesis

The pBudDR and pBudDM plasmids have been described previously (3, 8). Ii (p33 + p35), p33, p35 and p35LIML were subcloned into pcDNA3 (Invitrogen, ON). from previously described constructs (3). The pcDNA3 p33LIML mutant in which the two leucine-based sorting signals were changed for alanines was created by PCR (3). pcDNA3.1 YFP was obtained from Invitrogen. pNleA-GFP was previously described (9). To create the pBud αSCD encoding the single-chain dimer, the luminal domains of the mature DRα

(amino acids 1–191) was linked by PCR overlap to p33's luminal domain (amino acids 57–232) using a (Gly)3(Ser)1(Gly)3 linker.

Antibodies and Western blotting

The following mouse mAbs were described previously (3, 8): BU45 (C-terminal region of human Ii); Pin.1 (cytoplasmic tail of human Ii); L243 (HLA-DR); XD5 (DRα/DRβ, DRβ); CerCLIP.1 (CLIP). For the simultaneous detection of MHCII and Ii, pre-coupled BU45 (Alexa fluor 647) and XD5 (Alexa fluor 488) mAbs were used. Otherwise, Alexa Fluor 488- or 633-coupled goat anti-mouse secondary antibodies were used for flow cytometry (Invitrogen). For Western blotting, peroxidase-AffiniPure goat anti-mouse IgG (H + L) (Jackson Immunoresearch, PA) was used. For immunoprecipitations, cells were first lysed at 4 °C in 1% Triton-X100. Samples were then subjected to SDS–PAGE. Proteins on immunoblots were detected by chemiluminescence (Roche Applied Science, Qc).

Cell lines and flow cytometry

For transient expression, HEK 293T cells were transfected using polyethyleneimine (Polyscience, PA) and stained after 48 h. To determine surface expression, live cells were stained on ice and were analyzed by flow cytometry. To determine total expression of MHCII or Ii, cells were fixed in 4% paraformaldehyde, permeabilized in 0.5% saponin and stained, as described previously (8). In some experiments, cells were first surface stained before being permealized and stained.

2.6. Results

A soluble single-chain dimer between Ii and DRα (αSCD) is expressed at the plasma membrane with DRβ

To control the MHCII/Ii stoichiometry, we constructed a soluble Ii/MHC αSCD. To covalently attach MHCII and Ii, the cDNA for the soluble form of DRα was linked to a sequence coding for a flexible gly3/ser/gly3 linker and to the coding region of the luminal Ii N-terminus domain (Fig. 2-1A). This approach maintains intact the trimerization domain of Ii, a prerequisite to allow formation of high-order structures with co-expressed WT Ii units. Soluble Ii molecules were shown to trimerize and form nonamers with soluble MHCIIs in transfected HEK 293T epithelial cells (10). Thus, a co-transfected WT p35 will associate with the Ii moiety of αSCD, which is devoid of ER retention motifs. Upon co-expression of DRβ, a MHCII αβ heterodimer will fold around the Ii moiety of the αSCD. As the covalent link between DRα and Ii implies a stoichiometric interaction, no extra MHCII αβ dimer will be available to bind the co-transfected full length WT Iip35. Thus, if a (αSCD/β)+Iip35 complex egresses the ER, it will indicate that the MHCII β chain cytoplasmic tail is dominant and can override in *trans* the ER retention motif of the distant p35 moiety that is not in direct contact with the MHCII.

First, we ascertained that the soluble αSCD was stabilized at the membrane upon interaction with the full-length, transmembrane DRβ chain. When transiently co-transfected in HEK 293T cells, the DRβ chain and αSCD (αSCD/β) were both detected at the cell surface using the DR-specific XD5 and Ii-specific BU45 mAbs, respectively (Fig. 2-1B). As positive control, we used the WT DRα and DRβ chains co-expressed with an Ii mutant devoid of its two leucine-based motifs (Iip33LIML). The lack of such endosomal sorting signals mimics the situation created by the use of a soluble αSCD construct and results in a greater accumulation of MHCII/Ii complexes at the cell surface (3, 11). The αSCD/β complex passes through the Golgi and once at the plasma membrane, it is internalized and the Ii moiety is cleaved (data not shown). Transfected cells were recognized by the CerCLIP.1 mAb, which is specific for MHCIIs associated with the endosomal proteolytic

cleavage products of Ii (CLIP) sitting in the peptide-binding groove (12).

Overcoming the RxR motif requires a direct contact between Iip35 and the MHCII

To determine if the RxR motif can be inactivated in *trans*, we expressed p35 together with αSCD/β. Iip33 was used as a control since its interaction with the Ii moiety of αSCD should not prevent ER egress.

First, we ascertained that the co-expressed full-length Ii isoforms were able to complex with αSCD/β. Cells were co-transfected with αSCD/β and either p33 or p35. Cells were lyzed and a small fraction was used to immunoprecipitate p33 or p35 with Pin.1. The co-immunoprecipitation of DRβ was shown on immunoblots and confirmed qualitatively the association of the WT Ii isoforms with αSCD/β (Fig. 2-2A). Indeed, DRβ did not co-immunoprecipitate when expressed alone with Iip33 (Supplemental Fig. 2-4). A fraction of each cell lysate was included as control. DRβ did not co-immunoprecipitate in the absence of p33 or p35 since the αSCD is soluble and not recognized by Pin.1 (4).
Knowing that p35 can associate with αSCD/β, we could then determine if the sole presence of DR in the complex is sufficient to mask the neighboring RxR motif and to allow transport to the plasma membrane. The use of IiLIML mutants allows the assessment of both Ii and DR cell surface expression, providing an indirect functional read-out for ER egress (3). However, as the cell surface display will also depend on the transfection efficiency, we determined in parallel the total Ii and MHCII protein expression by staining permabilized cells (Fig. 2-2B). When the mean fluorescence intensities (MFIs) are plotted as the surface expression of a given molecule over its total cellular content (Fig. 2-2C), the resulting ratios tend to be low for ER-retained molecules (3).

As shown above, in the absence of additional Ii, αSCD/β was expressed at the plasma membrane and cells stained positive for both BU45 and L243 (Fig. 2-2B, left panels). As expected, co-expression of p33LIML did not impact on the αSCD/β. Indeed, the surface over total ratios for Ii (BU45) and MHCII (L243 and XD5) were not affected by the presence of Iip33LIML (Fig. 2-2C). In contrast, upon co-expression of p35LIML, cell surface expression of αSCD/β was greatly reduced and the surface/total ratios were low for

Ii and MHCII, indicating intracellular retention (Fig. 2-2B and C). Accordingly, the plasma membrane display of CLIP was reduced (Fig. 2-2D).

The above-described results demonstrate that Ii can bind αSCD/β. As Ii trimerization is rapid and precedes MHCII binding (13), the co-transfected Ii and the Ii moiety of the αSCD will most likely heterotrimerize (Ii1αSCD2 or Ii2αSCD1). Soon after or in parallel, the MHCII α and β chains fold together around the covalently-linked Ii, leaving the full length Ii in the complex but devoid of MHCII chains. The fact that p35 prevented cell surface expression of these complexes indicates that masking must not occur in *trans*, the MHCII having to be in direct contact with p35 to overcome the RxR retention signal.

p33 and p35 exit the ER through different routes

Unphosphorylated p35 undergoes retrograde transport in COPI coatamers from the ERGIC to the ER (14). Upon phosphorylation of p35, 14-3-3 adaptor proteins associate with Ii and block β-COP binding. However, little is known about the mechanism by which Ii actually exits the ER. COPII-coated vesicles form at ER exit sites (ERES) where specific cargos are concentrated (15). Cytoplasmic export signals have been identified in some transmembrane proteins, allowing active recruitment and enrichment into budding vesicles. Other membrane proteins, according to the bulk-flow model, enter various types of vesicles through a default pathway originating at non-specific sites physically distinct from ERES (16). To gain insights into the transport mode of DR and Ii isoforms, we perturbed trafficking in the early secretory pathway using the NleA protein from enterohaemorrhagic *E. coli*. One known function of the NleA virulence factor is to bind to Sec24, a main constituent of the COPII protein coat involved in the ER-to-Golgi anterograde transport, and to inhibit COPII-mediated transport (9). HEK 293T cells were transiently transfected with DR and Ii, together with NleA-GFP or control YFP. After 48 h, surface expression of DR was monitored by flow cytometry on cells expressing GFP (or YFP) (Fig. 2-3A). The data reveals that DR, when transfected alone or with Iip33LIML, is well expressed at the plasma membrane in NleA-expressing cells. On the other hand, when co-expressed with p35LIML, DR expression was markedly reduced in $NleA^+$ versus YFP^+ cells. However,

as cells are not usually p35 exclusive, we performed this assay on cells expressing both Ii isoforms. As a single cDNA was transfected to produce both p33 and p35, we confirmed on immunoblots that both isoforms were translated (Fig. 2-3B). Densitometry revealed that there was about 1.5-fold more p35 than p33 in these cells. As p35 is slightly overrepresented, we can assume that all Ii trimers will incorporate at least one p35 moiety. In these conditions, we found that p35 had a negative effect on the surface expression of DR (Fig. 2-3A). We also monitored Ii surface expression and the results confirmed the NleA-induced surface down-modulation of Iip35-containing complexes (Fig. 2-3C). The MFIs obtained for surface DR and Ii were normalized over the total expression of the proteins in permeabilized cells. Fig. 2-3D demonstrates the significant impact of NleA on the trafficking of p35-containing complexes. Importantly, the absence of CLIP at the cell surface corroborates the negative impact of NleA of the ER egress on this Ii isoform (Fig. 2-3E). Indeed, NleA appeared to only slightly affect Iip33 surface expression. As there was no down-regulation of MHCII or CLIP, these results may reflect a marginal effect of NleA on MHCII-free Ii trimers. Altogether, these results confirm the additional layers of complexity in the ER egress of Iip35 versus p33. Interestingly, the peculiar structural properties of Iip35 render the MHCII/Ii complexes susceptible to the negative effects of NleA on protein trafficking to the Golgi.

2.7. Discussion

Our data best fit a model where a co-expressed full length Ii associates with αSCD/β through its trimerization motif, thereby generating pseudo-heptamers ($\alpha SCD_2DR\beta_2Ii_1$) and -pentamers ($\alpha SCD_1DR\beta_1Ii_2$). When p35 incorporated the complex, the MHCIIs were unable to mask its RxR motif, demonstrating the need for a direct contact and the capacity of p35 to force the assembly of large complexes. However, normal cells make a wide variety of heterotrimeric Ii combinations by mixing the four isoforms. Our results do not rule out that trimers devoid of RxR motifs can also egress the ER loaded with only one (pentamer) or two (heptamer) MHCIIs. If stoichiometric variations can influence the functions of MHCIIs remains to be determined. This is

particularly relevant in the etiology of B chronic lymphocytic leukemia (B-CLL) where p35 is overexpressed and of type 1 diabetes, where a defect in p35 expression is thought to alter the presentation of disease-related antigens (17, 18).

The need to accumulate MHCIIs on the trimeric Ii backbone until all the p35 moieties are concealed is incompatible with a pentamer-only model (6). A stoichiometric interaction is also required for ER egress of the octameric (4α:4β) ATP-sensitive K^+ channel where each β chain masks the RxR motif of adjacent β and α subunits. ER egress occurs only when all the motifs are covered and the complex is fully assembled (19). It is also possible that p35 evolved to regulate surface expression of MHCII-free Ii trimers. Indeed, Ii has signaling properties and receptor functions that might require tight control via p35 expression and phosphorylation (20). In this context, stoichiometric MHCII variations may be a trivial collateral consequence of the mechanism by which p35 regulates Ii surface levels.

Finally, our results show that ER egress of p35- and/or p43-containing complexes is sensitive to the activity of NleA. Although NleA has been shown to inhibit the transport of COPII-dependent cargos (9), the result of budding experiments did not confirm the inclusion of p35 in such vesicles (Supplemental Fig. 2-5). This could be due to the limitations of the assay, namely that the reactions only sample a portion of proteins in the ER at steady state or that Iip35 needs additional factors that are limiting in our conditions. Also, we can- not rule out that NleA could be having an indirect or off-target effect. Still, the differential behavior of Ii isoforms in the presence of NleA offers the opportunity to shed light on mechanistic principles governing ER egress of RxR-containing protein complexes and, ultimately, to uncover a potential role for NleA in the subversion of antigen presentation by enterohaemorrhagic *E. coli*.

2.8. Funding

This research was funded by the National Science and Engineering Research Council of Canada (NSERC) (grant #298537).

2.9. Acknowledgements

We thank Peter Cresswell, Lisa Denzin and Rafick Sékaly for reagents, cells and antibodies.

2.10. Abbreviations

SCD, single chain dimer; RxR, di-arginine motif; ERES, ER exit sites

2.11. References

1. Strubin M, Berte C, Mach B. *Alternative splicing and alternative initiation of translation explain the four forms of the Ia antigen-associated invariant chain*. EMBO J. 1986;5(13):3483-8.
2. Schutze MP, Peterson PA, Jackson MR. *An N-terminal double-arginine motif maintains type II membrane proteins in the endoplasmic reticulum*. EMBO J. 1994;13(7):1696-705.
3. Khalil H, Brunet A, Thibodeau J. *A three-amino-acid-long HLA-DRbeta cytoplasmic tail is sufficient to overcome ER retention of invariant-chain p35*. J Cell Sci. 2005;118(Pt 20):4679-87.
4. Roche PA, Marks MS, Cresswell P. *Formation of a nine-subunit complex by HLA class II glycoproteins and the invariant chain*. Nature. 1991;354(6352):392-4.
5. Lamb CA, Cresswell P. *Assembly and transport properties of invariant chain trimers and HLA-DR-invariant chain complexes*. J Immunol. 1992;148(11):3478-82.
6. Koch N, Zacharias M, Konig A, Temme S, Neumann J, Springer S. *Stoichiometry of HLA class II-invariant chain oligomers*. PLoS One. 2011;6(2):e17257.
7. Anderson HA, Bergstralh DT, Kawamura T, Blauvelt A, Roche PA. *Phosphorylation of the invariant chain by protein kinase C regulates MHC class II trafficking to antigen-processing compartments*. J Immunol. 1999;163(10):5435-43.
8. Faubert A, Samaan A, Thibodeau J. *Functional analysis of tryptophans alpha 62 and beta 120 on HLA-DM*. J Biol Chem. 2002;277(4):2750-5.
9. Kim J, Thanabalasuriar A, Chaworth-Musters T, Fromme JC, Frey EA, Lario PI, et al. *The bacterial virulence factor NleA inhibits cellular protein secretion by disrupting mammalian COPII function*. Cell Host Microbe. 2007;2(3):160-71.

10. Majera D, Kristan KC, Neefjes J, Turk D, Mihelic M. *Expression, purification and assembly of soluble multimeric MHC class II-invariant chain complexes*. FEBS Lett. 2012;586(9):1318-24.
11. Bakke O, Dobberstein B. *MHC class II-associated invariant chain contains a sorting signal for endosomal compartments*. Cell. 1990;63(4):707-16.
12. Denzin LK, Robbins NF, Carboy-Newcomb C, Cresswell P. *Assembly and intracellular transport of HL*
A-DM and correction of the class II antigen-processing defect in T2 cells. Immunity. 1994;1(7):595-606.
13. Marks MS, Blum JS, Cresswell P. *Invariant chain trimers are sequestered in the rough endoplasmic reticulum in the absence of association with HLA class II antigens*. J Cell Biol. 1990;111(3):839-55.
14. O'Kelly I, Butler MH, Zilberberg N, Goldstein SA. *Forward transport. 14-3-3 binding overcomes retention in endoplasmic reticulum by dibasic signals*. Cell. 2002;111(4):577-88.
15. Sato K. *COPII coat assembly and selective export from the endoplasmic reticulum*. J Biochem. 2004;136(6):755-60.
16. Zanetti G, Pahuja KB, Studer S, Shim S, Schekman R. *COPII and the regulation of protein sorting in mammals*. Nat Cell Biol. 2012;14(1):20-8.
17. Veenstra H, Jacobs P, Dowdle EB. *Processing of HLA-class II invariant chain and expression of the p35 form is different in malignant and transformed cells*. Blood. 1993;82(8):2494-500.
18. Yan G, Shi L, Penfornis A, Faustman DL. *Impaired processing and presentation by MHC class II proteins in human diabetic cells*. J Immunol. 2003;170(1):620-7.
19. Zerangue N, Schwappach B, Jan YN, Jan LY. *A new ER trafficking signal regulates the subunit stoichiometry of plasma membrane K(ATP) channels*. Neuron. 1999;22(3):537-48.
20. Shachar I, Haran M. *The secret second life of an innocent chaperone: the story of CD74 and B cell/chronic lymphocytic leukemia cell survival*. Leuk Lymphoma. 2011;52(8):1446-54.

2.12. Figure legends

Figure 2-1. Schematic representation and trafficking of αSCD. (A) Schematic representation of DRα + DRβ + Ii and αSCD/DRβ complexes. The αSCD was designed as to have Ii and HLA-DRα luminal domains linked by a flexible gly3/ser/gly3 sequence. (B) DR (DRα + DRβ) + p33LIML and αSCD/β were transiently transfected in HEK293T cells. After 48 h, cells were stained to detect MHCII, Ii and CLIP using XD5, BU45 and CerCLIP.1 primary mAbs, respectively, followed by an Alexa Fluor 488-coupled goat anti-mouse IgG secondary mAb. Controls (Ctrl) represent mock-

transfected cells stained in the same conditions with the MHCII-specific mAb followed by the fluorescent secondary antibody.

Figure 2-2. Masking of the p35 ER retention motif requires a direct association with the MHCIIβ chain. (A) Cells were transfected with αSCD/β alone or with p33 or p35. Cell lysates (right lanes) and samples immunoprecipitated with the Ii-specific Pin.1 mAb (left lanes) were analyzed on immunoblots for the presence of the DRβ chain (XD5 mAb). Less material was loaded in the third lane from left, as judged by the fact that less of the immunoprecipitating antibody heavy chain is detected at 50 KDa. (B) Cells were transfected with αSCD/β alone or with p33LIML or p35 LIML. After 48 h, the cells were permeabilized or not and stained for surface MHCII or Ii. Control (Ctrl) mock-transfected cells were stained in the same conditions. (C) The MFIs obtained for live or permeabilized cells were plotted as a ratio. DRβ and DRαβ correspond to the values obtained with XD5 and L243, respectively. (D) Cells were stained for the presence of CLIP at the cell surface and the MFIs were plotted. Error bars indicate the SD from five independent experiments. Student's *t*-tests were performed; $*p \leq 0.05$ and $*p \leq 0.01$.

Figure 2-3. p33 and p35 exit the ER through different routes. (A) HEK293T cells were transfected with DR (DRα + DRβ) together with control YFP or NleA-GFP. Some conditions included p33LIML, p35LIML or Ii (p33 + p35). After 48 h, cells were analyzed by flow cytometry for the expression, in GFP- or YFP-positive cells, of DR using L243 and secondary Alexa Fluor 633 goat anti-mouse antibody. Histograms are plotted as % of max to account for the differences in transfection efficiencies. The shaded curves (Ctrl) represent the fluorescence background of mock-transfected cells stained in the same conditions. (B) HEK293T cells were mock-transfected or transfected with DR (DRα + DRβ) together with p33, p35 or Ii (p33 + p35). After 48 h, cells were lysed and the expression of Ii isoforms was analyzed on immunoblots using the Pin.1 mAb specific for both p33 and p35 (upper panel). In addition, cell lysates were analyzed with a rabbit serum specific for the p35 N-terminal 16 amino acids extension (lower panel). Top and bottom arrows show the p35 and p33 isoforms, respectively. Densitometry revealed a

relative p35:p33 expression ratio of 3:2. Arrows indicate the position of the two isoforms. (C) Aliquots of cells used in panel A were stained for the expression of Ii at the cell surface using BU45 and secondary Alexa Fluor 633 goat anti-mouse antibody. (D) The MFIs obtained for live or permeabilized cells were plotted as a ratio for MHCII (XD5) and Ii (BU45). (E) MFIs obtained for cell surface CLIP (CerCLIP.1 mAb). Error bars indicate the SD from five independent experiments. Paired Student's *t*-tests were performed; $^{*}p \leq 0.05$ and $^{*}p \leq 0.01$.

2.13. Figures

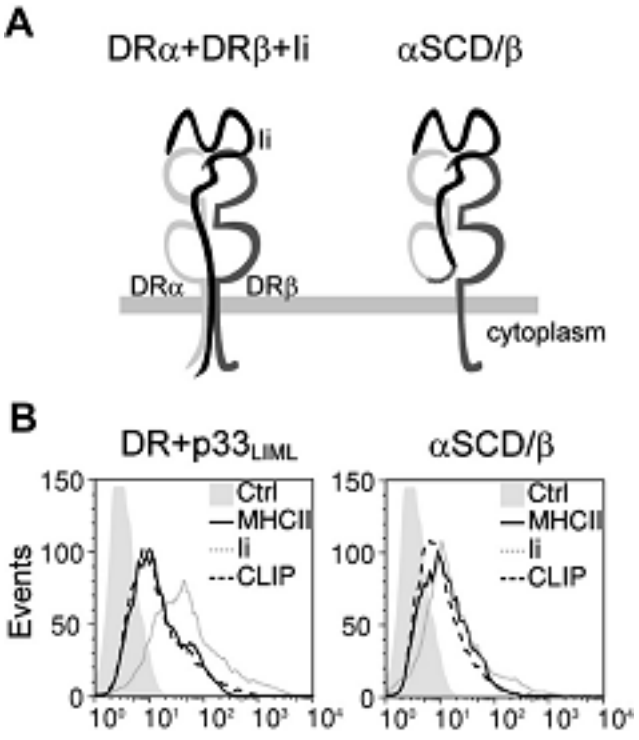

Figure 2-1. Schematic representation and trafficking of aSCD.

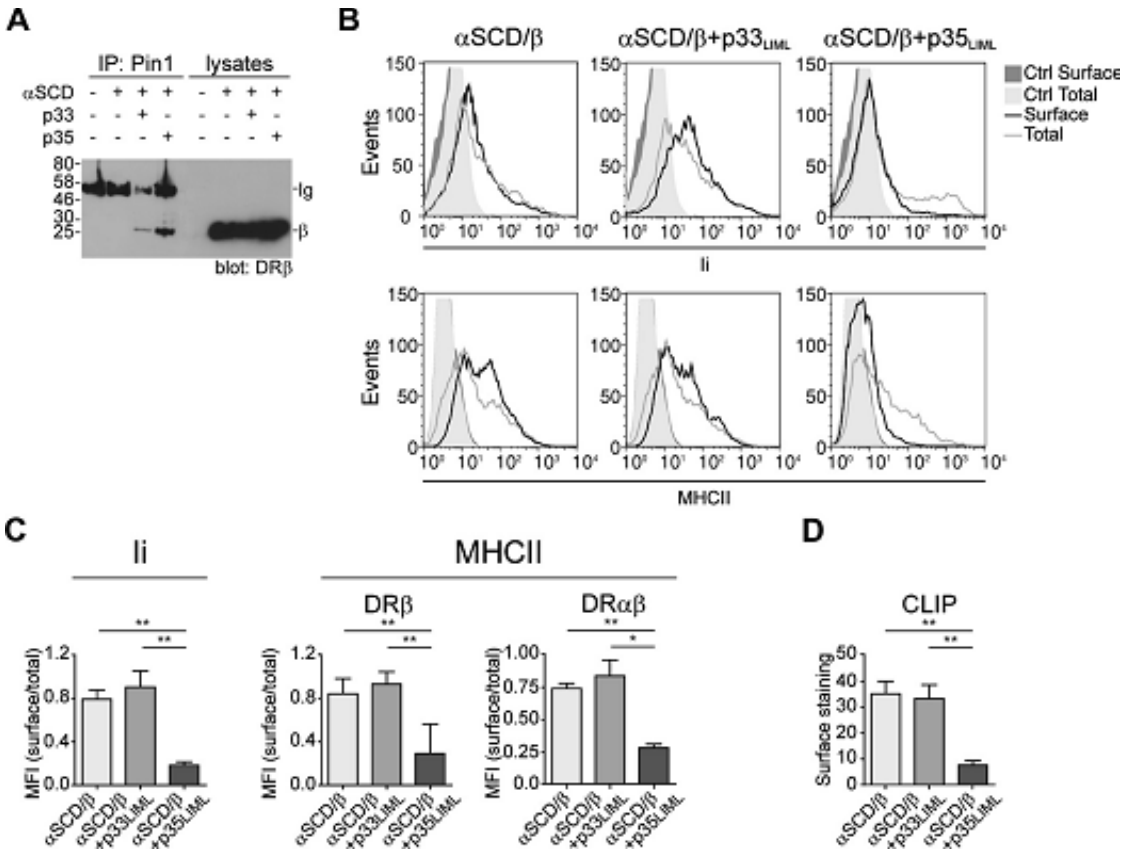

Figure 2-2. Masking of the p35 ER retention motif requires a direct association with the MHCIIβ chain.

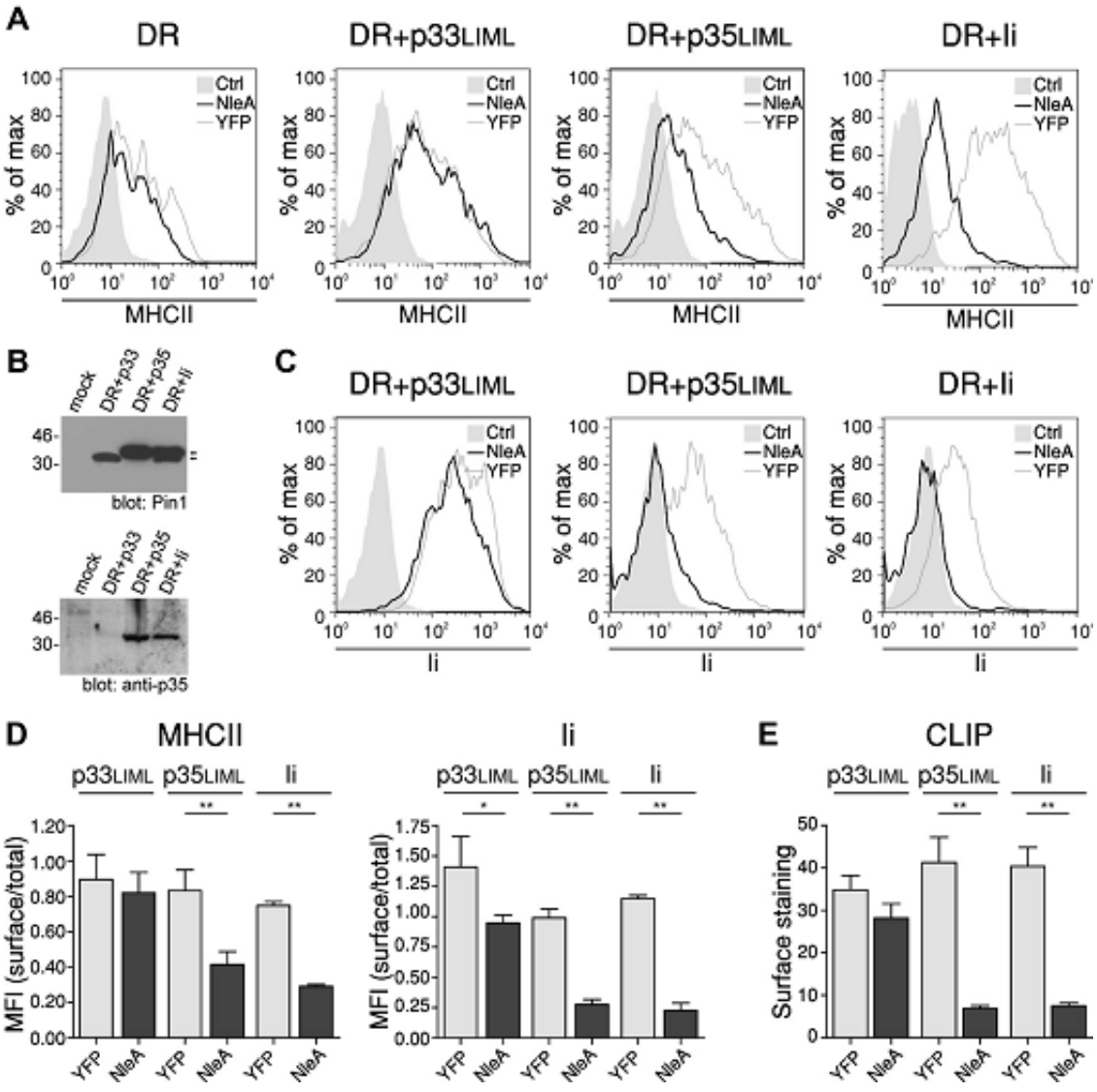

Figure 2-3. p33 and p35 exit the ER through different routes.

2.14. Supplementary data

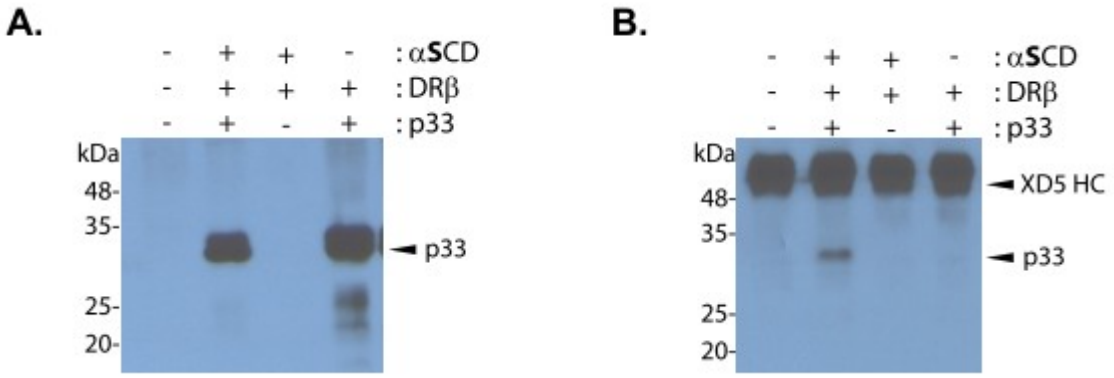

Figure 2-4. Iip33 interacts with DRβ only in presence of αSCD. (A) HEK 293XT cells were transiently transfected and lyzed after 48h. Whole cell lysates were separated in reducing conditions on SDS-PAGE and blotted for Ii using a combination of D-6 (Genève et al. Monoclon Antib Immunodiagn Immunother. 2014; 33:221-7), a mAb specific for the cytoplasmic tail of Ii (Santa Cruz Biotechnology Inc.), and HRP-coupled anti-mouse heavy chain antibody (Jackson ImmunoResearch). The arrow points to p33. **(B)** Protein G sepharose beads (GE Healthcare Bio-Sciences Inc.) were coupled to the XD5 mAb and used to immunoprecipitate DRβ from the lysates described in panel A. Samples were blotted with D-6 as in panel A. Arrows point to p33 and heavy chain of XD5 used for immunoprecipitations.

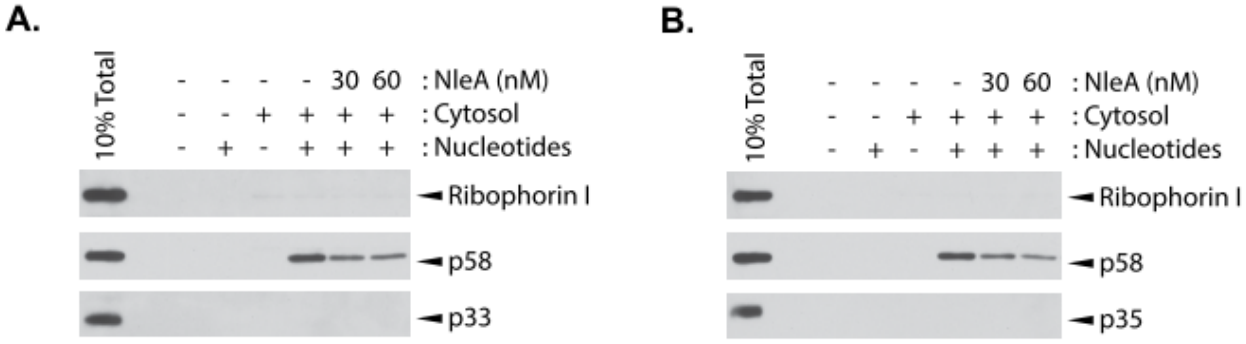

Figure 2-5. COPII vesicle formation assay. An in vitro COPII vesicle formation assay was performed as described previously (Kim et al., Cell Host Microbe. 2007; 2:160-71). Semi-intact cells were prepared using HeLa cells stably expressing HLA-DR1 with either p33 (A) or

p35 (B). Rat liver cytosol (4 mg/ml final concentration) was used as a source of COPII proteins. Nucleotides include GTP and an ATP regenerating system (Kim et al., Cell Host Microbe. 2007; 2:160-71). Isolated budded vesicle fractions and 10% of the total semi-intact cells (10% total) were solubilized, separated on an SDS-PAGE, and probed for ribophorin I (an ER resident protein), p58/ERGIC53/LMAN1 (an ER-Golgi recycling protein) and Ii. Ribophorin I should not be found in the vesicle fraction, whereas p58/ERGIC53/LMAN1 should be found in the vesicle fraction in a cytosol and nucleotide-dependent manner. Ii was not found in the COPII vesicle fraction under the current assay condition.

Chapitre 3. Résultats de l'article 2

Ce manuscrit est reproduit avec la permission de tous les auteurs.

3.1. Contribution des auteurs

J'ai procédé aux expériences et préparé toutes les figures. Jacques Thibodeau et moi avons planifié le projet, procédé aux analyses et écrit cet article.

3.2. The NleA virulence factor alters the trafficking of both Iip35 in a COPII-dependant manner and HLA-DQ independently of its β chain cytoplasmic tail

Catherine Gauthier,[*] and Jacques Thibodeau[*]

[*]Laboratoire d'Immunologie Moléculaire, Département de Microbiologie, Infectiologie et Immunologie, Université de Montréal, Montreal, Quebec HC3 3J7, Canada;

Status : In preparation

3.3. Abstract

Enteropathogenic *Escherichia coli* (EPEC) and enterohemorrhagic *E. coli* (EHEC) are important pathogens of humans. They induce attaching-effacing (A/E) lesions in the gut, where they take control over the host they infect while staying completely extracellular. They possess in their genome a locus of enterocyte effacement, or LEE, that codes for a variety of virulence factors, including a type 3 secretion system. Upon its translocation into the infected enterocyte, the non-LEE encoded factor A (NleA) interacts with Sec24, a core component of the COPII system, inducing its total disruption. A key mechanism used by the enterocytes in order to protect themselves is to react to the IFN-γ secreted by surrounding activated immune cells, leading to antigen presentation by MHC class II. Our group recently showed that NleA affects the trafficking of the human invariant chain p35 isoform. Here, we demonstrate that this impairment is COPII-dependant. Moreover, we provide evidence that NleA also subverts HLA-DQ surface expression. Altogether, this suggests that NleA is a very potent virulence factor that may partially counteract MHCII antigen presentation, which is one of the host's best defense mechanisms.

3.4. Introduction

Homeostasis between the intestinal epithelium of animals and commensal microorganisms of the microbiota must be tightly regulated to maintain health. Various strains of *Escherichia coli* are part of the human microbiota, whereas others are long known pathogens. Enteropathogenic *E. coli* (EPEC) causes severe diarrheas in children, and enterohemorrhagic *E. coli* (EHEC) is responsible for both hemorrhagic colitis and hemolytic-uremic syndrome (1-4). They induce in their host attaching-effacing (A/E) lesions as they attach to the apical face of enterocytes and destroy the microvilli architecture of the epithelium (1, 5, 6). A/E bacteria display in their genome a pathogenicity island essential to their virulence. This locus of enterocyte effacement (LEE) is expressed as the bacteria attaches to an enterocyte (2, 7). Numerous LEE and non-LEE encoded effectors are translocated directly from the bacteria into the targeted cell by a LEE-encoded type 3 secretion system (T3SS) (8-

10). This enables the pathogen to take control over the host cell's cytoskeleton machinery and create a pedestal structure at the top of the enterocyte (11-14).

Upon the onset of the immune response, activated antigen-presenting cells (APCs) secrete IL-12, which further activates macrophages, T cells and NK T cells (15, 16). In turn, the IFN-γ secreted by these cells induces the expression of MHC class II (MHCII) in enterocytes (16, 17). Both pathogens and hosts are continually evolving in order to develop attack and defense mechanisms against one another in a never ending arms race (18-27). It was recently shown that EHEC, but not EPEC, could subvert the IFN-γ pro-inflammatory pathway in order to evade the host immune response (28, 29). Surely, EPEC must have also evolved to counteract this key signaling pathway.

The non-LEE encoded effector A (NleA) is known to disrupt COPII vesicle trafficking by binding the COPII subunit Sec24 (30, 31). Ultimately, the tight junctions between enterocytes are destructed and the integrity of the intestinal epithelium is lost, as shown in infection experiments *in vitro* with EPEC and in mice with *Citrobacter rodentium*, an A/E pathogen (8, 32, 33). Our group showed that the expression of NleA in artificial APCs affects the trafficking of Iip35, an important player in antigen presentation by MHCII in humans (34). MHCII molecules, expressed in APCs and activated epithelial cells, are made of an α and a β chain that dimerize in the endoplasmic reticulum after biosynthesis (17, 35, 36). The invariant chain (Ii) facilitates αβ association, and then drives MHCII out of the ER and towards the endocytic compartment known as the MIIC (37, 38). There, MHCII meets and loads up a high-affinity exogenous peptide (39-41). The MHCII-peptide complex is then bound to the plasma membrane in order to be recognized by a specific CD4+ T cell (42). In humans, there are three isotypes of MHCII (HLA-DP, -DQ and -DR) and four isoforms of Ii (p33, p35, p41 and p43) (43, 44). The two predominant forms of Ii (p33 and p35) differ in a 16 amino acid extension bore by p35 at its N-terminal end (44, 45). It has been suggested that this extension drives the selection of Iip35, but not p33, in COPII vesicles (34, 46).

Considering the major role of IFN-γ in the clearance of A/E pathogens, our group focused on further dissecting the mechanism of action of NleA on the trafficking of the MHCII antigen presentation molecules. We provide evidence that Iip35 is dependent on

COPII for ER egress, strongly suggesting that NleA acts through this pathway in order to tone down antigen presentation. Finally, our data show that in addition to Iip35, HLA-DQ is also negatively regulated by NleA in artificial APCs. This highlights the idea that MHCII evolved and diversified to avoid being completely subverted by a single virulence factor or pathogen (47-49). On the other hand, considering the variability in the repertoire of peptides presented by the three MHCII isotypes, one can suggest that A/E pathogens found a way to alter antigen presentation by a MHCII isotype crucial to its clearance. Both scenarios corroborate the fact that the everlasting trench war between host and pathogen plays a great role in shaping these organisms.

3.5. Methods

Plasmids and cell lines

The following plasmids were already described: human pcDNA3.1 Iip33, Iip35, Ii (p33+p35), HLA-DRα and HLA-DRβ (50, 51); pBud HLA-DR (52); pLNCX HLA-DQ (53); pNleA-GFP (31). DRβ/DPcyto, DRβ/DQcyto and DRβAAA.1 cDNA were excised from previously described SRαpuro constructs and subcloned into pcDNA3. (52, 53). This plasmid and pcDNA3.1 YFP were purchased from Invitrogen. HEK293T cells were transiently transfected using polyethilenimine (Polyscience, PA). Cells were cultured in DMEM supplemented with 5% FBS (Wisent, Saint-Bruno, Canada).

Antibodies

The murine BU45 mAb recognizes the C-terminal region of human Ii, and L243 the HLA-DR dimer (54). For indicated experiments, FITC-coupled L243 and Alexa Fluor 647-coupled BU45 (Invitrogen, cat. no. A20186) were used. The Tu169 (mouse, anti-DQ) mAb was purchased from Biolegend (cat. no. 555562), the D-6 (mouse, N-terminal region of Ii) mAb and E19-R (rabbit, N-terminal region of Sec23)

mAb from Santa Cruz Biotechnology (cat. no. sc- 137217 and sc-12107-R) (50), and the rabbit anti-Sec13 pAb from Sigma-Aldrich (cat. no. SAB1411243). For secondary antibodies, the Alexa Fluor 488- and 633-coupled goat anti-mouse antibodies were used for flow cytometry (Invitrogen); HRP-coupled goat anti-mouse and anti-rabbit antibodies were used for Western blotting (Jackson Immunoresearch, PA).

Flow cytometry

24 or 48h after transfection, 10^6 cells were resuspended in staining buffer (PBS, BSA 1%). For total staining, cells were fixed 15 min in 4% paraformaldehyde, washed three times, and permeabilized for 15 min in staining buffer containing 0.05% saponin. Cells were then stained 30 min with the indicated primary antibodies in the appropriate staining buffer and washed. The previous step was repeated for secondary antibody staining when needed. Cells were analyzed on a FACSCalibur® flow cytometer (Becton Dickinson, Mississauga, Canada).

Western blotting

Cells were lyzed at 4°C in lysis buffer containing 1% CHAPS. Protein G sepharose beads (GE Healthcare) were coupled to the indicated antibodies and used for immunoprecipitation. Samples were subjected to SDS-PAGE. Proteins were detected by chemiluminescence (Roche)

3.6. Results and discussion

Iip35, but not Iip33, directly interacts with COPII subunits

Previous results from our team show that Iip35 surface expression is affected by NleA in artificial APCs, whereas Iip33 is not (34). To further understand the mechanism underlying

the effect of that virulence factor over Ii, we looked for direct interaction between Ii and COPII subunits. The COPII system is well characterized in yeast and mammals (reviewed in (55) and (56)): five subunits form the main core of these vesicles. These are Sar1, Sec23, Sec24, Sec13 and Sec31 (57). It is known that Sec24 is tightly related to cargo selection and it is also the subunit directly bound by NleA (58). Therefore, we assessed whether Ii could also bind to COPII subunits. Cells were transfected with either Iip33, p35 or both. The expression of these proteins was confirmed by intracellular staining and FACS analyses and by immunoblot (Fig. 3-1A-B). We used a biochemistry approach to detect an interaction between Sec23 and the different Ii isoforms. Figure 3-1C clearly shows that Iip35 expressed alone is co-immunoprecipitated with the COPII Sec23 subunit, whereas p33 is very slightly detected. This suggests an important interaction of Iip35 homotrimers with COPII components, and a minor one for Iip33 homotrimers with COPII. The two large bands detected in the $p33^{+}p35^{+}$ lane further confirm this. Since Ii heterotrimers can incorporate both p33 and p35 moieties, the p35 moiety interacts with COPII and is co-immunoprecipitated, taking p33 down. Results in Fig. 3-1D corroborate those in Fig. 3-1C : Iip35, but not p33, is detected upon CO-IP with Sec13. This is reminiscent of the results obtained earlier in NleA assays which showed impaired surface expression of Iip35 but not p33 (34).

Knowing that Iip33 and p35 differ only in the 16 amino acid extension bore by p35, the motif recognized by the COPII subunits must be encoded in this extension (44). However, none of the currently identified motifs recognized by Sec24 appears in that sequence (59). It has been put forward by Giraudo et al. that the COPII component Sar1 also plays a role in cargo selection and recognizes signals made of basic amino acids (46). In that regard, the Iip35 N-terminal RRR motif could explain the strong interaction observed with COPII components (46). The other arginine residues common to both Ii isoforms could be a signal of lesser importance, which would be coherent with the slight interaction detected between Iip33 and COPII subunits (44, 46, 60). Taken together, our results provide new insight into ER egress by Ii complexes, suggesting that the arginine residues common to Iip33 and p35, and the ones found in the Iip35 extension make up a strong signal recognized by COPII subunits, probably by Sar1. The effect of NleA over Iip35 must therefore be COPII-mediated.

Neither HLA-DR nor DQ directly interact with COPII subunits

Using the same technique, cells were co-transfected with the different isoforms of Ii with or without MHCII (HLA-DR or DQ), stained and analyzed by FACS to confirm protein expression (Fig. 3-1A), then lyzed and subjected to CO-IP with Sec23 or Sec13. Figure 3-1C shows the same Ii detection levels in lanes expressing p35 or the two isoforms, with or without MHCII. The slight band observed in the $p33^{+}MHCII^{-}$ cells lane also appears when HLA-DQ is co-expressed, but it seems to be lost upon co-expression of HLA-DR. The FACS plots of $Iip33^{+}$ and $Iip33^{+}DR^{+}$ cells show the same expression levels of Iip33, but there is a drastic difference in the corresponding cell lysates. This could indicate protein degradation in the $Iip33^{+}DR^{+}$ sample after cell lysis and explain the undetectable level of Iip33 on immunoblots. Another explanation would be the loss of minor interaction between Iip33 and COPII components upon co-expression of HLA-DR. That could be related to faster ER egress of p33 homotrimers bound to MHCII. Since this effect is not seen in the samples from $Iip33^{+}DQ^{+}$ cells, this effect could be specific to HLA-DR. What is common to both $Iip33^{+}MHCII^{+}$ lanes is that the detection level of Iip33 is not greater than in the $MHCII^{-}$ corresponding condition. These findings are corroborated in Fig. 3-1D. That suggests that MHCII does not add to the minor Iip33 interaction with COPII subunits and, therefore, the two MHCII isotypes would not interact directly with COPII. A simple way to address that issue would be to perform an immunoblot for MHCII with the same CO-IP conditions used in Fig. 3-1C-D.

Surface expression of HLA-DQ, but not HLA-DR, is affected by NleA

In order to deepen our understanding of the role played by NleA in affecting antigen presentation by MHCII, we then looked at the surface expression of different isotypes upon expression of NleA in artificial APCs. Cells were co-transfected with plasmids coding for either HLA-DR or DQ and YFP or GFP-tagged NleA. Intracellular staining and FACS analysis confirmed protein expression (Fig. 3-2A). Figure 3-2B clearly clearly shows slight but not significant decrease in the HLA-DR surface expression rate upon NleA expression. However, there is a dramatic decrease in HLA-DQ surface expression rate when the virulence

factor is co-transfected. That data implies that NleA somehow affects the intracellular trafficking of HLA-DQ, but not HLA-DR, thereby keeping it from reaching the cell surface. Taking together figure 3-1C-D and figure 3-2, we cannot rule out the possibility that the mechanism by which NleA affects DQ is COPII-related, but an MHCII immunoblot could possibly answer this question.

The NleA effect over HLA-DQ surface expression does not depend on DQβ cytoplasmic tail

COPII sorting of MHC class I (MHCI) is mediated by the conserved α chain C-terminal hydrophobic residue, an alanine or a valine, depending on the isotype and allele (61). This mechanism may also apply to ER egress by MHCII molecules. All three MHCII isotypes α chain bear a leucine residue at their C-terminal amino acid (GenBank M60334.1, NM_033554.3, HE965627.1). Leucine is a hydrophobic residue, just like valine and alanine. The C-terminal residue differs in every MHCII β chain: HLA-DRβ displays a conserved serine residue (UniProtKB O19730), HLA-DPβ an alanine (GenBank M57466.1) and HLA-DQβ a histidine (GenBank L34105.1). Serine and histidine are polar residues. We therefore inquired if the chemical properties of the MHCIIβ last amino acid could confer resistance to NleA. Cells were co-transfected with wild type (WT) HLA-DR, WT HLA-DQ or constructs of DR bearing a mutated β chain cytoplasmic region. They also received either YFP or GFP-tagged NleA plasmids. The first panel of figure 3-3A shows that the surface expression of WT HLA-DR is mostly unchanged upon NleA co-expression, as demonstrated in Fig. 3-2B. WT DR was used as a negative control for the following conditions. Again we observed a decrease in WT HLA-DQ when co-expressed with NleA on panel 5 of Fig. 3-3A. Its significant decrease, as compared to WT DR in Fig.3-3B, is coherent with Fig. 3-2B as well. Panels 2-4 of Fig.3B correspond to constructs bearing respectively an alanine, a histidine and an alanine at the C-terminal end of MHCIIβ. As shown on the plots (Fig. 3-3A) and as compared to WT DR on the bar chart (Fig. 3-3B), there is no significant difference in surface expression of these constructs upon co-expression with either YFP or GFP-tagged NleA. This suggests that there is no significant effect of NleA over their surface expression.

By relating the behavior of the above mentioned HLA-DR constructs to their sequence, it can be appreciated that whether they displayed the WT β chain C-terminal serine residue, or a mutated cytoplasmic tail bearing either an alanine or a histidine, their sorting was unchanged upon co-expression of NleA. That data shows no correlation between the last residue being hydrophobic or not and an effect on surface expression upon co-expression with NleA. Also, the simple fact that WT DQβ bears a histidine at this position and is still affected by NleA indicates that the last amino acid at this end of MHCIIβ does not dictate the MHCII fate. Furthermore, since all MHCII α chains bear a leucine residue at their C-terminal end but are differentially affected by NleA, then that residue cannot be accounted for NleA's effect. Considering, the direct effect of NleA over COPII vesicle formation, we may suggest that neither the C-terminal residues of MHCII α nor β chain mediate MHCII selection by COPII subunits. So to speak, our data concerning MHCII is not consistent with the theory put forward for MHCI (61).

Moreover, if the HLA-DR variant bearing the cytoplasmic region of DQβ could not reconstitute the NleA effect on DQ, and considering that COPII selection is usually mediated by the cytoplasmic tail signals (62), we may put forward that COPII subunits might recognize a signal in DQα which is absent in DRα. In that regard, the observed NleA effect over HLA-DQ could be attributed to such a motif in DQα.

3.7. Conclusion

Virulence factors are powerful effectors developed by pathogens in order to attack their hosts or subvert their defense mechanisms. The NleA molecule produced by enteropathogenic *Escherichia coli* (EPEC) is certainly a great example of a very effective virulence factor, since its translocation into human enterocytes induces both the disruption in intracellular trafficking and the destruction of the gut's epithelial architecture. It was recently shown that NleA also affects the trafficking of Iip35, which

is crucial to antigen presentation by MHCII. Our group now puts forward that this effect is the result of COPII disruption by NleA, since Iip35 interacts directly with COPII subunits, probably Sar1. We also demonstrate that HLA-DQ surface expression is toned down upon NleA expression, unlike HLA-DR which is not affected as much. The underlying mechanism could be COPII-related, but it is surely different from the way MHCI molecules are selected by COPII subunits. Taken together, our results show that EPEC has evolved to develop a very efficient virulence factor able to dramatically affect key players from one of vertebrate's best defense mechanisms: MHCII antigen presentation.

3.8. Funding

This project was funded by the National Science and Engineering Research Council of Canada (NSERC) [grant no.298537]. CG was supported by studentships from the Canadian Institutes of Health Research (CIHR), the UdeM Medicine faculty and the UdeM Microbiology, Infectiology and Immunology department.

3.9. Acknowledgements

We thank Dr Samantha Gruenheid for the GFP-tagged NleA plasmid and Serge Sénéchal for helping with the flow cytometry.

3.10. Author disclosure statement

The authors have no financial interests to disclose.

3.11. Abbreviations

A/E, attaching-effacing; APC, antigen presenting cell; CO-IP, co-immunoprecipitation; *E. coli*, *Escherichia coli*; EHEC, enterohemorrhagic *E. coli*; EPEC, enteropathogenic *E. coli*; ER, endoplasmic reticulum; Ii, invariant chain; LEE, locus of enterocyte effacement; MHCI, major histocompatibility complex class I; MHCII, major histocompatibility complex class I; MIIC, MHCII rich compartment; T3SS, type 3 secretion system.

3.12. References

1. Levine MM. *Escherichia coli that cause diarrhea: enterotoxigenic, enteropathogenic, enteroinvasive, enterohemorrhagic, and enteroadherent*. J Infect Dis. 1987;155(3):377-89.
2. McDaniel TK, Jarvis KG, Donnenberg MS, Kaper JB. *A genetic locus of enterocyte effacement conserved among diverse enterobacterial pathogens*. Proc Natl Acad Sci U S A. 1995;92(5):1664-8.
3. Yoshioka K, Yagi K, Moriguchi N. *Clinical features and treatment of children with hemolytic uremic syndrome caused by enterohemorrhagic Escherichia coli O157:H7 infection: experience of an outbreak in Sakai City, 1996*. Pediatr Int. 1999;41(2):223-7.
4. Levine MM, Xu JG, Kaper JB, Lior H, Prado V, Tall B, et al. *A DNA probe to identify enterohemorrhagic Escherichia coli of O157:H7 and other serotypes that cause hemorrhagic colitis and hemolytic uremic syndrome*. J Infect Dis. 1987;156(1):175-82.
5. Griffin PM, Tauxe RV. *The epidemiology of infections caused by Escherichia coli O157:H7, other enterohemorrhagic E. coli, and the associated hemolytic uremic syndrome*. Epidemiol Rev. 1991;13:60-98.

6. Moon HW, Whipp SC, Argenzio RA, Levine MM, Giannella RA. *Attaching and effacing activities of rabbit and human enteropathogenic Escherichia coli in pig and rabbit intestines*. Infect Immun. 1983;41(3):1340-51.
7. Perna NT, Mayhew GF, Posfai G, Elliott S, Donnenberg MS, Kaper JB, et al. *Molecular evolution of a pathogenicity island from enterohemorrhagic Escherichia coli O157:H7*. Infect Immun. 1998;66(8):3810-7.
8. Deng W, Li Y, Vallance BA, Finlay BB. *Locus of enterocyte effacement from Citrobacter rodentium: sequence analysis and evidence for horizontal transfer among attaching and effacing pathogens*. Infect Immun. 2001;69(10):6323-35.
9. Zaharik ML, Gruenheid S, Perrin AJ, Finlay BB. *Delivery of dangerous goods: type III secretion in enteric pathogens*. Int J Med Microbiol. 2002;291(8):593-603.
10. Deng W, Puente JL, Gruenheid S, Li Y, Vallance BA, Vazquez A, et al. *Dissecting virulence: systematic and functional analyses of a pathogenicity island*. Proc Natl Acad Sci U S A. 2004;101(10):3597-602.
11. Knutton S, Baldwin T, Williams PH, McNeish AS. *Actin accumulation at sites of bacterial adhesion to tissue culture cells: basis of a new diagnostic test for enteropathogenic and enterohemorrhagic Escherichia coli*. Infect Immun. 1989;57(4):1290-8.
12. Nataro JP, Kaper JB. *Diarrheagenic Escherichia coli*. Clin Microbiol Rev. 1998;11(1):142-201.
13. Elliott SJ, Yu J, Kaper JB. *The cloned locus of enterocyte effacement from enterohemorrhagic Escherichia coli O157:H7 is unable to confer the attaching and effacing phenotype upon E. coli K-12*. Infect Immun. 1999;67(8):4260-3.
14. Elliott SJ, Sperandio V, Giron JA, Shin S, Mellies JL, Wainwright L, et al. *The locus of enterocyte effacement (LEE)-encoded regulator controls expression of both LEE- and non-LEE-encoded virulence factors in enteropathogenic and enterohemorrhagic Escherichia coli*. Infect Immun. 2000;68(11):6115-26.
15. Schroder K, Hertzog PJ, Ravasi T, Hume DA. *Interferon-gamma: an overview of signals, mechanisms and functions*. J Leukoc Biol. 2004;75(2):163-89.
16. Zhang SY, Boisson-Dupuis S, Chapgier A, Yang K, Bustamante J, Puel A, et al. *Inborn errors of interferon (IFN)-mediated immunity in humans: insights into the respective roles of IFN-alpha/beta, IFN-gamma, and IFN-lambda in host defense*. Immunol Rev. 2008;226:29-40.
17. Thelemann C, Eren RO, Coutaz M, Brasseit J, Bouzourene H, Rosa M, et al. *Interferon-gamma induces expression of MHC class II on intestinal epithelial cells and protects mice from colitis*. PLoS One. 2014;9(1):e86844.
18. Dennehy JJ. *What Can Phages Tell Us about Host-Pathogen Coevolution?* Int J Evol Biol. 2012;2012:396165.
19. Coffin JM. *Virions at the gates: receptors and the host-virus arms race*. PLoS Biol. 2013;11(5):e1001574.
20. Koonin EV, Dolja VV. *A virocentric perspective on the evolution of life*. Curr Opin Virol. 2013;3(5):546-57.
21. Restif O. *An offer you cannot refuse: down-regulation of immunity in response to a pathogen's retaliation threat*. J Evol Biol. 2013;26(9):2021-30.
22. Wu B, Gong J, Yuan S, Zhang Y, Wei T. *Patterns of evolutionary selection pressure in the immune signaling protein TRAF3IP2 in mammals*. Gene. 2013;531(2):403-10.

23. Best A, White A, Boots M. *The coevolutionary implications of host tolerance*. Evolution. 2014;68(5):1426-35.
24. Kodaman N, Pazos A, Schneider BG, Piazuelo MB, Mera R, Sobota RS, et al. *Human and Helicobacter pylori coevolution shapes the risk of gastric disease*. Proc Natl Acad Sci U S A. 2014;111(4):1455-60.
25. Lei BR, Olival KJ. *Contrasting patterns in mammal-bacteria coevolution: bartonella and leptospira in bats and rodents*. PLoS Negl Trop Dis. 2014;8(3):e2738.
26. Schlesinger KJ, Stromberg SP, Carlson JM. *Coevolutionary immune system dynamics driving pathogen speciation*. PLoS One. 2014;9(7):e102821.
27. Tellier A, Moreno-Gamez S, Stephan W. *Speed of adaptation and genomic footprints of host-parasite coevolution under arms race and trench warfare dynamics*. Evolution. 2014;68(8):2211-24.
28. Ho NK, Crandall I, Sherman PM. *Identifying mechanisms by which Escherichia coli O157:H7 subverts interferon-gamma mediated signal transducer and activator of transcription-1 activation*. PLoS One. 2012;7(1):e30145.
29. Ho NK, Ossa JC, Silphaduang U, Johnson R, Johnson-Henry KC, Sherman PM. *Enterohemorrhagic Escherichia coli O157:H7 Shiga toxins inhibit gamma interferon-mediated cellular activation*. Infect Immun. 2012;80(7):2307-15.
30. Gruenheid S, Sekirov I, Thomas NA, Deng W, O'Donnell P, Goode D, et al. *Identification and characterization of NleA, a non-LEE-encoded type III translocated virulence factor of enterohaemorrhagic Escherichia coli O157:H7*. Mol Microbiol. 2004;51(5):1233-49.
31. Kim J, Thanabalasuriar A, Chaworth-Musters T, Fromme JC, Frey EA, Lario PI, et al. *The bacterial virulence factor NleA inhibits cellular protein secretion by disrupting mammalian COPII function*. Cell Host Microbe. 2007;2(3):160-71.
32. Thanabalasuriar A, Koutsouris A, Weflen A, Mimee M, Hecht G, Gruenheid S. *The bacterial virulence factor NleA is required for the disruption of intestinal tight junctions by enteropathogenic Escherichia coli*. Cell Microbiol. 2010;12(1):31-41.
33. Thanabalasuriar A, Kim J, Gruenheid S. *The inhibition of COPII trafficking is important for intestinal epithelial tight junction disruption during enteropathogenic Escherichia coli and Citrobacter rodentium infection*. Microbes Infect. 2013;15(10-11):738-44.
34. Cloutier M, Gauthier C, Fortin JS, Geneve L, Kim K, Gruenheid S, et al. *ER egress of invariant chain isoform p35 requires direct binding to MHCII molecules and is inhibited by the NleA virulence factor of enterohaemorrhagic Escherichia coli*. Hum Immunol. 2015.
35. Machamer CE, Cresswell P. *Biosynthesis and glycosylation of the invariant chain associated with HLA-DR antigens*. J Immunol. 1982;129(6):2564-9.
36. Klein J, Sato A. *The HLA system. First of two parts*. N Engl J Med. 2000;343(10):702-9.
37. Roche PA, Cresswell P. *Proteolysis of the class II-associated invariant chain generates a peptide binding site in intracellular HLA-DR molecules*. Proc Natl Acad Sci U S A. 1991;88(8):3150-4.
38. Romagnoli P, Layet C, Yewdell J, Bakke O, Germain RN. *Relationship between invariant chain expression and major histocompatibility complex class II transport into early and late endocytic compartments*. J Exp Med. 1993;177(3):583-96.

39. Guagliardi LE, Koppelman B, Blum JS, Marks MS, Cresswell P, Brodsky FM. *Co-localization of molecules involved in antigen processing and presentation in an early endocytic compartment*. Nature. 1990;343(6254):133-9.
40. Neefjes JJ, Stollorz V, Peters PJ, Geuze HJ, Ploegh HL. *The biosynthetic pathway of MHC class II but not class I molecules intersects the endocytic route*. Cell. 1990;61(1):171-83.
41. Peters PJ, Neefjes JJ, Oorschot V, Ploegh HL, Geuze HJ. *Segregation of MHC class II molecules from MHC class I molecules in the Golgi complex for transport to lysosomal compartments*. Nature. 1991;349(6311):669-76.
42. Cresswell P. *Assembly, transport, and function of MHC class II molecules*. Annu Rev Immunol. 1994;12:259-93.
43. Simpson E. *Function of the MHC*. Immunol Suppl. 1988;1:27-30.
44. Koch N, Lauer W, Habicht J, Dobberstein B. *Primary structure of the gene for the murine Ia antigen-associated invariant chains (Ii). An alternatively spliced exon encodes a cysteine-rich domain highly homologous to a repetitive sequence of thyroglobulin*. EMBO J. 1987;6(6):1677-83.
45. Lamb CA, Cresswell P. *Assembly and transport properties of invariant chain trimers and HLA-DR-invariant chain complexes*. J Immunol. 1992;148(11):3478-82.
46. Giraudo CG, Maccioni HJ. *Endoplasmic reticulum export of glycosyltransferases depends on interaction of a cytoplasmic dibasic motif with Sar1*. Mol Biol Cell. 2003;14(9):3753-66.
47. Zhang M, He H. *Parasite-mediated selection of major histocompatibility complex variability in wild brandt's voles (Lasiopodomys brandtii) from Inner Mongolia, China*. BMC Evol Biol. 2013;13:149.
48. Sommer S. *The importance of immune gene variability (MHC) in evolutionary ecology and conservation*. Front Zool. 2005;2:16.
49. Spurgin LG, Richardson DS. *How pathogens drive genetic diversity: MHC, mechanisms and misunderstandings*. Proc Biol Sci. 2010;277(1684):979-88.
50. Geneve L, Gauthier C, Thibodeau J. *The D-6 mouse monoclonal antibody recognizes the CD74 cytoplasmic tail*. Monoclon Antib Immunodiagn Immunother. 2014;33(4):221-7.
51. Cloutier M, Gauthier C, Fortin JS, Thibodeau J. *The invariant chain p35 isoform promotes formation of nonameric complexes with MHC II molecules*. Immunol Cell Biol. 2014;92(6):553-6.
52. Khalil H, Brunet A, Thibodeau J. *A three-amino-acid-long HLA-DRbeta cytoplasmic tail is sufficient to overcome ER retention of invariant-chain p35*. J Cell Sci. 2005;118(Pt 20):4679-87.
53. Khalil H, Brunet A, Saba I, Terra R, Sekaly RP, Thibodeau J. *The MHC class II beta chain cytoplasmic tail overcomes the invariant chain p35-encoded endoplasmic reticulum retention signal*. Int Immunol. 2003;15(10):1249-63.
54. Faubert A, Samaan A, Thibodeau J. *Functional analysis of tryptophans alpha 62 and beta 120 on HLA-DM*. J Biol Chem. 2002;277(4):2750-5.
55. Budnik A, Stephens DJ. *ER exit sites--localization and control of COPII vesicle formation*. FEBS Lett. 2009;583(23):3796-803.
56. Brandizzi F, Barlowe C. *Organization of the ER-Golgi interface for membrane traffic control*. Nat Rev Mol Cell Biol. 2013;14(6):382-92.
57. Barlowe C. *COPII and selective export from the endoplasmic reticulum*. Biochim Biophys Acta. 1998;1404(1-2):67-76.

58. Wendeler MW, Paccaud JP, Hauri HP. *Role of Sec24 isoforms in selective export of membrane proteins from the endoplasmic reticulum*. EMBO Rep. 2007;8(3):258-64.
59. Mancias JD, Goldberg J. *Exiting the endoplasmic reticulum*. Traffic. 2005;6(4):278-85.
60. Bakke O, Dobberstein B. *MHC class II-associated invariant chain contains a sorting signal for endosomal compartments*. Cell. 1990;63(4):707-16.
61. Cho S, Ryoo J, Jun Y, Ahn K. *Receptor-mediated ER export of human MHC class I molecules is regulated by the C-terminal single amino acid*. Traffic. 2011;12(1):42-55.
62. Aridor M, Weissman J, Bannykh S, Nuoffer C, Balch WE. *Cargo selection by the COPII budding machinery during export from the ER*. J Cell Biol. 1998;141(1):61-70.

3.13. Figure legends

Figure 3-1. Iip35 directly interacts with components of the COPII system, whereas Iip33 does not. HEK293T cells were transiently transfected with different Ii isoforms with or without MHCII as indicated. 48h after transfection, cells were harvested. (A) The following antibody cocktails were used for total staining: Alexa Fluor 647-coupled BU45 (panels 1-3); FITC-coupled L243 and BU45-647 (panels 4-7). Cells for samples displayed in panels 8-11 were split and stained with either BU45-647 only or with Tu169 (anti-HLA-DQ, Biologend) followed by Alexa Fluor 488 goat anti-mouse (Invitrogen). Cells were analyzed by flow cytometry. Control conditions (Ctrl) represent background fluorescence emitted by non-transfected stained cells. (B) The rest of the cells was lyzed, (C) subjected to CO-IP with beads directed against Sec23 (E19-R, Santa Cruz) or (D) Sec13 (anti-Sec13, Sigma-Aldrich). (B,C,D) Samples were migrated on 12% SDS-PAGE and blotted for Ii with D-6 mAb (Santa Cruz) followed by HRP-coupled goat anti-mouse antibody (Jackson Immunoresearch).

Figure 3-2. Surface expression of HLA-DQ, but not HLA-DR, is affected by NleA. HEK293T cells were transiently transfected in triplicates with wild type WT HLA-DR or HLA-DQ, and either YFP or GFP-tagged NleA. (A) 24h after transfection, cells were harvested and split for surface or total staining. DR

transfected cells were stained with L243 and DQ transfected cells with Tu169 (anti-HLA-DQ, Biologend). Alexa Fluor 633 goat anti-mouse (Invitrogen) was used for all samples as secondary antibody. Cells were analyzed by flow cytometry. Control conditions (Ctrl) represent background fluorescence emitted by non-transfected stained cells. (B) Surface over total MFI ratios (surface expression rate) were plotted and analyzed with non-parametric Student *t* test.

Figure 3-3. Surface expression of HLA-DR constructs bearing mutations on the β chain cytoplasmic tail is not affected by NleA. HEK293T cells were transiently transfected in triplicates with either YFP or GFP-tagged NleA and with MHCII variants: WT DQ or WT DRα with either, WT DRβ, DRβAAA, DRβ/DQcyto or DRβ/DPcyto. (A) 24h after transfection, cells were harvested and split for surface or total staining. DR transfected cells were stained with L243 and DQ transfected cells with Tu169 (anti-HLA-DQ, Biologend). Alexa Fluor 633 goat anti-mouse (Invitrogen) was used for all samples as secondary antibody. Cells were analyzed by flow cytometry. Control conditions (Ctrl) represent background fluorescence emitted by non-transfected stained cells. (B) Surface expression rates of NleA over YFP were plotted and analyzed with one-way ANOVA and all compared to the WT DR control with the Dunnett method.

3.14. Figures

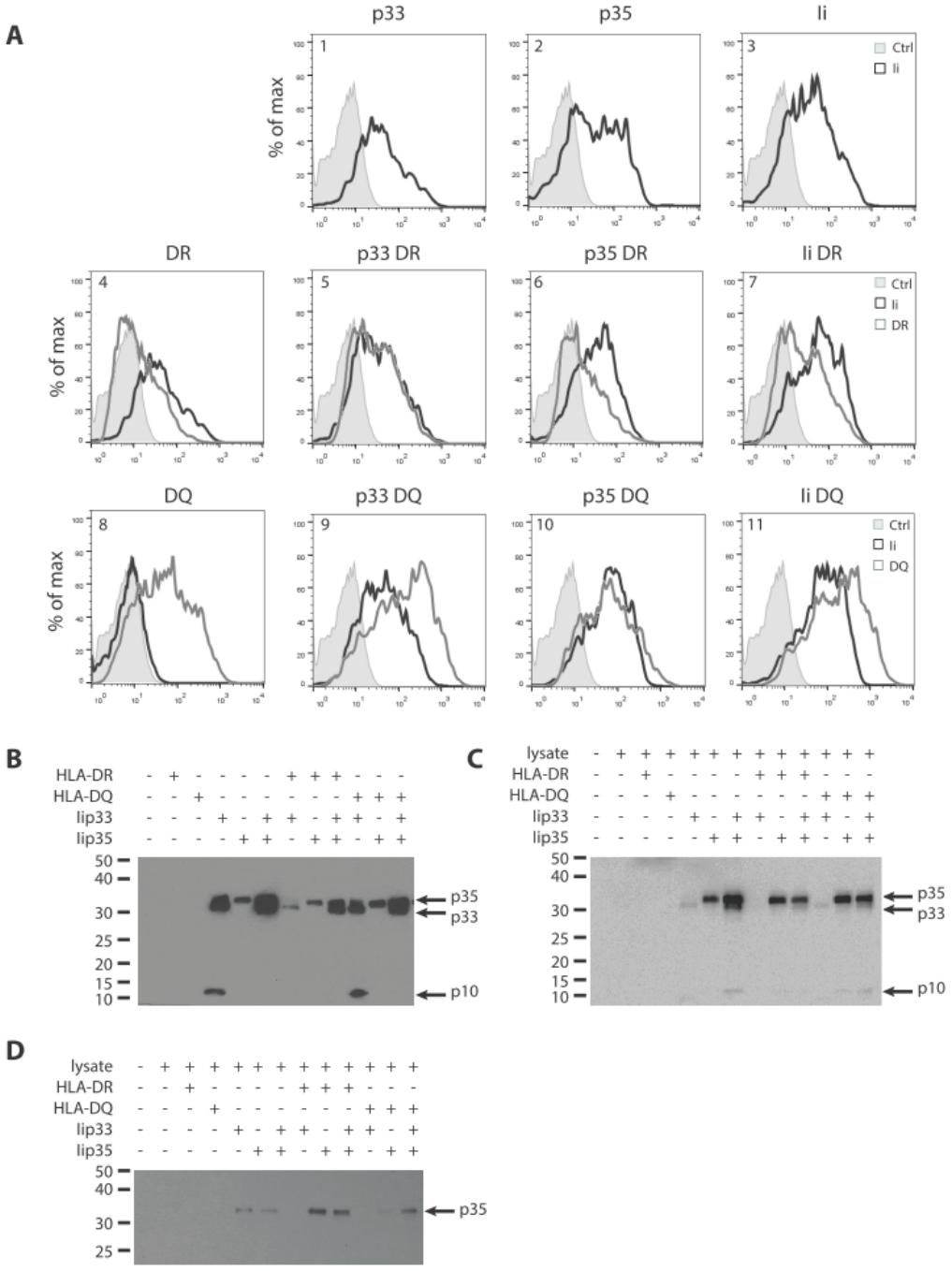

Figure 3-1. Iip35 directly interacts with components of the COPII system, whereas Iip33 does not.

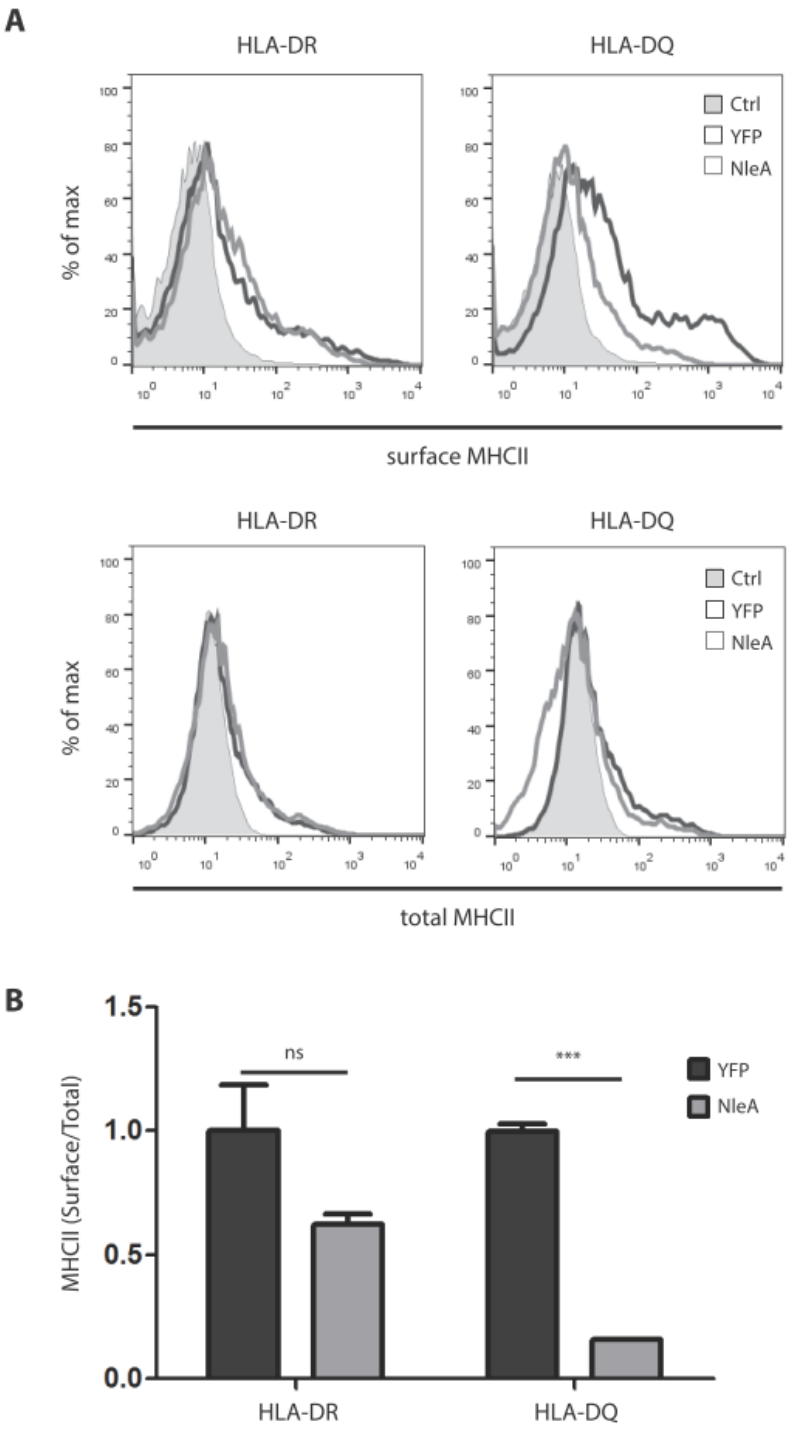

Figure 3-2. Surface expression of HLA-DQ, but not HLA-DR, is affected by NleA.

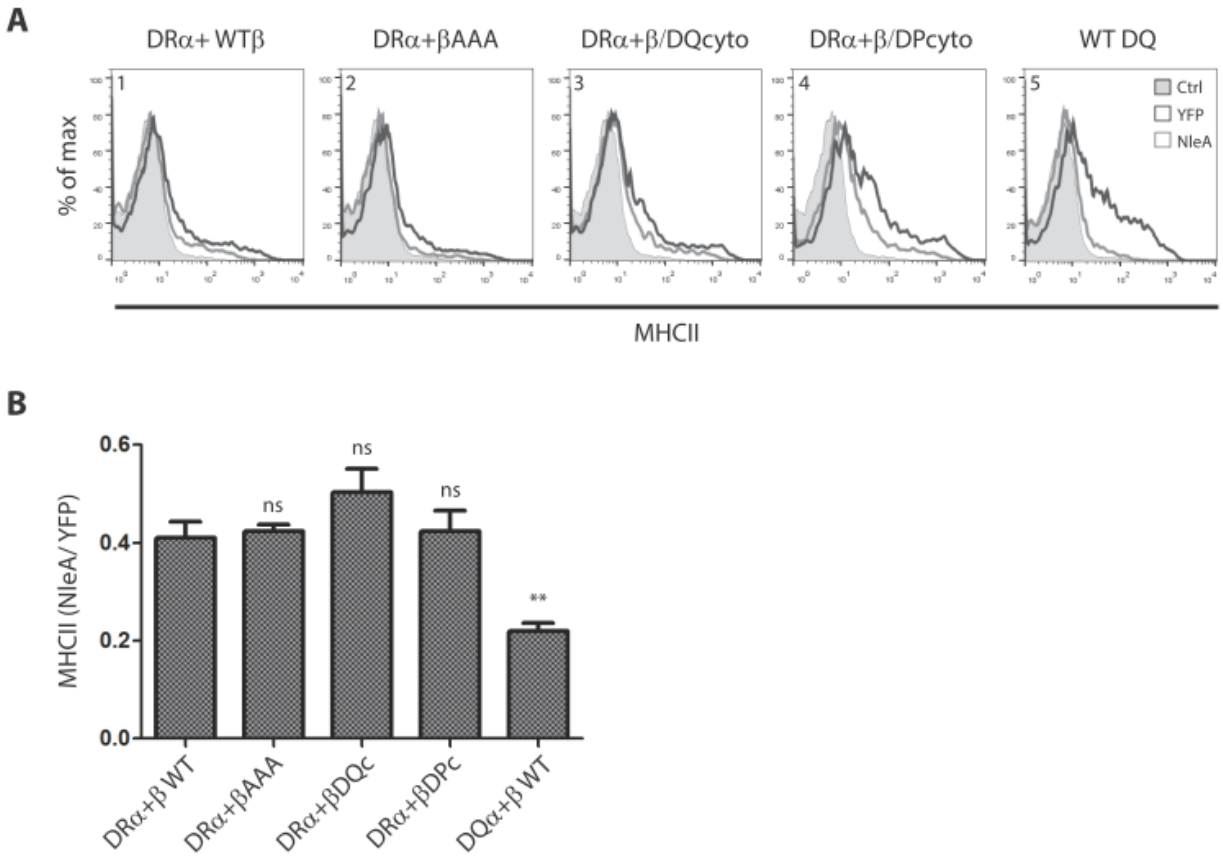

Figure 3-3. Surface expression of HLA-DR constructs bearing mutations on the β chain cytoplasmic tail is not affected by NleA.

Chapitre 4. Discussion

L'existence et le maintien dans l'évolution des vertébrés de quatre isoformes de la chaîne invariante doit impliquer des fonctions pour chacune d'elles qui sont non-redondantes. En ce qui a trait aux deux isoformes prédominantes de l'humain, Iip33 et p35, comme elles ne diffèrent que par l'extension cytosolique de 16 acides aminés de p35, cette extension supplémentaire doit procurer à Iip35 une variation de la fonction de son homologue p33 (92, 93). Le motif de rétention au réticulum endoplasmique de p35 est probablement central dans cette disparité fonctionnelle. Les contraintes reliées à la formation et au transport de complexes αβIi contenant Iip35 ont été investiguées et les résultats sont discutés ci-dessous.

4.1. Le rôle d'Iip35 dans l'assemblage de αβIi

Notre groupe a déjà montré que la région cytoplasmique de la chaîne β du CMH II est responsable du masquage du motif RXR chez Iip35 (118). De plus, une queue cytoplasmique longue de seulement trois acides aminés suffit au masquage (118). Par contre, le mode par lequel le masquage survient est méconnu : le CMH II y parvient-il peu importe sa localisation dans le complexe (interaction en *trans*), ou le dimère doit-il être associé directement à Iip35 (masquage en *cis*)? Pour déterminer le mode par lequel survient le masquage, des chimères couplant la région luminale de la chaîne invariante et celle de la chaîne α ou β de HLA-DR ont été réalisées. Ce système vise à forcer l'oligomérisation de ces protéines de manière à obtenir uniquement des complexes où DRβ est distant de tout Ii sauvage. De cette façon, l'interaction en *trans* est imposée entre leur queue cytoplasmique respective. L'impossibilité des complexes comprenant Iip35 à atteindre la surface cellulaire implique que la queue cytoplasmique de DRβ ne parvient pas à masquer l'ERM lorsqu'ils sont distants. Ces résultats suggèrent ainsi que l'interaction entre ces deux partenaires doit être directe, ou en *cis*, pour parvenir au masquage optimal.

Ce système présente néanmoins ses failles; les chimères produites représentent des protéines tronquées et hautement modifiées par rapport à leur homologue physiologique. Malgré qu'il ait été montré que leur comportement se compare aux protéines de type sauvage (Figure 2-1, p.53), l'important niveau d'altération des protéines est non-négligeable. Ainsi, un second modèle, beaucoup plus près des protéines sauvages, a été mis en place. Comme la région CLIP est le site majeur d'interaction entre Ii et le CMH II, son altération donne naissance à une chaîne invariante pour laquelle l'affinité pour le CMH II est hautement altérée (résultats non-montrés). L'attrait de ce modèle demeure simplement dans l'incapacité du CMH II à lier Ii; en co-exprimant la forme mutée d'Iip35 et la forme sauvage de p33, ces formes hétérotrimérisent et ne permettent l'interaction avec le CMH II qu'au niveau de p33 (Figure 4-1, p.78). Ainsi, comme avec le système chimérique, on obtient un modèle dans lequel l'interaction en *trans* est imposée, la différence étant que ce nouveau modèle implique du CMH II de type sauvage et une chaîne invariante mutée pour une région restreinte. Inversement, il serait également possible d'imposer une interaction en *cis* en utilisant Iip35 sauvage et Iip33 dont la région CLIP est mutée. Bref, il serait très intéressant de mettre à l'œuvre ce système afin de confirmer les résultats obtenus dans le système chimérique.

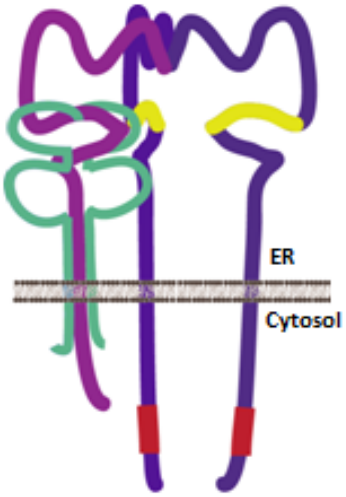

Figure 4-1. Représentation schématisée d'un complexe αβIi pentamérique. Illustration d'un complexe dans lequel la région CLIP (jaune) de l'isoforme p35 ne permet pas l'interaction avec le CMH II (vert). Le CMH II interagit avec la composante p33 du complexe. La queue cytoplasmique de la chaîne β du CMH II est distante par rapport à l'ERM de p35 (rouge).

Néanmoins, les résultats obtenus avec le système actuel mettent en lumière de nouveaux éléments visant à répondre à la controverse sur la stœchiométrie entourant l'oligomérisation d'Ii et du CMH II. L'implication générale de nos résultats pointe vers l'existence de structures de haut poids moléculaire, en ce sens qu'un homotrimère d'Iip35 doit avoir tous ses motifs masqués directement pour sortir du ER. Ainsi, pour atteindre la surface cellulaire, un homotrimère p35 doit porter trois dimères de CMH II, correspondant à un nonamère. Bien entendu, si ce phénomène est observable *in vitro* en présence de l'isoforme p35 exprimée seule, il n'est pas garanti que ces résultats puissent être extrapolés aux protéines sauvages dans les cellules présentatrices d'antigènes. Effectivement, il est connu que la balance entre les taux des différentes isoformes est scrupuleusement gardée. Comme Iip33 est présente en quantité jusqu'à quatre fois plus importante qu'Iip35 (94), alors la probabilité de rencontrer un homotrimère p35 est faible.

Nos résultats permettent d'ajouter de la puissance à l'argument de l'existence de structures heptamériques et nonamériques apporté il y a plusieurs années (122), et sont en contradiction directe avec le principe de pentamère obligatoire avancée dernièrement (134). Par contre, tel que mentionné plus haut, notre système ne récapitule pas exactement un système physiologique, en ce sens que les taux d'expression des isoformes ne sont pas respectés. Conséquemment, nos résultats ne peuvent exclure une possible prédominance de structures en pentamères en conditions physiologiques, où Iip35 se ferait plus rare.

4.2. Le rôle d'Iip35 dans l'export de αβIi du ER

Lorsqu'un complexe αβIi est en mesure de sortir du ER et d'entamer sa progression vers le MIIC, plusieurs directions peuvent être prises : le Golgi ou la surface cellulaire (33, 96). Cependant, les modes de transport empruntés pour entreprendre cette progression demeurent nébuleux à ce jour. La protéine NleA, un facteur de virulence produit par plusieurs entérobactéries pathogènes, est un outil de choix pour aborder cette question. En effet, NleA parvient à contrecarrer le système vésiculaire COPII en liant sa sous-unité Sec24 (277).

Lorsque NleA est transfecté en lignée cellulaire, l'export protéique depuis le ER par COPII est inhibé à 50% (278).

Ainsi, dans un système de transfection en lignée cellulaire, un effet drastique de NleA sur l'atteinte de la surface cellulaire par les complexes αβIi contenant Iip35 a pu être montré. Cette analyse révèle également un effet moindre de NleA sur les complexes contenant seulement Iip33. Considérant la relation bien établie entre l'expression de NleA et l'inhibition de COPII, ces résultats tendent à montrer un rôle de COPII dans l'export d'αβIi à partir du ER. Le degré de co-immunoprécipitation des deux isoformes d'Ii avec des constituants de COPII montre une importante corrélation avec l'effet observé en surface lors d'expériences avec NleA. Ceci permet donc d'avancer que l'effet de NleA sur Ii soit médié par l'inhibition de COPII. L'effet moins important sur Iip33 serait attribuable à sa faible affinité avec COPII. Néanmoins, il faut considérer que la plus faible détection de p33 peut être reliée à sa progression rapide depuis le ER, puisqu'elle ne subit pas de recyclage au même titre que p35, en raison du ERM.

Si les co-immunoprécipitations de composantes du complexe αβIi avec les sous-unités de COPII donnent une bonne indication quant à leur interaction directe, une autre approche pour montrer que αβIi transite par ces vésicules serait d'inclure dans notre système des analogues dominants négatifs de Sar1. Les mutants SAR1[H79G] et [T39N] sont bien caractérisés pour altérer la formation des vésicules COPII. Le premier, restreint à l'état GTP permet l'assemblage des sous-unités de COPII et la sélection de cargo, mais pas la séparation du bourgeon depuis la membrane du ER; le second, restreint à l'état GDP, n'est pas en mesure de s'ancrer à la membrane et il n'y a pas formation de bourgeon (205). Dans les deux cas, aucune vésicule COPII ne peut émerger du ER. Le même système de transfection pourrait servir et être analysé par cytométrie en flux. Néanmoins, comme l'effet de ces variants de Sar1 a un effet dramatique sur l'export du ER, la viabilité des cellules doit être rapidement affectée en les exprimant. L'analyse de transfectants par microscopie confocale est une option attrayante, notamment parce qu'elle permettrait de visualiser clairement la sélection des différentes isoformes par les pré-bourgeons contenant Sar1[H79G]. Ceci ajouterait du poids à l'argument de l'interaction forte entre COPII et Iip35. De surcroît, ceci permettrait de

démontrer si l'interaction limitée avec p33 est une question de transit rapide à travers les organelles et vers la surface, ou si elle est attribuable au fait que les complexes comportant cette isoforme ne dépendent pas de COPII.

Une seconde approche pour approfondir nos connaissances en la matière serait de procéder à la mutagenèse de résidus clefs de la queue cytoplasmique d'Iip35 et p33. La sous-unité Sec24 de COPII est celle généralement associée à la sélection du cargo (166). Par contre, ni Iip33 ni p35 ne présentent des motifs identifiés comme reconnus par Sec24 (101, 166). Un rôle de sélection a déjà été suggéré pour Sar1, qui reconnaitrait des motifs composés de résidus basiques arginine et lysine (208). Ainsi, les quatre arginines présentes dans la région cytoplasmique d'Iip33 justifieraient la faible interaction, et les huit arginines et la lysine d'Iip35 expliqueraient la forte interaction avec les sous-unités de COPII (101). Des études de mutagenèse dirigée contre ces résidus permettraient de définir avec précision s'ils sont réellement cruciaux pour l'interaction avec COPII, et quels résidus sont essentiels.

En somme, nos observations tendent à montrer que l'isoforme p35 de la chaîne invariante est cruciale pour diriger l'export des complexes αβIi. Néanmoins, nos résultats concernant la susceptibilité du CMH II vis-à-vis NleA suggèrent qu'Iip35 ne soit pas seul à présenter des contraintes pour son transport intracellulaire. En effet, il semble que NleA module également l'expression de surface de HLA-DQ, mais nos résultats d'immunobuvardage de type Western ne permettent pas de déterminer si cet effet est médié par COPII. Bien entendu, l'analyse de la détection de p33 est une observation indirecte, et il serait optimal pour répondre à cette question de détecter directement le niveau de CMH II dans ces mêmes échantillons.

Malgré qu'une interaction directe avec les composantes du système COPII n'ait pu être démontrée, il peut être suggéré que la susceptibilité de HLA-DQ à NleA induise dans le complexe αβIi des contraintes rappelant celles provoquées par Iip35. Ceci illustre bien le rôle de la diversité dans le haut niveau de complexité de la voie de la présentation antigénique par le CMH II. Advenant qu'une interaction soit montrée entre COPII et DQ, donc que l'export de HLA-DQ exprimé seul soit dépendant de COPII, mais que DQ ne puisse entrainer la

précipitation de p33, il peut être proposé que l'affinité d'Ii pour COPII prévale sur celle du CMH II. Ceci serait probablement explicable par le masquage de motifs reconnus par COPII sur le CMH II par la queue cytoplasmique d'Ii.

Une autre alternative pour expliquer les phénotypes observés résiderait dans le niveau d'interaction entre DQ et Ii. Notre groupe a déjà montré que DQ n'est pas aussi compétent que DR pour masquer l'ERM de p35 et induire son expression à la surface cellulaire, suggérant que cet isotype ait effectivement une faible affinité pour Ii, voir qu'il soit Ii-indépendant (118). Ainsi, il peut être proposé que DQ ait évolué pour présenter des propriétés caractéristiques de la chaîne invariante, en l'occurrence d'Iip35, et médier lui-même sa sélection dans les vésicules COPII. Dans ce cas, il serait intéressant d'ajouter HLA-DP à notre système, qui montre un phénotype intermédiaire dans le masquage de l'ERM de p35 (118); HLA-DP pourrait également être affecté par NleA et médier sa sélection par COPII.

Nos résultats montrent que le principe s'appliquant au CMH I pour sa sélection par COPII ne semble pas s'appliquer au CMH II. Par ailleurs, la construction pour laquelle la queue cytoplasmique de DRβ a été substituée pour celle de DQβ ne confère pas à DR la susceptibilité à NleA qui est démontrée chez DQ. Ceci semble indiquer que l'effet de NleA sur le CMH II est indépendant de la chaîne β. Il peut donc être supposé que cet effet soit plutôt attribuable à un motif de la queue cytoplasmique de la chaîne α qui soit indépendant du résidu C-terminal (Figure 4-2, p.82).

```
DQB1*0602;  SGVGGFVLGL IFLGLGLIIR QRSRKG.... ....LLH
DRB1*01:01; SGVGGFVLGL LFLGAGLFIY FRNQKGHSGL QPTGFLS
DRA1*01:01; VGLV...GII IGTIFIIKGV RKSNAAERRG PL
DQA1*01:01; GLSVGLVGIV VGTVFIIQGL RSVGASRHQG PL
```

Figure 4-2. Alignement de séquence des régions transmembranaires et cytoplasmiques des allèles de HLA-DR et HLA-DQ utilisés dans cette étude. Les séquences proviennent des bases de données GenBank (L34105.1 DQB1*05 :602, M60334.1 DRA1*01 :01, HE965627.1 DQA1*01 :01) et UniProtKB (O19730 DRB1*01 :01).

Pour répondre à cette hypothèse, une analyse de la séquence de la région cytoplasmique de la chaîne α des différents isotypes de CMH II devraient être effectuée, afin d'y trouver des motifs interagissant avec COPII. Nos observations suggèrent que ces motifs soient présents chez DQ, mais pas chez DR. Tel que suggéré pour Iip33 et p35, des études de mutagenèse dirigée permettraient d'identifier des résidus clefs dans cette interaction. Évidemment, pour tracer un portrait complet, il serait important d'inclure dans cette étude le troisième isotype de CMH II : HLA-DP.

4.3. Perspectives

Ce projet a permis d'obtenir plus de précisions en ce qui a trait à l'effet d'Iip35 dans les étapes précoces menant à la présentation antigénique. Dans le but d'approfondir les connaissances obtenues grâce à ce projet, plusieurs expériences additionnelles pourraient être effectuées.

4.3.1. Le mécanisme de masquage du motif RXR d'Iip35 par la chaîne β du CMH II

Nos observations suggèrent fortement que l'interaction distale entre DRβ et la queue cytoplasmique d'Iip35 ne permet pas le masquage du motif RXR et indique ainsi que le masquage en *cis* soit requis pour éviter la recapture par COPI dans l'ERGIC ou le Golgi. Néanmoins, le mécanisme d'action entourant le masquage n'a pas été élucidé. Est-ce une question d'encombrement stérique ou de changement de conformation restreignant l'accès de COPI au ERM? Trois principes sont mis de l'avant à ce jour, tous par notre laboratoire : pour qu'il y ait masquage efficace, il faut à la chaîne β du CMH II une queue longue d'au moins trois acides aminés (118), la seule conservation de l'extension de 16 acides aminés au niveau cytosolique d'Iip35 ne suffit pour la rétention au ER (302), et le masquage doit être effectué en *cis* ((303), présenté dans ce mémoire). Cette problématique pourrait être abordée en produisant des mutants d'Iip35 portant des altérations au niveau cytoplasmique : en changeant le positionnement du RXR par rapport à la membrane, la théorie de l'encombrement stérique

pourrait être testée. Des mutants dont la taille de la queue cytoplasmique est inchangée, mais pour lesquels la séquence est altérée pourraient également être mis à l'étude. Il s'agirait donc d'utiliser un système de transfection impliquant la co-expression des mutants d'Iip35 avec le CMH II et d'observer la rétention du complexe ou son accès à la surface cellulaire.

4.3.2 Le rôle d'Iip35 dans la présentation antigénique

Comme nos résultats touchent les stades précoces menant à la présentation antigénique par le CMH II, il serait intéressant de vérifier si la composition du complexe αβIi peut ultimement affecter cette présentation d'antigènes aux cellules T (94). Une manière d'aborder cette question *in vitro* serait en procédant à des tests fonctionnels. Des transfectants exprimant diverses isoformes de la chaîne invariante pourraient être évalués pour l'apprêtement du virus de l'influenza X31 inactivé et la présentation du peptide $HA_{307-318}$, restreint à la présentation par le CMH II (25, 163, 304-306). Ces résultats pourraient procurer un tout nouveau rôle aux différentes isoformes. Des peptides divers pourraient être testés pour évaluer si telle isoforme permet une meilleure présentation de tel peptide; il pourrait être observé qu'une isoforme induit généralement une présentation plus efficace, ou alors que les isoformes de la chaîne invariante modulent chacune le répertoire de peptides présentés (297).

En ce sens, l'étude du répertoire de peptides présentés par des APCs exprimant différents variants d'Ii serait de prime intérêt. Pour ce faire, la technologie CRISPR permettrait d'abord d'empêcher l'expression d'Ii endogène soit *in vitro* dans des lignées de cellules B; pour des études *in vivo*, notre laboratoire détient déjà une souris n'exprimant pas Ii (Ii *knock-out*). Par la suite, les lignées cellulaires pourraient être transfectées de façon stable avec des plasmides codant pour chacune des isoformes d'Ii ou les deux. Pour la souris, il faudrait créer des *knock-in* exprimant les mêmes conditions énumérées. Ceci pallierait à l'absence de p35 chez la souris (91). La spectrométrie de masse serait une technologie de choix pour l'analyse du répertoire de peptides portés dans la niche des molécules de CMH II selon la ou les isoforme(s) d'Ii exprimée(s). Évidemment, les études de peptidome dans le contexte du CMH II sont nettement compliquées par rapport au CMH I en ce sens que la

longueur des peptides est beaucoup plus variable. Néanmoins, ce champ de recherche est actuellement en croissance et gagne à être investigué (307, 308).

Pour fournir encore plus d'informations, les différentes souris *knock-in* et la *knock-out* pourraient être infectées avec la bactérie *Citrobacter rodentium* de type sauvage ou exprimant un NleA inactif (281). L'infection d'animaux de laboratoire permettrait ultimement de confirmer le rôle du facteur de virulence NleA dans l'altération de la présentation antigénique par le CMH II. Pour y parvenir, la charge bactérienne du côlon, la charge en eau des fèces des souris et la période de temps nécessaire pour résilier l'infection sont trois facteurs qui pourraient être mesurés. Cette étude démontrerait que les pathogènes causant des lésions d'attachement-effacement ont acquis en NleA une arme favorisant leur évasion du système immunitaire humain par la subversion de la présentation antigénique.

Chapitre 5. Conclusion

La chaîne invariante joue un rôle important dans la présentation antigénique par le CMH II, que ce soit par sa fonction de chaperon, de protecteur de la niche ou de guide (154). Néanmoins, même si ses différentes isoformes sont largement caractérisées en ce qui a trait à leur séquence ou à leurs caractéristiques post-traductionnelles individuelles, peu d'études se sont concentrées sur les particularités de complexes comprenant diverses isoformes d'Ii à la fois (7, 12, 88, 93, 94, 106-111, 113, 114, 282). De surcroît, dans l'optique où quatre isoformes sont conservées chez l'humain, il peut être supposé que celles-ci occupent des fonctions distinctes et non-redondantes, justifiant cette conservation. Comme les deux isoformes humaines prédominantes – Iip33 et p35 – ne diffèrent que par une extension cytosolique de 16 acides aminés portée par Iip35, cette petite région doit nécessairement procurer à p35 une fonction particulière. Entre autres, un motif connu de rétention au réticulum endoplasmique y est encodé. Ainsi, ce projet visait à évaluer l'effet de cette extension sur l'assemblage des complexes αβIi et leur export du réticulum endoplasmique.

Nos résultats montrent que la nécessité du masquage en *cis* du motif de rétention promeut la formation de structures de haute complexité pour la sortie du ER. Par ailleurs, Iip35 favorise l'export du ER des complexes αβIi via les vésicules COPII. Ainsi, il peut être affirmé que cette extension, et particulièrement son ERM, font d'Iip35 un régulateur clef dans la formation et l'export des complexes αβIi. Afin d'étendre le rôle d'Iip35 jusqu'aux événements de présentation antigénique, des analyses de fonction et de peptidome gagneraient à être réalisées. Comme Iip35 promeut la formation de structures αβIi de plus haute complexité, plus de dimères de CMH II doivent se trouver dirigés vers le MIIC pour y rencontrer un peptide. Ainsi, il est probable que la présence de l'isoforme p35 de la chaîne invariante favorise une présentation antigénique plus efficace.

L'homme présente une chaîne invariante unique, en ce sens qu'aucun analogue de p35 n'est répertorié chez les autres vertébrés (17, 309-311). L'équilibre dans l'expression des

isoformes d'Ii étant strictement régulé, il est de prime importance de comprendre les distinctions fonctionnelles entre Iip33 et p35. Ce sujet est d'une importance clinique certaine, considérant l'observation de déséquilibre dans le taux des isoformes d'Ii dans plusieurs pathologies, notamment dans des cas de diabète auto-immun et de leucémie lymphoïde chronique (295-297). Ainsi, le développement des connaissances concernant les particularités des isoformes d'Ii est certainement un outil dans la compréhension de ces pathologies.

Bibliographie

1. Klein J, Sato A. *The HLA system. First of two parts*. N Engl J Med. 2000;343(10):702-9.
2. Simpson E. *Function of the MHC*. Immunol Suppl. 1988;1:27-30.
3. Kaufman JF, Auffray C, Korman AJ, Shackelford DA, Strominger J. *The class II molecules of the human and murine major histocompatibility complex*. Cell. 1984;36(1):1-13.
4. Miller J, Germain RN. *Efficient cell surface expression of class II MHC molecules in the absence of associated invariant chain*. J Exp Med. 1986;164(5):1478-89.
5. Ohtsuka M, Inoko H, Kulski JK, Yoshimura S. *Major histocompatibility complex (Mhc) class Ib gene duplications, organization and expression patterns in mouse strain C57BL/6*. BMC Genomics. 2008;9:178.
6. Cresswell P, Ackerman AL, Giodini A, Peaper DR, Wearsch PA. *Mechanisms of MHC class I-restricted antigen processing and cross-presentation*. Immunol Rev. 2005;207:145-57.
7. Cresswell P. *Assembly, transport, and function of MHC class II molecules*. Annu Rev Immunol. 1994;12:259-93.
8. Roche PA, Cresswell P. *Proteolysis of the class II-associated invariant chain generates a peptide binding site in intracellular HLA-DR molecules*. Proc Natl Acad Sci U S A. 1991;88(8):3150-4.
9. Biron CA. *Interferons alpha and beta as immune regulators – a new look*. Immunity. 2001;14(6):661-4.
10. Kobayashi KS, van den Elsen PJ. *NLRC5: a key regulator of MHC class I-dependent immune responses*. Nat Rev Immunol. 2012;12(12):813-20.
11. Pessara U, Koch N. *Tumor necrosis factor alpha regulates expression of the major histocompatibility complex class II-associated invariant chain by binding of an NF-kappa B-like factor to a promoter element*. Mol Cell Biol. 1990;10(8):4146-54.
12. Machamer CE, Cresswell P. *Biosynthesis and glycosylation of the invariant chain associated with HLA-DR antigens*. J Immunol. 1982;129(6):2564-9.
13. Brown JH, Jardetzky TS, Gorga JC, Stern LJ, Urban RG, Strominger JL, et al. *Three-dimensional structure of the human class II histocompatibility antigen HLA-DR1*. Nature. 1993;364(6432):33-9.
14. Anderson MW, Gorski J. *Cooperativity during the formation of peptide/MHC class II complexes*. Biochemistry. 2005;44(15):5617-24.
15. Denzin LK, Cresswell P. *HLA-DM induces CLIP dissociation from MHC class II alpha beta dimers and facilitates peptide loading*. Cell. 1995;82(1):155-65.
16. Denzin LK, Sant'Angelo DB, Hammond C, Surman MJ, Cresswell P. *Negative regulation by HLA-DO of MHC class II-restricted antigen processing*. Science. 1997;278(5335):106-9.
17. Borghese F, Clanchy FI. *CD74: an emerging opportunity as a therapeutic target in cancer and autoimmune disease*. Expert Opin Ther Targets. 2011;15(3):237-51.

18. Thelemann C, Eren RO, Coutaz M, Brasseit J, Bouzourene H, Rosa M, et al. *Interferon-gamma induces expression of MHC class II on intestinal epithelial cells and protects mice from colitis*. PLoS One. 2014;9(1):e86844.
19. Steimle V, Siegrist CA, Mottet A, Lisowska-Grospierre B, Mach B. *Regulation of MHC class II expression by interferon-gamma mediated by the transactivator gene CIITA*. Science. 1994;265(5168):106-9.
20. Zinkernagel RM, Doherty PC. *Restriction of in vitro T cell-mediated cytotoxicity in lymphocytic choriomeningitis within a syngeneic or semiallogeneic system*. Nature. 1974;248(5450):701-2.
21. Zinkernagel RM, Doherty PC. *MHC-restricted cytotoxic T cells: studies on the biological role of polymorphic major transplantation antigens determining T-cell restriction-specificity, function, and responsiveness*. Adv Immunol. 1979;27:51-177.
22. Zinkernagel RM, Doherty PC. *H-2 compatability requirement for T-cell-mediated lysis of target cells infected with lymphocytic choriomeningitis virus. Different cytotoxic T-cell specificities are associated with structures coded for in H-2K or H-2D*. J Exp Med. 1975;141(6):1427-36.
23. Peaper DR, Cresswell P. *Regulation of MHC class I assembly and peptide binding*. Annu Rev Cell Dev Biol. 2008;24:343-68.
24. Hansen TH, Bouvier M. *MHC class I antigen presentation: learning from viral evasion strategies*. Nat Rev Immunol. 2009;9(7):503-13.
25. Roche PA, Teletski CL, Karp DR, Pinet V, Bakke O, Long EO. *Stable surface expression of invariant chain prevents peptide presentation by HLA-DR*. EMBO J. 1992;11(8):2841-7.
26. Wright CA, Kozik P, Zacharias M, Springer S. *Tapasin and other chaperones: models of the MHC class I loading complex*. Biol Chem. 2004;385(9):763-78.
27. Serwold T, Gonzalez F, Kim J, Jacob R, Shastri N. *ERAAP customizes peptides for MHC class I molecules in the endoplasmic reticulum*. Nature. 2002;419(6906):480-3.
28. Saric T, Chang SC, Hattori A, York IA, Markant S, Rock KL, et al. *An IFN-gamma-induced aminopeptidase in the ER, ERAP1, trims precursors to MHC class I-presented peptides*. Nat Immunol. 2002;3(12):1169-76.
29. York IA, Chang SC, Saric T, Keys JA, Favreau JM, Goldberg AL, et al. *The ER aminopeptidase ERAP1 enhances or limits antigen presentation by trimming epitopes to 8-9 residues*. Nat Immunol. 2002;3(12):1177-84.
30. Guagliardi LE, Koppelman B, Blum JS, Marks MS, Cresswell P, Brodsky FM. *Co-localization of molecules involved in antigen processing and presentation in an early endocytic compartment*. Nature. 1990;343(6254):133-9.
31. Neefjes JJ, Stollorz V, Peters PJ, Geuze HJ, Ploegh HL. *The biosynthetic pathway of MHC class II but not class I molecules intersects the endocytic route*. Cell. 1990;61(1):171-83.
32. Peters PJ, Neefjes JJ, Oorschot V, Ploegh HL, Geuze HJ. *Segregation of MHC class II molecules from MHC class I molecules in the Golgi complex for transport to lysosomal compartments*. Nature. 1991;349(6311):669-76.
33. Romagnoli P, Layet C, Yewdell J, Bakke O, Germain RN. *Relationship between invariant chain expression and major histocompatibility complex class II transport into early and late endocytic compartments*. J Exp Med. 1993;177(3):583-96.

34. Bevan MJ. *Cross-priming for a secondary cytotoxic response to minor H antigens with H-2 congenic cells which do not cross-react in the cytotoxic assay*. J Exp Med. 1976;143(5):1283-8.
35. Kurts C, Heath WR, Carbone FR, Allison J, Miller JF, Kosaka H. *Constitutive class I-restricted exogenous presentation of self antigens in vivo*. J Exp Med. 1996;184(3):923-30.
36. Kreer C, Rauen J, Zehner M, Burgdorf S. *Cross-presentation: how to get there - or how to get the ER*. Front Immunol. 2011;2:87.
37. Rock KL, Gamble S, Rothstein L. *Presentation of exogenous antigen with class I major histocompatibility complex molecules*. Science. 1990;249(4971):918-21.
38. Grant EP, Rock KL. *MHC class I-restricted presentation of exogenous antigen by thymic antigen-presenting cells in vitro and in vivo*. J Immunol. 1992;148(1):13-8.
39. Pfeifer JD, Wick MJ, Roberts RL, Findlay K, Normark SJ, Harding CV. *Phagocytic processing of bacterial antigens for class I MHC presentation to T cells*. Nature. 1993;361(6410):359-62.
40. Kovacsovics-Bankowski M, Clark K, Benacerraf B, Rock KL. *Efficient major histocompatibility complex class I presentation of exogenous antigen upon phagocytosis by macrophages*. Proc Natl Acad Sci U S A. 1993;90(11):4942-6.
41. Rock KL, Rothstein L, Gamble S, Fleischacker C. *Characterization of antigen-presenting cells that present exogenous antigens in association with class I MHC molecules*. J Immunol. 1993;150(2):438-46.
42. Harding CV, Song R. *Phagocytic processing of exogenous particulate antigens by macrophages for presentation by class I MHC molecules*. J Immunol. 1994;153(11):4925-33.
43. Norbury CC, Hewlett LJ, Prescott AR, Shastri N, Watts C. *Class I MHC presentation of exogenous soluble antigen via macropinocytosis in bone marrow macrophages*. Immunity. 1995;3(6):783-91.
44. Reis e Sousa C, Germain RN. *Major histocompatibility complex class I presentation of peptides derived from soluble exogenous antigen by a subset of cells engaged in phagocytosis*. J Exp Med. 1995;182(3):841-51.
45. Malaviya R, Twesten NJ, Ross EA, Abraham SN, Pfeifer JD. *Mast cells process bacterial Ags through a phagocytic route for class I MHC presentation to T cells*. J Immunol. 1996;156(4):1490-6.
46. Norbury CC, Chambers BJ, Prescott AR, Ljunggren HG, Watts C. *Constitutive macropinocytosis allows TAP-dependent major histocompatibility complex class I presentation of exogenous soluble antigen by bone marrow-derived dendritic cells*. Eur J Immunol. 1997;27(1):280-8.
47. Heath WR, Carbone FR. *Cross-presentation in viral immunity and self-tolerance*. Nat Rev Immunol. 2001;1(2):126-34.
48. Crotzer VL, Blum JS. *Autophagy and its role in MHC-mediated antigen presentation*. J Immunol. 2009;182(6):3335-41.
49. Yewdell JW, Norbury CC, Bennink JR. *Mechanisms of exogenous antigen presentation by MHC class I molecules in vitro and in vivo: implications for generating CD8+ T cell responses to infectious agents, tumors, transplants, and vaccines*. Adv Immunol. 1999;73:1-77.
50. Neefjes J, Sadaka C. *Into the intracellular logistics of cross-presentation*. Front Immunol. 2012;3:31.

51. Valujskikh A, Hartig C, Heeger PS. *Indirectly primed CD8+ T cells are a prominent component of the allogeneic T-cell repertoire after skin graft rejection in mice. Transplantation*. 2001;71(3):418-21.
52. Valujskikh A, Lantz O, Celli S, Matzinger P, Heeger PS. *Cross-primed CD8(+) T cells mediate graft rejection via a distinct effector pathway*. Nat Immunol. 2002;3(9):844-51.
53. Fink PJ, Matis LA, McElligott DL, Bookman M, Hedrick SM. *Correlations between T-cell specificity and the structure of the antigen receptor*. Nature. 1986;321(6067):219-26.
54. Winoto A, Urban JL, Lan NC, Goverman J, Hood L, Hansburg D. *Predominant use of a V alpha gene segment in mouse T-cell receptors for cytochrome c*. Nature. 1986;324(6098):679-82.
55. White J, Herman A, Pullen AM, Kubo R, Kappler JW, Marrack P. *The V beta-specific superantigen staphylococcal enterotoxin B: stimulation of mature T cells and clonal deletion in neonatal mice*. Cell. 1989;56(1):27-35.
56. Janeway CA, Jr., Yagi J, Conrad PJ, Katz ME, Jones B, Vroegop S, et al. *T-cell responses to Mls and to bacterial proteins that mimic its behavior*. Immunol Rev. 1989;107:61-88.
57. Herman A, Kappler JW, Marrack P, Pullen AM. *Superantigens: mechanism of T-cell stimulation and role in immune responses*. Annu Rev Immunol. 1991;9:745-72.
58. Ford D, Burger D. *Precursor frequency of antigen-specific T cells: effects of sensitization in vivo and in vitro*. Cell Immunol. 1983;79(2):334-44.
59. Fraser JD, Proft T. *The bacterial superantigen and superantigen-like proteins*. Immunol Rev. 2008;225:226-43.
60. Acha-Orbea H, Shakhov AN, Scarpellino L, Kolb E, Muller V, Vessaz-Shaw A, et al. *Clonal deletion of V beta 14-bearing T cells in mice transgenic for mammary tumour* virus. Nature. 1991;350(6315):207-11.
61. Woodland DL, Happ MP, Gollob KJ, Palmer E. *An endogenous retrovirus mediating deletion of alpha beta T cells?* Nature. 1991;349(6309):529-30.
62. Woodland DL, Lund FE, Happ MP, Blackman MA, Palmer E, Corley RB. *Endogenous superantigen expression is controlled by mouse mammary tumor proviral loci*. J Exp Med. 1991;174(5):1255-8.
63. Choi YW, Kotzin B, Lafferty J, White J, Pigeon M, Kubo R, et al. *A method for production of antibodies to human T-cell receptor beta-chain variable regions*. Proc Natl Acad Sci U S A. 1991;88(19):8357-61.
64. Marrack P, Kushnir E, Kappler J. *A maternally inherited superantigen encoded by a mammary tumour virus*. Nature. 1991;349(6309):524-6.
65. Marrack P, Kappler J. *The staphylococcal enterotoxins and their relatives*. Science. 1990;248(4956):705-11.
66. Langford MP, Stanton GJ, Johnson HM. *Biological effects of staphylococcal enterotoxin A on human peripheral lymphocytes*. Infect Immun. 1978;22(1):62-8.
67. Peavy DL, Adler WH, Smith RT. *The mitogenic effects of endotoxin and staphylococcal enterotoxin B on mouse spleen cells and human peripheral lymphocytes*. J Immunol. 1970;105(6):1453-8.
68. Scherer MT, Ignatowicz L, Winslow GM, Kappler JW, Marrack P. *Superantigens: bacterial and viral proteins that manipulate the immune system*. Annu Rev Cell Biol. 1993;9:101-28.

69. Kim J, Urban RG, Strominger JL, Wiley DC. *Toxic shock syndrome toxin-1 complexed with a class II major histocompatibility molecule HLA-DR1*. Science. 1994;266(5192):1870-4.
70. Fraser JD. *High-affinity binding of staphylococcal enterotoxins A and B to HLA-DR*. Nature. 1989;339(6221):221-3.
71. Fleischer B, Schrezenmeier H. *T cell stimulation by staphylococcal enterotoxins. Clonally variable response and requirement for major histocompatibility complex class II molecules on accessory or target cells*. J Exp Med. 1988;167(5):1697-707.
72. Fleischer B, Schrezenmeier H, Conradt P. *T lymphocyte activation by staphylococcal enterotoxins: role of class II molecules and T cell surface structures*. Cell Immunol. 1989;120(1):92-101.
73. Babbitt BP, Allen PM, Matsueda G, Haber E, Unanue ER. *Binding of immunogenic peptides to Ia histocompatibility molecules*. Nature. 1985;317(6035):359-61.
74. Buus S, Sette A, Colon SM, Miles C, Grey HM. *The relation between major histocompatibility complex (MHC) restriction and the capacity of Ia to bind immunogenic peptides*. Science. 1987;235(4794):1353-8.
75. Bjorkman PJ, Saper MA, Samraoui B, Bennett WS, Strominger JL, Wiley DC. *The foreign antigen binding site and T cell recognition regions of class I histocompatibility antigens*. Nature. 1987;329(6139):512-8.
76. Bjorkman PJ, Saper MA, Samraoui B, Bennett WS, Strominger JL, Wiley DC. *Structure of the human class I histocompatibility antigen, HLA-A2*. Nature. 1987;329(6139):506-12.
77. Brown JH, Jardetzky T, Saper MA, Samraoui B, Bjorkman PJ, Wiley DC. *A hypothetical model of the foreign antigen binding site of class II histocompatibility molecules*. Nature. 1988;332(6167):845-50.
78. Herman A, Labrecque N, Thibodeau J, Marrack P, Kappler JW, Sekaly RP. *Identification of the staphylococcal enterotoxin A superantigen binding site in the beta 1 domain of the human histocompatibility antigen HLA-DR*. Proc Natl Acad Sci U S A. 1991;88(22):9954-8.
79. Jardetzky TS, Brown JH, Gorga JC, Stern LJ, Urban RG, Chi YI, et al. *Three-dimensional structure of a human class II histocompatibility molecule complexed with superantigen*. Nature. 1994;368(6473):711-8.
80. Thibodeau J, Cloutier I, Lavoie PM, Labrecque N, Mourad W, Jardetzky T, et al. *Subsets of HLA-DR1 molecules defined by SEB and TSST-1 binding*. Science. 1994;266(5192):1874-8.
81. Thibodeau J, Labrecque N, Denis F, Huber BT, Sekaly RP. *Binding sites for bacterial and endogenous retroviral superantigens can be dissociated on major histocompatibility complex class II molecules*. J Exp Med. 1994;179(3):1029-34.
82. Hudson KR, Tiedemann RE, Urban RG, Lowe SC, Strominger JL, Fraser JD. *Staphylococcal enterotoxin A has two cooperative binding sites on major histocompatibility complex class II*. J Exp Med. 1995;182(3):711-20.
83. Herman A, Croteau G, Sekaly RP, Kappler J, Marrack P. *HLA-DR alleles differ in their ability to present staphylococcal enterotoxins to T cells*. J Exp Med. 1990;172(3):709-17.
84. Lavoie PM, Thibodeau J, Cloutier I, Busch R, Sekaly RP. *Selective binding of bacterial toxins to major histocompatibility complex class II-expressing cells is controlled by invariant chain and HLA-DM*. Proc Natl Acad Sci U S A. 1997;94(13):6892-7.

85. Lavoie PM, Thibodeau J, Erard F, Sekaly RP. *Understanding the mechanism of action of bacterial superantigens from a decade of research*. Immunol Rev. 1999;168:257-69.
86. Fortin JS, Geneve L, Gauthier C, Shoukry NH, Azar GA, Younes S, et al. *MMTV superantigens coerce an unconventional topology between the TCR and MHC class II*. J Immunol. 2014;192(4):1896-906.
87. Jones PP, Murphy DB, Hewgill D, McDevitt HO. *Detection of a common polypeptide chain in I--A and I--E sub-region immunoprecipitates*. Mol Immunol. 1979;16(1):51-60.
88. Marks MS, Blum JS, Cresswell P. *Invariant chain trimers are sequestered in the rough endoplasmic reticulum in the absence of association with HLA class II antigens*. J Cell Biol. 1990;111(3):839-55.
89. Claesson-Welsh L, Barker PE, Larhammar D, Rask L, Ruddle FH, Peterson PA. *The gene encoding the human class II antigen-associated gamma chain is located on chromosome 5*. Immunogenetics. 1984;20(1):89-93.
90. Collins T, Korman AJ, Wake CT, Boss JM, Kappes DJ, Fiers W, et al. *Immune interferon activates multiple class II major histocompatibility complex genes and the associated invariant chain gene in human endothelial cells and dermal fibroblasts*. Proc Natl Acad Sci U S A. 1984;81(15):4917-21.
91. Koch N, Lauer W, Habicht J, Dobberstein B. *Primary structure of the gene for the murine Ia antigen-associated invariant chains (Ii). An alternatively spliced exon encodes a cysteine-rich domain highly homologous to a repetitive sequence of thyroglobulin*. EMBO J. 1987;6(6):1677-83.
92. Lamb CA, Cresswell P. *Assembly and transport properties of invariant chain trimers and HLA-DR-invariant chain complexes*. J Immunol. 1992;148(11):3478-82.
93. Arunachalam B, Lamb CA, Cresswell P. *Transport properties of free and MHC class II-associated oligomers containing different isoforms of human invariant chain*. Int Immunol. 1994;6(3):439-51.
94. Anderson HA, Bergstralh DT, Kawamura T, Blauvelt A, Roche PA. *Phosphorylation of the invariant chain by protein kinase C regulates MHC class II trafficking to antigen-processing compartments*. J Immunol. 1999;163(10):5435-43.
95. O'Sullivan DM, Noonan D, Quaranta V. *Four Ia invariant chain forms derive from a single gene by alternate splicing and alternate initiation of transcription/translation*. J Exp Med. 1987;166(2):444-60.
96. Lotteau V, Teyton L, Peleraux A, Nilsson T, Karlsson L, Schmid SL, et al. *Intracellular transport of class II MHC molecules directed by invariant chain*. Nature. 1990;348(6302):600-5.
97. Michelsen K, Yuan H, Schwappach B. Hide and run. *Arginine-based endoplasmic-reticulum-sorting motifs in the assembly of heteromultimeric membrane proteins*. EMBO Rep. 2005;6(8):717-22.
98. Simonsen A, Momburg F, Drexler J, Hammerling GJ, Bakke O. *Intracellular distribution of the MHC class II molecules and the associated invariant chain (Ii) in different cell lines*. Int Immunol. 1993;5(8):903-17.
99. Odorizzi CG, Trowbridge IS, Xue L, Hopkins CR, Davis CD, Collawn JF. *Sorting signals in the MHC class II invariant chain cytoplasmic tail and transmembrane region determine trafficking to an endocytic processing compartment*. J Cell Biol. 1994;126(2):317-30.

100. Bremnes B, Madsen T, Gedde-Dahl M, Bakke O. *An LI and ML motif in the cytoplasmic tail of the MHC-associated invariant chain mediate rapid internalization*. J Cell Sci. 1994;107 (Pt 7):2021-32.
101. Bakke O, Dobberstein B. *MHC class II-associated invariant chain contains a sorting signal for endosomal compartments*. Cell. 1990;63(4):707-16.
102. Pond L, Kuhn LA, Teyton L, Schutze MP, Tainer JA, Jackson MR, et al. *A role for acidic residues in di-leucine motif-based targeting to the endocytic pathway*. J Biol Chem. 1995;270(34):19989-97.
103. Arneson LS, Miller J. *Efficient endosomal localization of major histocompatibility complex class II-invariant chain complexes requires multimerization of the invariant chain targeting sequence*. J Cell Biol. 1995;129(5):1217-28.
104. Tietze C, Schlesinger P, Stahl P. *Chloroquine and ammonium ion inhibit receptor-mediated endocytosis of mannose-glycoconjugates by macrophages: apparent inhibition of receptor recycling*. Biochem Biophys Res Commun. 1980;93(1):1-8.
105. Kornfeld S, Mellman I. *The biogenesis of lysosomes*. Annu Rev Cell Biol. 1989;5:483-525.
106. Koch N, Hammerling GJ. *Ia-associated invariant chain is fatty acylated before addition of sialic acid*. Biochemistry. 1985;24(22):6185-90.
107. Anderson HA, Roche PA. *Phosphorylation regulates the delivery of MHC class II invariant chain complexes to antigen processing compartments*. J Immunol. 1998;160(10):4850-8.
108. Spiro RC, Quaranta V. *The invariant chain is a phosphorylated subunit of class II molecules*. J Immunol. 1989;143(8):2589-94.
109. Kuwana T, Peterson PA, Karlsson L. *Exit of major histocompatibility complex class II-invariant chain p35 complexes from the endoplasmic reticulum is modulated by phosphorylation*. Proc Natl Acad Sci U S A. 1998;95(3):1056-61.
110. Miller J, Hatch JA, Simonis S, Cullen SE. *Identification of the glycosaminoglycan-attachment site of mouse invariant-chain proteoglycan core protein by site-directed mutagenesis*. Proc Natl Acad Sci U S A. 1988;85(5):1359-63.
111. Lamb CA, Yewdell JW, Bennink JR, Cresswell P. *Invariant chain targets HLA class II molecules to acidic endosomes containing internalized influenza virus*. Proc Natl Acad Sci U S A. 1991;88(14):5998-6002.
112. Neumann J, Koch N. *Assembly of major histocompatibility complex class II subunits with invariant chain*. FEBS Lett. 2005;579(27):6055-9.
113. Simonis S, Cullen SE. *Fatty acylation of murine Ia alpha, beta, and invariant chains*. J Immunol. 1986;136(8):2962-7.
114. Sant AJ, Zacheis M, Rumbarger T, Giacoletto KS, Schwartz BD. *Human Ia alpha- and beta-chains are sulfated*. J Immunol. 1988;140(1):155-60.
115. Bijlmakers MJ, Benaroch P, Ploegh HL. *Mapping functional regions in the lumenal domain of the class II-associated invariant chain*. J Exp Med. 1994;180(2):623-9.
116. Ashman JB, Miller J. *A role for the transmembrane domain in the trimerization of the MHC class II-associated invariant chain*. J Immunol. 1999;163(5):2704-12.
117. Bertolino P, Staschewski M, Trescol-Biemont MC, Freisewinkel IM, Schenck K, Chretien I, et al. *Deletion of a C-terminal sequence of the class II-associated invariant chain abrogates invariant chains oligomer formation and class II antigen presentation*. J Immunol. 1995;154(11):5620-9.

118. Khalil H, Brunet A, Saba I, Terra R, Sekaly RP, Thibodeau J. *The MHC class II beta chain cytoplasmic tail overcomes the invariant chain p35-encoded endoplasmic reticulum retention signal*. Int Immunol. 2003;15(10):1249-63.
119. Koch N, McLellan AD, Neumann J. *A revised model for invariant chain-mediated assembly of MHC class II peptide receptors*. Trends Biochem Sci. 2007;32(12):532-7.
120. Helenius A, Marquardt T, Braakman I. *The endoplasmic reticulum as a protein-folding compartment*. Trends Cell Biol. 1992;2(8):227-31.
121. Anderson KS, Cresswell P. *A role for calnexin (IP90) in the assembly of class II MHC molecules*. EMBO J. 1994;13(3):675-82.
122. Roche PA, Marks MS, Cresswell P. *Formation of a nine-subunit complex by HLA class II glycoproteins and the invariant chain*. Nature. 1991;354(6352):392-4.
123. Riberdy JM, Newcomb JR, Surman MJ, Barbosa JA, Cresswell P. *HLA-DR molecules from an antigen-processing mutant cell line are associated with invariant chain peptides*. Nature. 1992;360(6403):474-7.
124. Ghosh P, Amaya M, Mellins E, Wiley DC. *The structure of an intermediate in class II MHC maturation: CLIP bound to HLA-DR3*. Nature. 1995;378(6556):457-62.
125. Sette A, Southwood S, Miller J, Appella E. *Binding of major histocompatibility complex class II to the invariant chain-derived peptide, CLIP, is regulated by allelic polymorphism in class II*. J Exp Med. 1995;181(2):677-83.
126. Karp DR, Jenkins RN, Long EO. *Distinct binding sites on HLA-DR for invariant chain and staphylococcal enterotoxins*. Proc Natl Acad Sci U S A. 1992;89(20):9657-61.
127. Romagnoli P, Germain RN. *The CLIP region of invariant chain plays a critical role in regulating major histocompatibility complex class II folding, transport, and peptide occupancy*. J Exp Med. 1994;180(3):1107-13.
128. Kropshofer H, Vogt AB, Hammerling GJ. *Structural features of the invariant chain fragment CLIP controlling rapid release from HLA-DR molecules and inhibition of peptide binding*. Proc Natl Acad Sci U S A. 1995;92(18):8313-7.
129. Vogt AB, Stern LJ, Amshoff C, Dobberstein B, Hammerling GJ, Kropshofer H. *Interference of distinct invariant chain regions with superantigen contact area and antigenic peptide binding groove of HLA-DR*. J Immunol. 1995;155(10):4757-65.
130. Stumptner P, Benaroch P. *Interaction of MHC class II molecules with the invariant chain: role of the invariant chain (81-90) region*. EMBO J. 1997;16(19):5807-18.
131. Siebenkotten IM, Carstens C, Koch N. *Identification of a sequence that mediates promiscuous binding of invariant chain to MHC class II allotypes*. J Immunol. 1998;160(7):3355-62.
132. Wilson NA, Wolf P, Ploegh H, Ignatowicz L, Kappler J, Marrack P. *Invariant chain can bind MHC class II at a site other than the peptide binding groove*. J Immunol. 1998;161(9):4777-84.
133. de Kretser TA, Crumpton MJ, Bodmer JG, Bodmer WF. *Demonstration of two distinct light chains in HLA-DR-associated antigens by two-dimensional gel electrophoresis*. Eur J Immunol. 1982;12(3):214-21.
134. Koch N, Zacharias M, Konig A, Temme S, Neumann J, Springer S. *Stoichiometry of HLA class II-invariant chain oligomers*. PLoS One. 2011;6(2):e17257.
135. Cloutier M, Gauthier C, Fortin JS, Thibodeau J. *The invariant chain p35 isoform promotes formation of nonameric complexes with MHC II molecules*. Immunol Cell Biol. 2014;92(6):553-6.

136. Stumptner-Cuvelette P, Benaroch P. *Multiple roles of the invariant chain in MHC class II function*. Biochim Biophys Acta. 2002;1542(1-3):1-13.
137. Harding CV, Geuze HJ. *Class II MHC molecules are present in macrophage lysosomes and phagolysosomes that function in the phagocytic processing of Listeria monocytogenes for presentation to T cells*. J Cell Biol. 1992;119(3):531-42.
138. Kleijmeer MJ, Ossevoort MA, van Veen CJ, van Hellemond JJ, Neefjes JJ, Kast WM, et al. *MHC class II compartments and the kinetics of antigen presentation in activated mouse spleen dendritic cells*. J Immunol. 1995;154(11):5715-24.
139. Kleijmeer MJ, Raposo G, Geuze HJ. *Characterization of MHC Class II Compartments by Immunoelectron Microscopy*. Methods. 1996;10(2):191-207.
140. Kleijmeer MJ, Morkowski S, Griffith JM, Rudensky AY, Geuze HJ. *Major histocompatibility complex class II compartments in human and mouse B lymphoblasts represent conventional endocytic compartments*. J Cell Biol. 1997;139(3):639-49.
141. Blum JS, Cresswell P. *Role for intracellular proteases in the processing and transport of class II HLA antigens*. Proc Natl Acad Sci U S A. 1988;85(11):3975-9.
142. Matza D, Kerem A, Shachar I. *Invariant chain, a chain of command*. Trends Immunol. 2003;24(5):264-8.
143. Newcomb JR, Cresswell P. *Structural analysis of proteolytic products of MHC class II-invariant chain complexes generated in vivo*. J Immunol. 1993;151(8):4153-63.
144. Matza D, Wolstein O, Dikstein R, Shachar I. *Invariant chain induces B cell maturation by activating a TAF(II)105-NF-kappaB-dependent transcription program*. J Biol Chem. 2001;276(29):27203-6.
145. Matza D, Lantner F, Bogoch Y, Flaishon L, Hershkoviz R, Shachar I. *Invariant chain induces B cell maturation in a process that is independent of its chaperonic activity*. Proc Natl Acad Sci U S A. 2002;99(5):3018-23.
146. Roche PA. *HLA-DM: an in vivo facilitator of MHC class II peptide loading*. Immunity. 1995;3(3):259-62.
147. Karlsson L, Peleraux A, Lindstedt R, Liljedahl M, Peterson PA. *Reconstitution of an operational MHC class II compartment in nonantigen-presenting cells*. Science. 1994;266(5190):1569-73.
148. Sanderson F, Kleijmeer MJ, Kelly A, Verwoerd D, Tulp A, Neefjes JJ, et al. *Accumulation of HLA-DM, a regulator of antigen presentation, in MHC class II compartments*. Science. 1994;266(5190):1566-9.
149. Marks MS, Roche PA, van Donselaar E, Woodruff L, Peters PJ, Bonifacino JS. *A lysosomal targeting signal in the cytoplasmic tail of the beta chain directs HLA-DM to MHC class II compartments*. J Cell Biol. 1995;131(2):351-69.
150. Sloan VS, Cameron P, Porter G, Gammon M, Amaya M, Mellins E, et al. *Mediation by HLA-DM of dissociation of peptides from HLA-DR*. Nature. 1995;375(6534):802-6.
151. Denzin LK, Hammond C, Cresswell P. *HLA-DM interactions with intermediates in HLA-DR maturation and a role for HLA-DM in stabilizing empty HLA-DR molecules*. J Exp Med. 1996;184(6):2153-65.
152. Sherman MA, Weber DA, Jensen PE. *DM enhances peptide binding to class II MHC by release of invariant chain-derived peptide*. Immunity. 1995;3(2):197-205.
153. Long EO. *Intracellular traffic and antigen processing*. Immunol Today. 1989;10(7):232-4.

154. Fortin JS, Cloutier M, Thibodeau J. *Exposing the Specific Roles of the Invariant Chain Isoforms in Shaping the MHC Class II Peptidome*. Front Immunol. 2013;4:443.
155. Anderson MS, Miller J. *Invariant chain can function as a chaperone protein for class II major histocompatibility complex molecules*. Proc Natl Acad Sci U S A. 1992;89(6):2282-6.
156. Schaiff WT, Hruska KA, Jr., McCourt DW, Green M, Schwartz BD. *HLA-DR associates with specific stress proteins and is retained in the endoplasmic reticulum in invariant chain negative cells*. J Exp Med. 1992;176(3):657-66.
157. Sekaly RP, Tonnelle C, Strubin M, Mach B, Long EO. *Cell surface expression of class II histocompatibility antigens occurs in the absence of the invariant chain*. J Exp Med. 1986;164(5):1490-504.
158. Viville S, Neefjes J, Lotteau V, Dierich A, Lemeur M, Ploegh H, et al. *Mice lacking the MHC class II-associated invariant chain*. Cell. 1993;72(4):635-48.
159. Roche PA, Cresswell P. *Invariant chain association with HLA-DR molecules inhibits immunogenic peptide binding*. Nature. 1990;345(6276):615-8.
160. Teyton L, O'Sullivan D, Dickson PW, Lotteau V, Sette A, Fink P, et al. *Invariant chain distinguishes between the exogenous and endogenous antigen presentation pathways*. Nature. 1990;348(6296):39-44.
161. Newcomb JR, Cresswell P. *Characterization of endogenous peptides bound to purified HLA-DR molecules and their absence from invariant chain-associated alpha beta dimers*. J Immunol. 1993;150(2):499-507.
162. Bijlmakers MJ, Benaroch P, Ploegh HL. *Assembly of HLA DR1 molecules translated in vitro: binding of peptide in the endoplasmic reticulum precludes association with invariant chain*. EMBO J. 1994;13(11):2699-707.
163. Long EO, LaVaute T, Pinet V, Jaraquemada D. *Invariant chain prevents the HLA-DR-restricted presentation of a cytosolic peptide*. J Immunol. 1994;153(4):1487-94.
164. Kreis TE, Lowe M, Pepperkok R. *COPs regulating membrane traffic*. Annu Rev Cell Dev Biol. 1995;11:677-706.
165. Bi X, Corpina RA, Goldberg J. *Structure of the Sec23/24-Sar1 pre-budding complex of the COPII vesicle coat*. Nature. 2002;419(6904):271-7.
166. Mancias JD, Goldberg J. *Exiting the endoplasmic reticulum*. Traffic. 2005;6(4):278-85.
167. Barlowe C. *COPII and selective export from the endoplasmic reticulum*. Biochim Biophys Acta. 1998;1404(1-2):67-76.
168. Schekman R, Orci L. *Coat proteins and vesicle budding*. Science. 1996;271(5255):1526-33.
169. Rothman JE, Wieland FT. *Protein sorting by transport vesicles*. Science. 1996;272(5259):227-34.
170. Sollner T, Whiteheart SW, Brunner M, Erdjument-Bromage H, Geromanos S, Tempst P, et al. *SNAP receptors implicated in vesicle targeting and fusion*. Nature. 1993;362(6418):318-24.
171. Parlati F, McNew JA, Fukuda R, Miller R, Sollner TH, Rothman JE. *Topological restriction of SNARE-dependent membrane fusion*. Nature. 2000;407(6801):194-8.
172. Mossessova E, Bickford LC, Goldberg J. *SNARE selectivity of the COPII coat*. Cell. 2003;114(4):483-95.
173. Barlowe C, Orci L, Yeung T, Hosobuchi M, Hamamoto S, Salama N, et al. *COPII: a membrane coat formed by Sec proteins that drive vesicle budding from the endoplasmic reticulum*. Cell. 1994;77(6):895-907.

174. Presley JF, Cole NB, Schroer TA, Hirschberg K, Zaal KJ, Lippincott-Schwartz J. *ER-to-Golgi transport visualized in living cells*. Nature. 1997;389(6646):81-5.
175. Pearse BM. *Clathrin: a unique protein associated with intracellular transfer of membrane by coated vesicles*. Proc Natl Acad Sci U S A. 1976;73(4):1255-9.
176. Keen JH, Willingham MC, Pastan IH. *Clathrin-coated vesicles: isolation, dissociation and factor-dependent reassociation of clathrin baskets*. Cell. 1979;16(2):303-12.
177. Harrison SC, Kirchhausen T. *Clathrin, cages, and coated vesicles*. Cell. 1983;33(3):650-2.
178. Szul T, Sztul E. *COPII and COPI traffic at the ER-Golgi interface*. Physiology (Bethesda). 2011;26(5):348-64.
179. Venditti R, Wilson C, De Matteis MA. *Exiting the ER: what we know and what we don't*. Trends Cell Biol. 2014;24(1):9-18.
180. Novick P, Field C, Schekman R. *Identification of 23 complementation groups required for post-translational events in the yeast secretory pathway*. Cell. 1980;21(1):205-15.
181. Baker D, Hicke L, Rexach M, Schleyer M, Schekman R. *Reconstitution of SEC gene product-dependent intercompartmental protein transport*. Cell. 1988;54(3):335-44.
182. Rothblatt JA, Deshaies RJ, Sanders SL, Daum G, Schekman R. *Multiple genes are required for proper insertion of secretory proteins into the endoplasmic reticulum in yeast*. J Cell Biol. 1989;109(6 Pt 1):2641-52.
183. Hicke L, Schekman R. *Yeast Sec23p acts in the cytoplasm to promote protein transport from the endoplasmic reticulum to the Golgi complex in vivo and in vitro*. EMBO J. 1989;8(6):1677-84.
184. Hicke L, Schekman R. *Molecular machinery required for protein transport from the endoplasmic reticulum to the Golgi complex*. Bioessays. 1990;12(6):253-8.
185. Kaiser CA, Schekman R. *Distinct sets of SEC genes govern transport vesicle formation and fusion early in the secretory pathway*. Cell. 1990;61(4):723-33.
186. Deshaies RJ, Schekman R. *Structural and functional dissection of Sec62p, a membrane-bound component of the yeast endoplasmic reticulum protein import machinery*. Mol Cell Biol. 1990;10(11):6024-35.
187. Paccaud JP, Reith W, Carpentier JL, Ravazzola M, Amherdt M, Schekman R, et al. *Cloning and functional characterization of mammalian homologues of the COPII component Sec23*. Mol Biol Cell. 1996;7(10):1535-46.
188. Klumperman J. *Transport between ER and Golgi*. Curr Opin Cell Biol. 2000;12(4):445-9.
189. Lippincott-Schwartz J, Roberts TH, Hirschberg K. *Secretory protein trafficking and organelle dynamics in living cells*. Annu Rev Cell Dev Biol. 2000;16:557-89.
190. Gorelick FS, Shugrue C. *Exiting the endoplasmic reticulum*. Mol Cell Endocrinol. 2001;177(1-2):13-8.
191. Kaiser C, Ferro-Novick S. *Transport from the endoplasmic reticulum to the Golgi*. Curr Opin Cell Biol. 1998;10(4):477-82.
192. Lee MC, Miller EA. *Molecular mechanisms of COPII vesicle formation*. Semin Cell Dev Biol. 2007;18(4):424-34.
193. Haucke V. *Vesicle budding: a coat for the COPs*. Trends Cell Biol. 2003;13(2):59-60.
194. Brandizzi F, Barlowe C. *Organization of the ER-Golgi interface for membrane traffic control*. Nat Rev Mol Cell Biol. 2013;14(6):382-92.

195. Tang BL, Kausalya J, Low DY, Lock ML, Hong W. *A family of mammalian proteins homologous to yeast Sec24p*. Biochem Biophys Res Commun. 1999;258(3):679-84.
196. Fromme JC, Ravazzola M, Hamamoto S, Al-Balwi M, Eyaid W, Boyadjiev SA, et al. *The genetic basis of a craniofacial disease provides insight into COPII coat assembly*. Dev Cell. 2007;13(5):623-34.
197. Boyadjiev SA, Justice CM, Eyaid W, McKusick VA, Lachman RS, Chowdry AB, et al. *A novel dysmorphic syndrome with open calvarial sutures and sutural cataracts maps to chromosome 14q13-q21*. Hum Genet. 2003;113(1):1-9.
198. Quintero CA, Giraudo CG, Villarreal M, Montich G, Maccioni HJ. *Identification of a site in Sar1 involved in the interaction with the cytoplasmic tail of glycolipid glycosyltransferases*. J Biol Chem. 2010;285(39):30340-6.
199. Antonny B, Schekman R. *ER export: public transportation by the COPII coach*. Curr Opin Cell Biol. 2001;13(4):438-43.
200. Belden WJ, Barlowe C. *Distinct roles for the cytoplasmic tail sequences of Emp24p and Erv25p in transport between the endoplasmic reticulum and Golgi complex*. J Biol Chem. 2001;276(46):43040-8.
201. Barlowe C. *Signals for COPII-dependent export from the ER: what's the ticket out?* Trends Cell Biol. 2003;13(6):295-300.
202. Lee MC, Miller EA, Goldberg J, Orci L, Schekman R. *Bi-directional protein transport between the ER and Golgi*. Annu Rev Cell Dev Biol. 2004;20:87-123.
203. Otte S, Barlowe C. *The Erv41p-Erv46p complex: multiple export signals are required in trans for COPII-dependent transport from the ER*. EMBO J. 2002;21(22):6095-104.
204. Springer S, Schekman R. *Nucleation of COPII vesicular coat complex by endoplasmic reticulum to Golgi vesicle SNAREs*. Science. 1998;281(5377):698-700.
205. Aridor M, Fish KN, Bannykh S, Weissman J, Roberts TH, Lippincott-Schwartz J, et al. *The Sar1 GTPase coordinates biosynthetic cargo selection with endoplasmic reticulum export site assembly*. J Cell Biol. 2001;152(1):213-29.
206. Aridor M, Weissman J, Bannykh S, Nuoffer C, Balch WE. *Cargo selection by the COPII budding machinery during export from the ER*. J Cell Biol. 1998;141(1):61-70.
207. Aridor M, Traub LM. *Cargo selection in vesicular transport: the making and breaking of a coat*. Traffic. 2002;3(8):537-46.
208. Giraudo CG, Maccioni HJ. *Endoplasmic reticulum export of glycosyltransferases depends on interaction of a cytoplasmic dibasic motif with Sar1*. Mol Biol Cell. 2003;14(9):3753-66.
209. Spiliotis ET, Manley H, Osorio M, Zuniga MC, Edidin M. *Selective export of MHC class I molecules from the ER after their dissociation from TAP*. Immunity. 2000;13(6):841-51.
210. Cho S, Ryoo J, Jun Y, Ahn K. *Receptor-mediated ER export of human MHC class I molecules is regulated by the C-terminal single amino acid*. Traffic. 2011;12(1):42-55.
211. Cosson P, Lefkir Y, Demolliere C, Letourneur F. *New COP1-binding motifs involved in ER retrieval*. EMBO J. 1998;17(23):6863-70.
212. Orci L, Stamnes M, Ravazzola M, Amherdt M, Perrelet A, Sollner TH, et al. *Bidirectional transport by distinct populations of COPI-coated vesicles*. Cell. 1997;90(2):335-49.
213. Hong W. *Protein transport from the endoplasmic reticulum to the Golgi apparatus*. J Cell Sci. 1998;111 (Pt 19):2831-9.

214. Martinez-Menarguez JA, Geuze HJ, Slot JW, Klumperman J. *Vesicular tubular clusters between the ER and Golgi mediate concentration of soluble secretory proteins by exclusion from COPI-coated vesicles*. Cell. 1999;98(1):81-90.
215. Wieland FT, Gleason ML, Serafini TA, Rothman JE. *The rate of bulk flow from the endoplasmic reticulum to the cell surface*. Cell. 1987;50(2):289-300.
216. Pelham HR. *Evidence that luminal ER proteins are sorted from secreted proteins in a post-ER compartment*. EMBO J. 1988;7(4):913-8.
217. Doms RW, Russ G, Yewdell JW. *Brefeldin A redistributes resident and itinerant Golgi proteins to the endoplasmic reticulum*. J Cell Biol. 1989;109(1):61-72.
218. Sciaky N, Presley J, Smith C, Zaal KJ, Cole N, Moreira JE, et al. *Golgi tubule traffic and the effects of brefeldin A visualized in living cells*. J Cell Biol. 1997;139(5):1137-55.
219. Peyroche A, Antonny B, Robineau S, Acker J, Cherfils J, Jackson CL. *Brefeldin A acts to stabilize an abortive ARF-GDP-Sec7 domain protein complex: involvement of specific residues of the Sec7 domain*. Mol Cell. 1999;3(3):275-85.
220. Niu TK, Pfeifer AC, Lippincott-Schwartz J, Jackson CL. *Dynamics of GBF1, a Brefeldin A-sensitive Arf1 exchange factor at the Golgi*. Mol Biol Cell. 2005;16(3):1213-22.
221. Richter S, Geldner N, Schrader J, Wolters H, Stierhof YD, Rios G, et al. *Functional diversification of closely related ARF-GEFs in protein secretion and recycling*. Nature. 2007;448(7152):488-92.
222. Oprins A, Duden R, Kreis TE, Geuze HJ, Slot JW. *Beta-COP localizes mainly to the cis-Golgi side in exocrine pancreas*. J Cell Biol. 1993;121(1):49-59.
223. Rothman JE, Orci L. *Molecular dissection of the secretory pathway*. Nature. 1992;355(6359):409-15.
224. Eugster A, Frigerio G, Dale M, Duden R. *COP I domains required for coatomer integrity, and novel interactions with ARF and ARF-GAP*. EMBO J. 2000;19(15):3905-17.
225. Cosson P, Letourneur F. *Coatomer interaction with di-lysine endoplasmic reticulum retention motifs*. Science. 1994;263(5153):1629-31.
226. Cosson P, Demolliere C, Hennecke S, Duden R, Letourneur F. *Delta- and zeta-COP, two coatomer subunits homologous to clathrin-associated proteins, are involved in ER retrieval*. EMBO J. 1996;15(8):1792-8.
227. Cabrera M, Muniz M, Hidalgo J, Vega L, Martin ME, Velasco A. *The retrieval function of the KDEL receptor requires PKA phosphorylation of its C-terminus*. Mol Biol Cell. 2003;14(10):4114-25.
228. Girod A, Storrie B, Simpson JC, Johannes L, Goud B, Roberts LM, et al. *Evidence for a COP-I-independent transport route from the Golgi complex to the endoplasmic reticulum*. Nat Cell Biol. 1999;1(7):423-30.
229. O'Kelly I, Butler MH, Zilberberg N, Goldstein SA. *Forward transport. 14-3-3 binding overcomes retention in endoplasmic reticulum by dibasic signals*. Cell. 2002;111(4):577-88.
230. Yuan H, Michelsen K, Schwappach B. *14-3-3 Dimers Probe the Assembly Status of Multimeric Membrane Proteins*. Curr Biol. 2003;13(8):638-46.
231. Nufer O, Hauri H-P. *ER Export: Call 14-3-3*. Curr Biol. 2003;13(10):R391-R3.
232. Levine MM, Xu JG, Kaper JB, Lior H, Prado V, Tall B, et al. *A DNA probe to identify enterohemorrhagic Escherichia coli of O157:H7 and other serotypes that cause hemorrhagic colitis and hemolytic uremic syndrome*. J Infect Dis. 1987;156(1):175-82.

233. McDaniel TK, Jarvis KG, Donnenberg MS, Kaper JB. *A genetic locus of enterocyte effacement conserved among diverse enterobacterial pathogens*. Proc Natl Acad Sci U S A. 1995;92(5):1664-8.
234. De Rycke J, Comtet E, Chalareng C, Boury M, Tasca C, Milon A. *Enteropathogenic Escherichia coli O103 from rabbit elicits actin stress fibers and focal adhesions in HeLa epithelial cells, cytopathic effects that are linked to an analog of the locus of enterocyte effacement*. Infect Immun. 1997;65(7):2555-63.
235. Goffaux F, China B, Janssen L, Pirson V, Mainil J. *The locus for enterocyte effacement (LEE) of enteropathogenic Escherichia coli (EPEC) from dogs and cats*. Adv Exp Med Biol. 1999;473:129-36.
236. An H, Fairbrother JM, Desautels C, Mabrouk T, Dugourd D, Dezfulian H, et al. *Presence of the LEE (locus of enterocyte effacement) in pig attaching and effacing Escherichia coli and characterization of eae, espA, espB and espD genes of PEPEC (pig EPEC) strain 1390*. Microb Pathog. 2000;28(5):291-300.
237. Goffaux F, China B, Mainil J. *Organisation and in vitro expression of esp genes of the LEE (locus of enterocyte effacement) of bovine enteropathogenic and enterohemorrhagic Escherichia coli*. Vet Microbiol. 2001;83(3):275-86.
238. McNally A, Roe AJ, Simpson S, Thomson-Carter FM, Hoey DE, Currie C, et al. *Differences in levels of secreted locus of enterocyte effacement proteins between human disease-associated and bovine Escherichia coli O157*. Infect Immun. 2001;69(8):5107-14.
239. Zhu C, Agin TS, Elliott SJ, Johnson LA, Thate TE, Kaper JB, et al. *Complete nucleotide sequence and analysis of the locus of enterocyte Effacement from rabbit diarrheagenic Escherichia coli RDEC-1*. Infect Immun. 2001;69(4):2107-15.
240. Yoshioka K, Yagi K, Moriguchi N. *Clinical features and treatment of children with hemolytic uremic syndrome caused by enterohemorrhagic Escherichia coli O157:H7 infection: experience of an outbreak in Sakai City, 1996*. Pediatr Int. 1999;41(2):223-7.
241. Levine MM. *Escherichia coli that cause diarrhea: enterotoxigenic, enteropathogenic, enteroinvasive, enterohemorrhagic, and enteroadherent*. J Infect Dis. 1987;155(3):377-89.
242. Griffin PM, Tauxe RV. *The epidemiology of infections caused by Escherichia coli O157:H7, other enterohemorrhagic E. coli, and the associated hemolytic uremic syndrome*. Epidemiol Rev. 1991;13:60-98.
243. Moon HW, Whipp SC, Argenzio RA, Levine MM, Giannella RA. *Attaching and effacing activities of rabbit and human enteropathogenic Escherichia coli in pig and rabbit intestines*. Infect Immun. 1983;41(3):1340-51.
244. Elliott SJ, Sperandio V, Giron JA, Shin S, Mellies JL, Wainwright L, et al. *The locus of enterocyte effacement (LEE)-encoded regulator controls expression of both LEE- and non-LEE-encoded virulence factors in enteropathogenic and enterohemorrhagic Escherichia coli*. Infect Immun. 2000;68(11):6115-26.
245. Knutton S, Baldwin T, Williams PH, McNeish AS. *Actin accumulation at sites of bacterial adhesion to tissue culture cells: basis of a new diagnostic test for enteropathogenic and enterohemorrhagic Escherichia coli*. Infect Immun. 1989;57(4):1290-8.
246. Nataro JP, Kaper JB. *Diarrheagenic Escherichia coli*. Clin Microbiol Rev. 1998;11(1):142-201.
247. Deng W, Li Y, Vallance BA, Finlay BB. *Locus of enterocyte effacement from Citrobacter rodentium: sequence analysis and evidence for horizontal transfer among attaching and effacing pathogens*. Infect Immun. 2001;69(10):6323-35.

248. Perna NT, Mayhew GF, Posfai G, Elliott S, Donnenberg MS, Kaper JB, et al. *Molecular evolution of a pathogenicity island from enterohemorrhagic Escherichia coli O157:H7*. Infect Immun. 1998;66(8):3810-7.
249. Elliott SJ, Yu J, Kaper JB. *The cloned locus of enterocyte effacement from enterohemorrhagic Escherichia coli O157:H7 is unable to confer the attaching and effacing phenotype upon E. coli K-12*. Infect Immun. 1999;67(8):4260-3.
250. Donnenberg MS, Lai LC, Taylor KA. *The locus of enterocyte effacement pathogenicity island of enteropathogenic Escherichia coli encodes secretion functions and remnants of transposons at its extreme right end*. Gene. 1997;184(1):107-14.
251. Kaper JB. *The locus of enterocyte effacement pathogenicity island of Shiga toxin-producing Escherichia coli O157:H7 and other attaching and effacing E. coli*. Jpn J Med Sci Biol. 1998;51 Suppl:S101-7.
252. Sperandio V, Kaper JB, Bortolini MR, Neves BC, Keller R, Trabulsi LR. *Characterization of the locus of enterocyte effacement (LEE) in different enteropathogenic Escherichia coli (EPEC) and Shiga-toxin producing Escherichia coli (STEC) serotypes*. FEMS Microbiol Lett. 1998;164(1):133-9.
253. Friedberg D, Umanski T, Fang Y, Rosenshine I. *Hierarchy in the expression of the locus of enterocyte effacement genes of enteropathogenic Escherichia coli*. Mol Microbiol. 1999;34(5):941-52.
254. Mellies JL, Elliott SJ, Sperandio V, Donnenberg MS, Kaper JB. *The Per regulon of enteropathogenic Escherichia coli : identification of a regulatory cascade and a novel transcriptional activator, the locus of enterocyte effacement (LEE)-encoded regulator (Ler)*. Mol Microbiol. 1999;33(2):296-306.
255. Laaberki MH, Janabi N, Oswald E, Repoila F. *Concert of regulators to switch on LEE expression in enterohemorrhagic Escherichia coli O157:H7: interplay between Ler, GrlA, HNS and RpoS*. Int J Med Microbiol. 2006;296(4-5):197-210.
256. Deng W, Puente JL, Gruenheid S, Li Y, Vallance BA, Vazquez A, et al. *Dissecting virulence: systematic and functional analyses of a pathogenicity island*. Proc Natl Acad Sci U S A. 2004;101(10):3597-602.
257. Zaharik ML, Gruenheid S, Perrin AJ, Finlay BB. *Delivery of dangerous goods: type III secretion in enteric pathogens*. Int J Med Microbiol. 2002;291(8):593-603.
258. Kenny B. *Mechanism of action of EPEC type III effector molecules*. Int J Med Microbiol. 2002;291(6-7):469-77.
259. Dean P, Maresca M, Kenny B. *EPEC's weapons of mass subversion*. Curr Opin Microbiol. 2005;8(1):28-34.
260. de Grado M, Abe A, Gauthier A, Steele-Mortimer O, DeVinney R, Finlay BB. *Identification of the intimin-binding domain of Tir of enteropathogenic Escherichia coli*. Cell Microbiol. 1999;1(1):7-17.
261. Kenny B. *Phosphorylation of tyrosine 474 of the enteropathogenic Escherichia coli (EPEC) Tir receptor molecule is essential for actin nucleating activity and is preceded by additional host modifications*. Mol Microbiol. 1999;31(4):1229-41.
262. Luo Y, Frey EA, Pfuetzner RA, Creagh AL, Knoechel DG, Haynes CA, et al. *Crystal structure of enteropathogenic Escherichia coli intimin-receptor complex*. Nature. 2000;405(6790):1073-7.

263. Goosney DL, DeVinney R, Pfuetzner RA, Frey EA, Strynadka NC, Finlay BB. *Enteropathogenic E. coli translocated intimin receptor, Tir, interacts directly with alpha-actinin*. Curr Biol. 2000;10(12):735-8.
264. Gruenheid S, Finlay BB. *Microbial pathogenesis and cytoskeletal function*. Nature. 2003;422(6933):775-81.
265. Crane JK, McNamara BP, Donnenberg MS. *Role of EspF in host cell death induced by enteropathogenic Escherichia coli*. Cell Microbiol. 2001;3(4):197-211.
266. McNamara BP, Koutsouris A, O'Connell CB, Nougayrede JP, Donnenberg MS, Hecht G. *Translocated EspF protein from enteropathogenic Escherichia coli disrupts host intestinal barrier function*. J Clin Invest. 2001;107(5):621-9.
267. Guttman JA, Finlay BB. *Tight junctions as targets of infectious agents*. Biochim Biophys Acta. 2009;1788(4):832-41.
268. Marches O, Ledger TN, Boury M, Ohara M, Tu X, Goffaux F, et al. *Enteropathogenic and enterohaemorrhagic Escherichia coli deliver a novel effector called Cif, which blocks cell cycle G2/M transition*. Mol Microbiol. 2003;50(5):1553-67.
269. Mundy R, Petrovska L, Smollett K, Simpson N, Wilson RK, Yu J, et al. *Identification of a novel Citrobacter rodentium type III secreted protein, EspI, and roles of this and other secreted proteins in infection*. Infect Immun. 2004;72(4):2288-302.
270. Campellone KG, Robbins D, Leong JM. *EspFU is a translocated EHEC effector that interacts with Tir and N-WASP and promotes Nck-independent actin assembly*. Dev Cell. 2004;7(2):217-28.
271. Elliott SJ, Krejany EO, Mellies JL, Robins-Browne RM, Sasakawa C, Kaper JB. *EspG, a novel type III system-secreted protein from enteropathogenic Escherichia coli with similarities to VirA of Shigella flexneri*. Infect Immun. 2001;69(6):4027-33.
272. Matsuzawa T, Kuwae A, Yoshida S, Sasakawa C, Abe A. *Enteropathogenic Escherichia coli activates the RhoA signaling pathway via the stimulation of GEF-H1*. EMBO J. 2004;23(17):3570-82.
273. Viswanathan VK, Lukic S, Koutsouris A, Miao R, Muza MM, Hecht G. *Cytokeratin 18 interacts with the enteropathogenic Escherichia coli secreted protein F (EspF) and is redistributed after infection*. Cell Microbiol. 2004;6(10):987-97.
274. Garmendia J, Phillips AD, Carlier MF, Chong Y, Schuller S, Marches O, et al. *TccP is an enterohaemorrhagic Escherichia coli O157:H7 type III effector protein that couples Tir to the actin-cytoskeleton*. Cell Microbiol. 2004;6(12):1167-83.
275. Schauer DB, Falkow S. *The eae gene of Citrobacter freundii biotype 4280 is necessary for colonization in transmissible murine colonic hyperplasia*. Infect Immun. 1993;61(11):4654-61.
276. Gruenheid S, Sekirov I, Thomas NA, Deng W, O'Donnell P, Goode D, et al. *Identification and characterization of NleA, a non-LEE-encoded type III translocated virulence factor of enterohaemorrhagic Escherichia coli O157:H7*. Mol Microbiol. 2004;51(5):1233-49.
277. Kim J, Thanabalasuriar A, Chaworth-Musters T, Fromme JC, Frey EA, Lario PI, et al. *The bacterial virulence factor NleA inhibits cellular protein secretion by disrupting mammalian COPII function*. Cell Host Microbe. 2007;2(3):160-71.
278. Thanabalasuriar A, Bergeron J, Gillingham A, Mimee M, Thomassin JL, Strynadka N, et al. *Sec24 interaction is essential for localization and virulence-associated function of the bacterial effector protein NleA*. Cell Microbiol. 2012;14(8):1206-18.

279. Thanabalasuriar A, Koutsouris A, Hecht G, Gruenheid S. *The bacterial virulence factor NleA's involvement in intestinal tight junction disruption during enteropathogenic E. coli infection is independent of its putative PDZ binding domain*. Gut Microbes. 2010;1(2):114-8.
280. Thanabalasuriar A, Koutsouris A, Weflen A, Mimee M, Hecht G, Gruenheid S. *The bacterial virulence factor NleA is required for the disruption of intestinal tight junctions by enteropathogenic Escherichia coli*. Cell Microbiol. 2010;12(1):31-41.
281. Thanabalasuriar A, Kim J, Gruenheid S. *The inhibition of COPII trafficking is important for intestinal epithelial tight junction disruption during enteropathogenic Escherichia coli and Citrobacter rodentium infection*. Microbes Infect. 2013;15(10-11):738-44.
282. Sand KMK, Landsverk O, Bakke O, Gregers T. *Intracellular trafficking of the human invariant chain isoforms, Iip33 and Iip35*. Mol Immunol. 2012;51(1):30.
283. Knudsen Sand KM, Landsverk OJ, Berg-Larsen A, Bakke O, Gregers TF. *The human-specific invariant chain isoform Iip35 modulates Iip33 trafficking and function*. Immunol Cell Biol. 2014;92(9):791-8.
284. Ishigami S, Natsugoe S, Tokuda K, Nakajo A, Iwashige H, Aridome K, et al. *Invariant chain expression in gastric cancer*. Cancer Lett. 2001;168(1):87-91.
285. Koide N, Yamada T, Shibata R, Mori T, Fukuma M, Yamazaki K, et al. *Establishment of perineural invasion models and analysis of gene expression revealed an invariant chain (CD74) as a possible molecule involved in perineural invasion in pancreatic cancer*. Clin Cancer Res. 2006;12(8):2419-26.
286. Vivarelli M, D'Urbano LE, Insalaco A, Lunt M, Jury F, Tozzi AE, et al. *Macrophage migration inhibitory factor (MIF) and oligoarticular juvenile idiopathic arthritis (o-JIA): association of MIF promoter polymorphisms with response to intra-articular glucocorticoids*. Clin Exp Rheumatol. 2007;25(5):775-81.
287. Cuthbert RJ, Wilson JM, Scott N, Coletta PL, Hull MA. *Differential CD74 (major histocompatibility complex Class II invariant chain) expression in mouse and human intestinal adenomas*. Eur J Cancer. 2009;45(9):1654-63.
288. Lin X, Wang X, Capek HL, Simone LC, Tuli A, Morris CR, et al. *Effect of invariant chain on major histocompatibility complex class I molecule expression and stability on human breast tumor cell lines*. Cancer Immunol Immunother. 2009;58(5):729-36.
289. Maharshak N, Cohen S, Lantner F, Hart G, Leng L, Bucala R, et al. *CD74 is a survival receptor on colon epithelial cells*. World J Gastroenterol. 2010;16(26):3258-66.
290. Lapter S, Ben-David H, Sharabi A, Zinger H, Telerman A, Gordin M, et al. *A role for the B-cell CD74/macrophage migration inhibitory factor pathway in the immunomodulation of systemic lupus erythematosus by a therapeutic tolerogenic peptide*. Immunology. 2011;132(1):87-95.
291. Lee YH, Bae SC, Song GG. *The association between the functional PTPN22 1858 C/T and MIF -173 C/G polymorphisms and juvenile idiopathic arthritis: a meta-analysis*. Inflamm Res. 2012;61(5):411-5.
292. Herrero LJ, Sheng KC, Jian P, Taylor A, Her Z, Herring BL, et al. *Macrophage migration inhibitory factor receptor CD74 mediates alphavirus-induced arthritis and myositis in murine models of alphavirus infection*. Arthritis Rheum. 2013;65(10):2724-36.
293. Llamas-Covarrubias MA, Valle Y, Bucala R, Navarro-Hernandez RE, Palafox-Sanchez CA, Padilla-Gutierrez JR, et al. *Macrophage migration inhibitory factor (MIF): genetic*

evidence for participation in early onset and early stage rheumatoid arthritis. Cytokine. 2013;61(3):759-65.
294. Chen Z, Ma T, Huang C, Zhang L, Hu T, Li J. *MIF, a potential therapeutic target for rheumatoid arthritis?* Rheumatol Int. 2014;34(10):1481-2.
295. Veenstra H, Jacobs P, Dowdle EB. *Processing of HLA-class II invariant chain and expression of the p35 form is different in malignant and transformed cells*. Blood. 1993;82(8):2494-500.
296. Veenstra H, Jacobs P, Dowdle EB. *Abnormal association between invariant chain and HLA class II alpha and beta chains in chronic lymphocytic leukemia*. Cell Immunol. 1996;171(1):68-73.
297. Yan G, Shi L, Penfornis A, Faustman DL. *Impaired processing and presentation by MHC class II proteins in human diabetic cells*. J Immunol. 2003;170(1):620-7.
298. Mellanby RJ, Koonce CH, Monti A, Phillips JM, Cooke A, Bikoff EK. *Loss of invariant chain protects nonobese diabetic mice against type 1 diabetes*. J Immunol. 2006;177(11):7588-98.
299. Binsky I, Lantner F, Grabovsky V, Harpaz N, Shvidel L, Berrebi A, et al. *TAp63 regulates VLA-4 expression and chronic lymphocytic leukemia cell migration to the bone marrow in a CD74-dependent manner*. J Immunol. 2010;184(9):4761-9.
300. Burster T, Boehm BO. *Processing and presentation of (pro)-insulin in the MHC class II pathway: the generation of antigen-based immunomodulators in the context of type 1 diabetes mellitus*. Diabetes Metab Res Rev. 2010;26(4):227-38.
301. Shachar I, Haran M. *The secret second life of an innocent chaperone: the story of CD74 and B cell/chronic lymphocytic leukemia cell survival*. Leuk Lymphoma. 2011;52(8):1446-54.
302. Khalil H, Brunet A, Thibodeau J. *A three-amino-acid-long HLA-DRbeta cytoplasmic tail is sufficient to overcome ER retention of invariant-chain p35*. J Cell Sci. 2005;118(Pt 20):4679-87.
303. Cloutier M, Gauthier C, Fortin JS, Geneve L, Kim K, Gruenheid S, et al. *ER egress of invariant chain isoform p35 requires direct binding to MHCII molecules and is inhibited by the NleA virulence factor of enterohaemorrhagic Escherichia coli*. Hum Immunol. 2015.
304. Pinet V, Malnati MS, Long EO. *Two processing pathways for the MHC class II-restricted presentation of exogenous influenza virus antigen*. J Immunol. 1994;152(10):4852-60.
305. Wedderburn LR, Searle SJ, Rees AR, Lamb JR, Owen MJ. *Mapping T cell recognition: the identification of a T cell receptor residue critical to the specific interaction with an influenza hemagglutinin peptide*. Eur J Immunol. 1995;25(6):1654-62.
306. Pinet VM, Long EO. *Peptide loading onto recycling HLA-DR molecules occurs in early endosomes*. Eur J Immunol. 1998;28(3):799-804.
307. Muntasell A, Carrascal M, Alvarez I, Serradell L, van Veelen P, Verreck FAW, et al. *Dissection of the HLA-DR4 Peptide Repertoire in Endocrine Epithelial Cells: Strong Influence of Invariant Chain and HLA-DM Expression on the Nature of Ligands*. The Journal of Immunology. 2004;173(2):1085-93.
308. Collado JA, Alvarez I, Ciudad MT, Espinosa G, Canals F, Pujol-Borrell R, et al. *Composition of the HLA-DR-associated human thymus peptidome*. Eur J Immunol. 2013;43(9):2273-82.

309. Bremnes B, Rode M, Gedde-Dahl M, Nordeng TW, Jacobsen J, Ness SA, et al. *The MHC class II-associated chicken invariant chain shares functional properties with its mammalian homologs*. Exp Cell Res. 2000;259(2):360-9.
310. Fujiki K, Smith CM, Liu L, Sundick RS, Dixon B. *Alternate forms of MHC class II-associated invariant chain are not produced by alternative splicing in rainbow trout (Oncorhynchus mykiss) but are encoded by separate genes*. Dev Comp Immunol. 2003;27(5):377-91.
311. Zhong D, Yu W, Liu Y, Liu J, Li J. *Molecular cloning and expression of two chicken invariant chain isoforms produced by alternative splicing*. Immunogenetics. 2004;56(9):650-6.

Annexe 1. Article non-discuté dans ce mémoire n°1

MMTV Superantigens Coerce an Unconventional Topology between the TCR and MHC Class II

Jean-Simon Fortin,[*,†,1] Laetitia Genève,[*,1] Catherine Gauthier,[*] Naglaa H. Shoukry,[‡] Georges A. Azar,[*,2] Souheil Younes,[‡] Bader Yassine-Diab,[‡] Rafick-Pierre Sékaly,[x] Daved H. Fremont,[†] and Jacques Thibodeau[*]

[*]Laboratoire d'Immunologie Moléculaire, Département de Microbiologie, Infectiologie et Immunologie, Université de Montréal, Montreal, Quebec HC3 3J7, Canada;

[†]Department of Pathology and Immunology, Washington University School of Medicine, St. Louis, MO 63110;

[‡]Département de Médecine, Université de Montréal and Centre de Recherche du Centre Hospitalier de l'Université de Montréal, Montreal, Quebec H2L 4M1, Canada;

[x]Division of Infectious Diseases, Vaccine and Gene Therapy Institute of Florida, Port Saint Lucie, FL 34987

[1]J.-S.F. and L.G. contributed equally to this work.

[2]Current address: Axenis, Centre de Biologie Integrative des Maladies Émergentes, Institut Pasteur, Paris, France.

Status: published in Journal of Immunology

Address correspondence and reprint requests to Dr. Jacques Thibodeau, Laboratoire d'Immunologie Moléculaire, Département de Microbiologie, Infectiologie et Immunologie, Université de Montréal, CP 6128, Succursale Centre-Ville, Montreal, QC H3C 3J7, Canada.

Abstract

Mouse mammary tumor virus superantigens (vSAGs) are notorious for defying structural characterization, and a consensus has yet to be reached regarding their ability to bridge the TCR to MHC class II (MHCII). In this study, we determined the topology of the T cell signaling complex by examining the respective relation of vSAG7 with the MHCII molecule, MHCII-associated peptide, and TCR. We used covalently linked peptide/MHCII complexes to demonstrate that vSAG presentation is tolerant to variation in the protruding side chains of the peptide, but can be sensitive to the nature of the protruding N-terminal extension. An original approach in which vSAG was covalently linked to either MHCII chain confirmed that vSAG binds outside the peptide binding groove. Also, whereas the C-terminal vSAG segment binds to the MHCII α-chain in a conformation-sensitive manner, the membrane-proximal N-terminal domain binds the β-chain. Because both moieties of the mature vSAG remain noncovalently associated after processing, our results suggest that vSAG crosslinks MHCII molecules. Comparing different T cell hybridomas, we identified key residues on the MHCII α-chain that are differentially recognized by the CDR3β when engaged by vSAG. Finally, we show that the highly conserved tyrosine residue found in the vSAg TGXY motif is required for T cell activation. Our results reveal a novel SAG/MHCII/TCR architecture in which vSAGs coerce a near-canonical docking between MHCII and TCR that allows eschewing of traditional CDR3 binding with the associated peptide in favor of MHCII α-chain binding. Our findings highlight the plasticity of the TCR CDRs.

Introduction

Superantigens (SAGs) are bacterial or viral proteins that have the ability to stimulate up to 20% of the total T cell population, bypassing conventional MHC class II (MHCII) Ag processing and presentation (1). SAG-activated T cells undergo a strong proliferation phase that is followed by either anergy or deletion (2). In contrast to canonical MHCII/TCR docking, which relies on the intimate binding of the CDRs to the MHCII *a* helixes and associated peptide, TCR bridging to MHCII by SAGs relies on distinct strategies (3). On the one side, they commonly bind to the TCR CDR2, framework region 3 (FR3), and hypervariable region (HV4) that are within a specific V family (4). On the other side, they either bind 1) the MHCII *a*-chain, 2) a binding interface composed of the MHCII α-chain and associated peptide, 3) the MHCII βHis81 residue through coordination of a zinc ion, or 4) the entire MHCII membrane-distal surface spanning the *a*-chain, β-chain, and the associated peptide (4, 5). Moreover, a handful of SAGs have the ability to crosslink or oligomerize MHCII molecules by using both the α- and β-chain binding sites (6). SAGs of viral origin have yet to provide a clear picture in terms of their ability to compel such interactions.

The best characterized viral SAGs (vSAGs) are those encoded by the mouse mammary tumor viruses (MMTVs). Contrary to other SAGs, vSAGs are produced by the host cell machinery and must undergo posttranslational modifications to stimulate T cells (7). First, a precursor polypeptide forming a type II transmembrane protein of 37 kDa is modified by the addition of up to five N- linked glycans (8). Then, the 45-kDa glycoprotein transits to the Golgi where it is cleaved at two specific RXXR dibasic motifs, resulting in the luminal N-vSAG and C-vSAG (also called 18 kDa) moieties. After processing, both N- and C-terminal domains remain noncovalently associated and detached from the membrane (9). This maturation allows cells to shed vSAGs, even when devoid of MHCIIs, a feature called paracrine transfer (10). Finally, by binding both MHCII and TCR, the C-vSAG domain is responsible for cognate T cell stimulation (9, 11). Within this fragment is the most polymorphic region of the MMTV

SAGs, the C-terminal 21–38 residues responsible for Vβ specificity (12). Extensive TCR mutagenesis has revealed that the TCR binding site of C-vSAG includes the TCR Vβ FR3 and HV4 (13–17). Interaction with MHCIIs, in contrast, is puzzling and has been reasoned from competition experiments in which vSAG and the staphylococcal enterotoxin A (SEA) compete for binding on both the α- and β-chains (10, 18).

The molecular basis for successful T cell stimulation by vSAG7 is an interesting conundrum. Our group and others have described vSAG presentation to be influenced by the peptide repertoire (19, 20). However, it is unknown whether this characteristic is linked to vSAG binding to MHCII or TCR recognition of the vSAG-bound MHCII complex. Conflicting data of vSAG binding to the MHCII α-chain, β-chain, or peptide-binding groove exist in the literature and none provided a consensual model on how they successfully generate the T cell signaling complex (10, 18, 21, 22). In the present study, we sought to determine the topology of the vSAG/MHCII/TCR complex by examining the respective relationship of vSAG7 with the MHCII chains, associated peptide, and TCR. To this end, we used a panel of covalently linked peptide/MHCII molecules, point mutants, and MHCII/vSAG single chain (SC) constructs. Altogether, our results define a novel MHCII/SAG/TCR architecture.

Methods

Plasmids and mutagenesis

The vSAG7 sequence was codon optimized using GeneOptimizer (Invitrogen). pBUD-DRα and -DRβ have been described elsewhere (23). Lumenal portions of DRα (aa 1–191) and DRβ (aa 1–199) were linked to the lumenal part of vSAG7 (aa 67–322) or Ii (aa 72–297) by the PCR overlap extension method (24). The chains were joined by a small glycine-serine linker (G3-S-G3) introduced in DR chains, Ii and vSAG7 using complementary overlapping primers. DRα mutants, peptide-linked DRβ (25), hemagglutinin SC trimer (HASCT) and SC dimer (SCD)*D*Ct were generated by the PCR overlap

extension method using the Phusion polymerase (New England BioLabs). The resulting cDNAs were cloned into pCDNA3 vector (Invitrogen) and sequenced. The lHADR, CLIP-HADR, and GSPS- HADR peptide-linked DRβ coding sequences were obtained by chemical synthesis (Life Technologies) and cloned in pCDNA3.

Abs and reagents

The VS7 (IgG1) mouse mAb is specific to the C-terminal end of MMTV7 SAG (26). L243 (mouse IgG2a mAb) and ISCR3 (mouse IgG2b mAb) bind specific DRα conformational epitopes (27). XD5 (mouse IgG1 mAb) binds a linear epitope in the β1 domain of all HLA-DR molecules (28). BU45 (mouse IgG1 mAb) binds the C-terminal portion of human Ii (29), and CerCLIP.1 (mouse IgG1 mAb) recognizes the N-terminal portion of CLIP (30). The anti-DRα (antiserum against the DRα-chain) and anti-DRβ (anti- serum against the DRβ*0101 chain) were obtained following the immunization of rabbits with proteins purified from SDS-PAGE (R.P.S., unpublished). The anti-SEA mAb was a gift of Dr. W. Mourad (University of Montreal) (31). SEA was purchased from Sigma-Aldrich (St. Louis, MO).

Cell lines and transfections

Human epithelial HEK 293T, HeLa DM.5 and HeLa CIITA cells (20), and murine DAP cells were culture in DMEM (Wisent) with 5% FBS (Wisent), whereas Kmls 13.11 and Kmls 12.6 T cell hybridomas (32) were cultured in DMEM with 10% FBS. CTLL-2 (TIB-214; American Type Culture Collection) and HA1.7 TCR^+ Jurkat cell line, CH7C17 (33), were cultured in RPMI 1640 (Wisent) with 10% FBS and 4 μM 2-ME. HeLa and DAP cells were transfected using Lipofectamine LTX reagent (Invitrogen) according to the manufacturer's instructions. The cells were selected for resistance against geneticin (500 μg/ml; Wisent), and $MHCII^+$ cells were sorted by flow cytometry on a FACSVantage SE (BD Biosciences). HEK 293T cells were transfected using the calcium phosphate method as described previously (34) using 8 μg plasmid DNA. Cells were harvested and analyzed 48 h after transfection.

Flow cytometry

Cells were incubated in PBS with the primary Ab for 30 min on ice. Cells were washed twice with PBS and incubated a further 30 min with the Alexa Fluor 488–coupled goat anti-mouse IgG Ab (Invitrogen) for 30 min on ice. After two more washes, cells were analyzed by flow cytometry using a FACSCalibur (BD Biosciences). Alternatively, cells were incubated for 1 h with SEA on ice and washed twice with PBS prior to the addition of Abs. Intracellular stainings were performed as mentioned on fixed, permeabilized cells (4% paraformaldehyde, 0.05% saponin).

T cell stimulation assays

vSAG7-expressing APCs were cocultured at a 1:1 ratio with 5 3 10^4 T cell hybridomas for 18 h at 37˚C. IL-2 production was determined by the ability of the coculture supernatant to sustain the proliferation of the IL-2– dependent T cell line CTLL-2 and was measured by [^{3}H]thymidine in- corporation (35). Alternatively, the IL-2 concentration was determined by cytometric bead array (BD Biosciences). For indirect presentation, APCs (donors) were cocultured with BJAB cells (acceptors) and responder T cell hybridomas at a ratio of 1:1:1.

Immunoblots

Cells were lysed for 30 min on ice at a density of 2×10^7 cells/ml in 1% (v/v) Triton X-100 in lysis buffer (20 mM Tris-HCl, 150 mM NaCl) and complete protease inhibitor (Roche). Heated (65˚C) or boiled total protein extracts were then separated by SDS-PAGE (10%) under reducing conditions, unless mentioned otherwise. Samples were transferred to Hybond-ECL nitrocellulose membrane (Amersham Biosciences). Membranes were blocked for 1 h with 5% (w/v) dry milk in TBST (TBS with 0.1% [v/v] Tween 20). The following steps were also performed in TBST with 5% dry milk. Primary Abs to DRα, DRβ, and vSAG7 were incubated for 1 h at room temperature. Membranes were washed three times for 10 min and incubated for 1 h with HRP-conjugated secondary Abs (Bio/Can Scientific) followed by three more 10-min washes. Bands were visualized by the BM chemiluminescence blotting substrate (Roche). For

endo H sensitivity, 500 U endoglycosidase H (New England BioLabs) was added to the protein extract and incubated for 1 h at 37˚C. Samples were analyzed on SDS-PAGE as above.

Results

MHCII-associated peptide influences vSAG7 presentation

It was previously shown that DM-deficient human cells could not present the toxic shock syndrome toxin-1 or vSAGs (20, 36). Similarly, presentation of these SAGs by cells from H2-DM–deficient mice was inefficient (37–39). DM edits the peptide repertoire by exchanging CLIP for a variety of peptides with better kinetic stability (40). Thus, we wondered whether the accumulation of CLIP/MHCII complexes observed in DM^{-} cells was responsible for the lack of vSAG7 presentation. We used the well- characterized DM^{-} T2-DR3 cell line (41). In these cells, >90% of the DR molecules are loaded with CLIP, a phenotype that is lost upon transfection of DM (30). As shown in Fig. 1A, whereas T2- DR3 cells failed to present vSAG7, T2-DR3-DM^{+} cells led to strong T cell proliferation, similar to that observed with DM- proficient BJAB and COX B cell lines. Of note, in this experiment, vSAG was provided by coculturing APCs with the $MHCII^{-}$ DAP- $vSAG7^{+}$ cell line (10). These results suggest that CLIP/DR3 complexes do not support vSAG7 presentation.

We next aimed to determine how the CLIP peptide could affect vSAG7 presentation. Considering the MHCII-associated peptide, vSAG presentation can be influenced by 1) peptide flanking residues (PFRs) extending outside the groove, 2) peptide protruding side chains, or 3) peptide-induced MHCII conformational change. To discriminate between these possibilities, we generated cell lines displaying distinct homogenous pMHCII populations by transfecting DRα with various peptide/DRβ fusion proteins (42). The mouse DAP cells were chosen as model APCs because they

are easily transfected and allow vSAG7-specific T cell stimulation upon cotransfection of MHCIIs and vSAG (43). Once stable peptide/DR1 DAP cell lines were obtained, we transiently transfected vSAG7 and monitored proliferation of mouse vSAG7-responsive T cell hybridomas (44). We used two different hybridomas bearing Vβ6 regions cognate for vSAG7. Because vSAG7 expression is low, we coexpressed a reporter GFP to monitor transfection efficiencies and plotted mean fluorescence intensity (MFI) in bar graphs.

First, we tested whether the PFRs of CLIP were affecting vSAG stimulation. We hypothesized that the hallmark N-terminal extension of CLIP would affect vSAG7 presentation based on analyses of CLIP peptides found in T2-DR3 cells, which all bear four to six PFRs (35, 45). We generated cell lines expressing MHCIIs charged with either long $CLIP_{81–101}$ (lCLIP) or core $CLIP_{87–101}$ (cCLIP) peptides (Fig. 1B). To ensure that the quaternary structure of the different complexes was not disturbed by the peptide, we used two different mAbs: L243, which binds a conformational epitope on the DRα-chain, and XD5.117, which binds a linear epitope on the DRβ-chain (28, 46). Fig. 1C shows for each cell line the MHCII cell surface expression and the MFI of the reporter GFP (*lower panels*). Both cell lines expressed similar amount of MHCIIs and were similarly receptive to DNA upon the subsequent transient transfection of vSAG7 and GFP.

After vSAG7 transfection, cells were incubated with the $Vβ6^+$ T cell hybridomas Kmls 13.11 or 12.6. As shown in Fig. 1D, vSAG7 presentation by lCLIP-DR was inefficient compared with cCLIP-DR, the latter giving rise to strong T cell response. Interestingly, we also observed a decrease in L243 mAb reactivity with the lCLIP-DR1 transfectant (Fig. 1C), better portrayed by the graph in Fig. 1E showing normalized MFI for L243 over XD5. The reduced L243 reactivity for lCLIP/MHCII complexes can either stem from an MHCII conformation alteration or steric hindrance between the $CLIP_{81–86}$ extension and L243. This result suggests that vSAG7 presentation is sensitive to variations in pMHCII that are also sensed by the mAb L243.

However, it is hard to pinpoint whether it is one of these effects, or a combination of both, that accounts for the reduction in stimulatory capacity of vSAG7. On the one hand, it was reported that the L243- like 14-4-4S mAb, specific for mouse MHCII, competes against vSAG7 on I-E^d (47). Likewise, staphylococcal enterotoxin B (SEB), which binds to the MHCII α-chain and competes with L243, is also affected by lCLIP (48, 49). On the other hand, superimposition of the crystal structures of DR1 bound to either CLIP86–101 or CLIP90–101 showed conformational alteration in the loop connecting the third and fourth strands of the MHCII β-sheet platform that includes lysine α39 (50). Mutation of K39 abolishes L243 and SEB binding but does not affect vSAG presentation (51). Therefore, although there is a known conformational change between CLIP-MHCII variants, it is unlikely to affect vSAG7 presentation. Taken together, these results suggest that the reduced vSAG7 stimulation observed when presented by lCLIP-DR1 is due to steric hindrance of vSAG7 by terminal PFRs of CLIP. This conclusion is strengthened by the fact that a HA peptide bearing the N-terminal extension of CLIP (CLIP81–87) was much less permissive in allowing vSAG7 stimulation than the wild-type (wt) HA sequence of the corresponding length (Supplemental Fig. 1). Also, the above-described data corroborate the notion that vSAG7 binds to the MHCII α-chain (10).

Secondly, we sought to evaluate the contribution of TCR- contacting peptide residues by comparing the capacity of peptides with distinct protruding side chains to present vSAG7. To this end, we employed a covalently linked HA307–319 peptide (HADR1). We selected this peptide over CLIP given the availability of the HA peptide/DR1/HA1.7 TCR structure and of the modified Jurkat cell line expressing the HA1.7 TCR (hereafter simply referred to as Jurkat) (33, 52). Our rationale was to be able to distinguish both the conventional and vSAG presentation in the same setting, using different T cells. Additionally, to minimize adverse effects linked to the bound peptide's primary sequence, we performed the same assays using another peptide supporting vSAG presentation, the tetanus toxin peptide (TT829–842). Similar to HA-DR1, TT-DR1 has great kinetic stability and also fills the P1 pocket with a tyrosine,

thus providing a system to test the exclusive contribution of peptide-protruding side chains (Fig. 1B) (53, 54). The TCR contacting side chains of these two peptides were interchanged, resulting in the backbone (b) HA$_b$ and TT$_b$ variants, and involved a charge modification at P-1 (K-Q), a change of a small residue (V) to a bulkier one (I) at P2, and finally a change from a positively charged residue to a highly hydro- phobic one (K-F) at P8. When any of the peptide-protruding side chains were implicated in specific vSAG7 contacts, one should expect to see differential stimulation between these peptides, independently of the T cell Vβ specificity. The stably transfected HAβ and TTβ constructs (Fig. 1F, 1H) were then tested for their capacity to stimulate T cells (Fig. 1G, 1I). Every variant successfully presented vSAG7, suggesting that a peptide's protruding side chains are not critical for vSAG7-mediated response (Fig. 1G, 1I). Conversely, presentation of HA$_b$ failed to stimulate Jurkat T cells (Fig. 1J), as specific TCR contact residues have been modified (52). Many covalently-linked peptides supported strong vSAG7 presentation, ruling out a role for the peptide's C-terminal linker and thus PFR at this end. Altogether, these results suggest a model in which vSAG7 presentation is tolerant to the nature of the peptide's protruding side chains, but can be sensitive to the conformation adopted by the N-terminal extension of some peptides.

N-vSAG7 has an overlapping binding site with SEA on the DRb-chain

The above-described data support the notion that C-vSAG7 binds to the MHCII α-chain. However, it has been proposed that the vSAG7 polypeptide has two binding sites on MHCII, one of which shares the same interface as SEA on the β-chain or binds the peptide-binding groove (18, 21, 22). Maturing vSAGs are composed of two domains that remain noncovalently associated upon processing. C-vSAG participates in MHCII/TCR bridging but the role of N-vSAG is less clear. To gain insight on the role of the latter, we designed two SC polypeptides in which the luminal domain of either DR chain is linked to that of vSAG7. These straightforward SCDs were inspired by a similar fusion between MHCII and Ii (55). Such SCDs were made possible because HLA-DR and vSAG7 are type I and type II proteins, respectively, allowing fusion of the C

terminus of DR chains to the N terminus of vSAG7. The resulting DRα- and DRβ-based fusion molecules were named αSCD and βSCD, respectively, and are depicted in Fig. 2A. For brevity, when an SCD is mentioned in an experimental setting, it is always cotransfected with its matching complementary wt DR chain partner; for example, DRα plus βSCD is referred to as βSCD.

First, we characterized the interaction between the SCDs and their complementary MHCII chain partner. For these experiments, we used HEK 293T cells given their high transfection efficiency. First, the αSCD apparently failed to form a functional complex with DRβ, as judged by the lack of L243 surface staining and the fact that DRβ remained entirely EndoH-sensitive (Fig. 2B, Supplemental Fig. 2, *left panel*). Also, the αSCD migrates as two major bands, which are smaller than βSCD and appear to be devoid of sugars (Supplemental Fig. 2, *middle* and *right panels*). In contrast, the βSCD properly associated into heterodimers with DRα, trafficked to the plasma membrane, and was recognized by a conformational mAb (Fig. 2B, *left panel*). Using the anti–C-vSAG7 mAb VS7, we also observed MHCII-bound vSAGs at the cell surface (Fig 2B, *right panel*). Al- together, these results indicate that only the βSCD can generate ordered complexes and allow vSAG surface expression.

Next, to confirm that vSAG7 behaved similar to the wt vSAG when part of the βSCD, we verified whether it still competed the binding of SEA. We transfected HEK 293T cells with either wt DR or βSCD and performed SEA binding assays monitored by flow cytometry. Fig. 2C shows the DR (*left panel*) and SEA (*right panel*) staining profiles, which reveal weak SEA binding to cells expressing βSCD. Once normalized for MHCII surface expression, we noted a marked reduction in the binding of SEA for βSCD compared with the wt or a control βIi-SCD controls (Fig. 2A, 2D). These results indicated that the vSAG moiety on DRβ interferes with SEA binding. However, because SEA has a minor low-affinity binding site on the MHCII α-chain, the possibility remained that the observed competition was due to the presence of vSAG7 on DR*α* (56, 57). To test this, we performed the same experiment using a DRα mutant that is unable to bind SEA (DRαK39A) (56). As shown in Fig. 2E, binding of SEA is the same whether

DRβ is associated with wt MHCII α-chain or K39A mutant. Moreover, truncating C-vSAG from βSCD, generating the βSCDΔCt, still reduced SEA binding, confirming that N-vSAG7 and SEA have an overlapping binding interface (Fig. 2D). The high SEA concentration and affinity for βHis81 are factors likely to favor displacement of some of the vSAG7 molecules and could explain why competition was not total. Likewise, processing of the vSAG7 moiety is observed and could favor its dissociation from the *β*-chain (Supplemental Fig. 2). These data confirmed that N-vSAG has an overlapping binding site with SEA on the MHCII β-chain.

vSAG7 does not bind the MHCII peptide groove

Our results described so far define the binding site of C-vSAG7 and N-vSAG to the MHCII α-chain and β-chain, respectively. Thus, it was difficult to envision a model where vSAG7 interacted with both DR chains at once. Huber and colleagues (22) proposed that a segment of MMTV SAGs (called the MHCII peptide-binding motif) interacts with the MHCII peptide-binding groove upon synthesis in the endoplasmic reticulum. The MHCII peptide- binding motif is part of N-vSAG and could bridge both vSAG segments through the MHCII cleft. To verify whether vSAG7 occupies the MHCII groove, we designed a new construct, HASCT, in which the HA peptide was appended to the βSCD N terminus (Fig. 2A). Based on the Hsu et al. (22) premise, our rationale was that N-vSAG7 would prevent HA binding to the groove. Fig. 3A shows the surface DR expression for both βSCD and HASCT in comparison with wt DR and HADR. Interestingly, DR surface staining was increased in both transfectants expressing the linked HA peptide. These data corroborate well with the in- creased stability of MHCIIs when optimal peptide occupies the groove (25). Soluble versions of DRβ and HAβ (sβ and sHAβ) chains were used as controls and ruled out transmembrane domain–mediated bias between the transmembrane-devoid βSCD and controls. L243 MFI ratios of sβ and βSCD against sHAβ and HASCT, respectively, showed a 4-fold increase in expression when HA was fused to DRβ (Fig. 3B). That the tethered HA peptide increased expression of DR is incompatible with a model in which vSAG would occupy the binding groove.

To confirm that the HA peptide was lodged inside the groove and not displaced by the immature vSAG7 polypeptide, we tested the complex for SDS sensitivity. Indeed, HA/DR1 complexes resist SDS denaturation and migrate as compact peptide-loaded heterodimers under nonboiled conditions (58). Cell lysates obtained from the transfectants presented in Fig. 3A as well as a *β*IiSCD control were analyzed by SDS-PAGE. XD5 mAb was used to probe the immunoblots. As expected, in absence of HLA-DM, neither Ii nor vSAG7 SCDs formed compact complexes with DRα (Fig. 3C, *lanes 4* and *6*). In contrast, when HA was linked to either DRβ or βSCD (*lanes 2* and *8*), compact, SDS-resistant heterodimers were observed, confirming that the HA peptide was present in the groove.

To unequivocally prove that vSAG7 did not bind to the MHCII cleft, we tested whether the HASCT could induce both Jurkat and vSAG-specific T cell responses. To this end, we moved from the HEK 293T to HeLa cells, the former being unable to present vSAG (20). Of note, although the molecular basis of this defect remains obscure, HeLa cells are unable to present vSAGs unless transfected with CIITA or treated with IFN-γ (20). This provided a useful system to evaluate the presentation of HA independently of vSAG in the absence of CIITA and of both HA and vSAG7 in the presence of CIITA. We transiently transfected our various β-chains into either HeLa or HeLa CIITA^{+} cells and assessed the response of Jurkat or Kmls 13.11 cells. As expected, vSAG7 presentation only occurred in the presence of CIITA, whether from the SCD or SCT (Fig. 3E). Surprisingly, HeLa cells transfected with HASCT failed to stimulate Jurkat cells in contrast to the control sHAβ (Fig. 3D). The lack of HA presentation can be attributed to either an MHCII conformation flaw or to the vSAG moiety of the HASCT hampering proper TCR docking. We argue for the latter alternative because the tested mAbs did not distinguished the HASCT from the sHAβ control (Fig. 3A), and in the presence of CIITA, HA presentation was restored (Fig. 3D). However, that Jurkat failed to respond to the HASCT in CIITA^{-} cells was puzzling. This is not due to degradation of the SCT-HA peptide and its subsequent association to endogenously expressed MHCIIs, as the DR*b**0102 allele in the homozygous HeLa CIITA^{+} cells does not present HA307–318

to Jurkat T cells (59) and therefore must arise from the HA-DR1 moiety of the SCT. One explanation is that in presence of a pool of MHCIIs, C-vSAG is transferred from the processed SCT onto the endogenous pMHCIIs (supporting vSAG presentation), thus revealing HA to the HA1.7 TCR-bearing Jurkat T cells. The implications of this finding are discussed below.

vSAG7 presentation relies on MHCIIa/TCR interactions

To better pinpoint the C-vSAG7 binding site on DRα and investigate the TCR binding topology, we generated an array of mutants of the α helix lining the peptide groove. Most mutants were modeled from DQ2 and I-A^q, which present vSAG poorly and span aa 63–68, the interface associated with SEB binding (12). Fig. 4A shows the point mutants on the HA-DR1 model (Protein Data Bank no. 1FYT) as well as DRα residues implicated in L243 mAb binding (27, 52). Flow cytometry analysis of the resulting stable DR expression in DAP cells is given in Fig. 4B as assessed by L243 and XD5 staining. As above, stable cell lines were transiently cotransfected with vSAG7 and the reporter GFP. Then, cells were cocultured with Kmls 13.11 and Kmls 12.6 T cells and IL-2 production was measured. In an effort to minimize the effect of the cells' intrinsic associated peptides, we coexpressed each DRα variant with the HADRβ-chain. Additionally, this allowed us to monitor the stimulation of HA-specific Jurkat cells, which could be impeded by the α-chain mutations (Fig. 4D). As predicted from the HA/DR1/HA1.7 TCR cocrystal (52), only mutation of TCR contact residues α64, α65, and α67 abrogated presentation of HA to Jurkat cells.

Of note, the reactivity of L243 was strongly decreased toward DR mutants α63 and α67 (Fig. 4B). This is best portrayed by the graph in Fig. 4C showing L243 MFI over the MFI of the conformation-insensitive XD5 mAb. Surprisingly, those same DR mutants had a dramatically reduced ability to present vSAG7 (Fig. 4E, 4F), suggesting again overlapping binding regions between L243 and vSAG. Because the side-chain of α63 points laterally, the weakened stimulation observed with both hybridomas by the αI63E MHCII mutant cell line suggests that C-vSAG7 binding is somehow affected by

this mutation. Indeed, a less obstructive mutation, αI63A, restored vSAG7 stimulation (Supplemental Fig. 3A, 3B).

Interestingly, whereas DRαA64R allowed a strong Kmls 13.11 stimulation, Kmls 12.6 failed to respond (Fig. 4E, 4F). This result indicates a TCR recognition effect unrelated to vSAG7 binding and highlights the importance of specific DRα/TCR contacts for efficient T cell stimulation. In line with this, it became difficult to evaluate whether the effect of DRα K67A on vSAG presentation is actually linked to a weakened association between vSAG and DRα or to a TCR recognition defect. Indeed, DRα K67 is characterized by a lack of both L243 reactivity and inefficient presentation of HA peptide to Jurkat cells, making both outcomes plausible (Fig. 2C, 2D). Although weak, the stimulatory response observed exclusively with the Kmls 13.11 hybridoma suggests that TCR recognition is a factor.

The solvent-exposed DRα α helix is used by SEB to bridge TCRs (61). The fact that vSAG7 presentation implicates DRα/ TCR interactions demonstrates that the topology of the ternary complex is different from the one involving SEB. Interestingly, only the DRα mutant A64R cell line was unable to support SEB presentation (Supplemental Fig. 3C). The highly conserved A64 is buried inside the SEB/DRα interface and the Arg substitute is likely to sterically hinder SEB association, probably reflecting the effect of I63E on vSAG7 presentation. Overall, it is apparent that the mechanism leading to TCR recognition of the vSAG/MHCII complexes differs from SEB and canonical peptide/MHCII recognition.

vSAG7 mediates TCR activation through a conserved TGXY motif

The specific interactions between the TCR and the MHCII α-chain suggest the existence of conserved vSAG/TCR contacts. Given the numerous responsive Vβs for all vSAGs, it is unlikely that the TCR interaction is solely based on the polymorphic vSAG C terminus, as it would severely impede the likelihood of a cognate partnership. Interestingly, an alignment of MMTV SAGs and MMTV SAG-related domain from other viruses (e.g., herpesvirus) revealed a conserved TGXY motif (Fig. 5A) located at

residues 226–229 of C-vSAG. We mutated the Tyr229 to a Phe and assessed the ability of vSAG7-YF to stimulate different T cell hybridomas. Fig. 5B indicates that the Y229F mutation introduced either in full length or SC vSAG7 abrogated the activity. The TGXY motif could impact vSAG activity in many ways. On the one hand, it could perturb C-vSAG binding to MHCIIs or its overall structural integrity. Both of these hypotheses are refuted by the fact that the mutation did not affect surface expression of MHCIIs or vSAG7 (Fig. 5C, 5D). On the other hand, the Tyr229 could be implicated in direct TCR contact. Supporting this mechanism is the presence of a similar motif, LGNY, on a SEB contacting loop that interacts with the HV4 region of the TCRβ. Accordingly, mutation of the Tyr on SEB prevents its presentation (63, 64). Furthermore, Digglemann and colleagues (65) described the region of C-vSAG bearing the TGXY motif as part of the TCR-interacting domain. These results suggest that in addition to highly polymorphic regions responsible for Vβ specificities, vSAG binding also relies on conserved vSAG-specific TCR interactions.

Discussion

The data presented in this study define how vSAG7 bridges MHCII to the TCR. C-vSAG binds the MHCII α-chain in a conformation- sensitive manner at the interface formed between the α helix and the β-sheet platform. We demonstrated that, when coerced by vSAG, the TCR recognizes the MHCII in a near canonical manner, which constitutes a unique topology among those previously described for SAGs. Next, our results suggest that maturing N- and C-vSAG7 bind the MHCII β- and α-chains, respectively, on distinct MHCIIs. Finally, we identified a conserved motif in MMTV SAGs responsible for TCR binding independently of the TCR Vβ specificity. Based on our results and those of others, we propose a model in which the N- and C-terminal domains of a single vSAG crosslink two MHCIIs and bridge only specific TCR-bearing Vβ elements that can be skewed to recognize the MHCII α-chain instead of the associated peptide (Fig. 4G).

C-vSAG7 binding to the MHCII α-chain is influenced by the associated peptide

Presentation of vSAG7 requires that MHCIIs be filled with a diverse peptide repertoire (11, 20, 38). In the present study, we demonstrated that a single peptide supports vSAG7 presentation. However, the MHCII associated peptide must meet certain criteria to be part of a permissive pMHCII. By comparing cell lines expressing either cCLIP-DR1, lCLIP-DR1, and CLIP-HADR1, we showed that the CLIP81–86 PFRs inhibit vSAG presentation (Fig. 1D, Supplemental Fig. 1). Interestingly, it was previously described that CLIP N-terminal extensions also interfered with SEB binding to MHCII (49). The crystal structures of CLIP-DR3 and CLIP–I-A^b show that the CLIP81–86 N-terminal extension is disordered, suggesting an idiosyncratic effect of this CLIP region on vSAG function (66, 67). Future studies will address this issue by characterizing the impact of a larger panel of N-terminal extensions linked to various core peptides. Nevertheless, knowing the profound effect of PFRs on canonical and toxic shock syndrome toxin-1 T cell responses (39, 68, 69), and that DM favors the binding of peptides that tightly fit the groove, our findings point to N-terminal peptide trimming as a potentially important determinant for vSAG presentation (40, 70). These results explain why DM-deficient cells, either murine or human, are unable to present vSAG7, as they are predominantly charged with CLIP peptide bearing a 4- to 6-aa extension (34, 45, 71). Hsu et al. (22) reported that a DM^- B cell line was able to present vSAG7. However, as opposed to T2 cells expressing a single MHCII (DR3) or our DAP cell lines (DR1), the proportion of the various alleles of DR, DQ, or DP that are bound to CLIP at steady-state, or which form of CLIP is bound, was not determined in this DM^- model.

It is unclear whether the previously reported need for peptide diversity reflects a direct contribution of the peptide's sequence to part of the vSAG binding site or is an indirect negative effect echoed in the MHCII conformation. The findings presented in this study support the latter hypothesis. It is unlikely that vSAG7 interacts with the MHCII-bound peptide's protruding side chains because severe changes in charge or size

between those of HA, TT, and CLIP did not affect their ability to activate Vβ6- and Vβ8.1-bearing T cells (Fig. 1, Supplemental Fig. 3D). Although we did not conduct a thorough saturation mutagenesis of the peptides, our observation of DRα/TCR contacts portrays a setting in which vSAG7/peptide interactions are improbable (see below). Our results suggest that C-vSAG7 binds to the lateral interface formed by the solvent-exposed DRα α helix/β-sheet junction (Fig. 4A), an area highly susceptible to peptide-induced conformational changes (72). That HA-DR1αI63E, but not HA-DR1αI63A, reduced both L243 mAb reactivity and vSAG7 presentation capabilities points to an MHCII conformation defect (Fig. 4C, 4D, Supplemental Fig. 3A, 3B). It was previously reported that mice expressing Eα-bound I-A^b as the sole pMHCII were unable to mount vSAG7-specific responses, supporting the conclusion that a diverse MHCII peptide repertoire was required (38). In light of our results, we can speculate as to why this pMHCII failed to present vSAG. The Eα(52–68) peptide bears no N-terminal PFRs, and the C-terminal linker between the peptide and the MHCII β-chain does not influence vSAG presentation. Thus, as previously presented by the authors, the inability of Eα–I-A^b to successfully present vSAG must be due to its intrinsic conformation (38). In- deed, whereas the 25-9-17 mAb binds a panel of peptide-bound I-A^b, Eα–I-A^b was not recognized (73, 74). One possibility is that vSAG7 binding is affected by the aF24 residue, reported to be pushed outward by the bulky p1-filling Phe of Eα at the C-vSAG7 binding site (75). Although we did not observe an effect of a Y-A substitution at the p1 HA residue (Supplemental Fig. 3E), it would be interesting to determine whether a bulkier amino acid (e.g., Trp) substitution would reduce vSAG7 presentation accordingly. Collectively, these results indicate that the interface formed on the DRα α helix/β-sheet junction is paramount for vSAG7 binding and that its presentation is vulnerable to both peptide-mediated conformational changes and N-terminal PFRs.

TCR engagement by vSAG7 is unique among SAGs

Most of the SAG-mediated T cell signaling complexes outline a typical interaction between the TCR Vβ and the SAG, where the Vα sometimes participates in MHCII β-chain binding (4, 76, 77). Consequently, Vβ/MHCII α-chain contacts are

sterically precluded by the bound bacterial SAGs. Given the lack of an MMTV SAG crystal structure, it is challenging to predict how vSAGs force MHCII/TCR association. Previous analyses of the response of mature peripheral T cells against vSAGs have clearly established that non-Vβ components of the TCR are involved in the pMHCII/vSAG7 complex recognition (78–81). The Vα-chain was shown to be an important part of the complex, and a skewed repertoire in responding cells has been identified (82, 83). Within a given Vα family, reactivity was seen with only certain Vβ subfamily members (83, 84). Thus, the variations in the CDR regions, especially CDR3, are likely to affect the capacity of these TCRs to bind the MHCIIs and might be at the origin of many of the reported cases of MHCII allelic/isotype restriction (32, 47, 83, 85).

Based on these facts and our results demonstrating that DRα A64R and K67A mutant cell lines differentially stimulated distinct hybridomas bearing the same Vβ, it is clear that the TCR/MHCII contacts are imperative to vSAG7 signal transduction (Fig. 4E, 4F). Moreover, these findings highlight direct MHCII α-chain/ TCRβ contacts and would imply that vSAG7-mediated TCR engagement resembles that of conventional peptides, as hypothesized by the Marrack and Kappler group following their discovery that the TCR βT24Y mutant abrogated both conventional Ag and vSAG presentation (13, 86). Along the same lines, our MHCII α64 and α67 mutants were also unable to trigger HA-specific activation of Jurkat cells (Fig. 4D). Based on the crystal structure of HA/DR1/HA1.7 TCR, DRα A64 and K67 are bound to the CDR2β D51 (52). However, one must be cautious in unifying these results. Indeed, as we have shown with our many different peptide/MHCII combinations, the peptide's protruding side chain did not affect vSAG response by the tested hybridomas, as would be expected in a traditional pMHCII-TCR setting (Fig. 1). Furthermore, mutations at residues α65 and α68, which are also implicated in TCR binding (52), had no effect on the ability of MHCIIs to present vSAG7 (Fig. 4D, 4E). Thus, it is fitting to picture a near canonical docking between MHCII and TCR that is coerced by vSAG. Such architecture allows eschewing of traditional CDR1/3 binding with the associated peptide in favor of

MHCII chain binding as proposed by Nguyen et al. (87). These Vα/MHCIIβ and Vβ/MHCIIα contacts remain to be verified biochemically (88).

A large body of literature suggests that the β-chain junctional region could influence TCR recognition of vSAGs (79, 89–91). Especially relevant was the demonstration by many groups that Vβ6 thymic deletion is incomplete in vSAG7^{+} mice and that Vβ junctional diversity regulates vSAG reactivity (91, 92). At first glance, the need for a diverse peptide repertoire and the importance of Vβ junctional diversity may seem paradoxical. Because many peptides support vSAG binding, we do not expect skewing in CDR3. However, our results point to the existence of nonpermissive peptides regulating vSAG binding and to unconventional interactions between MHCII and TCR. In order words, there may be extra pressure on CDR3s to have more intimate contacts with the MHCII chains than during canonical peptide recognition. In- deed, thymic positive selection does not directly influence the fine specificity of T cells toward MHCII, and it has been suggested that TCR/MHCII interactions taking place during vSAG presentation are unconventional and linked to TCR recognition of haplotype- specific MHCII residues (79, 87). This is in line with the recent demonstration by Kilgannon et al. (92) that three of eight Vβ6^{+} T cells, although all specific for the same pMHCII (K5–I-A^{d}), did not respond to vSAG7.

A recent report by Stadinski et al. (93) stressed the fact that TCR specificity for pMHC ligands is not driven by germline-encoded pairwise interactions. Notably, they described a single TCR Vβ using alternate strategies to bind pMHC when paired with different Vα. The authors argued that because CDR1 and CDR2 loops have the flexibility to bind their ligands in many ways, this could not fit a pairwise coevolution model. Accordingly, it demonstrated that the CDR3 loops can markedly alter those evolutionarily selected contacts (94). Canonical CDR/pMHCII contacts can differ under different pressures, supporting a model in which vSAG enforces such unconventional docking.

vSAG7 moieties bind distinct MHCIIs

Given that vSAG7 N- and C-terminal moieties bind respectively the MHCII β1 and α1 domains, one must ask how such binding is possible while remaining noncovalently associated. We propose a model where C-vSAG binds the *α*-chain of an adjacent MHCII, while still bound to N-vSAG, with the latter attached to the β-chain. In other words, unable to reach the α-chain of its MHCII partner in *cis*, C-vSAG interacts with another MHCII in *trans*. This model highly resembles the manner in which SEA crosslinks MHCII molecules via a low-affinity binding site to the α-chain and the Zn-dependent binding site on the β-chain (95, 96). In the context of the SCT, our results showing that HA presentation to Jurkat cells is null in endogenous $MHCII^{-}$ as opposed to $MHCII^{+}$ cell lines strongly support such a model (Fig. 3D). Indeed, we speculate that in the absence of surrounding endogenous pMHCIIs, both vSAG7 moieties remain associated with the parent MHCII, blocking the groove and preventing the TCR from recognizing the HA peptide. Also, because each MHCII is covalently linked to vSAG, it is possible the C-vSAG prevents any approaching vSAG from contacting the *a*-chain in *trans*. In contrast, in HeLa CIITA cells, C-vSAG7 will find numerous vSAG-free endogenous MHCII α-chains to associate with, freeing the MHCII membrane-distal region for the HA-1.7 TCR binding. Although our data best fit a model where vSAG crosslinks MHCII molecules, we cannot entirely rule out that vSAG binds across the groove on the α- and β-chains of a single molecule. Biochemical and crystallographic studies will be needed to decisively demonstrate the binding of a single vSAG to two distinct MHCII molecules.

Highly conserved TCR binding motif in vSAGs

Our results indicate a more intricate vSAG7 presentation than previously acknowledged. vSAG stimulatory activity is paired to the TCR interaction of DRα, a structural aspect that will likely modulate its potency in terms of the responding T cell repertoire and the strength of the signal. Additionally, vSAG recognition of specific TCR vβ elements is mediated through its C-terminal 30 or so highly variable amino acids,

complicating speculation as to how this family of vSAGs could mediate such a broad immune response without a conserved binding scheme.

In conclusion, our observation that conserved DRα residues are implicated in the recognition of the vSAG/peptide/MHCII by the TCR suggests that T cell activation is influenced by the polymorphic CDR3β region, linked to the recognition of the MHCII *a*-chain. To our knowledge, this represents a novel SAG-mediated MHCII/TCR architecture. According to a recent study by Nur-ur Rahman et al. suggesting that the TCR CDR2β is the critical determinant for the functional recognition of bacterial SAGs, it is clear that the topology of vSAG differs from those previously described (97). Because both the MHCII allele and associated peptide influence the potential interaction between MHCII and TCR, a given TCR could only recognize a fraction of the vSAG/ pMHCII complexes (79). MMTV SAGs are expressed at very low density on the cell surface and still remain highly potent T cell activators. This expression pattern is of great importance, as it mimics the low density of conventional antigenic peptide/MHCII complexes, critical for T cell activation (98, 99).

Funding

This work was supported by Canadian Institutes of Health Research Grants MOP 36355 and 93592.

Acknowledgements

We thank Julie Chase and Christopher K. Salmon for proofreading and critical input on the manuscript. We also thank Walid Mourad for providing mAbs and Serge Sénéchal for assistance with cell sorting.

Disclosures

The authors have no financial conflicts of interest.

Abbreviations

Abbreviations used in this article: b, backbone; cCLIP, core CLIP; C-vSAG, C-terminal viral superantigen; FR3, framework region 3; HA, hemagglutinin; HASCT, hemagglutinin single chain trimer; HV4, hypervariable region 4; lCLIP, long CLIP; MFI, mean fluorescence intensity; MHCII, MHC class II; MMTV, mouse mammary tumor virus; N-vSAG, N-terminal viral superantigen; PFR, peptide flanking residue; s, soluble; SAG, superantigen; SC, single chain; SCD, single chain dimer; SCT, single chain trimer; SEA, staphylococcal enterotoxin A; SEB, staphylococcal enterotoxin B; TT, tetanus toxin; vSAG, viral superantigen; wt, wild-type.

References

1. Fraser, J. D., and T. Proft. 2008. The bacterial superantigen and superantigen-like proteins. *Immunol. Rev.* 225: 226–243.
2. Acha-Orbea, H., A. N. Shakhov, and D. Finke. 2007. Immune response to MMTV infection. *Front. Biosci.* 12: 1594–1609.
3. Scherer, M. T., L. Ignatowicz, G. M. Winslow, J. W. Kappler, and P. Marrack. 1993. Superantigens: bacterial and viral proteins that manipulate the immune system. *Annu. Rev. Cell Biol.* 9: 101–128.
4. Sundberg, E. J., L. Deng, and R. A. Mariuzza. 2007. TCR recognition of peptide/MHC class II complexes and superantigens. *Semin. Immunol.* 19: 262–271.
5. Bueno, C., G. Criado, J. K. McCormick, and J. Madrenas. 2007. T cell signalling induced by bacterial superantigens. *Chem. Immunol. Allergy* 93: 161–180.
6. Li, H., A. Llera, E. L. Malchiodi, and R. A. Mariuzza. 1999. The structural basisof T cell activation by superantigens. *Annu. Rev. Immunol.* 17: 435–466.
7. Korman, A. J., P. Bourgarel, T. Meo, and G. E. Rieckhof. 1992. The mouse mammary tumour virus long terminal repeat encodes a type II transmembrane glycoprotein. *EMBO J.* 11: 1901–1905.

8. McMahon, C. W., L. Y. Bogatzki, and A. M. Pullen. 1997. Mouse mammary tumor virus superantigens require N-linked glycosylation for effective presen- tation to T cells. *Virology* 228: 161–170.
9. Winslow, G. M., P. Marrack, and J. W. Kappler. 1994. Processing and major histocompatibility complex binding of the MTV7 superantigen. *Immunity* 1: 23– 33.
10. Delcourt, M., J. Thibodeau, F. Denis, and R. P. Sekaly. 1997. Paracrine transfer of mouse mammary tumor virus superantigen. *J. Exp. Med.* 185: 471–480.
11. Grigg, M. E., C. W. McMahon, S. Morkowski, A. Y. Rudensky, and M. Pullen. 1998. Mtv-1 superantigen trafficks independently of major his- tocompatibility complex class II directly to the B-cell surface by the exocytic pathway. *J. Virol.* 72: 2577–2588.
12. Acha-Orbea, H., and H. R. MacDonald. 1995. Superantigens of mouse mammary tumor virus. *Annu. Rev. Immunol.* 13: 459–486.
13. Pullen, A. M., J. Bill, R. T. Kubo, P. Marrack, and J. W. Kappler. 1991. Analysis of the interaction site for the self superantigen Mls-1a on T cell receptor V*b*. *J. Exp. Med.* 173: 1183–1192.
14. Pullen, A. M., T. Wade, P. Marrack, and J. W. Kappler. 1990. Identification of the region of T cell receptor *b* chain that interacts with the self-superantigen MIs-1a. *Cell* 61: 1365–1374.
15. Cazenave, P. A., P. N. Marche, E. Jouvin-Marche, D. Voegtlé, F. Bonhomme, Bandeira, and A. Coutinho. 1990. V*b*17 gene polymorphism in wild-derived mouse strains: two amino acid substitutions in the V*b*17 region greatly alter T cell receptor specificity. *Cell* 63: 717–728.
16. Herman, A., J. W. Kappler, P. Marrack, and A. M. Pullen. 1991. Superantigens: mechanism of T-cell stimulation and role in immune responses. *Annu. Rev. Immunol.* 9: 745–772.
17. MacNeil, D., E. Fraga, and B. Singh. 1992. Inhibition of superantigen recognition by peptides of the variable region of the T cell receptor *b* chain. *Eur. J. Immunol.* 22: 937–941.
18. Torres, B. A., N. D. Griggs, and H. M. Johnson. 1993. Bacterial and retroviral superantigens share a common binding region on class II MHC antigens. *Nature* 364: 152–154.
19. Pullen, A. M., and L. Y. Bogatzki. 1996. Receptors on T cells escaping superantigen-mediated deletion lack special beta-chain junctional region struc- tural characteristics. *J. Immunol.* 156: 1865–1872. .
20. Azar, G. A., R. P. Sékaly, and J. Thibodeau. 2005. A defective viral superantigen-presenting phenotype in HLA-DR transfectants is corrected by CIITA. *J. Immunol.* 174: 7548–7557.
21. Mottershead, D. G., P. N. Hsu, R. G. Urban, J. L. Strominger, and B. T. Huber. 1995. Direct binding of the Mtv7 superantigen (Mls-1) to soluble MHC class II molecules. *Immunity* 2: 149–154.
22. Hsu, P. N., P. Wolf Bryant, N. Sutkowski, B. McLellan, H. L. Ploegh, and B. T. Huber. 2001. Association of mouse mammary tumor virus super- antigen with MHC class II during biosynthesis. *J. Immunol.* 166: 3309– 3314.
23. Faubert, A., A. Samaan, and J. Thibodeau. 2002. Functional analysis of tryptophans *a*62 and *b*120 on HLA-DM. *J. Biol. Chem.* 277: 2750–2755.

24. Ho, S. N., H. D. Hunt, R. M. Horton, J. K. Pullen, and L. R. Pease. 1989. Site-directed mutagenesis by overlap extension using the polymerase chain reaction. *Gene* 77: 51–59.
25. Kozono, H., J. White, J. Clements, P. Marrack, and J. W. Kappler. 1994. Production of soluble MHC class II proteins with covalently bound single peptides. *Nature* 369: 151–154.
26. Winslow, G. M., M. T. Scherer, J. W. Kappler, and P. Marrack. 1992. Detection and biochemical characterization of the mouse mammary tumor virus 7 superantigen (Mls-1a). *Cell* 71: 719–730.
27. Fu, X. T., and R. W. Karr. 1994. HLA-DR *a* chain residues located on the outer loops are involved in nonpolymorphic and polymorphic antibody-binding epitopes. *Hum. Immunol.* 39: 253–260.
28. Radka, S. F., C. E. Machamer, and P. Cresswell. 1984. Analysis of monoclonal antibodies reactive with human class II *b* chains by two-dimensional electro- phoresis and Western blotting. *Hum. Immunol.* 10: 177–186.
29. Wraight, C. J., P. van Endert, P. Mo̧ller, J. Lipp, N. R. Ling, I. C. MacLennan, N. Koch, and G. Moldenhauer. 1990. Human major histocompatibility complex class II invariant chain is expressed on the cell surface. *J. Biol. Chem.* 265: 5787–5792.
30. Denzin, L. K., N. F. Robbins, C. Carboy-Newcomb, and P. Cresswell. 1994. Assembly and intracellular transport of HLA-DM and correction of the class II antigen-processing defect in T2 cells. *Immunity* 1: 595–606.
31. Mahana, W., R. al-Daccak, C. Léveillé, J. P. Valet, J. Hébert, M. Ouellette, and W. Mourad. 1995. A natural mutation of the amino acid residue at position 60 destroys staphylococcal enterotoxin A murine T-cell mitogenicity. *Infect. Immun.* 63: 2826–2832.
32. Herman, A., G. Croteau, R. P. Sekaly, J. Kappler, and P. Marrack. 1990. HLA-DR alleles differ in their ability to present staphylococcal enterotoxins to T cells. *J. Exp. Med.* 172: 709–717.
33. Hewitt, C. R. A., J. R. Lamb, J. Hayball, M. Hill, M. J. Owen, and R. E. O'Hehir. 1992. Major histocompatibility complex independent clonal T cell anergy by direct interaction of *Staphylococcus aureus* enterotoxin B with the T cell antigen receptor. *J. Exp. Med.* 175: 1493–1499.
34. Graham, F. L., and A. J. van der Eb. 1973. A new technique for the assay of infectivity of human adenovirus 5 DNA. *Virology* 52: 456–467.
35. Sette, A., S. Ceman, R. T. Kubo, K. Sakaguchi, E. Appella, D. F. Hunt, T. A. Davis, H. Michel, J. Shabanowitz, R. Rudersdorf, et al. 1992. Invariant chain peptides in most HLA-DR molecules of an antigen-processing mutant. *Science* 258: 1801–1804.
36. Lavoie, P. M., J. Thibodeau, I. Cloutier, R. Busch, and R. P. Sékaly. 1997. Selective binding of bacterial toxins to major histocompatibility complex class II-expressing cells is controlled by invariant chain and HLA-DM. *Proc. Natl. Acad. Sci. USA* 94: 6892–6897.
37. Tourne, S., T. Miyazaki, A. Oxenius, L. Klein, T. Fehr, B. Kyewski, C. Benoist, and D. Mathis. 1997. Selection of a broad repertoire of $CD4^+$ T cells in H-2Ma0/ 0 mice. *Immunity* 7: 187–195.

38. Golovkina, T., Y. Agafonova, D. Kazansky, and A. Chervonsky. 2001. Diverse repertoire of the MHC class II-peptide complexes is required for presentation of viral superantigens. *J. Immunol.* 166: 2244–2250.
39. Hogan, R. J., J. VanBeek, D. R. Broussard, S. L. Surman, and D. L. Woodland. 2001. Identification of MHC class II-associated peptides that promote the pre- sentation of toxic shock syndrome toxin-1 to T cells. *J. Immunol.* 166: 6514– 6522.
40. Schulze, E. D., and K. W. Wucherpfennig. 2012. The mechanism of HLA-DM induced peptide exchange in the MHC class II antigen presentation pathway.*Curr. Opin. Immunol.* 24: 105–111.
41. Mellins, E., L. Smith, B. Arp, T. Cotner, E. Celis, and D. Pious. 1990. Defective processing and presentation of exogenous antigens in mutants with normal HLA class II genes. *Nature* 343: 71–74.
42. Ignatowicz, L., G. Winslow, J. Bill, J. Kappler, and P. Marrack. 1995. Cell surface expression of class II MHC proteins bound by a single peptide. *J. Immunol.* 154: 3852–3862.
43. Labrecque, N., H. Mcgrath, M. Subramanyam, B. T. Huber, and R. P. Sékaly.1993. Human T cells respond to mouse mammary tumor virus-encoded superantigen: Vβ restriction and conserved evolutionary features. *J. Exp. Med.* 177: 1735–1743.
44. Subramanyam, M., B. McLellan, N. Labrecque, R. P. Sekaly, and B. T. Huber. 1993. Presentation of the Mls-1 superantigen by human HLA class II molecules to murine T cells. *J. Immunol.* 151: 2538–2545.
45. Riberdy, J. M., J. R. Newcomb, M. J. Surman, J. A. Barbosa, and P. Cresswell. 1992. HLA-DR molecules from an antigen-processing mutant cell line are as- sociated with invariant chain peptides. *Nature* 360: 474–477.
46. Gorga, J. C., P. J. Knudsen, J. A. Foran, J. L. Strominger, and S. J. Burakoff. 1986. Immunochemically purified DR antigens in liposomes stimulate xenogeneic cytolytic T cells in secondary in vitro cultures. *Cell. Immunol.* 103: 160– 173.
47. Blackman, M. A., F. E. Lund, S. Surman, R. B. Corley, and D. L. Woodland. 1992. Major histocompatibility complex-restricted recognition of retroviral superantigens by V*b*17$^+$ T cells. *J. Exp. Med.* 176: 275–280.
48. Sundberg, E., and T. S. Jardetzky. 1999. Structural basis for HLA-DQ binding bythe streptococcal superantigen SSA. *Nat. Struct. Biol.* 6: 123–129.
49. Vogt, A. B., L. J. Stern, C. Amshoff, B. Dobberstein, G. J. Hämmerling, and H. Kropshofer. 1995. Interference of distinct invariant chain regions with superantigen contact area and antigenic peptide binding groove of HLA-DR. *J. Immunol.* 155: 4757–4765.
50. Günther, S., A. Schlundt, J. Sticht, Y. Roske, U. Heinemann, K.-H. Wiesmüller, G. Jung, K. Falk, O. Rötzschke, and C. Freund. 2010. Bidirectional binding of invariant chain peptides to an MHC class II molecule. *Proc. Natl. Acad. Sci. USA* 107: 22219–22224.
51. Thibodeau, J., N. Labrecque, F. Denis, B. T. Huber, and R. P. Sékaly. 1994. Binding sites for bacterial and endogenous retroviral superantigens can be dissociated on major histocompatibility complex class II molecules. *J. Exp. Med.* 179: 1029–1034.

52. Hennecke, J., A. Carfi, and D. C. Wiley. 2000. Structure of a covalently stabilized complex of a human *ab* T-cell receptor, influenza HA peptide and MHC class II molecule, HLA-DR1. *EMBO J.* 19: 5611–5624.
53. O'Sullivan, D., T. Arrhenius, J. Sidney, M. F. Del Guercio, M. Albertson, M. Wall, C. Oseroff, S. Southwood, S. M. Colón, et al. 1991. On the interaction of promiscuous antigenic peptides with different DR alleles. Identification of common structural motifs. *J. Immunol.* 147: 2663–2665.
54. De Magistris, M. T., J. Alexander, M. Coggeshall, A. Altman, F. C. Gaeta, H. M. Grey, and A. Sette. 1992. Antigen analog-major histocompatibility complexes act as antagonists of the T cell receptor. *Cell* 68: 625–634.
55. Thayer, W. P., C. T. Dao, L. Ignatowicz, and P. E. Jensen. 2003. A novel single chain I-A^b molecule can stimulate and stain antigen-specific T cells. *Mol. Immunol.* 39: 861–870.
56. Thibodeau, J., M. Dohlsten, I. Cloutier, P. M. Lavoie, P. Bjork, F. Michel, C. Léveillé, W. Mourad, T. Kalland, and R. P. Sékaly. 1997. Molecular characterization and role in T cell activation of staphylococcal enterotoxin A binding to the HLA-DR alpha-chain. *J. Immunol.* 158: 3698–3704.
57. Labrecque, N., J. Thibodeau, and R. P. Sékaly. 1993. Interactions between staphylococcal superantigens and MHC class II molecules. *Semin. Immunol.* 5: 23–32.
58. Natarajan, S. K., L. J. Stern, and S. Sadegh-Nasseri. 1999. Sodium dodecyl sulfate stability of HLA-DR1 complexes correlates with burial of hydrophobic residues in pocket 1. *J. Immunol.* 162: 3463–3470.
59. Stumptner-Cuvelette, P., S. Morchoisne, M. Dugast, S. Le Gall, G. Raposo, O. Schwartz, and P. Benaroch. 2001. HIV-1 Nef impairs MHC class II antigen presentation and surface expression. *Proc. Natl. Acad. Sci. USA* 98: 12144– 12149.
60. Blackman, M. A., and D. L. Woodland. 1996. Role of the T cell receptor alpha-chain in superantigen recognition. *Immunol. Res.* 15: 98–113.
61. Jardetzky, T. S., J. H. Brown, J. C. Gorga, L. J. Stern, R. G. Urban, Y. I. Chi, C. Stauffacher, J. L. Strominger, and D. C. Wiley. 1994. Three-dimensional structure of a human class II histocompatibility molecule complexed with superantigen. *Nature* 368: 711–718.
62. Crooks, G. E., G. Hon, J. Chandonia, and S. E. Brenner. 2004. WebLogo : a sequence logo generator. *Genome Res.* 14: 1188–1190.
63. Kappler, J. W., A. Herman, J. Clements, and P. Marrack. 1992. Mutations defining functional regions of the superantigen staphylococcal enterotoxin B. *J. Exp. Med.* 175: 387–396.
64. Li, H., A. Llera, D. Tsuchiya, L. Leder, X. Ysern, P. M. Schlievert, K. Karjalainen, and R. A. Mariuzza. 1998. Three-dimensional structure of the complex between a T cell receptor *b* chain and the superantigen staphylococcal enterotoxin B. *Immunity* 9: 807–816.
65. Wirth, S., A. Vessaz, C. Krummenacher, F. Baribaud, H. Acha-Orbea, and H. Diggelmann. 2002. Regions of mouse mammary tumor virus superantigen involved in interaction with the major histocompatibility complex class II I-A molecule. *J. Virol.* 76: 11172–11175.

66. Ghosh, P., M. Amaya, E. Mellins, and D. C. Wiley. 1995. The structure of an intermediate in class II MHC maturation: CLIP bound to HLA-DR3. *Nature* 378: 457–462.
67. Zhu, Y., A. Y. Rudensky, A. L. Corper, L. Teyton, and I. A. Wilson. 2003. Crystal structure of MHC class II I-Ab in complex with a human CLIP peptide: pre- diction of an I-Ab peptide-binding motif. *J. Mol. Biol.* 326: 1157–1174.
68. Carson, R. T., K. M. Vignali, D. L. Woodland, and D. A. A. Vignali. 1997. T cell receptor recognition of MHC class II-bound peptide flanking residues enhances immunogenicity and results in altered TCR V region usage. *Immunity* 7: 387– 399.
69. Wen, R., D. R. Broussard, S. Surman, T. L. Hogg, M. A. Blackman, and D. L. Woodland. 1997. Carboxy-terminal residues of major histocompatibility complex class II-associated peptides control the presentation of the bacterial superantigen toxic shock syndrome toxin-1 to T cells. *Eur. J. Immunol.* 27: 772– 781.
70. Suri, A., S. B. Lovitch, and E. R. Unanue. 2006. The wide diversity and complexity of peptides bound to class II MHC molecules. *Curr. Opin. Immunol.* 18: 70–77.
71. Miyazaki, T., P. Wolf, S. Tourne, C. Waltzinger, A. Dierich, N. Barois, H. Ploegh, C. Benoist, and D. Mathis. 1996. Mice lacking H2-M complexes, enigmatic elements of the MHC class II peptide-loading pathway. *Cell* 84: 531– 541.
72. Painter, C. A., M. P. Negroni, K. A. Kellersberger, Z. Zavala-Ruiz, J. E. Evans, and L. J. Stern. 2011. Conformational lability in the class II MHC 310 helix and adjacent extended strand dictate HLA-DM susceptibility and peptide exchange. *Proc. Natl. Acad. Sci. USA* 108: 19329–19334.
73. Chervonsky, A. V., R. M. Medzhitov, L. K. Denzin, A. K. Barlow, Y. Rudensky, and C. A. Janeway, Jr. 1998. Subtle conformational changes induced in major histocompatibility complex class II molecules by binding peptides. *Proc. Natl. Acad. Sci. USA* 95: 10094–10099.
74. Wong, P., and A. Y. Rudensky. 1996. Phenotype and function of $CD4^+$ T cells in mice lacking invariant chain. *J. Immunol.* 156: 2133–2142.
75. Tobita, T., M. Oda, H. Morii, M. Kuroda, A. Yoshino, T. Azuma, and H. Kozono. 2003. A role for the P1 anchor residue in the thermal stability of MHC class II molecule I-Ab. *Immunol. Lett.* 85: 47–52.
76. Saline, M., K. E. J. Rö dströ m, G. Fischer, V. Y. Orekhov, B. G. Karlsson, and K. Lindkvist-Petersson. 2010. The structure of superantigen complexed with TCR and MHC reveals novel insights into superantigenic T cell activation. *Nat. Commun.* 1: 119.
77. Wang, L., Y. Zhao, Z. Li, Y. Guo, L. L. Jones, D. M. Kranz, W. Mourad, and H. Li. 2007. Crystal structure of a complete ternary complex of TCR, super- antigen and peptide-MHC. *Nat. Struct. Mol. Biol.* 14: 169–171.
78. Blackman, M. A., H. G. Burgert, D. L. Woodland, E. Palmer, J. W. Kappler, and P. Marrack. 1990. A role for clonal inactivation in T cell tolerance to Mls-1a. *Nature* 345: 540–542.
79. Woodland, D. L., H. P. Smith, S. Surman, P. Le, R. Wen, and M. A. Blackman. 1993. Major histocompatibility complex-specific recognition of Mls-1 is medi- ated by multiple elements of the T cell receptor. *J. Exp. Med.* 177: 433–442.

80. Pircher, H., T. W. Mak, R. Lang, W. Ballhausen, E. Rüedi, H. Hengartner, R. M. Zinkernagel, and K. Bürki. 1989. T cell tolerance to Mlsa encoded anti- gens in T cell receptor V*b*8.1 chain transgenic mice. *EMBO J.* 8: 719–727.
81. Yui, K., S. Komori, M. Katsumata, R. M. Siegel, and M. I. Greene. 1990. Self-reactive T cells can escape clonal deletion in T-cell receptor V*b*8.1 transgenic mice. *Proc. Natl. Acad. Sci. USA* 87: 7135–7139.
82. Vacchio, M. S., O. Kanagawa, K. Tomonari, and R. J. Hodes. 1992. Influence of T cell receptor V*a* expression on Mlsa superantigen-specific T cell responses. *J. Exp. Med.* 175: 1405–1408.
83. Smith, H. P., P. Le, D. L. Woodland, and M. A. Blackman. 1992. T cell receptor *a*-chain influences reactivity to Mls-1 in V*b*8.1 transgenic mice. *J. Immunol.* 149: 887-896.
84. Aude-Garcia, C., A. Attinger, D. Housset, H. R. MacDonald, H. Acha-Orbea, P. N. Marche, and E. Jouvin-Marche. 2000. Pairing of V*b*6 with certain V*a*2 family members prevents T cell deletion by Mtv-7 superantigen. *Mol. Immunol.* 37: 1005–1012.
85. Kang, J., C. A. Chambers, J. Pawling, and C. Scott. 1994. Conserved amino acid residues in the complementarity-determining region 1 of the TCR *b*-chain are involved in the recognition of conventional Ag and Mls-1 superantigen. *J. Immunol.* 152: 5305–5317.
86. Marrack, P., G. M. Winslow, Y. Choi, M. Scherer, A. Pullen, J. White, and J. W. Kappler. 1993. The bacterial and mouse mammary tumor virus superantigens; two different families of proteins with the same functions. *Immunol. Rev.* 131: 79–92.
87. Nguyen, P., D. L. Woodland, and M. A. Blackman. 1996. MHC bias of Mls-1 recognition is not influenced by thymic positive selection. *Cell. Immunol.* 167: 224–229.
88. Andersen, P. S., P. M. Lavoie, R. P. Sékaly, H. Churchill, D. M. Kranz, P. M. Schlievert, K. Karjalainen, and R. A. Mariuzza. 1999. Role of the T cell receptor *a* chain in stabilizing TCR-superantigen-MHC class II complexes. *Immunity* 10: 473–483.
89. Ciurli, C., D. N. Posnett, R. P. Sékaly, and F. Denis. 1998. Highly biased CDR3 usage in restricted sets of β chain variable regions during viral superantigen 9 response. *J. Exp. Med.* 187: 253–258.
90. Candéias, S., C. Waltzinger, C. Benoist, and D. Mathis. 1991. The V*b*17$^+$ T cell repertoire: skewed J*b* usage after thymic selection; dissimilar CDR3s in CD4 versus CD8+ cells. *J. Exp. Med.* 174: 989–1000.
91. Chies, J. A., G. Marodon, A. M. Joret, A. Regnault, M. P. Lembezat, B. Rocha, and A. A. Freitas. 1995. Persistence of V*b*6$^+$ T cells in Mls-1a mice. A role for the third complementarity-determining region (CDR3) of the T cell receptor beta chain in superantigen recognition. *J. Immunol.* 155: 4171–4178.
92. Kilgannon, P., Z. Novak, A. Fotedar, and B. Singh. 2010. Junctional diversity prevents negative selection of an antigen-specific T cell repertoire. *Mol. Immunol.* 47: 1154–1160.
93. Stadinski, B. D., P. Trenh, R. L. Smith, B. Bautista, P. G. Huseby, G. Li, L. J. Stern, and E. S. Huseby. 2011. A role for differential variable gene pairing in creating T cell receptors specific for unique major histocompatibility ligands. *Immunity* 35: 694–704.

94. Deng, L., R. J. Langley, Q. Wang, S. L. Topalian, and R. A. Mariuzza. 2012. Structural insights into the editing of germ-line-encoded interactions between T-cell receptor and MHC class II by V*a* CDR3. *Proc. Natl. Acad. Sci. USA* 109: 14960–14965.
95. Mehindate, K., J. Thibodeau, M. Dohlsten, T. Kalland, R. P. Se´kaly, and W. Mourad. 1995. Cross-linking of major histocompatibility complex class II molecules by staphylococcal enterotoxin A superantigen is a requirement for inflammatory cytokine gene expression. *J. Exp. Med.* 182: 1573–1577.
96. Petersson, K., M. Thunnissen, G. Forsberg, and B. Walse. 2002. Crystal structure of a SEA variant in complex with MHC class II reveals the ability of SEA to crosslink MHC molecules. *Structure* 10: 1619–1626.
97. Nur-ur Rahman, A. K., D. A. Bonsor, C. A. Herfst, F. Pollard, M. Peirce, W. Wyatt, K. J. Kasper, J. Madrenas, E. J. Sundberg, and J. K. McCormick. 2011. The T cell receptor *b*-chain second complementarity determining region loop (CDR2*b* governs T cell activation and V*b* specificity by bacterial super- antigens. *J. Biol. Chem.* 286: 4871–4881.
98. Woodland, D. L., R. Wen, and M. A. Blackman. 1997. Why do superantigens care about peptides? *Immunol. Today* 18: 18–22.
99. Proft, T., and J. Fraser. 1998. Superantigens: just like peptides only different. *J. Exp. Med.* 187: 819–821.

Figure legends

FIGURE 1. vSAG7 presentation is dictated by the MHCII-associated peptide. (A) vSAG presentation by DM^+ and DM^- B cell lines following vSAG transfer from the $vSAG7^+$ DAP cell line (10). Presentation is monitored by the stimulation of Vβ6- and 8.1-bearing T cell hybridoma Kmls 13.11 and $KR3^+$. BJAB (DR3) is used as a positive B cell control and COX is a $DR3^+DM^+$ B cell line. (B) Sequence alignment of different peptide constructs covalently linked to DRβ used to assess vSAG presentation. Peptides are aligned according to the residue filling the P1 pocket. Asterisks above the sequences mark the protruding side chains at positions P1, P2, and P8. MHCII cell surface expression of DAP cells transfected with DRα and cCLIP or lCLIP (C), HA or HAb (F), or TT or TTb (H) stained with either L243 or XD5 anti-DR mAbs. The MFI values for cell surface expression are shown are shown in the lower right corner of each histogram and are colored according to the legend. Bar graphs below the histograms represent the MFI of the GFP control plasmid cotransfected with vSAG7 to monitor the

transfection efficiency. L243/XD5 MFI ratio of the two CLIP variants, cCLIP87–101 and lCLIP81–101, are shown in (E).

FIGURE 2. The N-terminal domain of vSAG7 overlaps the SEA binding site on the MHCII *β*-chain. (A) Schematic representations of the constructs used throughout this study. Different peptides were appended to DRβ (pepDRβ) C terminus based on the strategy by Kozono et al. (25). The C terminus of DR1 β -chains was covalently attached to the N terminus of Ii (IiSCD), vSAG7 (SCD), or N-vSAG (SCDΔCt) by a flexible GLY-SER linker. Similarly, the C terminus of DR1 α-chain was covalently attached to the N terminus of vSAG7 (αSCD). In the SCT, a peptide was also linked to the N terminus of the SCD. The linkers between DR and either the peptide, vSAG7 or Ii, are represented as light gray boxes. The arrowheads represent the three vSAG7 cleavage sites. (B) L243 and VS7 cell surface staining of HEK 293T cells transfected with the αSCD or βSCD and the appropriate complementary DR chain or a wt DR and vSAG7 control. L243 and VS7 mAbs recognize a conformational epitope on DRα and the C-terminal end of vSAG7, respectively. (C) HEK 293T cells were transiently transfected with wt DR and vSAG7, DRα and the βSCDs, or βIiSCDs. Forty-eight hours after transfection, cells were harvested, split, and incubated on ice with L243 or SEA for 3h. After washing, bound SEA was detected by flow cytometry using an anti-SEA mAb. These staining profiles are representative of at least five independent experiments. (D) The MFIs were plotted as a ratio where the error bars represent the SD to the mean of three stainings on independent populations of transfected cells. (E) Same as (D), but using DRα K39A mutant, which prevents SEA binding to the α-chain. All data are representative of at least three independent experiments.

FIGURE 3. vSAG7 binding to MHCII α- and β-chains occurs on distinct MHCII molecules. (A) Cell surface expression of MHCII on HEK 293T cells transfected with DRβ or HAβ (*left panel*) and βSCD or HASCT (*right panel*) stained with the L243 mAb. (B) The MFIs of the transfectants bearing the HA peptide were plotted as a ratio against the ones without HA. The error bars represent the SD to the mean of three

stainings on independent populations of transfected cells. (C) Compact SDS-resistant and -sensitive forms of DR were assessed by immunoblot (IB) analysis of total protein extracts (boiled or heated to 65˚C) from the transfectants in (A). Ii-SCD (βIi) was used as control. The IB was revealed with the anti-DRβ mAb XD5. The two compact complexes are marked with I or II (*lanes 2* and *8*) and schematized next to the gel. (D) Com- parison of HA-specific T cell stimulation between endogenous $MHCII^{+}$ or $MHCII^{2}$ HeLa cells transfected with different MHCII β-chains. (E) Same as (D) but comparing vSAG7-specific T cell stimulation. All data are representative of at least three independent experiments.

FIGURE 4. Residues on the MHCII α-chain act in tandem with vSAG to engage TCRs. (A) Depiction of the MHCII with a close-up on the peptide- binding groove that highlights DRα *α* helix spanning mutants (pink) and the L243 mAbs binding site (red), depicted as sticks. The α-chain, β-chain, and peptide are green, blue, and yellow, respectively. (B) MHCII cell surface profiles of DAP cell lines transfected with HADRβ and different DRα mutants as stained with L243 and XD5 mAbs. The MFIs are shown in the lower right corner of each histogram and are colored according to the legend. Cotransfected GFP protein was used to monitor the transfection efficiency of vSAG7, and MFIs are shown as bar graphs next to histograms. (C) L243 and XD5 MFI ratios derived from (B). Cell lines from (B) were transfected with vSAG7 or a mock control before monitoring Jurkat (D), Kmls 13.11 (E), and Kmls 12.6 (F) T cell proliferation. All data are representative of at least three independent experiments. (G) Model of vSAG7 binding to MHCII and TCR in which the multiple binding regions between vSAG7, both MHCII chains, and the TCRs are highlighted. The N-vSAG and C-vSAG moieties remain noncovalently associated after processing and lead to the crosslinking of MHCII molecules. Binding of C-vSAG7 to the MHCII *α*-chain is conformation-dependent and abrogated by a peptide N-terminal extension. The TCRβ CDR3 binds the MHCII α-chain specifically instead of the peptide, whereas vSAG binds the FR3 and HV4 region of the Vβ. The exact nature of Vα binding to the MHCII β remains to be fully characterized (60).

FIGURE 5. A conserved *TGXY* motif is central to the activity of vSAG7. (A) Sequence similarity among 18 MMTV SAG proteins or vSAG-like domains. The height of a particular position is proportional to the frequency of the corresponding residue type between the aligned sequences and to the sequence information in the alignment and its given bits (62). The residue numbering is based on the vSAG7 protein (GenBank ID M90535.1). T, G, and Y of the motif are colored a lighter shade of gray. (B) Functional assay of transiently transfected HeLa CIITA cells with multiple β-chains against the vSAG7-reactive Kmls 13.11 T cell hybridoma. (C) L243 cell surface expression profiles of DRα transiently cotransfected with either the βSCD or the Y229F mutant. (D) Ratios between DR and vSAG MFIs were plotted from the transfectants in (C), and the error bars represent the SD to the mean of three independent experiments.

Figures

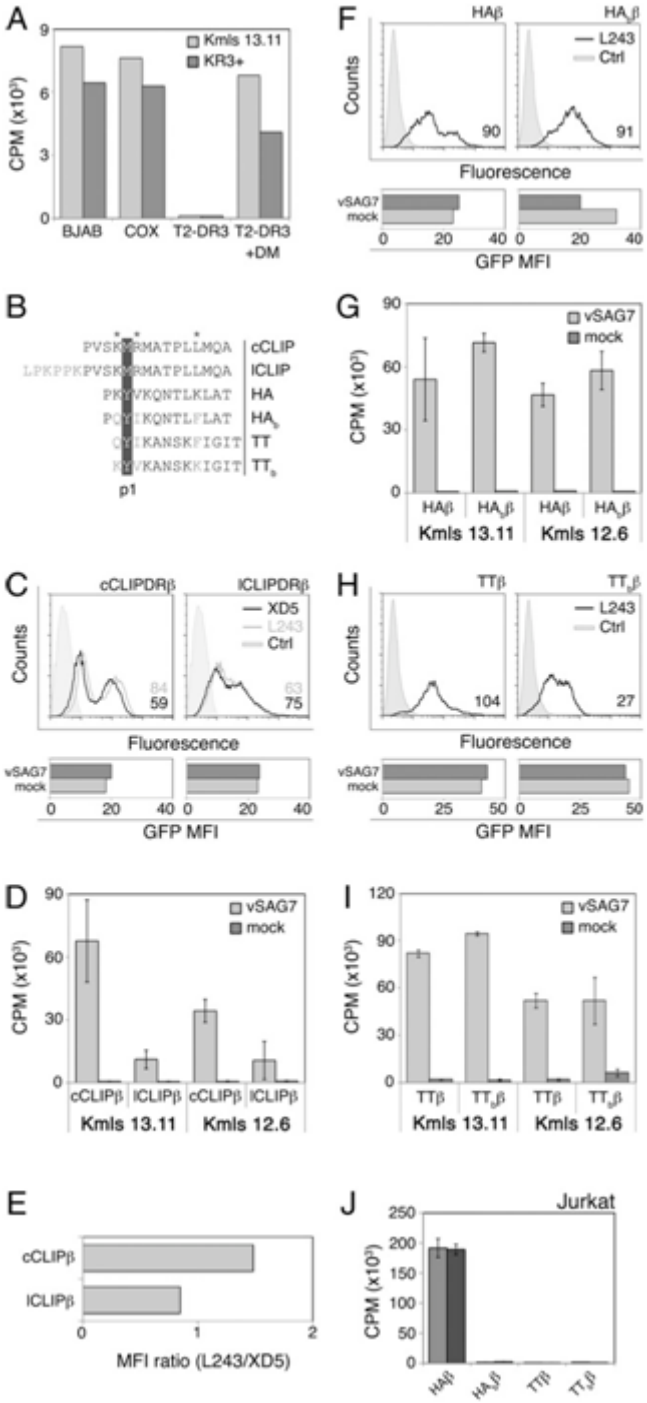

FIGURE 1. vSAG7 presentation is dictated by the MHCII-associated peptide.

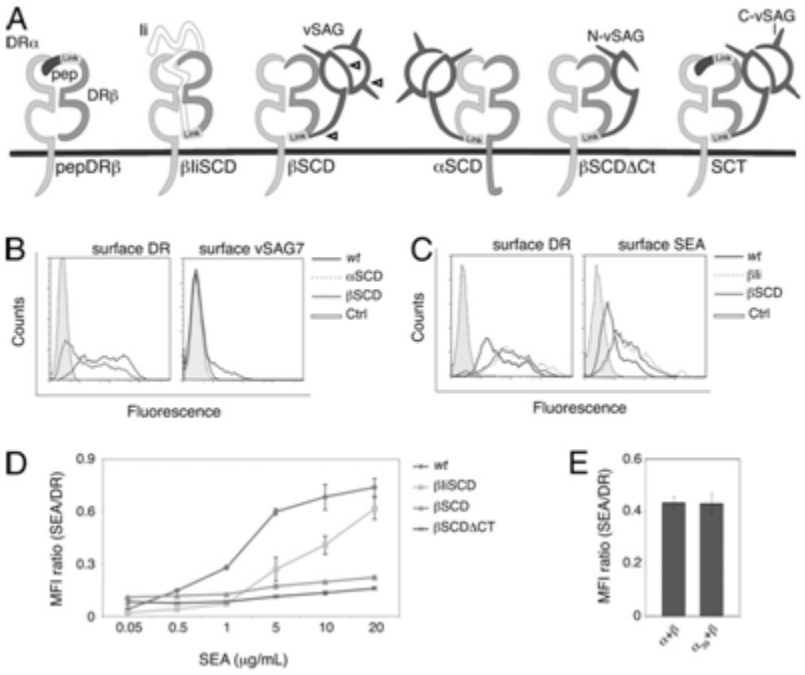

FIGURE 2. The N-terminal domain of vSAG7 overlaps the SEA binding site on the MHCII β-chain.

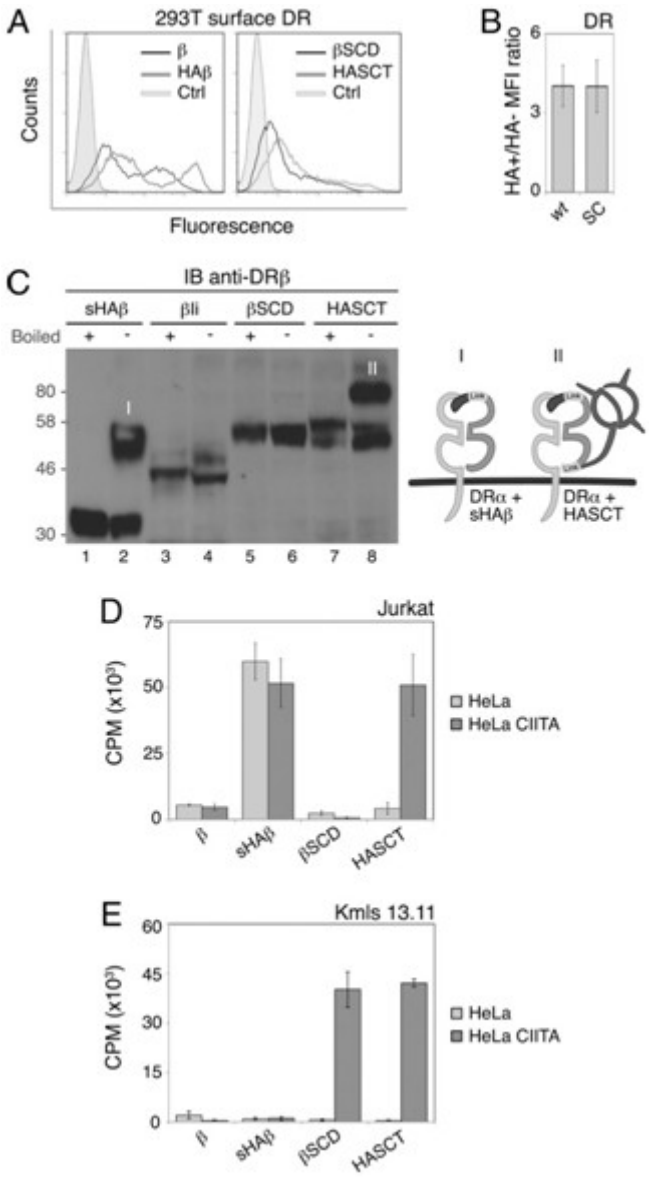

FIGURE 3. vSAG7 binding to MHCII α- and β-chains occurs on distinct MHCII molecules.

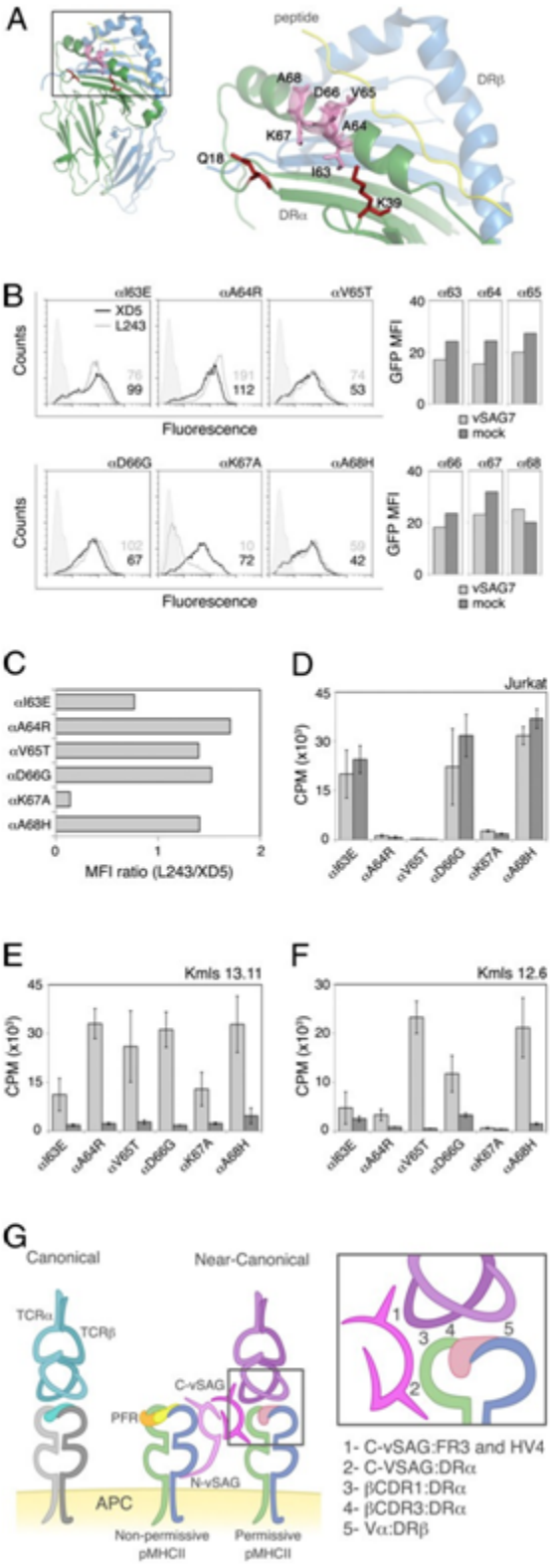

FIGURE 4. Residues on the MHCII α-chain act in tandem with vSAG to engage TCRs.

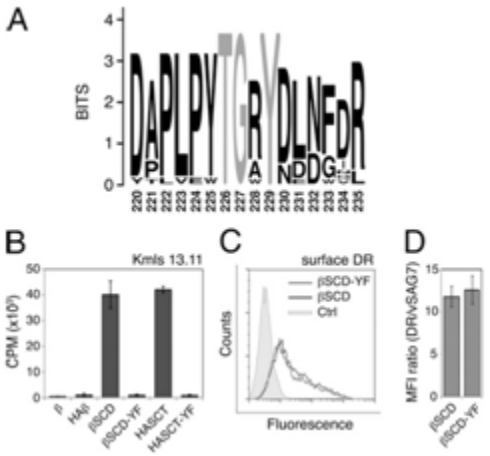

FIGURE 5. A conserved *TGXY* motif is central to the activity of vSAG7.

Supplementary data

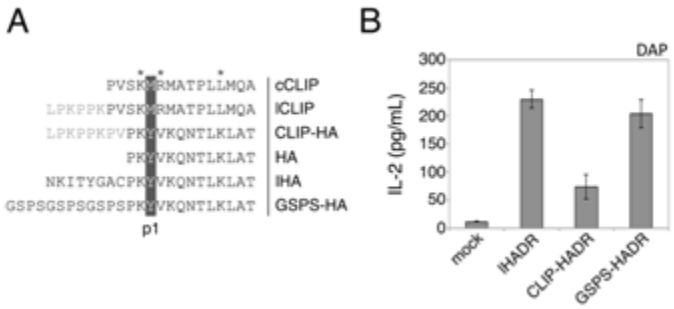

Supplemental figure 1: The N-terminal extension of CLIP ($CLIP_{81-87}$) negatively modulates the presentation of vSAG7. (A) Primary sequence alignment of the peptide-DRβ constructs used in this study. Peptides are aligned according to the residue filling the P1 pocket. Asterisks above the sequences mark the protruding side chains at positions P-1, P2 and P8. (B) DAP cells were stably transfected with vSAG7, DRα and the various peptide-DRβ SCDs. Cells expressing MHCIIs were sorted by flow cytometry using L243 (MFI for lHADR: 83; CLIP-HADR: 110; GSPS-HADR:140). Cells were co-cultured overnight with the T cell hybridoma Kmls13.11 at an equal cell ratio and IL-2 production was assessed by cytometric bead array. Co-cultures were done in triplicates and error bars represent the

standard deviation to the mean. The data is representative of two experiments performed with independent stable transfections.

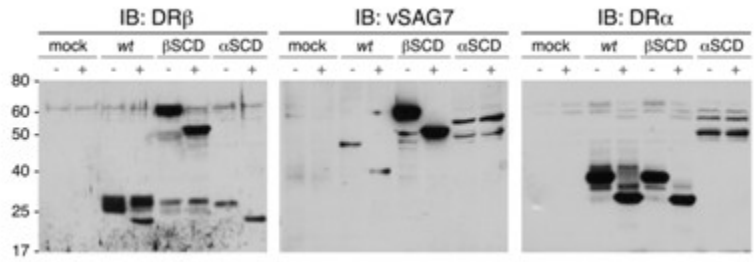

Supplemental figure 2: Maturation and proteolytic cleavage of the SCDs. Lysates of cells trans- fected with the αSCD or βSCD and their respective complementary MHCII chains were split in two and treated or not with EndoH. Samples were separated by SDS-PAGE and immunoblotted for DRα, vSAG7 or DR . Control (untransfected or wt DR) and vSAG7 transfected cells were also given the same treatment. The molecular weight (kDa) is given on the left side and the + or - signs indicate whether EndoH treatment was performed.

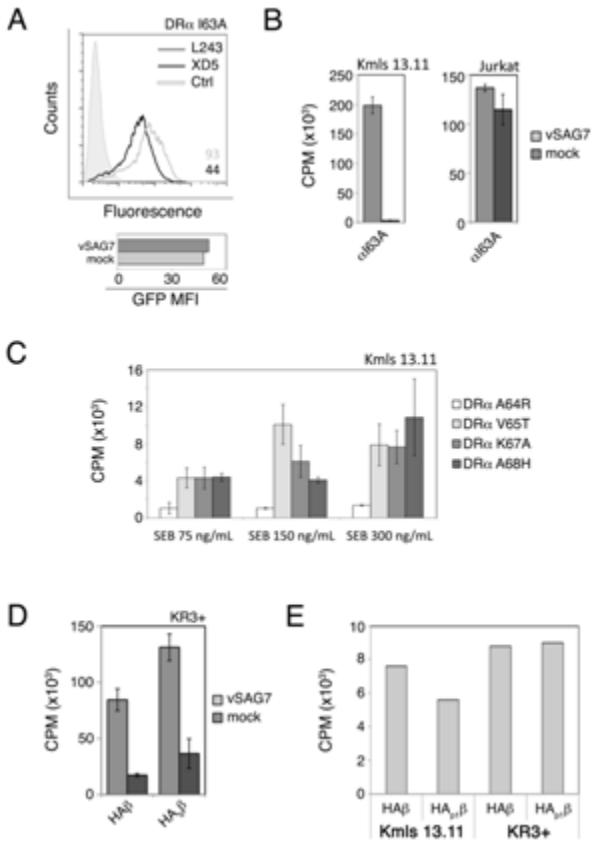

Supplemental figure 3: C-vSAG7 binding to the MHCII α chain is conformation sensitive. (A) Cell surface profiles of DAP cell lines expressing HADRβ and the I63A DRα mutant stained with the L243 and XD5 mAb. The MFI are shown in the lower right corner of each histogram and are colored with respect to the legend. Co-transfected YFP protein was used to monitor the transfection efficiency of vSAG7 and MFI are shown as bar graphs below histograms. (B) Cell lines from A were transfected with vSAG7 or a mock control before monitoring Kmls 13.11 and Jurkat T cell proliferation. (C) SEB presentation to Kmls 13.11 T cell hybridoma of multiple DRα mutant cell lines. (D) Peptide protruding side chains do not affect vSAG7 presentation. Transfected cell lines from Fig. 1F were used as APCs to stimulate Vβ8.1+ bearing T cell hybridoma KR3+. (E) Small peptide anchor residue substitution at p1 does not affect vSAG presentation. DAP cell lines expressing DRα and HAβ or HAp1β mutant Y-A were transfected with vSAG7 or a mock control prior to T cell presentation to the Vβ6 and Vβ8.1 bearing Kmls 13.11 or KR3+ T cell hybridomas, respectively. The HAp1β mutant encodes a HA peptide with the Tyr P1 anchor residue mutated for an Ala.

Annexe 2. Article non-discuté dans ce mémoire n°2

The invariant chain p35 isoform promotes formation of nonameric complexes with MHC II molecules

Maryse Cloutier, Catherine Gauthier[1], Jean-Simon Fortin[1] and Jacques Thibodeau

[1]These authors contributed equally to this work

Status: published in Immunology and Cell Biology.

Address correspondence and reprint requests to Dr. Jacques Thibodeau, Laboratoire d'Immunologie Moléculaire, Département de Microbiologie, Infectiologie et Immunologie, Université de Montréal, CP 6128, Succursale Centre-Ville, Montreal, QC H3C 3J7, Canada.

Abstract

Four different isoforms of the human invariant chain (Ii) have been described (p33, p35, p41 and p43). These heterotrimerize in the endoplasmic reticulum (ER) before associating with MHC class II molecules (MHCIIs). However, the final stoichiometry of the Ii/MHCII complex remains debated. This is particularly interesting as both p35 and p43 include a di-arginine motif that requires masking by MHCII to allow ER egress. Here, to functionally address the requirement for stoichiometric interactions, we used a recombinant DR heterodimer bearing its own cytoplasmic di-lysine ER-retention motif (DRKKAA). When

coexpressed with p33 and a control myc-tagged DR (DR_{myc}), DRKKAA was retained in the ER but had little impact on surface expression of DR_{myc}. However, when coexpressed with p35, DRKKAA restricted the surface expression of DR_{myc}, indicating that Ii trimers can be loaded with more than one MHCII. Similar results were obtained using HLA-DQ instead of DR_{myc}, showing that a single trimeric Ii scaffold can include distinct MHCII isotypes. Altogether, these results demonstrate that the subunit stoichiometry of oligomeric Ii/MHCII complexes is influenced by p35.

Introduction

In the endoplasmic reticulum (ER), the invariant chain (Ii; CD74) functions as a scaffold protein for MHC class II molecules (MHCIIs) (1). As a result of alternative splicing and different start codon usage, humans express four Ii isoforms (p33, p35, p41 and p43), of which p33 and p35 are the most predominantly expressed (2-4). Both p35 and p43 bear a 16-amino acid cytoplasmic extension including a strong di-arginine (RxR) ER-retention motif (5,6). Our earlier work has shown that the 'masking' of the RxR motif is strictly dependent on MHCII binding and requires the β chain cytoplasmic domain (7).

All Ii isoforms contain cytoplasmic leucine-based endosomal sorting signals as well as a luminal class II-associated invariant chain peptide (CLIP) and a C-terminal trimerization domain (8,9). According to the current model proposed by Roche *et al.* (3), three MHCII αβ heterodimers associate with a preformed Ii trimer, creating a stoichiometric structure ($\alpha 3\beta 3Ii3$) that exits the ER. Once in endosomes, Ii is degraded, leading to disruption of the nonamer and the generation of CLIP in the peptide-binding groove of MHCII (10). HLA-DM catalyzes the exchange of CLIP for high-affinity peptides (11).

A recent report showed that soluble human Ii and MHCII coproduced in cell lines are secreted around a trimeric Ii scaffold as either pentamers, heptamers or nonamers (12). However, Koch *et al.* (13), challenged the existence of high-order structures and postulated that due to structural constraints imposed by the anchoring membrane, Ii and MHCIIs can only form pentamers ($\alpha 1\beta 1Ii_3$). Given the divergent results obtained so far using traditional biochemistry techniques (3,13), we chose to shed new light on the assembly and stoichiometry of the complex using a functional approach. Our data revealed that although nonamer formation is not a prerequisite for ER egress, the presence of p35 favors the inclusion of more than one MHCII per Ii trimer.

Methods

Plasmids and mutagenesis

The pBud DRαβ and pLNCX DQ plasmids have been described previously (7,24). The DRβ chain was subcloned into pcDNA3.1/myc (Invitrogen, Burlington, ON, Canada) to generate $DR\beta_{myc}$. DRα and $p35LIML$, $p33LIML$, pBud $p35LIMLS6,8A$ and DRβKKAA were subcloned into pcDNA3.1 from previously described constructs or were generated by PCR using mutagenic primers (7,15). All Ii molecules used in this study had mutations disrupting their cytoplasmic leucine-based endosomal sorting signals (p33LIML, p35LIML and $p35LIMLS6,8A$). This maximizes the surface expression of Ii upon ER egress, allowing us to easily ascertain transfection efficiency (15).

Antibodies

The following mouse monoclonal antibodies were described previously (7,24): L243 (HLA-DR); CerCLIP.1 (CLIP); HLA-DQ FITC (Life Science, Memphis, TM, USA) and 9e10 (myc-tag; Biolegend, San Diego, CA, USA). Secondary Alexa-fluor-coupled antibodies (Invitrogen) were used for flow cytometry.

Transfections and flow cytometry

HEK 293 T cells (3.5 million; ATCC CRL-11268) were plated in Dulbecco's Modified Eagle's Medium supplemented with 5% fetal bovine serum (Wisent, St-Bruno, QC, Canada) in a six-well plate. After 8 h, cells were transiently transfected in triplicates using 3 μg polyethylenimine (Polysciences, Warrington, PA, USA) per mg of DNA. Two μg of each DNA were transfected for each condition and, when necessary, empty plasmids were used to adjust the final DNA concentrations. After 48 h at 37°C, cells were harvested and washed in phosphate-buffered saline. To determine surface expression, live cells were stained on ice and analyzed by flow cytometry on a FACSCalibur (Becton Dickinson, San Jose, CA, USA). For total expression, cells were fixed in 4% paraformaldehyde, permeabilized with saponin 0.05% and stained, as described previously (24).

Results and discussion

p35 affects the stoichiometry of the MHCII/Ii complex

To determine functionally if more than one MHCII incorporate a given Ii trimer, we needed a cellular system expressing two distinct MHCIIs, one of which was unable to egress from the ER. This was achieved by designing a MHCIIβ chain bearing its own di-lysine (β_{KKAA}) ER-retention motif (Figure 1a). The C-terminal cytoplasmic di-lysine sequence acts as a strong retention signal for ER-resident type I proteins and recombinant reporter molecules displaying this motif localize in the ER (14). Also, we engineered a distinct control MHCIIβ chain bearing a myc tag (DR_{myc}) instead of the di-lysine signal (Figure 1a). We reasoned that if an Ii trimer was to bind more than one MHCII, the ER-retained variant of DR (DRKKAA) would indirectly prevent cell surface expression of coexpressed DR_{myc} that stochastically integrated the complex. In contrast, if only pentamers can form ($DR\alpha 1DR\beta KKAA1Ii3$ or $DR\alpha 1DR\beta myc1Ii3$), the fate of DRKKAA and DR_{myc} molecules should be independent.

We first confirmed that DRKKAA could not reach the plasma membrane. HEK293T cells were transiently transfected with DRKKAA or DRmyc and analyzed by flow cytometry (Figure 1b). In line with the presence of a functional ER-retention motif, DRKKAA was almost absent from the cell surface but could be detected upon membrane permeabilization. Confocal microscopy confirmed the ER retention of DRKKAA (Supplementary Figure 1). Then, we assessed the fate of DRmyc when coexpressed with DRKKAA. As expected, DRmyc was expressed at the plasma membrane independent of the presence of the ER-retained DRKKAA (Figure 1b, right panel). To quantify these findings and to account for variations in the transfection efficiencies, the mean fluorescence intensities were plotted as ratios between surface and total staining (Figure 1c). Such ratios are lower for ER-retained molecules versus those that efficiently traffic to the cell surface (15). That the relative proportion of MHCIIs at the surface was somewhat intermediate when the two types of DR were coexpressed is probably due to the fact that DRKKAA contributed to increase only the 'total' pool of molecules. Also, expression of the DRmyc is usually slightly less efficient in cotransfection experiments (Figure 1d).

We then assessed the impact of DRKKAA on the surface expression of βmyc in the presence of Iip33. First, when the control DRmyc was the sole source of β chains, MHCIIs were found at the surface (Figure 1e). Importantly, CLIP was detected as well, indicating that MHCIIs trafficked in association with Ii (Figure 1f). As expected, MHCII and CLIP were almost absent from the surface when DRKKAA was transfected with p33. Interestingly, when both β chains were coexpressed together with p33, MHCIIs were detected at the plasma membrane (Figure 1e). Confocal microscopy confirmed the ER egress of DRmyc (Supplementary Figure 2A). Because it is unlikely that nonamers formed simultaneously and exclusively of either DRmyc or DRKKAA without the inclusion of at least one competing DR counterpart, the detection of MHCIIs and CLIP at the surface strongly suggests that some DRmyc-associated but unsaturated Ii trimers (most likely pentamers) egressed from the ER before DRKKAA could integrate the complex (Figures 1e and f). The DR over CLIP surface mean fluorescence intensity ratios were identical for

DRmyc in the presence or absence of DRKKAA, confirming that the MHCIIs trafficked with Ii (Figure 1g).

Finally, we repeated these experiments with p35. We postulated that p35 homotrimers would incorporate MHCIIs until a nonamer is formed and all RxR motifs are masked. Indeed, p35 must form a stoichiometric complex with MHCII to egress the ER, precluding egress of pentamers or heptamers (7). Thus, stochastic incorporation of DRKKAA in unsaturated DRmyc/Ii complexes (or vice-versa) should result in the downmodulation of DRmyc surface expression. We expressed DRKKAA and/or DRmyc alongside p35 homotrimers. When p35 was expressed with DRmyc, MHCII and CLIP were found at the plasma membrane (Figures 1e and f). Remarkably, when DRmyc and DRKKAA were coexpressed in the presence of p35, neither MHCII nor CLIP was found at the cell surface (Figures 1e and f). Confocal microscopy revealed that the MHCIIs remained in the ER (Supplementary Figure 2). On the basis of these findings, we conclude that p35 trimers were retained in the ER until saturated with MHCIIs. However, as β chains are incorporated randomly, it is likely that most nonamers contained at least one βKKAA chain, thereby causing retention of associated DRmyc.

Iip35 generates nonamers composed of mixed MHCII isotypes

The ability of p35 to generate high-order structures implies that different MHCII isotypes can be part of a given heptamer or nonamer. To test this possibility, we evaluated the capacity of the DRKKAA mutant to retain DQ in the ER. Cells were transfected with either DQ alone, DQ and DR or DQ and DRKKAA in the presence of either p33 or p35. First, when coexpressed with p33 or p35, DQ was detected at the plasma membrane along with CLIP (Figures 2a and b). This result is in line with our previous report showing that DQ efficiently masks the RxR motif of Iip35 (7). Interestingly, in the presence of p33, DQ surface expression was not affected by DRKKAA (Figure 2a). As for DRmyc, this suggests that non-saturated DQ/p33 complexes can egress the ER, independently of DRKKAA. However, the need for stoichiometric MHCII/p35 interactions resulted in the formation of doomed complexes including both DQ and DRKKAA. The DRKKAA-mediated ER

retention of DQ was specific as it was not observed with WT DR. Noteworthy, the trafficking toward the cell surface of DQ was not totally abolished by p35 and DRKKAA. Given that no CLIP was detected at the cell surface (Figure 2b), we hypothesized that these cell surface DQ molecules did not interact with Ii and trafficked on their own. To test this possibility, we compared the capacity of DR and DQ with escape ER retention by p35S6,8A, an unphosphorylable Ii variant that never leaves the ER (16,17). Figures 2c and d show that although both DQ and DR are well expressed at the plasma membrane and yield CLIP with Iip33, only DQ was detected at the cell surface with p35S6,8A. As there was no trace of CLIP, we conclude that some DQ molecules egressed the ER without Ii. Altogether, these results demonstrate the existence of mixed heptamers or nonamers containing different MHCII isotypes.

Model for the assembly of Ii/MHCII complexes

In the ER, nascent Ii chains homo- or heterotrimerize before interacting with MHCIIs (Supplementary Figure 3). As Ii is often in vast excess and half of the Ii pool exists as p33 homotrimers, some MHCII-free or unsaturated Iip33 trimers (pentamers and/or heptamers) may exit the ER (16,18,19). However, the p33/p35 ratio will also have a key impact on the stoichiometry of the complex. Indeed, the presence of p35 in any Ii heterotrimer will force the sequential addition of MHCII units until each and every RxR motif is masked. Thus, depending on which Ii subunit binds the MHCII first and assuming that all p35 molecules are rapidly phosphorylated, an Ii heterotrimer containing one p35 should have a 33% chance of being released from the ER as a pentamer. As the sequential binding of MHCIIs on the Ii trimer was shown to be non-cooperative (20), Ii trimers will compete with newly formed pentamers for the available MHCIIs. Although Ii is required for DP to reach the endocytic pathway (21), it remains to be determined if mixed complexes include any of the three MHCII allotypes.

In conclusion, our findings do not support the hypothesis that pentameric MHCII–Ii complexes are bent towards the cell membrane, thereby inhibiting the binding of additional MHCIIs (13). As the expression of p33 and p35 is differentially regulated in

diseases such as chronic lymphocytic leukemia and type I diabetes, stoichiometric MHCII/Ii variations may prove to be clinically relevant (22,23).

Funding

This research was funded by a grant from the National Science and Engineering Research Council of Canada (NSERC) to JT (grant number 298537).

Acknowledgements

We thank P Cresswell and L Denzin for the Cer.CLIP.1 antibody and RP Se´kaly for the Ii cDNA and the L243 hybridoma.

Conflict of interest

The authors declare no conflict of interest.

References

1. Cresswell P. Invariant chain structure and MHC class II function. *Cell* 1996; 84: 505–507.
2. Strubin M, Berte C, Mach B. Alternative splicing and alternative initiation of translation explain the four forms of the Ia antigen-associated invariant chain. *EMBO J* 1986; 5: 3485–3488.
3. Roche PA, Marks MS, Cresswell P. Formation of a nine-subunit complex by HLA class II glycoproteins and the invariant chain. *Nature* 1991; 354: 392–394.
4. Lamb CA, Cresswell P. Assembly and transport properties of invariant chain trimers and HLA-DR-invariant chain complexes. *J Immunol* 1992; 148: 3478–3482.

5. Strubin M, Long EO, Mach B. Two forms of the Ia antigen-associated invariant chain result from alternative initiations at two in-phase AUGs. *Cell* 1986; 47: 619–625.
6. Schutze M-P, Peterson PA, Jackson MR. An N-terminal double-arginine motif maintains type II membrane proteins in the endoplasmic reticulum. *EMBO J* 1994; 13: 1696–1705.
7. Khalil H, Brunet A, Saba I, Terra R, Sekaly RP, Thibodeau J. The MHC class II beta chain cytoplasmic tail overcomes the invariant chain p35-encoded endoplasmic reticulum retention signal. *Int Immunol* 2003; 15: 1249–1263.
8. Singer PA, Lauer W, Dembic Z, Mayer WE, Lipp J, Koch N *et al.* Structure of the murine Ia-associated invariant (Ii) chain as deduced from a cDNA clone. *EMBO J* 1984; 3: 873–877.
9. Cresswell P. Chemistry and functional role of the invariant chain. *Curr Opin Immunol* 1992; 4: 87–92.
10. Riberdy JM, Newcomb JR, Surman MJ, Barbosa JA, Cresswell P. HLA-DR molecules from an antigen-processing mutant cell line are associated with invariant chain peptides. *Nature* 1992; 360: 474–477.
11. Denzin LK, Cresswell P. HLA-DM induces CLIP dissociation from MHC class II αβ dimers and facilitates peptide loading. *Cell* 1995; 82: 155–165.
12. Majera D, Kristan KC, Neefjes J, Turk D, Mihelic M. Expression, purification and assembly of soluble multimeric MHC class II-invariant chain complexes. *FEBS Lett* 2012; 586: 1318–1324.
13. Koch N, Zacharias M, Konig A, Temme S, Neumann J, Springer S. Stoichiometry of HLA class II-invariant chain oligomers. *PLoS One* 2011; 6: e17257.
14. Teasdale RD, Jackson MR. Signal-mediated sorting of membrane proteins between the endoplasmic reticulum and the golgi apparatus. *Annu Rev Cell Dev Biol* 1996; 12: 27–54.
15. Khalil H, Brunet A, Thibodeau J. A three-amino-acid-long HLA-DRbeta cytoplasmic tail is sufficient to overcome ER retention of invariant-chain p35. *J Cell Sci* 2005; 118: 4679–4687.
16. Anderson HA, Bergstralh DT, Kawamura T, Blauvelt A, Roche PA. Phosphorylation of the invariant chain by protein kinase C regulates MHC class II trafficking to antigen-processing compartments. *J Immunol* 1999; 163: 5435–5443.
17. Kuwana T, Peterson PA, Karlsson L. Exit of major histocompatibility complex class II-invariant chain p35 complexes from the endoplasmic reticulum is modulated by phosphorylation. *Proc Natl Acad Sci USA* 1998; 95: 1056–1061.
18. Marks MS, Blum JS, Cresswell P. Invariant chain trimers are sequestered in the rough endoplasmic reticulum in the absence of association with HLA class II antigens. *J Cell Biol* 1990; 111: 839–855.
19. Warmerdam PA, Long EO, Roche PA. Isoforms of the invariant chain regulate transport of MHC class II molecules to antigen processing compartments. *J Cell Biol* 1996; 133: 281–291.
20. Jasanoff A, Song S, Dinner AR, Wagner G, Wiley DC. One of two unstructured domains of Ii becomes ordered in complexes with MHC class II molecules. *Immunity* 1999; 10: 761–768.
21. van LM, McEwen-Smith RM, Benham AM. HLA-DP HLA-DQ, and HLA-DR have different requirements for invariant chain and HLA-DM. *J Biol Chem* 2010; 285: 40800–40808.
22. Veenstra H, Jacobs P, Dowdle EB. Processing of HLA-class II invariant chain and expression of the p35 form is different in malignant and transformed cells. *Blood* 1993; 82: 2494–2500.
23. Yan G, Shi L, Penfornis A, Faustman DL. Impaired processing and presentation by MHC class II proteins in human diabetic cells. *J Immunol* 2003; 170: 620–627.

24. Faubert A, Samaan A, Thibodeau J. Functional analysis of tryptophans alpha 62 and beta 120 on HLA-DM. *J Biol Chem* 2002; 277: 2750–2755.

Figure legends

Figure 1. p35 favors the formation of high-order oligomers with MHCII. (a) Schematic representation of DR_{myc} and DR_{KKAA}. (b) HEK293T cells were transfected with DRα and either DRb_{myc} (DR_{myc}), DRb_{KKAA} (DR_{KKAA}) or both DR_{myc} and DR_{KKAA}. Cells were stained for the cell surface expression of MHCII using L243. Alternatively, cells were permeabilized with saponin and stained. The controls (ctrl) represent mock-transfected cells stained in the same conditions. (c) The mean fluorescence intensities (MFIs) obtained in b were plotted. (d) DR_{myc}- and DR_{myc} + DR_{KKAA}-expressing cells were permeabilized and stained with a myc tag-specific monoclonal antibody. (e) HEK293T cells were transfected with DR_{myc} and/or DR_{KKAA} together with p33 or p35. Cells were analyzed by flow cytometry using L243 to evaluate the efficiency of transport of MHCII. (f) Cells from e were stained for cell surface expression of CLIP. (g) The CLIP/MHCII expression ratios were calculated for a representative experiment. Paired Student's *t*-tests were performed; $*P \leq 0.05$, $**P \leq 0.01$; NS, non-significant $P \leq 0.1$. Error bars indicate the s.d. from at least three independent experiments.

Figure 2. Different MHCII isotypes can bind the same Ii trimer. (a–c) HEK293T cells were transiently transfected with DQ, DQ and DR or DQ and DR_{KKAA} alongside p33 or p35. (a) After 48 h, cells were analyzed by flow cytometry to derive DQ surface over total expression ratios using anti-DQ specific antibody. (b) Surface CLIP expression was assessed by flow cytometry and the mean fluorescence intensities (MFIs) were plotted. (c) Cells transiently transfected with DQ and DR, or DQ and DR_{KKAA}, alongside p33 or p35 were stained for DR (d, e) HEK293T cells were transiently transfected with DQ or DR together with p33, or $p35_{S6,8\,A}$. After 48 h, cells were analyzed by flow cytometry to evaluate DQ and DR surface to total expression ratio using anti-DQ and L243 antibodies, respectively or CLIP surface expression (e). MFIs were plotted and paired Student's *t*-tests were performed;

*$P \leq 0.05$, **$P \leq 0.01$; NS, non-significant $P \leq 0.1$. Error bars indicate the s.d. from at least three independent experiments

Figures

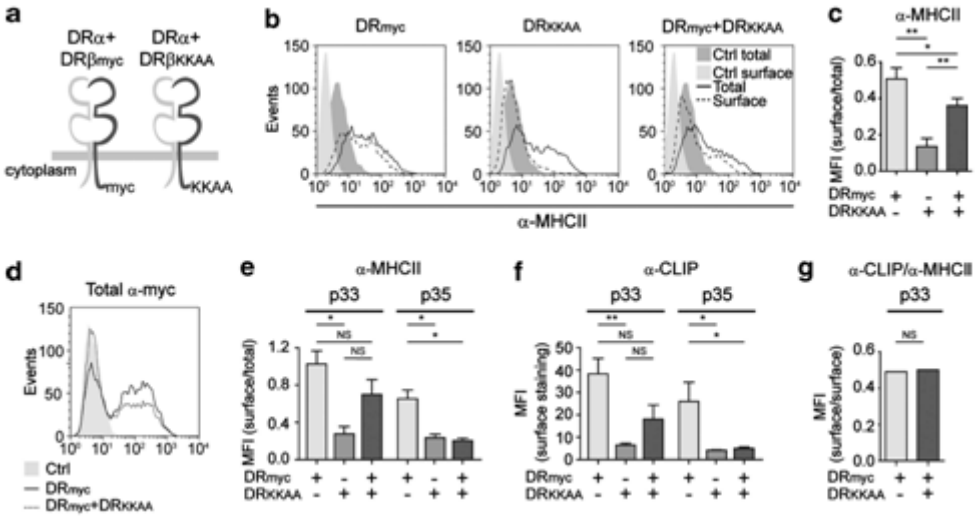

Figure 1. p35 favors the formation of high-order oligomers with MHCII

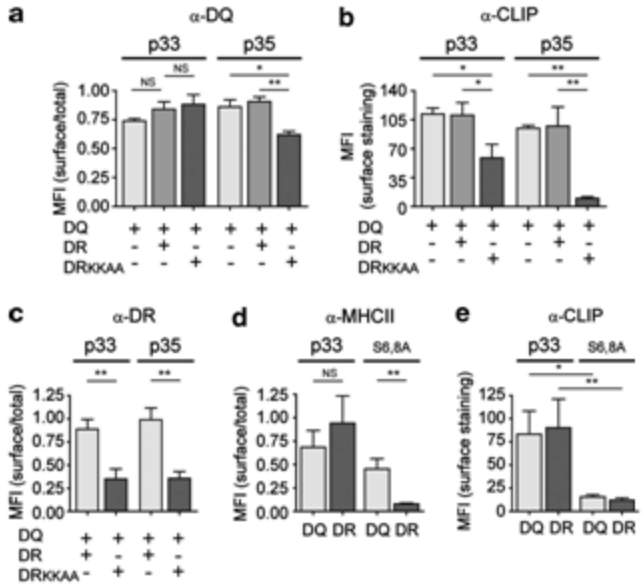

Figure 2. Different MHCII isotypes can bind the same Ii trimer.

Supplementary data

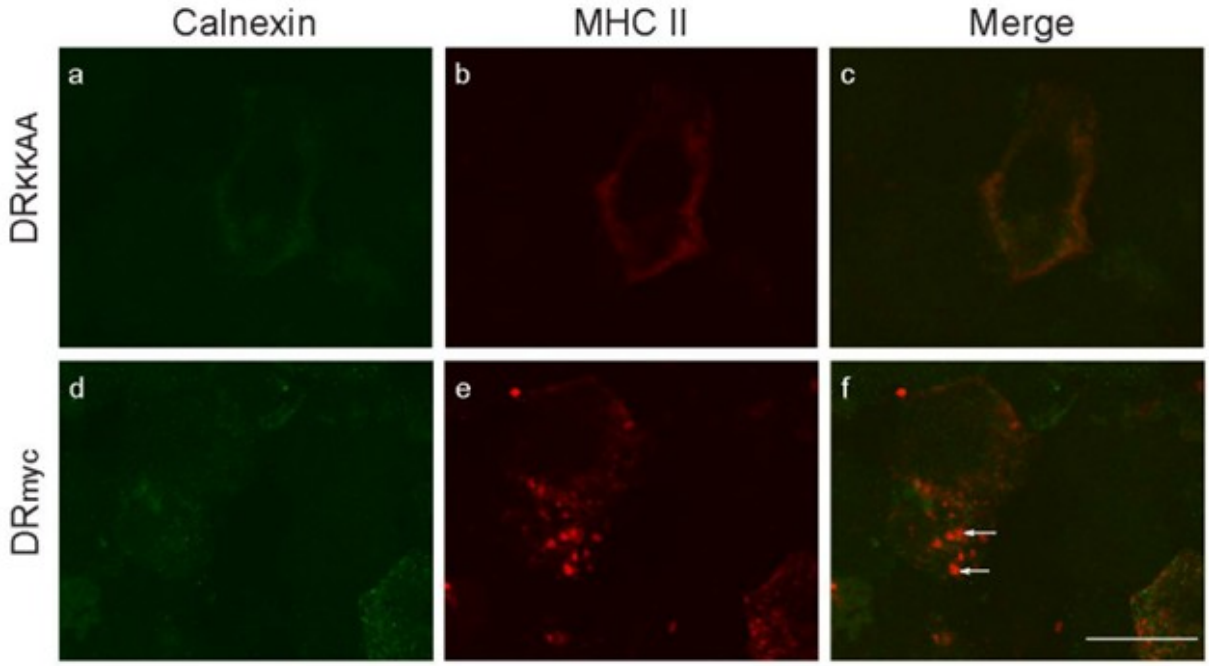

Supplemental Figure 1A. A di-lysine motif at the C-terminus of DRβ retains HLA-DR in the ER. HEK 293 cells were seeded on poly-L-lysine-treated coverslips and transiently transfected using HLA-DRα and the p33 isoform of **Ii** with alternatively $DR\beta_{KKAA}$ or $DR\beta_{myc}$. After 48h, cells were fixed with 4% PFA, permeabilized in 0.05% saponin and stained for calnexin (a, d) and class II (L243) (b, e). The secondary antibodies used were goat anti-rabbit coupled to Alexa Fluor 488 (a, d) and goat anti-mouse IgG2a coupled to Alexa Fluor 568 (b, e). Cells were analyzed by confocal microscopy on a Zeiss LSM 510 Laser Scanning confocal microscope. Panels c and f show the merge of calnexin and MHC class II. Arrows point to vesicular structures. The white scale bar in f corresponds to 10μm

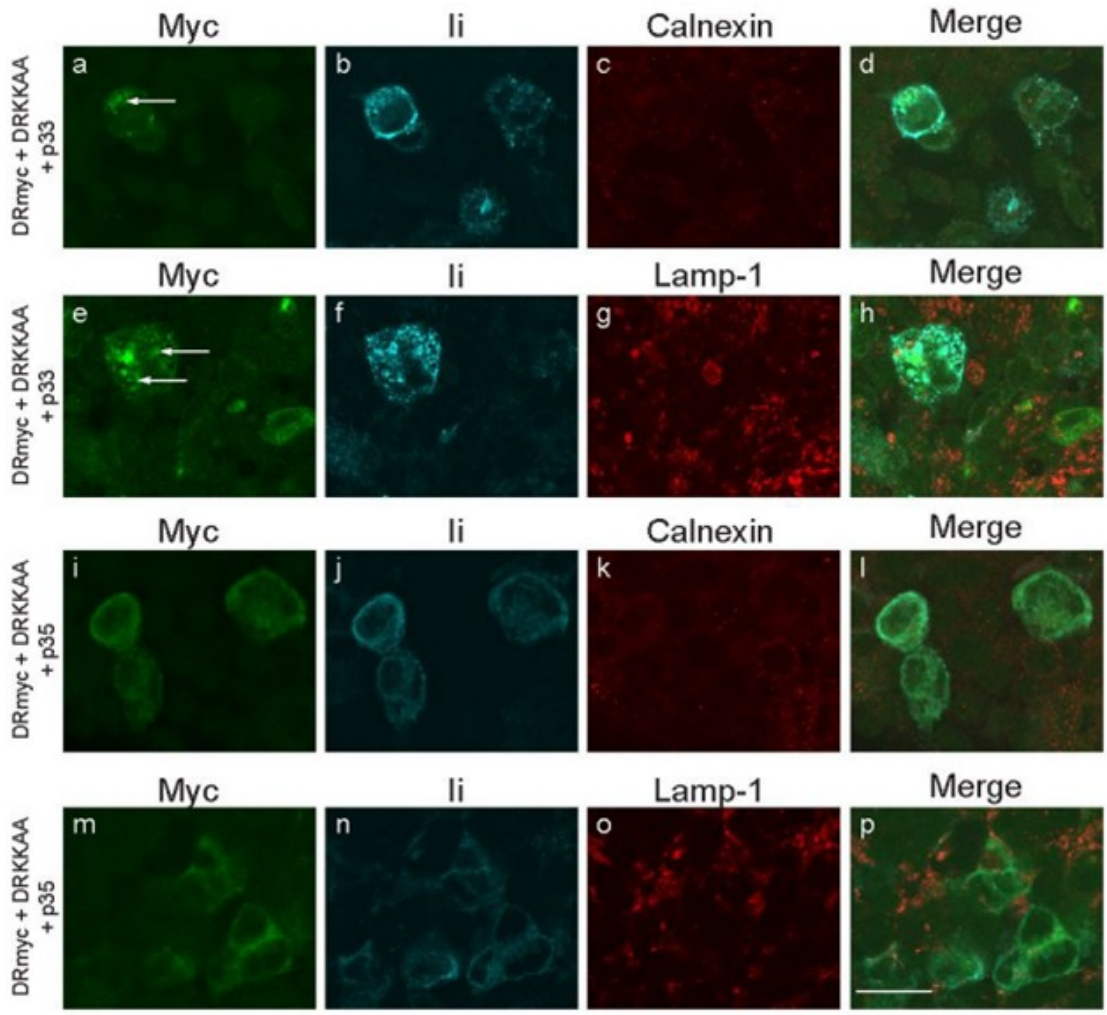

Supplemental Figure 2A. DR_{myc} is retained in the ER in the presence of DR_{KKAA} and lip35 but not lip33. HEK 293 cells were seeded on poly-L-lysine-treated coverslips and transiently transfected using HLA-DRα, $DR\beta_{KKAA}$ and $DR\beta_{myc}$ with altematively the p33 or p35 isoform of li. After 48h, cells were fixed with 4% PFA, permeabilized in 0.05% saponin and stained for Mye (9E10 coupled to FITC) (a, e, i, m), li (Pin.1 coupled to Alexa Fluor 647) (b, f, j, n) and calnexin (c, k) or Lamp-1 (g, o). The secondary antibodies used were and goat anti-rabbit coupled to Alexa Fluor 633 (c, g, k, o). Cells were analyzed by confocal microscopy on a Zeiss LSM 510 Laser Scanning confocal microscope. Panels d and 1 show the merge of calnexin, li and MHC class 11, whereas panels h and p show the merge of Lamp-1, li and MHC Il. Arrows point to vesicular structures. The white scale bar in p corresponds to 10μm.

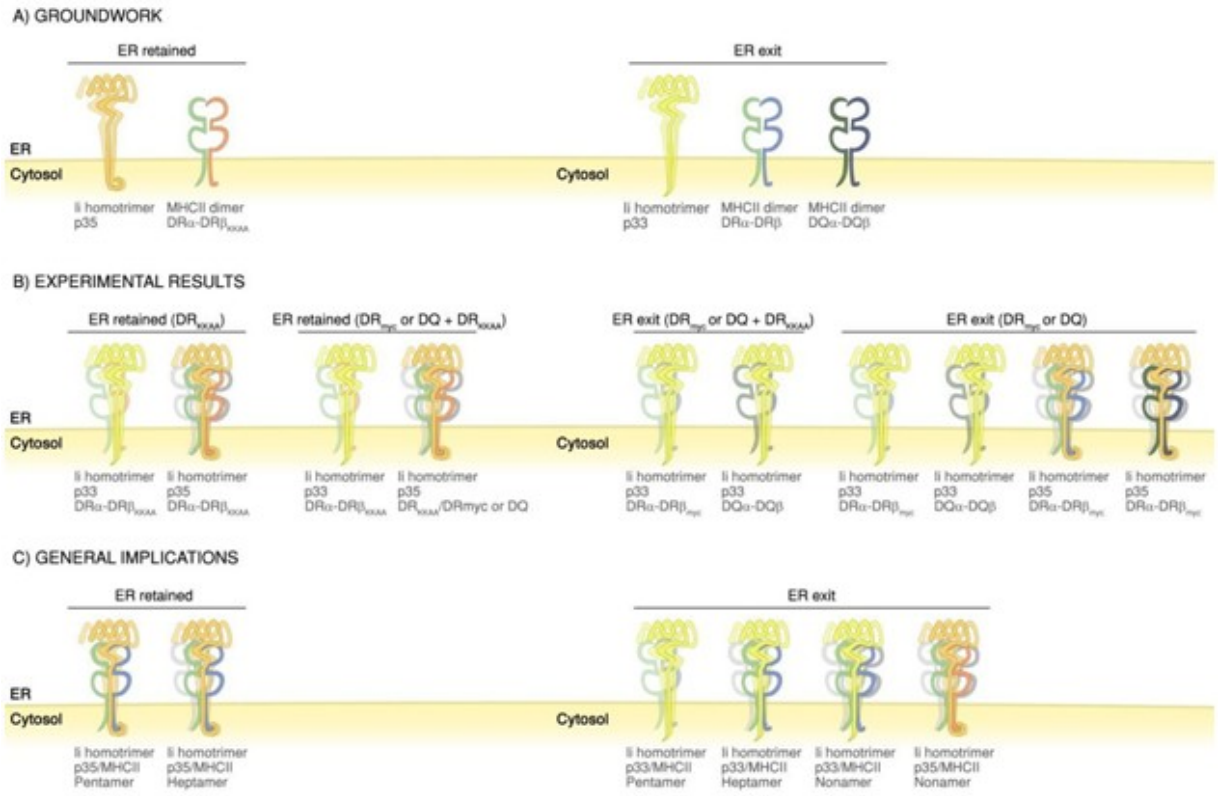

Supplemental Figure 3. Iip35 promotes formation of nonameric complexes with MHCIIs. (A) Groundwork on MHCII/Ii trafficking has established that while p35 homotrimers are retained in the ER by the RxR motif, Iip33 homotrimers, MHCII DR and DQ exit the ER. A DR mutant bearing the KKAA motif is also retained in the ER. (B) Our results show that p35 or p33 expressed with DRKKAA are retained in the ER. Meanwhile, expression with WT DR or DQ shows expression at the cell surface. When co-expressed with both DRKKAA and WT DR or DQ, cell surface level of p33/MHCII is reduced suggesting that one part of the pool is retained in the ER (p33/DRKKAA) while the other reaches the cell surface (p33/DR). Co-expression of DRKKAA and WT DR or DQ with p35 shows no cell surface expression of p35/MHCII. **C)** General implications of our model for the formation of Ii/MHCII complexes. Our experiments suggest that while p33 can exit the ER as pentamers, p35 promotes formation of stoichiometric complexes.

Annexe 3. Article non-discuté dans ce mémoire n°3

The D-6 Mouse Monoclonal Antibody Recognizes the CD74 Cytoplasmic Tail

Laetitia Genève,[*] Catherine Gauthier,[*] and Jacques Thibodeau[*]

[*]Laboratoire d'Immunologie Moléculaire, Département de Microbiologie, Infectiologie et Immunologie, Université de Montréal, Montreal, Quebec HC3 3J7, Canada;

Status : published in Monoclonal Antibobies in Immunodiagnosis and Immunotherapy

Address correspondence and reprint requests to Dr. Jacques Thibodeau, Laboratoire d'Immunologie Moléculaire, Département de Microbiologie, Infectiologie et Immunologie, Université de Montréal, CP 6128, Succursale Centre-Ville, Montreal, QC H3C 3J7, Canada.

Abstract

The invariant chain (Ii; CD74) is a multifunctional protein of the immune system and a major player in the presentation of exogenous antigens to T cells. In the endoplasmic reticulum (ER), Ii assists the folding and trafficking of MHC class II molecules. In the present study, we characterized the recently commercialized D-6 monoclonal antibody (MAb) made against a polypeptide spanning the entire sequence of the p33 isoform of human Ii. Using transgenic mice expressing the human p35

isoform, we showed by flow cytometry that D-6 only slightly cross-reacts with mouse Ii in permeabilized splenocytes. Analysis of the human B lymphoblastoid cell line LG2 revealed that D-6 recognizes Ii only upon membrane permeabilization. Variants of Ii bearing specific mutations or deletions were transfected in human cells to map the D-6 epitope. Our results showed that this MAb binds to the N-terminal cytoplasmic domain of Ii and that the epitope was destroyed upon mutagenesis of the two leucine-based endosomal targeting motifs. Thus, D-6 cannot be used for rapid flow cytometric assessment of CD74 cell surface expression and would be ineffective as a drug conjugate for the treatment of hematological malignancies.

Introduction

The invariant chain (Ii; CD74) was first described as a monomorphic component of MHC class II (MHCII) molecules (1). It is now recognized that Ii is a key chaperone in the MHCII antigen presentation pathway. As such, it is principally expressed in B cells, dendritic cells (DCs), monocytes/ macrophages, and thymic epithelial cells (2). Over the years, however, Ii was found to chaperone other molecules, such as CD70 (3). Also, it was ascribed very diverse cellular functions such as the regulation of DCs motility, B cell maturation, and macrophage response to macrophage migration inhibitoryfactor (MIF) (4-6).

The invariant chain is a glycosylated type II transmembrane protein of 216 amino acids (aa) organized in different functional domains (2). The N-terminal 28 aa constitute the cytoplasmic tail and the protein is membrane-anchored by a 26 aa-long hydrophobic domain. The 160 aa-long extracellular region can be further subdivided in a membrane-proximal disordered region, the class II-associated invariant chain peptide (CLIP) region, and the C-terminal trimerization domain (7). Alternative splicing of exon 6b results in two mRNAs, which in humans encode two different isoforms called hIip33 and hIip41 (mIip31 and mIip41 in mice) according to their molecular

mass (8,9). Exon 6b codes for a 64 aa extracellular do- main, inserted at residue 192, and capable of binding cathepsin to regulate Ag processing and presentation(10). In humans, the mRNAs coding for hIip33 and hIip41 both contain an alternative translation initiation codon, resulting in the synthesis of two additional isoforms, hIip35 and hIip43, of 35 and 43 kDa, respectively (9,11,12). The 16 aa N-terminal extension specific to these two isoforms contains a di-arginine (RxR) endoplasmic reticulum (ER) retention motif that presumably regulates for- mation of the Ii/MHCII complex (13,14).

As the main regulator of antigen presentation, Ii heterotrimerizes in the ER and associates with up to three MHCII αβ heterodimers to form pentamers, heptamers, and nonamers (15). Ii assists MHCII folding and prevents the loading of nascent endogenous ER polypeptides (16-18). For hIip35- and/or hIip43-containing Ii heterotrimers, ER egress occurs only upon binding of MHCII, which β chain masks the RxR motif (19). Two leucine-based motifs in the cytoplasmic tail of all isoforms target Ii and associated MHCIIs to the endocytic pathway, principally following internalization from the plasma membrane (20-22). Once in acidic compartments, Ii is degraded by a variety of proteases, freeing the MHCII groove and allowing the capture of exogenous peptides to be presented to $CD4^+$ T cells (2).

The transient cell surface expression of Ii trimers or Ii/ MHCII complexes has been exploited in cancer immunotherapy (23). A CD74-specific LL1 mouse MAb, which has been humanized and called milatuzumab, has antitumor activity on B cell malignancies (24,25). This antibody exerts a variety of effects on tumor cells, such as anti-proliferative activity (26,27). Moreover, it has been radiolabelled and shown to be rapidly internalized by B cell lymphomas (28). Consequently, the possibility of finding new CD74-specific MAbs of greater affinity and potency is of interest. The CD74 D-6 MAb (D-6) has recently been produced and commercialized by Santa Cruz Biotechnology. In this study, we characterized this antibody and mapped its epitope to the cytoplasmic tail of Ii.

Methods

Antibodies

BU45 and PIN-1 mouse hybridomas secrete IgG1 antibodies recognizing the C-terminal and the N-terminal part of human Ii, respectively (29,30). In-1 is a rat IgG2b MAb specific for the N-terminal part of murine Ii (BD-Pharmingen, Mississauga, Canada). The CD74 D-6 mouse MAb (IgG1) was purchased from Santa Cruz Biotechnology (cat. no. sc- 137217; Santa Cruz, CA). All MAbs were coupled to Alexa- 647 (Invitrogen, San Diego, CA).

Plasmids and cell lines

hIip33, hIip35, hIip33LIML, and hIi (hIip33 + hIip35) were subcloned from previously described constructs into pcDNA3.1 plasmids (31,32). pREP4-hIip33Δ20 and pBud-DRα + DRβ have been described previously (33). The murine DAP cell line stably expresses CIITA and has been described previously (34). The human HeLa cells and mouse Raw 264.7 (Raw) cells were stably transfected using Lipofectamine and Plus reagents (Invitrogen, Carlsbad, CA) according to the manufacturer's protocol. Cell populations were cloned by limiting dilution, and clones ex- pressing Ii were identified by intracellular staining with BU45. Cells were cultured in DMEM supplemented with 10% FBS (Wisent, Saint-Bruno, Canada).

Mice

Transgenic mice expressing the hIip35 isoform of human Ii have been described previously (35,36). The C57BL/6 (B6) and BALB/c mice were purchased from Charles River Laboratories International (Wilmington, MA). The CBA/CaHN-*Btk*^{xid}/J (Xid) mice were obtained from Jackson Laboratories (Bar Harbor, ME). All experiments were done in accordance with the Canadian Council of Animal Care guidelines.

Flow cytometry

Spleens were dissociated to obtain single cell suspensions. Red blood cells were lysed in 0.83% NH_4Cl. For cell lines, adherent cells were detached with EDTA 0.5 mM. All cells were resuspended (10^6) in staining buffer (PBS, FBS 3%, Hepes 10 mM). For total staining, cells were fixed 5 min in 4% paraformaldehyde (except for primary cells), washed three times, and then permeabilized for 10 min in staining buffer containing 0.1% saponin. Finally, cells were stained 30 min with the indicated antibodies in staining buffer with saponin and washed. Cells were analyzed on a FACSCalibur® flow cytometer (Becton Dickinson, Mississauga, Canada).

Results and discussion

D-6 can be used for detection of mouse and human Ii by flow cytometry

The D-6 MAb was obtained following immunization of mice with a synthetic polypeptide corresponding to the entire hIip33 isoform of human Ii (37). The sequence included the cytoplasmic, transmembrane, and luminal regions of the protein. D-6 was recommended for detection of CD74 of mouse, rat, and human origin by Western blot analysis, immunoprecipitation, immunofluorscence, and ELISA. We tested the capacity of D-6 to recognize Ii by flow cytometry in primary cells permeabilized with saponin. Indeed, Ii is mainly expressed in the endoplasmic reticulum (ER) and in the endocytic pathway (38). Splenocytes from C57BL/6 mice were isolated, permeabilized, and stained with D-6. As controls, we used splenocytes from mIi-deficient mice (mIiKO) and from transgenic mIiKO mice expressing the human hIip35 isoform (Tgp35/mIiKO).[35,39] As shown in Figure 1A, the mouse CD74-specific In-1 control MAb efficiently stained mIi in WT splenocytes whereas no signal was detected in mIiKO or Tgp35/mIiKO cells. On the other hand, the human-specific BU45 control MAb confirmed the strong hIip35 ex- pression in the Tgp35/mIiKO mice. As expected, the D-6 staining profile was similar to the one obtained with BU45 in Tgp35/mIiKO cells,

showing that both MAbs recognize hIi. The results also showed that D-6 recognizes mIi but the signal was much reduced compared to that of In-1. To determine if the weak binding of D-6 to mIi was a particularity of splenic B cells, we tested the same MAbs in the mouse RAW264.7 macrophage cell line that expresses mIi and MHCII molecules following the stable transfection of the transcription factor CIITA (RAW CIITA) (40). In addition, we tested RAW CIITA cells super-transfected with either hIip33 (RAW CIITA hIip33) or hIip35 (RAW CIITA hIip35). As shown in Figure 1B, In-1 recognized the endogenous mIi in all three cell lines (left panel). D-6 and BU45 showed very similar staining patterns, suggesting again that cross-reactivity of D-6 with mIi is weak.

To decisively conclude that the recognition of mIi by D-6 was poor, we stained the mouse fibroblast cell line DAP stably transfected with CIITA, the B cell line CH12, and splenocytes from two other mouse strains (BALB/c and Xid) (Fig. 2). While In-1 staining profiles revealed strong mIi expression in all conditions (DAP cells express some mIi constitutively), the low signals obtained with D-6 confirmed the differential ability of these MAbs to detect mIi. Altogether, these results showed that D-6 can be used for the detection of Ii by flow cytometry and that it is only slightly cross-reactive with mouse Ii.

D-6recognizes Ii only upon membrane permeabilization

In human antigen-presenting cells, hIi and the hIi/MHCII complex can be detected at the plasma membrane (29). As a first step in mapping the region recognized by D-6, we stained the human B lymphoblastoid cell line LG2 with D-6 and BU45. Figure 3 shows that only BU45 was capable of binding hIi at the cell surface. However, when cells were fixed and permabilized, the staining was found to be positive for both MAbs. These results suggest that D-6 either specifically recognizes an intracellular subset of the Ii pool or is directed at the cytoplasmic tail domain.

D-6 binds N-terminal cytoplasmic domain of hIi

To determine if D-6 binds the cytoplasmic or luminal region of Ii, we used a panel of HeLa cells transfected with different forms of hIi. The truncated hIi mutant devoid of its cytoplasmic tail (D20) is anchored in the membrane and still associates with MHCII molecules (41). Cells expressing Δ20 were permeabilized and stained with BU45 and D-6. Figure 4 reveals that D-6 does not recognize hIi devoid of its first N-terminal 20 residues. To confirm this finding, we conducted a competition experiment between D-6 and the well-characterized PIN-1 mouse MAb, which is specific for the cytoplasmic tail of all human Ii isoforms (30). The results showed that preincubation of the permeabilized cells with D-6 reduced the binding of PIN-1 (Fig. 4B).

As PIN-1 binding is inhibited following site-directed muta- genesis of the two leucine-based motifs located in the cytoplasmic tail (19), we tested the reactivity of D-6 against an hIi variant (hIip33LIML) having its Leu7Iso8 and Met16Leu17 amino acids changed for alanines (Fig. 4C). While HeLa cells transfected with hIip33 or hIip33LIML were recognized by BU45, D-6 failed to bind the hIi mutant devoid of its endosomal sorting signals.

Conclusion

The invariant chain is critical for many immune functions such as antigen presentation, thymic selection, B cell maturation and DC motility. It is expressed at the plasma membrane, principally in B cells, and has been attributed the cluster of differentiation 74 (CD74) (42). The cell surface expression and rapid internalization of Ii make it an effective target for antibody-mediated immunotherapy of lymphoma (24). Thus, it is crucial that we further our understanding of Ii's biology and assemble a panel of antibodies capable of detecting all subsets and isoforms. In this study, we characterized the new D-6 monoclonal antibody generated by Santa Cruz Biotechnology. We

showed that D-6 efficiently binds to human Ii and slightly cross-reacts with murine Ii in primary cells. The D-6 epitope clearly overlaps but may not be identical to the one of PIN-1, the latter MAb being human-specific. However, we cannot rule out that a difference in the affinity of PIN-1 and D-6 is responsible for the apparent species specificity of PIN-1. The epitope recognized by D-6 is localized in the portion of the cytoplasmic tail common to hIip33 and hIip35, more specifically in a segment encompassing the first 20 aa of the former (Fig. 5). The fact that D-6 recognizes the denatured and reduced Ii on immunoblots suggests that the epitope is not conformational (35). Although we have not specifically mapped the key residues in the epitope, the differential recognition of mIi and hIi points to the participation of at least one of the amino acids 11, 16 and 19, which diverged between the two species (Fig. 5, triangle). Moreover, this 9 aa region encompasses one of the two leucine-based motifs, which simultaneous mutation abolished D-6 reactivity. While the precise mapping of the epitope will await the thorough and systematic characterization of each amino acid, our results clearly demonstrate that D-6 recognizes the intracytoplasmic portion of Ii.

Funding

This project was funded by the Cancer Research Society. LG was supported in part by a studentship from INSERM (U-743).

Acknowledgements

We thank Serge Sénéchal for helping with the flow cytometry.

Author disclosure statement

The authors have no financial interests to disclose.

References

1. Cresswell P: Invariant chain structure and MHC class II function. Cell 1996;84:505–507.
2. Stumptner-Cuvelette P, and Benaroch P: Multiple roles of the invariant chain in MHC class II function. Biochim Biophys Acta 2002;1542:1–13.
3. Zwart W, Peperzak V, de VE, Keller AM, van der Horst G, Veraar EA, Geumann U, Janssen H, Janssen L, Naik SH, Neefjes J, and Borst J: The invariant chain transports TNF family member CD70 to MHC class II compartments in dendritic cells. J Cell Sci 2010;123:3817–3827.
4. Binsky I, Haran M, Starlets D, Gore Y, Lantner F, Harpaz N, Leng L, Goldenberg DM, Shvidel L, Berrebi A, Bucala R, and Shachar I: IL-8 secreted in a macrophage migration- inhibitory factor- and CD74-dependent manner regulates B cell chronic lymphocytic leukemia survival. Proc Natl Acad Sci USA 2007;104:13408–13413.
5. Lantner F, Starlets D, Gore Y, Flaishon L, Yamit-Hezi A, Dikstein R, Leng L, Bucala R, Machluf Y, Oren M, and Shachar I: CD74 induces TAp63 expression leading to B- cell survival. Blood 2007;110:4303–4311.
6. Faure-Andre G, Vargas P, Yuseff MI, Heuze M, Diaz J, Lankar D, Steri V, Manry J, Hugues S, Vascotto F, Bou- langer J, Raposo G, Bono MR, Rosemblatt M, Piel M, and Lennon-Dumenil AM: Regulation of dendritic cell migra- tion by CD74, the MHC class II-associated invariant chain. Science 2008;322:1705–1710.
7. Bijlmakers ME, Benaroch P, and Ploegh HL: Mapping functional regions in the lumenal domain of the class II- associated invariant chain. J Exp Med 1994;180:623–629.
8. Yamamoto K, Koch N, Steinmetz M, and Hammerling GJ: One gene encodes two distinct Ia-associated invariant chains. J Immunol 1985;134:3461–3467.

9. Strubin M, Berte C, and Mach B: Alternative splicing and al- ternative initiation of translation explain the four forms of the Ia antigen-associated invariant chain. EMBO J 1986;5:3485– 3488.
10. Koch N, Lauer W, Habicht J, and Dobberstein B: Primary structure of the gene for the murine Ia antigen-associated invariant chains (Ii). An alternatively spliced exon encodes a cysteine-rich domain highly homologous to a repetitive sequence of thyroglobulin. EMBO J 1987;6:1677–1683.
11. Strubin M, Long EO, and Mach B: Two forms of the Ia antigen-associated invariant chain result from alternative initiations at two in-phase AUGs. Cell 1986;47:619–625.
12. O'Sullivan DM, Noonan D, and Quaranta V: Four Ia in- variant chain forms derive from a single gene by alternative splicing and alternate initiation of transcription/translation. J Exp Med 1987;166:444–450.
13. Schutze M-P, Peterson PA, and Jackson MR: An N-terminal double-arginine motif maintains type II membrane proteins in the endoplasmic reticulum. EMBO J 1994;13:1696–1705.
14. Warmerdam PA, Long EO, and Roche PA: Isoforms of the invariant chain regulate transport of MHC class II mole- cules to antigen processing compartments. J Cell Biol 1996;133:281–291.
15. Roche PA, Marks MS, and Cresswell P: Formation of a nine-subunit complex by HLA class II glycoproteins and the invariant chain. Nature 1991;354:392–394.
16. Roche PA, and Cresswell P: Invariant chain association with HLA-DR molecules inhibits immunogenic peptide binding. Nature 1990;345:615–618.
17. Roche PA, and Cresswell P: Proteolysis of the class II- associated invariant chain generates a peptide binding site in intracellular HLA-DR molecules. Proc Natl Acad Sci USA 1991;88:3150–3154.
18. Anderson MS, and Miller J: Invariant chain can function as a chaperone protein for class II major histocompatibility complex molecules. Proc Natl Acad Sci USA 1992;89:2282–2286.
19. Khalil H, Brunet A, Saba I, Terra R, Sekaly RP, and Thibodeau J: The MHC class II beta chain cytoplasmic tail overcomes the invariant chain p35-encoded endoplasmic reticulum retention signal. Int Immunol 2003;15:1249–1263.
20. Bremnes B, Madsen T, Gedde-Dahl M, and Bakke O: An LI and ML motif in the cytoplasmic tail of the MHC-as- sociated invariant chain mediate rapid internalization. J Cell Sci 1994;107(Pt 7):2021–2032.
21. Odorizzi CG, Trowbridge IS, Xue L, Hopkins CR, Davis CD, and Collawn JF: Sorting signals in the MHC class II invariant chain cytoplasmic tail and transmembrane region determine trafficking to an endocytic processing compart- ment. J Cell Biol 1994;126:317–330.
22. Pieters J, Bakke O, and Dobberstein B: The MHC class II- associated invariant chain contains two endosomal targeting signals within its cytoplasmic tail. J Cell Sci 1993;106(Pt 3):831–846.
23. Thibodeau J, Bourgeois-Daigneault MC, and Lapointe R: Targeting the MHC Class II antigen presentation pathway in cancer immunotherapy. Oncoimmunology 2012;1:908–916.

24. Stein R, Mattes MJ, Cardillo TM, Hansen HJ, Chang CH, Burton J, Govindan S, and Goldenberg DM: CD74: a new candidate target for the immunotherapy of B-cell neo- plasms. Clin Cancer Res 2007;13:5556s–5563s.
25. Mark T, Martin P, Leonard JP, and Niesvizky R: Milatuzu- mab: a promising new agent for the treatment of lymphoid malignancies. Expert Opin Invest Drugs 2009;18:99–104.
26. Stein R, Qu Z, Cardillo T, Chen S, Rosario A, Horak ID, Hansen HJ, and Goldenberg DM: Anti-proliferative activity of a humanized anti-CD74 monoclonal antibody, hLL1, on B-cell malignancies. Blood 2004;104(12):3705–3711.
27. Frolich D, Blabetafeld D, Reiter K, Giesecke C, Daridon C, Mei HE, Burmester GR, Goldenberg DM, Salama A, and Dorner T: The anti-CD74 humanized monoclonal antibody, milatuzumab, which targets the invariant chain of MHC II complexes, alters B-cell proliferation, migration, and adhe- sion molecule expression. Arthritis Res Ther 2012;14:R54.
28. Hansen HJ, Ong GL, Diril H, Valdez A, Roche PA, Grif- fiths GL, Goldenberg DM, and Mattes MJ: Internalization and catabolism of radiolabelled antibodies to the MHC class-II invariant chain by B-cell lymphomas. Biochem J 1996;320(Pt 1):293–300.
29. Wraight CJ, Van Endert P, Moller P, Lipp J, Ling NR, Ma- cLennan IC, Koch N, and Moldenhauer G: Human major his- tocompatibility complex class II invariant chain is expressed on the cell surface. J Biol Chem 1990;265:5787–5792.
30. Lamb CA, and Cresswell P: Assembly and transport properties of invariant chain trimers and HLA-DR-invariant chain complexes. J Immunol 1992;148:3478–3482.
31. Brunet A, Samaan A, Deshaies F, Kindt TJ, and Thibodeau J: Functional characterization of a lysosomal sorting motifin the cytoplasmic tail of HLA-DObeta. J Biol Chem 2000;275:37062–37071.
32. Khalil H, Deshaies F, Bellemare-Pelletier A, Brunet A, Faubert A, Azar GA, and Thibodeau J: Class II transacti- vator-induced expression of HLA-DOb in HeLa cells. Tiss Antigens 2002;60:372–382.
33. Khalil H, Brunet A, and Thibodeau J: A three-amino-acid- long HLA-DRbeta cytoplasmic tail is sufficient to over- come ER retention of invariant-chain p35. J Cell Sci 2005;118:4679–4687.
34. Pezeshki AM, Cote MH, Azar GA, Routy JP, Boulassel MR, and Thibodeau J: Forced expression of HLA-DM at the surface of dendritic cells increases loading of synthetic peptides on MHC Class II molecules and modulates T cell responses. J Immunol 2011;187;74–81.
35. Geneve L, Menard C, Labrecque N, and Thibodeau J: The p35 human invariant chain in transgenic mice restores mature B cells in the absence of endogenous CD74. Int Immunol 2012;24:645–660.
36. Geneve L, Chemali M, Desjardins M, Labrecque N, and Thibodeau J: Human invariant chain isoform p35 restores thymic selection and antigen presentation in CD74-defi- cient mice. Immunol Cell Biol 2012;90:896–902.
37. Santa Cruz Biotechnology, Inc. http://www.scbt.com. Ac- cessed October 29, 2013.

38. Cresswell P: Assembly, transport, and function of MHC class II molecules. Annu Rev Immunol 1994;12:259–293.
39. Bikoff EK, Huang L-Y, Episkopou V, van Meerwijk J, Germain RN, and Robertson EJ: Defective major histocompatibility complex class II assembly, transport, peptide acquisition, and CD4 + T cell selection in mice lacking invariant chain ex- pression. J Exp Med 1993;177:1699–1712.
40. Steimle V, Siegrist C-A, Mottet A, Lisowska-Grospierre B, and Mach B: Regulation of MHC class II expression by interferon-gamma mediated by the transactivator gene CIITA. Science 1994;265:106–109.
41. Karp DR, Jenkins RN, and Long EO: Distinct binding sites on HLA-DR for invariant chain and staphylococcal en- terotoxins. Proc Natl Acad Sci USA 1992;89:9657–9661.
42. Möller P, Pezzutto A, Schwartz-Albiez R, Moldenhauer G, and Dörken B: Cluster report: CD74 in leukocyte typing IV. In: White Cell Differentiation Antigens. Knapp W, Dörken B, Rieber EP, Stein H, Gilks WR, Schmidt RE, and Von Dem Borne AEGK, Eds. Oxford University Press, Oxford, United Kingdom, 1989.

Figure legends

FIG. 1. D-6 recognizes human and mouse Ii in saponin-permeabilized primary cells. Cells were permeabilized with saponin and stained with In-1, BU45, or D-6. (A) Splenocytes were isolated from WT, mIiKO, and Tgp35/mIiKO mice. (B) Raw 264.7 cells (Raw) stably expressing CIITA were either mock-transfected (Raw CIITA) or transfected with hIip33 (Raw CIITA hIip33) or hIip35 (Raw CIITA hIip35). Cells were detached in EDTA, fixed in paraformaldehyde, permeabilized, and stained with antibodies. Data are representative of at least three independent experiments.

FIG. 2. The weak cross-reactivity of D-6 toward mIi is observed in different cell types. (A) Control DAP cells and DAP cells stably expressing CIITA were detached in EDTA, fixed in paraformaldehyde, permeabilized, and stained with D-6 or In-1. (B) Non-adherent CH12 B cells were fixed, permeabilized, and stained with D-6 or In-1. The control represents intrinsic cellular autofluorescence. (C) Splenocytes were isolated from C57BL/6 (B6), BALB/c, or CBA/CaHN-*Btk*^{xid}/J (Xid) mice.

Cells were permeabilized and stained with D-6 or In-1. Data are representative of at least two independent experiments.

FIG. 3. D-6 recognizes Ii only upon cell permeabilization. (A) The human LG2 B cells were washed in PBS and stained with D-6 or BU45. (B) LG2 cells were fixed, permeabilized with saponin, and stained with either D-6 or BU45. The staining profiles (neg) represent the intrinsic autofluorescence of the fixed and permeabilized cells. Data are representative of at least two independent experiments.

FIG. 4. D-6 recognizes the cytoplasmic tail of Ii. Cells were detached in EDTA, fixed, and permeabilized with saponin. (A) HeLa cells stably expressing DR1 alone, DR1 and hIip33D20 (DR1 D20), or DR1 and hIip35 (DR1 hIip35) were stained with D-6 or BU45. DR1 D20 expresses an hIi mutant form lacking the first 20 N-terminal residues of the hIip33 isoform. (B) HeLa cells stably expressing DR1 and hIip33 (DR1 hIip33) were incubated with PIN-1- Alexa647 (left bar). Alternatively, DR1 hIip33 cells were pre-incubated with unlabeled D-6, washed, and incubated with PIN-1-Alexa647 (right bar). The results are expressed as a percentage of the binding observed for cells incubated with PIN-1 alone. (C) HeLa cells stably expressing either hIip33 (p33), DR1 hIip33, or a hIip33 mutant with its two leucine-based sorting signals changed for alanines (hIip33LIML) were stained with D-6 or BU45. Data are representative of at least two independent experiments.

FIG. 5. Epitope mapping of the D-6 MAb. Schematic representation of the N-terminal region of the human Iip35 isoform (top row). The sequence of the mouse Iip31 is represented below. Only the non-conserved amino acids are shown. The two leucine-based motifs at positions 7–8 and 17–18 are identified with circles. The cytoplasmic tail and the transmembrane domain are identified. The start of the human Iip33 isoform and the following 20 amino acids deleted in the D20 mutant are marked. The arrowhead indicates the region encoding some or all of the amino acids forming the D-6 epitope.

Figures

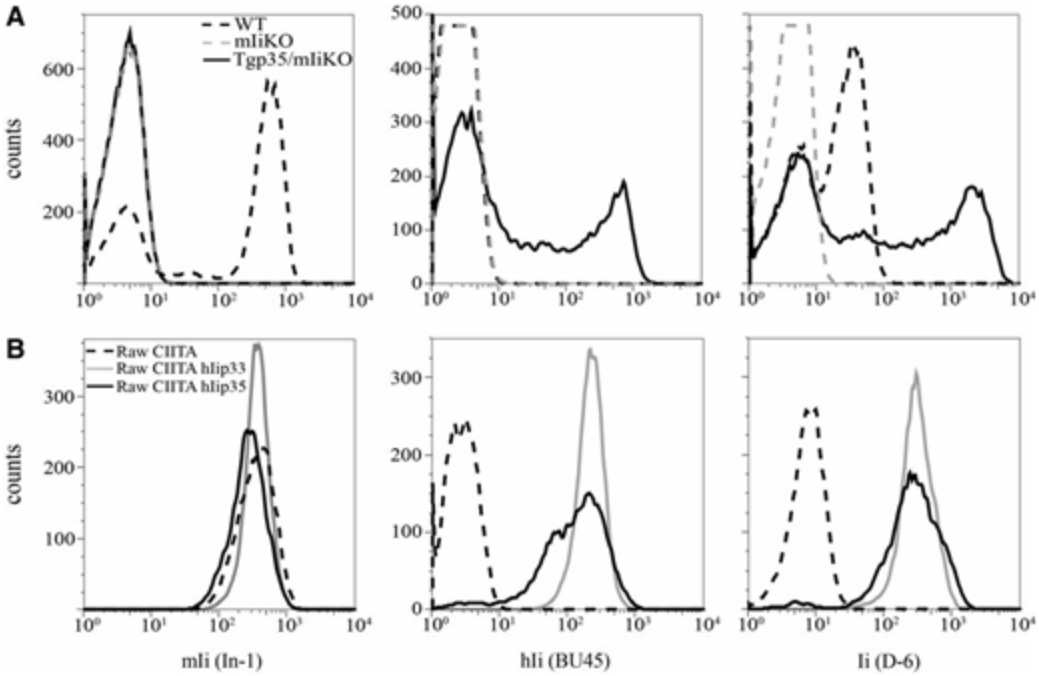

FIG. 1. D-6 recognizes human and mouse Ii in saponin-permeabilized primary cells.

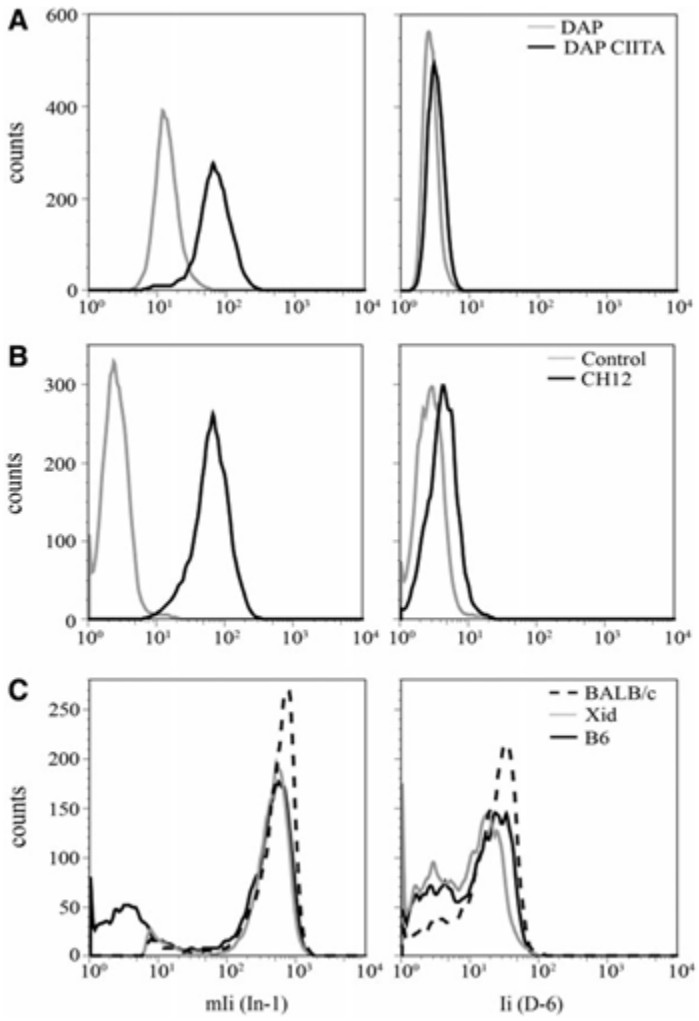

FIG. 2. The weak cross-reactivity of D-6 toward mIi is observed in different cell types.

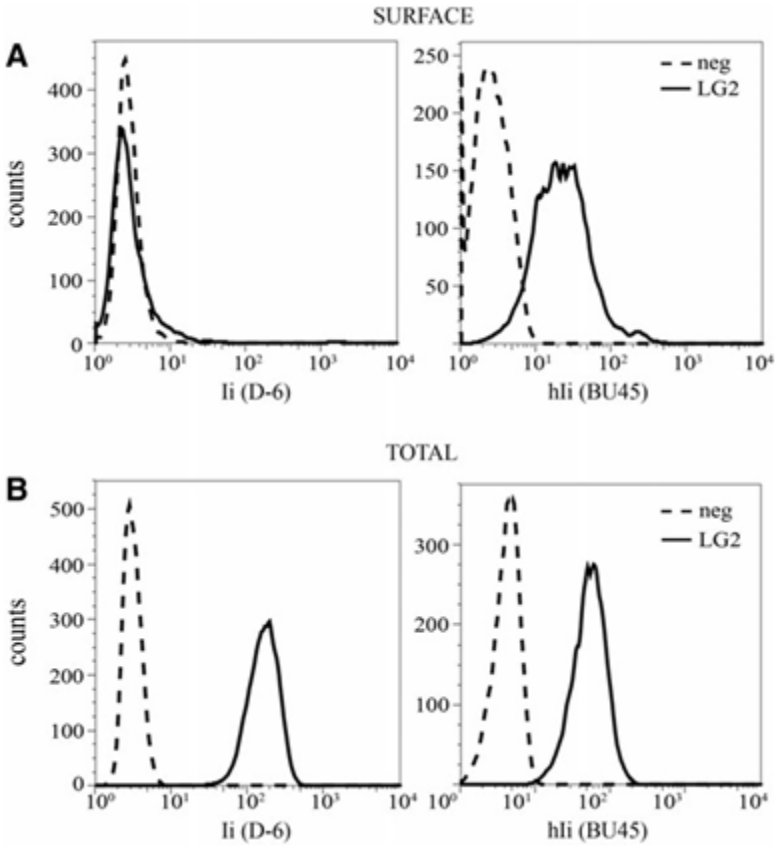

FIG. 3. D-6 recognizes Ii only upon cell permeabilization.

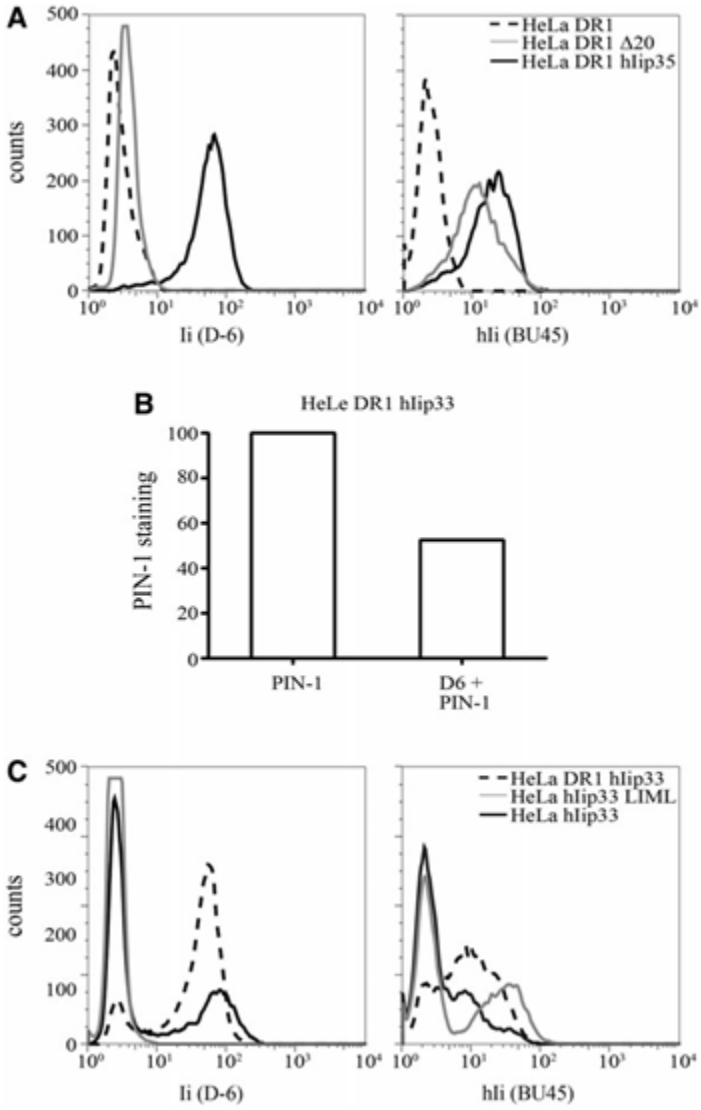

FIG. 4. D-6 recognizes the cytoplasmic tail of Ii.

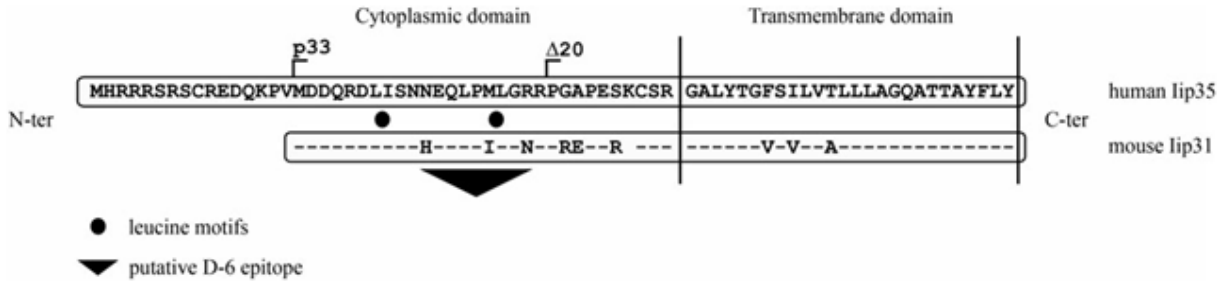

FIG. 5. Epitope mapping of the D-6 MAb.